UNIVERSIDAD AUTÓNOMA DE MADRID

DEPARTAMENTO DE BIOQUÍMICA

The role of VPS13 proteins in autophagy

TESIS DOCTORAL

SANDRA MUÑOZ BRACERAS

MADRID, 2017

DEPARTAMENTO DE BIOQUÍMICA
FACULTAD DE MEDICINA
UNIVERSIDAD AUTÓNOMA DE MADRID

The role of VPS13 proteins in autophagy

Sandra Muñoz Braceras
Licenciada en Biotecnología por la Universidad de Salamanca

Director de la Tesis:
Dr. Ricardo Escalante Hernández

Instituto de Investigaciones Biomédicas "Alberto Sols", Madrid
Consejo Superior de Investigaciones Científicas - Universidad Autónoma de Madrid

MINISTERIO
DE ECONOMÍA, INDUSTRIA
Y COMPETITIVIDAD

CSIC

UAM UNIVERSIDAD AUTÓNOMA DE MADRID

INSTITUTO DE INVESTIGACIONES BIOMÉDICAS "ALBERTO SOLS", IIBM

Dr. Ricardo Escalante Hernández, Científico Titular del Consejo Superior de Investigaciones Científicas en el Instituto de Investigaciones Biomédicas "Alberto Sols" de Madrid (CSIC/UAM)

CERTIFICA:

que **Sandra Muñoz Braceras**, Licenciada en Biotecnología por la Universidad de Salamanca ha realizado bajo mi dirección el trabajo de investigación titulado:

"The role of VPS13 proteins in autophagy"

Dicho trabajo reúne las condiciones requeridas por la legislación vigente, así como la originalidad y calidad científica necesarias para poder ser presentado y defendido con el fin de optar al grado de Doctor por la Universidad Autónoma de Madrid.

Y para que conste donde proceda, firmo el presente documento en Madrid a 4 de Mayo de 2017.

Fdo: Dr. Ricardo Escalante Hernández

http://www.iib.uam.es

C/ Arturo Duperier, nº 4
28029 MADRID ESPAÑA
TEL.: +34 91 585 4400
FAX: +34 91 585 4401

Esta Tesis Doctoral ha sido realizada gracias a la concesión de un contrato predoctoral para la Formación de Personal Investigador de la Universidad Autónoma de Madrid (FPI-UAM).

Agradecimientos

La primera persona a la que quiero agradecer este trabajo es a Ricardo. Muchas gracias Ricardo por ofrecerme la oportunidad de realizar la tesis en tu laboratorio y por ser un perfecto director. Recuerdo como si fuera ayer la ilusión con la que me presentaste a los tip y la idea de que en especial uno de ellos pudiera tener defectos en autofagia. La suerte quiso que así fuera y así comenzó el proyecto. El número 13 no parecía entonces tener nada que ver con la mala suerte y, aunque en múltiples ocasiones posteriores he maldecido mi mala suerte (y en especial al "monstruo" de proteína que tenía entre manos), en realidad no he podido tener mejor suerte que la de tenerte como director. Se quedan cortas las palabras para agradecer toda tu dedicación y todo lo que he aprendido de ti, tanto a nivel profesional como personal. Muchísimas gracias.

Muchas gracias también a todos aquellos con los que he compartido momentos en el laboratorio durante estos años. De todos he aprendido algo y todos habéis contribuido a que esta aventura sea inolvidable. Sergio, Javi y Dani, ¡menudo trío! A pesar de lo desconcertantes que fueron alguno de los momentos iniciales con vosotros, os he echado mucho de menos desde que os fuisteis. ¡Ojalá hubiéramos compartido más tiempo juntos! Y también contigo, Natalia, ya que tu buen rollo y entusiasmo con mil proyectos transmitían muchísima alegría y ganas de hacer cosas. Ana, nos quedamos solas durante un tiempo, pero era imposible aburrirse contigo. Cuando había un rato para hablar, daba igual de lo que fuera; nos hemos reído mucho, gracias por esos buenos ratos. ¡Qué gracioso también Montero con sus "bolas"! Gracias por traer ese salero andaluz al labo, aunque fuera por poco tiempo. Como buena burgalesa, mis piques he tenido contigo, Luisca; y es que yo creo que la catedral de Burgos es más amplia que la de León y que por eso no me gusta confluencia, jeje. Bromas aparte, gracias por todas aquellas rayadas experimentales que hemos compartido ya que, aunque cada uno tenía su proyecto, han sido muchas. ¡Qué bien que estabas tú, Eunice, para poner orden! (y también orden en su sentido más literal). Gracias por eso, por tu predisposición a ayudar siempre y, en general, por todo el tiempo compartido. ¡Cuánto me alegro de que tu estancia se alargue y se alargue! me gustaría que te quedaras por aquí mucho más. Con vosotras, Bea y María, sí que he compartido una parte del proyecto, muchas gracias por hacer los KOs A y B de dicty y los experimentos oportunos en esos mutantes; un gran trabajo y una gran compañía la vuestra. For some months, I shared with you, Hannes, my thoughts about Vps13; thank you for that and for teaching me how to differentiate neurons. Sumi, thank you for being a very good labmate and a good friend in a new city. And, in general, thank you to everyone in Andreas' lab for those nice months in Dresden. De vuelta al IIB, muchas gracias Rosa por tu ayuda con las cuantitativas y por tu alegría constante. Olivier, muchas gracias por tu idea del gap repair y tu ayuda con la transformación de levaduras. Diego, gracias por las innumerables horas en el confocal y por aguantar mi ritmo desde la primera sesión; la verdad es que son más aburridas las horas siendo autónomo. Daniela, Sol, Petri, León, Pilar, Lara, Bárbara, y Marta entre otros (por no hacer infinita la lista) gracias por todas aquellas comidas en las que de ciencia era casi de lo último de lo que se hablaba y por todos esos ratos en vuestra compañía, tanto en el IIB como fuera del trabajo.

Fuera del IIB también hay mucha gente a la que quiero agradecer ya que, de una manera u otra, una pequeña parte de esta tesis es suya. Silvia, Elvira y Ane, son muchas las conversaciones que os tengo que agradecer acerca de experimentos o del doctorado, pero, puestos a agradecer, más os agradezco muchas otras y el tiempo con vosotras durante estos años en Madrid.

Hasta Madrid no hubiera llegado sin vosotros: Amparo, Belén, Edu, Bea y María; grandes compañeros de carrera en Salamanca pero especialmente grandes amigos. Aunque cada uno actualmente en un lugar, vuestro apoyo a lo largo de este camino ha sido muy valioso. Tanto como aquel inocente comentario tuyo, Ángel, mencionando lo ilusionada que me veías cacharreando en las prácticas de laboratorio los primeros años de carrera.

A mis amigos de toda la vida quiero darles las gracias por entender a "mis bichos que se comen a otros bichos" y especialmente por entender el tiempo que me comían también a mí. Sara, María, Vero, Verolado, Noe, Lara, Miguel, Víctor, Abraham, Sergio, Jona, Hugo... Gracias por creer, desde que éramos pequeños, que de mayor iba a trabajar en un laboratorio.

Pero si alguien creyó desde siempre, y más que nadie, que podía dedicarme a la investigación fuiste tú, Raquel. Muchas gracias tata por eso y por ser mi mejor ejemplo a seguir. Papá y mamá, muchos han sido los días que os decía que había estado "contando puntos" y con ironía me decíais que si era contable. Tendría que serlo para llevar la cuenta de todas las cosas que habéis hecho por mí (¡incluso sin idea de ciencia habéis tratado de aportar soluciones cuando algo se complicaba en el laboratorio!). Os lo digo mucho menos de lo que debería así que quiero que aquí quede escrito en grande: ¡MUCHÍSIMAS GRACIAS!

Y a ti, Jose, muchísimas gracias una y otra vez. Sin ti no creo que hubiera podido acabar esta tesis. Gracias por comprender el tiempo dedicado al trabajo, especialmente en los últimos meses; gracias por ajustar nuestros planes a merced de mis experimentos cuando ha hecho falta; gracias por estar ahí siempre, incluso cuando estábamos a más de 2000 km de distancia; gracias por tu apoyo, por tus ánimos, por tu paciencia, por mantener mi cordura, por tus consejos, por tus abrazos, por tus besos, por compartir tu vida conmigo y, en definitiva, gracias por todo.

Resumen

Las proteínas de la familia VPS13 son un grupo de proteínas conservadas cuya ausencia conlleva la aparición o mayor riesgo de sufrir distintas enfermedades. En esta tesis hemos demostrado por primera vez que la ausencia de algunas proteínas VPS13 afecta a la autofagia, un proceso de degradación celular que es esencial para la homeostasis celular. Hemos usado mutantes de estas proteínas en la ameba social *Dictyostelium discoideum* y también células humanas HeLa en cultivo, en las que hemos inhibido la expresión de las proteínas VPS13 mediante el silenciamiento de RNA. Las células carentes de ciertas proteínas VPS13 muestran alteraciones de los patrones de marcadores autofágicos y un defecto parcial del flujo autofágico. Hemos descubierto que al menos algunas funciones de la proteína VPS13 de *D. discoideum* TipC, relacionadas con autofagia, están mediadas por el extremo C-terminal de la proteína y que éste es, hasta cierto punto, funcional por sí solo. Además, hemos demostrado que la función de las proteínas VPS13 en autofagia forma parte, probablemente, de un papel más general del tráfico vesicular, como así lo sugieren las alteraciones de marcadores de endosomas y lisosomas que hemos observado tras la inhibición de la expresión de la proteína VPS13A humana y que señalan posibles defectos en la capacidad degradativa de las células. También hemos revelado la conexión con la GTPasa RAB7, una proteína clave en la regulación de las rutas de endocitosis y autofagia. Nuestros resultados indican que VPS13A colocaliza de forma preferente con la mitocondria, lo que apunta a una interacción entre este orgánulo y el sistema endolisosomal. Basados en la asociación de la autofagia con muchas enfermedades neurodegenerativas entre otras enfermedades, consideramos que la contribución de VPS13A a una autofagia funcional podría ser relevante en la etiología de la corea acantocitosis (ChAc), la enfermedad neurodegenerativa rara causada por las mutaciones de VPS13A. Por tanto, proponemos estudiar el proceso autofágico a nivel de la participación de RAB7 y explorar la relación entre las mitocondrias y el sistema endolisosomal como áreas de investigación importantes que potencialmente podrían ayudar en el diseño racional de terapias futuras para la corea acantocitosis y, quizás, para otras enfermedades neurodegenerativas asociadas con las proteínas VPS13.

Summary

VPS13 proteins are a group of conserved proteins whose absence or mutations lead to the appearance or higher risk to suffering from different diseases. In this thesis we have demonstrated for the first time that the absence of some VPS13 proteins impairs autophagy, a degradative cellular process that is essential for cell homeostasis. We have used mutants of these proteins in the social amoeba *Dictyostelium discoideum* and human HeLa cells in culture in which VPS13 proteins have been downregulated by siRNA. Cells depleted of some VPS13 proteins show alterations in the pattern of autophagic markers and partial defects in autophagic flux. We have found that at least some autophagy-related roles of the TipC VPS13 *D. discoideum* protein are mediated by the conserved C terminus of the protein, able to function on its own to certain extent. Furthermore, we have shown that the VPS13 function in autophagy is very likely part of a more general role in vesicular trafficking, as suggested by the observed alterations of endocytic and lysosomal markers upon human VPS13A downregulation, which indicate an impairment of the efficient degradation capacity of the cells. We have also revealed a connection with the Rab GTPase RAB7, a key regulatory protein of both endocytic and autophagic pathways. Interestingly, our results indicate that VPS13A preferentially colocalizes with mitochondria, which points to an interplay between this organelle and the endolysosomal system. Based on the association of autophagy with several neurodegenerative diseases among other diseases, we consider that VPS13A contribution to a functional autophagy could be relevant for the etiology of chorea-acanthocytosis (ChAc), the rare neurodegenerative disease caused by mutations of VPS13A. Therefore, we propose the study of the autophagic process at the level of RAB7 participation and the exploration of the relationship between mitochondria and the endolysosomal system as important research fields that could potentially aid in the rational design of future therapies for ChAc and, perhaps, other neurodegenerative diseases associated to VPS13 proteins.

Table of contents

Resumen i

Summary iii

Table of contents v

Abbreviations ix

1 | INTRODUCTION 3

1.1 | The VPS13 family 3

1.1.1 | Evolution of the VPS13 family 3

1.1.2 | Alternative splicing and expression of the *VPS13* genes 3

1.1.3 | Implications of the VPS13 family for human health 5

1.1.4 | VPS13 proteins structure and functional domains 8

1.1.5 | Reported functions of VPS13 proteins 10

1.2 | Autophagy 15

1.2.1 | Types of autophagy 15

1.2.2 | The autophagic machinery 16

1.2.3 | Relevance of autophagy for human health 18

1.2.4 | An hypothetic role of VPS13 proteins in autophagy 19

1.3 | *Dictyostelium discoideum* 20

1.3.1 | Life cycle of *D. discoideum* 20

1.3.2 | General advantages of *D. discoideum* as a simple model 21

1.3.3 | *D. discoideum* to study autophagy 21

2 | OBJECTIVES 25

3 | MATERIALS AND METHODS 29

3.1 | DNA constructs 29

3.1.1 | PCR products for *vps13*$^{-}$ mutants production in *D. discoideum* 29

3.1.2 | DNA plasmids 30

3.2 | Specific *D. discoideum* techniques 32

3.2.1 | Strains, cell culture and development 32
3.2.2 | Generation of new *D. discoideum* strains 34
3.2.3 | Autophagy assays 34
3.2.4 | Phagocytosis assay 35
3.3 | Specific techniques for human cell lines 35
3.3.1 | Cell culture 35
3.3.2 | DNA and siRNA transfection and qPCR 35
3.3.3 | Autophagy assays 36
3.4 | Common methods 37
3.4.1 | Western blot and band densitometry 37
3.4.2 | Immunoprecipitation assays 37
3.4.3 | Mass-spectrometry 38
3.4.4 | Confocal microscopy and immunocytochemistry 39
3.4.5 | Electron microscopy 40
3.4.6 | Image analysis 40
3.4.7 | Statistical analysis 40
4 | RESULTS 43
4.1 | Autophagic flux in *D. discoideum tip*$^{-}$ mutants 43
4.2 | Autophagic flux in *D. discoideum vps13*$^{-}$ mutants 44
4.3 | Atg8 and Atg18 autophagic markers in the *tipC*$^{-}$ mutant 45
4.4 | Expression of TipC N and C termini 47
4.5 | Autophagy flux in VPS13A-depleted human cells 49
4.6 | Further study of autophagy in VPS13A-depleted cells 51
4.7 | Identification of *Dictyostelium* VPS13 proteins interactors 54
4.8 | Conserved interaction of TipC and VPS13A with RAB7 56
4.9 | VPS13A subcellular localization 56
4.10 | Endocytic traffic in VPS13A-depleted cells 59
4.11 | Ultrastructural analysis of VPS13A-depleted cells 63
5 | DISCUSSION 69

5.1 | Role of VPS13 proteins in autophagy and endocytic traffic 69

5.2 | VPS13 proteins localization and function 73

5.3 | VPS13 partners and related functions 75

5.4 | Concluding remarks and Future perspective 81

6 | CONCLUSIONS 85

7 | CONCLUSIONES 89

8 | REFERENCES 93

ANNEX: PUBLICATIONS 117

Abbreviations

ALPS	amphipathic lipid packing sensor
ATG	autophagy related
CCCP	carbonyl cyanide m-chlorophenyl hydrazine
ChAc	chorea-acanthocytosis
CK	creatine kinase
CMA	chaperone-mediated autophagy
CMT2	Charcot-Marie-Tooth type 2B
CQ	chloroquine
CS	cohen syndrome
CTSB	cathepsin B
DUF	domain of unknown function
EE	early endosome
EF-1a	elongation factor 1-alpha
ER	endoplasmic reticulum
ERMES	ER-mitochondria encounter structure
ESCRT	endosomal sorting complex required for transport
FFAT	two phenylalanines, FF, in an acidic tract
FYCO1	FYVE (Fab1-YotB-Vac1p-EEA1) and coiled-coil domain containing 1
$GABA_A$	gamma amino butyric acid
GDP	guanosine-5'-diphosphate
GFP	green fluorescent protein
GTP	guanosine-5'-triphosphate
HDAC6	histone deacetylase 6
HOPS	homotypic fusion and vacuole protein sorting
HSP	heat shock protein
ILV	intraluminal vesicle
iPSC	induced pluripotent stem cells
LAMP	lysosome-associated membrane protein
LC3	microtubule-associated protein 1 light chain 3 (MAPLC3)
LD	lipid droplet
LE	late endosome
LRRK	leucine-rich repeat kinase
MAMs	mitochondrial associated membranes

Mcp1	Mdm10 complementing protein 1
MCS	membrane contact site
mDAN	midbrain dopaminergic neurons
MSN	medium spiny neurons
MVB	multivesicular body
NA	neuroacanthocytosis
NVJ	nuclear vacuolar junction
OMM	outer mitochondrial membrane
OPI	overproduction and excretion of inositol
PA	phosphatidic acid
PAK1	p21-activated kinase 1
PAS	phagohore assembly site
PBS	phosphate buffered saline
PD	parkinson's disease
PE	Phosphoethanolamine
PH	pleckstrin homology
PI	phosphatidylinositol
PI(4,5)P	phosphatidylinositol-4,5- biphosphate
PI3P	phosphatidylinositol-3-phosphate
PI4P	phosphatidylinositol-4-phosphate
PIK3C3	phosphatidylinositol-3-kinase class III
PINK1	PTEN-induced putative kinase 1
PIP	phosphatidylinositol phosphoderivatives
PSM	prospore membrane
RAB	ras genes from rat brain
RAC1	ras-related C3 botunlinum toxin substrate 1
RBCs	red blood cells
RE	recycling endosome
RFP	red fluorescent protein
RILP	rab7-interacting lysosomal protein
Rubicon	RUN domain protein as Beclin 1 interacting and cysteine rich containing (RUN: RPIP8–UNC-14–NESCA)
SNARE	soluble N-ethylmaleimide–sensitive factor attachment protein receptors,
SQSTM1	sequestosome 1
SOI	suppressor of the rapid onset of impotence
TGN	*trans*-Golgi network

TLS	TGN localization signal
tTGase	tissue transglutaminase
UBA	ubiquitin associated
ULK1	unc-51 like autophagy activated kinase 1
UVRAG	UV radiation resistance associated gene
VAP	vesicle-associated membrane protein associated protein
vCLAMP	vacuole and mitochondria patch
VPL	vacuolar protein localization
VPS	vacuolar protein sorting
VPT	vacuolar protein targeting
WIPI	WD repeat domain phosphoinositide interacting
WT	wild-type

1 | INTRODUCTION

1 | INTRODUCTION

The aim of the research work presented in this thesis was to study if VPS13 (vacuolar protein sorting 13) proteins participate in autophagy. The hypothesis of such a role was partly inspired by the particular phenotype of a *vps13-* mutant in *Dictyostelium discoideum*, a simple organism that has been used in this thesis as a model system to advance in the knowledge of the role of VPS13 proteins, with special emphasis on autophagy. This section includes an overview of VPS13 proteins, autophagy, and *D. discoideum*.

1.1 | The VPS13 family

VPS13 proteins are a group of very large proteins with some common features according to their amino acid sequence. More than one VPS13 proteins are usually present in the same organism. However, their molecular functions are not totally redundant as exemplified by the distinct human diseases caused by mutations of the different *VPS13* genes. In order to gain insight into the etiology of these diseases, the roles of VPS13 proteins need to be discerned.

1.1.1 | Evolution of the VPS13 family

VPS13 proteins constitute a family of proteins widely conserved during eukaryotic evolution, from unicellular organisms to humans. One Vps13 protein is present in *Saccharomyces cerevisiae*, six in *Dictyostelium discoideum*, at least eight in *Tetrahymena thermophila*, three in *Arabidopsis thaliana*, two in *Caenorhabditis elegans,* three in *Drosophila melanogaster,* and four in *Mus musculus* and in *Homo sapiens.* In the case of the non-metazoan VPS13 proteins, homology of a particular protein with a specific member of the human VPS13 family is not obvious. Therefore, duplications of a common VPS13 ancestor might have independently occurred in plants, in dictyostelids and in ciliates after their divergence from fungi and metazoans and then similar duplications would have originated the different homologues in metazoans (FIG. 1).[311] Such enlargement of the VPS13 family suggests certain degree of specialization of the original functions of the protein or acquisition of new ones. Within the human family, VPS13B is the most divergent member while VPS13A and VPS13C are very similar, probably due to ancient and late duplications of the gene, respectively.[311]

1.1.2 | Alternative splicing and expression of the *VPS13* genes

If the existence of four human homologous genes makes this family complex, the degree of complexity increases by the alternative splicing of the resulting transcripts. Four different long isoforms have been described for *VPS13A*, two for *VPS13B*, four for *VPS13C*, and two for *VPS13D*. Shorter transcripts are reported but barely detected, being probably non-functional

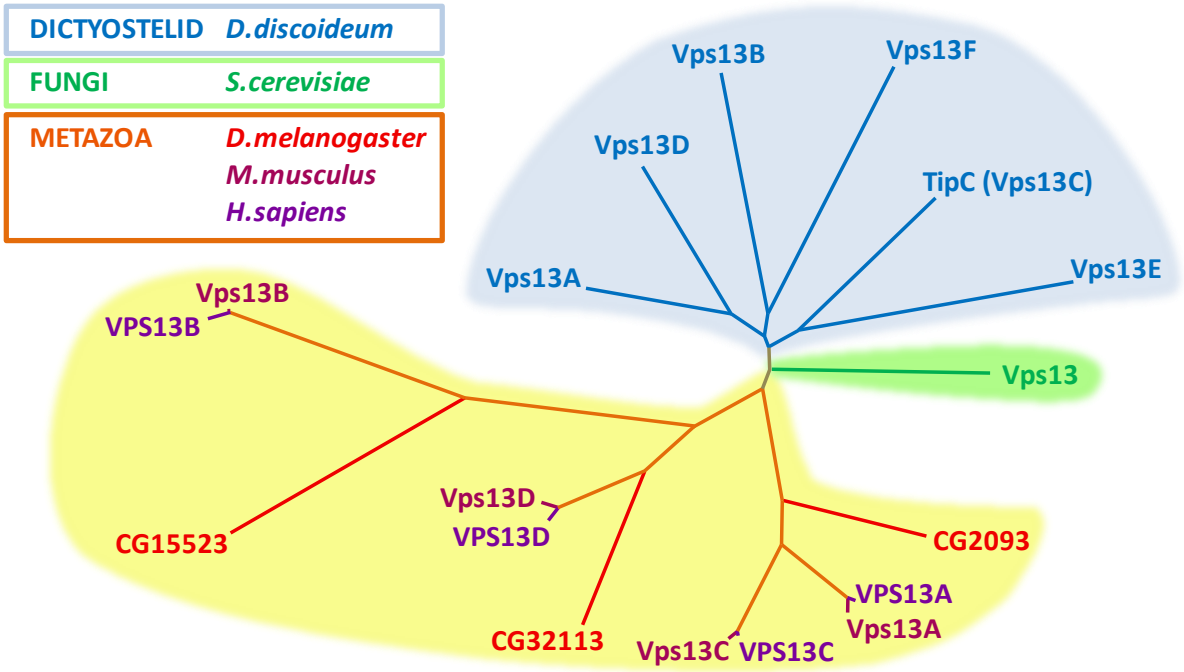

FIG. 1| **Distance-based phylogenetic tree of VPS13 proteins**. Figure modified from Leiba *et al.*,[160] in which an alignment of VPS13 protein sequences was performed excluding hyper variable regions and gaps.

and degraded,[310] although the possibility that they have some regulatory role cannot be fully neglected.[275] A detailed description of the transcripts can be found in an excellent review.[311]

Due to the large size of the gene, specific detection of the proteins derived from different transcripts is technically impractical due to the small variations. For instance, the molecular weights of human VPS13A range from 360 to 348 kDa. In order to assess the relative importance of each transcript, studies at the mRNA level have been performed. Two transcripts are mainly detected for each of the four human genes in a wide variety of tissues.[243,267,275,307,311] There are specific transcripts of *VPS13B*, *VPS13C* and *VPS13D* that are predominantly or exclusively expressed in the brain.[275,311] However, although brain-specific transcripts of *VPS13A* and *VPS13C* have been detected in the mouse brain,[192] no such specific transcripts have been detected in humans.[311] This is particularly interesting due to the association of *VPS13* genes with neurodegenerative diseases affecting distinct brain regions. However, mRNA levels showed similar expression of *VPS13A* and *VPS13B* regardless the brain region.[194,243] Accordingly, levels of human and mouse VPS13A proteins were similar in all the regions of the brain.[14,152] The brain, the blood, and specially the testes presented higher levels of VPS13A,[14,152] suggesting a special importance of this protein in those organs. Indeed, VPS13A absence causes a human neurodegenerative disease with abnormal red blood cells. No defect in spermatogenesis has been reported in humans but infertility has been observed in mice lacking VPS13A.[152]

1.1.3 | Implications of the VPS13 family for human health

The relevance of VPS13 proteins for human health is demonstrated by their association with different diseases. Two independent studies identified mutations in the *VPS13A* gene as the cause of a rare neurodegenerative disease known as chorea-acanthocytosis (ChAc).[243,307] This disorder is described in much more detail below as this thesis has been mainly focused on the function of VPS13A.

VPS13B mutations are at the cause of Cohen syndrome (CS), another rare neurodegenerative disease.[147] If interested in CS, good reviews of the condition and reported cases can be found elsewhere.[66,141,295]

VPS13C has been identified as a gene influencing the risk of suffering late onset Alzheimer's disease,[180] and also considered a Parkinson's disease (PD) susceptibility gene.[209] This later relationship has been questioned in different populations,[48,327,336] but affirmed in additional studies;[81,259] the discordance being likely due to methodological or environmental variations. Moreover, VPS13C mutations have been identified in an autosomal-recessive, early-onset, severe form of PD.[161]

In addition, genomic data have identified VPS13 variants in several cancers. For example, mutations in *VPS13A*, *VPS13B* and *VPS13C* and loss of *VPS13A* expression have been detected in gastric and colorectal cancers.[8] Similarly, reduced expression of *VPS13A* and *VPS13C* has been reported in primary osteosarcoma and refractory diffuse large B-cell lymphoma, respectively.[226,337] On the contrary, enhanced expression of *VPS13A* has been observed in gastric cancer stem cells.[196] *VPS13C* mutations have also been found in pancreatic tumors.[85]

Moreover, variants of *VPS13C* have been associated with altered glucose homeostasis,[94,330] although discrepancies exist,[334] perhaps due to technical or population aspects. It is debated if the cause of this association could be an altered insulin processing and secretion.[267,291,330]

A *VPS13D* variant has been associated to septic shock mortality, related to enhanced interleukin-6 production; but no other human condition has been described for this protein.[206]

A focus on chorea-acanthocytosis (ChAc)

As already mentioned, ChAc is caused by mutations in the *VPS13A* gene.[243,307] The mode of inheritance is autosomal recessive, although a non detected mutation in a family with ChAc led to confusion during years.[15,53,260,301] ChAc patients are either compound heterozygous or homozygous for one of the more than a hundred different mutations identified in the *VPS13A* gene.[64,301] The vast majority of mutations lead to truncated proteins that are probably degraded, as suggested by the pronounced or total absence of the protein in ChAc patients'

samples.[65] Therefore, absence of VPS13A is accepted in clinical practice as a valid sign to support a diagnosis of ChAc. This facilitates the molecular diagnosis because genetic analysis is challenging, as pathogenic mutations are distributed all over the gene, which spans 250 kb. Modern genomics will ease genetic testing for a precise diagnosis but western-blot is the most common diagnosis procedure to date (information is available at http://www.euro-hd.net/html/na/network/docs/chorein-wb-info.pdf). A very small percentage of the total reported mutations correspond to missense mutations or insertions/deletions not changing the frameshift. Even in those cases, the level of VPS13A protein is greatly reduced or absent.[65,301]

There is no apparent genotype-phenotype correlation in ChAc. Common signs of the disease are present despite the large number of different reported mutations and, at the same time, clinical heterogeneity is shown even among patients harboring the same mutation.[31,301]

Only 1 to 5 ChAc cases per million people are estimated.[133] However, the disease is likely underdiagnosed because, although distributed worldwide, many cases are recognized by a reduced number of clinicians. It is classified as a neuroacanthocytosis (NA) syndrome based on its two main features: the progressive neurological disorder and the presence of acanthocytes (misshapen red blood cells). Other NA syndromes are McLeod Syndrome, Huntington's Disease Like 2, and Pantothenate Kinase-Associated Neurodegeneration, each one caused by mutations in different genes.[319] Their clinical similarities make very difficult the differential diagnosis, only definitive after molecular confirmation. In addition, ChAc symptoms are diverse, especially at the onset of the disease,[166] about the second or third decade of life.[133] Given the heterogeneity of clinical manifestations, many molecular diagnosed cases and reviews of the disease are published to aid clinicians on the diagnosis.[68,93,106,107,233,320]

Acanthocytes are one of the features that characterize ChAc. They are red blood cells (RBCs) with irregular projections of the cytoplasm leading to a thorny morphology. Apart from the mentioned core NA syndromes, acanthocytes appear in other pathological conditions such as abetalipoproteinemia,[5] and anemia in liver cirrhosis.[237] Acanthocytes are more frequent in ChAc than in other NA syndromes. However, in some cases no acanthocytes have been observed,[23] and in others, the appearance of acanthocytes occurs in a late stage of the disease.[288] Therefore, the lack of acanthocytes cannot exclude ChAc as the underlying cause of neurological symptoms.

Another useful laboratory indicator for the diagnosis of the disease is the increased serum creatine kinase (CK) levels generally detected in ChAc patients,[107,133,242] even prior to neurological symptoms.[166] CK increase could be related to the muscular weakness and

atrophy observed in some ChAc cases;[54] however, it is detected regardless of the presence of other muscular signs.[261] In the line of muscle alterations, swollen mitochondria, many lipid droplets, lipofuscin granules and potential protein aggregates have been visualized at the ultrastructural level in ChAc patients' skeletal muscle.[181] On the contrary, protein aggregates have not been detected by diverse antibodies in other studies.[319]

There is no dispute regarding other clinical signs of ChAc such as progressive dyskinesia and dystonia, specially of trunk, legs and the orofacial region, respectively leading to gait difficulties and a "rubber man" appearance and feeding problems and dysarthria.[17,233,274] Biting of tongue, lip, cheek and fingers is probably the most distinctive sign of ChAc and serves to distinguish it from other resembling diseases.[54,93,321] Common psychiatric manifestations include personality changes, depression, anxiety, and obsessive-compulsive behaviour.[265,323] Cognitive dysfunction, manifested by attention problems and deteriorating memory, but only slight intellectual impairment, have also been observed.[55] Temporal lobe epilepsy and seizures are frequent,[16,242] and can appear as a first sign of the disease.[4,27,269,299] Parkinsonism has also been reported as presenting sign,[51] but it is usually developed at later stages.[205]

Many neurological signs are presumably consequence of the basal ganglia atrophy and degeneration observed by neuroimaging,[104,119,322] and by post-mortem analyses.[102,186] The most affected region is the striatum, particularly the head of the caudate nucleus,[104] although a reduction in the putamen volume has also been observed.[322] In those regions, glucose metabolism and dopaminergic neurotransmission can be reduced.[199,205] Reported cases presenting other marked neuropathological signs, such as iron deposition, are limited.[136,156]

To date, therapeutic approaches are based on a few empirical published observations and merely aim to mitigate the symptoms.[318] Regarding control of involuntary movements, the most used drugs are tetrabenazine, amantadine, valproate and levetiracetam.[106,133,318] Deep brain stimulation is applied only on selected cases, specially on those resistant to drugs, as controversy exits about some parameters (such as frequency or brain area) giving the best outcome,[38,77,158,190] and even about its effectiveness.[329] Botulinum toxin injections at located regions can also improve dystonia.[318] Neuropsychiatric symptoms are usually addressed with citalopram or quetiapine.[265,318,319] Speech and occupational therapies are helpful to deal with other issues like dysphagia, dysarthria, gait difficulties and general daily activities.[318]

In view of the lack of effective curative treatments, any finding about the molecular role of VPS13A could have enormous implications to set the basis of future potential therapies.

1.1.4 | VPS13 proteins structure and functional domains

One of the first approaches to infer the possible functions of a protein is to identify, within its amino acid sequence, the presence of conserved functional domains. Unfortunately, the conserved domains or structural features identified in the VPS13 protein family do not allow a confident prediction of its molecular function.

The amino- and carboxyl-terminal ends of VPS13 proteins probably constitute functional domains because, although some homology can be detected by sequence alignment throughout the entire length of the large VPS13 sequences, the similarity is much stronger at the N and C termini, where even the most divergent proteins of the family show high homology. An alignment of several VPS13 proteins is shown in the results section in figure 10. The same figure shows the putative domains, of unknown function, that can be detected by bioinformatics (NCBI conserved domain search using cdd.v.3.15 database, composition based adjustment, no low complexity filter, and an E-value threshold of 0.01) in almost all VPS13 proteins in the conserved regions: an N-terminal domain called Chorein_N, a domain called DUF1162 (currently SHR-BD), usually two MRS6 domains, and an ATG_C autophagy related C-terminal domain. At the present date, other VPS13 domains are identified (a VPS13 domain, a VPS13_mid_rpt domain and a VPS13_C domain) that indicate the conservation of other regions of the sequence but do not give any additional clue about the function of these proteins.

Interestingly, both the Chorein_N and the ATG_C domains are also identified in the human autophagic proteins ATG2A and ATG2B. ATG2 proteins participate in autophagy and in lipid droplet (LD) regulation.[312] Regarding a possible connection with LD related functions, putative ALPS (amphipathic lipid packing sensor) like motifs have been identified in yeast Vps13 and human VPS13A and VPS13B,[67] and yeast Vps13 was shown to localize at LDs in the absence of two proteins that stabilize contacts between the endoplasmic reticulum (ER) and LDs.[96]

PH (pleckstrin homology) domains, which are involved in the binding to phosphatidylinositol phosphoderivatives (PIPs) and the recruitment of proteins to specific locations, are identified in the middle of *T. thermophila* Vps13A sequence by conventional conserved domain search and a PH-like domain has been recently reported in the C terminus (but not in the most conserved region) of *S. cerevisiae* Vps13 by a more sophisticated bioinformatic search.[78] The lack of this domain hampered *S. cerevisiae* Vps13 localization to a particular membrane contact site (MCS; defined as the apposition of two membranes from different organelles) of the vacuole with the nucleus (nuclear vacuolar junction, NVJ) in early stationary phase.[78]

In accordance to that predicted interaction with PIPs, it has been very recently reported the binding of purified *S. cerevisiae* Vps13 full length protein and N and C termini to some lipids, primarily phosphatidic acid (PA) and mono-/diphosphorylated PIPs such as PI4P and $PI(4,5)P_2$ and, to a lesser extent, PI3P and other lipids.[58] In addition, the SHR_BD domain has been shown to mediate PIP binding together with a newly identified APT1 domain in the C-terminal region of VPS13 proteins (and also present in ATG2), which determines specific binding of yeast VPS13 to PI3P.[258] This binding is important for protein localization of C-terminus tagged Vps13 at small dots.[258] A particular missense mutation in the APT1 domain of yeast Vps13, equivalent to a ChAc causing mutation, diminished this interaction and hampered the recovery of some of the phenotypes of the null mutant.[258]

Supporting the importance of precise amino acids along the Vps13 sequence, other missense mutations (some of them also described as ChAc mutations) have been shown to favor or avoid yeast Vps13 localization to other MCS, those between the vacuole and the mitochondria (called vacuole and mitochondria patches, vCLAMPs) and alter Vps13 protein functions.[154,228] Vps13 localization and functionality can also be modified by the tagging of the protein at the N or C terminus.[154,228] The relevance of the C terminus of VPS13A was already suggested by the identification of disease causing mutations in the last exons of the *VPS13A* gene.[64,65]

Bioinformatic softwares differ in their prediction of transmembrane helices but experimental biochemical work has demonstrated a peripheral membrane association for VPS13 proteins. Yeast Vps13 was proposed to be part of a membrane-associated sedimentable complex, principally associated with Golgi membranes and traffic and secretory vesicles.[35] Peripheral association to membranes and cofractionation with proteins of endocytic vesicles has been demonstrated for a *D. melanogaster* homologue of VPS13A.[317] Human VPS13 proteins also interact with membranes as peripheral proteins.[310]

Regarding interaction with membranes, FFAT-like (two phenylalanines, FF, in an acidic tract) domains have been recognized in human VPS13A and VPS13C and other homologues in mice and *D. discoideum*.[187] FFAT domains are present in several lipid transfer proteins and they mediate the interaction with VAPs (vesicle-associated membrane protein-associated proteins), which are involved in the establishment of MCS between the ER and other organelles.[187]

According to electron microscopy visualization of negatively stained *S. cerevisiae* Vps13, it has a particular rod shape of about 20 nm long, similar to a hook at one end and with a loop at the other; both ends facing the same or opposite sides of the protein depending on its rotation.[58]

1.1.5 | Reported functions of VPS13 proteins

The molecular knowledge of VPS13 proteins was scarce at the time of starting this thesis and most of the information presented here has been only very recently published. In spite of the growing number of reports that involve VPS13 proteins in apparently disparate cellular processes, a global picture that explains their molecular function and the etiology of their associated diseases is still lacking.

S. cerevisiae

The first studies of VPS13 functions come from *S. cerevisiae*¸ in which only one VPS13 protein is present and thus potential functional redundancy with other members of the family is not possible, simplifying the analysis.

The *vps13Δ* mutant was identified as one of several mutants with altered vacuolar protein targeting (*vpt*) of carboxypeptidase Y to the vacuole (the equivalent of lysosomes in yeast) and called *vpt2*.[21] *vpt* mutants were later termed *vps*,[249,254] in order to include and organize within that nomenclature the *vpt*,[21,22,249] and the vacuolar protein localization (*vpl*) mutants;[255] which showed genetic overlap.[249,254] The *vps13* mutant has a normal vacuole morphology,[22,245] normal V-ATPase labeling of the vacuole membrane, and quinacrine acid-dependent staining; suggesting no gross defects in vacuole structure and acidification.[245] The same phenotype was observed in a loss of function mutant of *vps13* that was able to suppress loss of mating competence; and thus named *soi1* (suppressor of the rapid onset of impotence) in that work,[246] but *vps13* will be used here to avoid confusion. Yeast mutants in *vps13* displayed abnormalities in the trafficking of proteins between the *trans*-Golgi network (TGN) and the prevacuolar compartment (PVC), equivalent of late endosomes, and it was proposed that Vps13 participates in the cycling of proteins between these compartments through the regulation of TGN localization signals.[35,246] Further evidence supporting the role of Vps13 in targeting proteins to the vacuole was that the abnormal delivery of a mutated form of the plasma membrane protein Pma1 to the vacuole was suppressed in a *vps13* mutant.[168] In addition, FM4-64 (a lipophilic marker of bulk plasma membrane endocytosis) was normally internalized in that *vps13* mutant but it was more slowly delivered to the vacuole membrane, as suggested by its partial accumulation in a sort of small PVC.[168] Moreover, increased secretion of a chimeric protein that had to be delivered to the vacuole was shown in a *vps13* mutant.[342] Lastly, TGN homotypic fusion and TGN to PVC transport have been shown to require Vps13 interaction with Cdc31, a calmodulin-like calcium binding protein.[58]

A sporulation defect has been observed in *vps13* mutants,[35,74] which showed fewer and smaller prospore membranes (PSMs) unable to engulf the haploid nuclei.[207] During

sporulation, Vps13 localizes at the PSM by the recruitment of Spo71,[230] and it is required for proper PSM elongation and closure.[227] Spo71 and Spo73 could function in the regulation of Vps13 during PSM formation.[218,231] Vps13 is required for the accumulation at the PSM of PI4P and PI(4,5)P_2, which in turn activate Spo14, required for PA production and Spo20 recruitment, which is necessary for the fusion of PSM.[227] In addition, a membrane bending or scission activity has been proposed to be regulated by Vps13 since the majority of *vps13Δ* PSMs presented a sort of intralumenal vesicles not related to PA levels nor to the ESCRT (endosomal sorting complex required for transport) complex.[227]

The already mentioned interaction of Vps13 with PIPs could partly explain Vps13 membrane association.[58] A reciprocal regulation has been proposed by which the binding of Vps13 to PIPs might somehow influence their levels at membranes.[58] The mechanism of this interplay is yet unknown as no interaction with kinases or phosphatases involved in PIP metabolism have been detected.[230] Probably as a consequence of the Vps13 relationship with PIPs, an Opi1$^-$ (overproduction and excretion of inositol) phenotype was observed in the *vps13Δ* mutant.[101]

Vps13 subcellular localization is dynamic, adding complexity to the study of its functions. In non-sporulating cells, previous studies localized Vps13 at endosomes.[116] Recently, it has been described that Vps13 localizes at vCLAMPs and NVJ, two MCS connecting the vacuole with, respectively, the mitochondria or the nucleus.[154,228] In cells growing on a fermentable carbon source, Vps13 localizes vCLAMPs. This localization of Vps13 is essential to compensate the absence of another MCS, that of mitochondria with the ER, called ERMES (ER-mitochondria encounter structure);[154,228] suggesting that Vps13 at vCLAMPs participates in the trafficking of lipids, ions or other metabolites from and to mitochondria, which are the functions attributed to ERMES. Mitochondrial homeostasis is altered in *vps13Δ* mutants, in which mitochondrial integrity was defective and mitophagy (a selective form of autophagy to degrade mitochondria) was increased.[228] Vps13 changes the localization to NVJ when cells are grown on a non-fermentable carbon source.[154,228]

T. thermophila

The study of VPS13 proteins in the protozoan *T. thermophila* indicates a role in phagocytosis, a process not present in yeast cells. One, or possibly two, VPS13 homologues were identified as components of phagosomes in a mass spectrometry analysis.[122] Accordingly, one of them, TtVps13A, was GFP-tagged at the C terminus by homologous recombination and observed at the membrane of phagosomes.[264] Although the mechanism of association was not elucidated, the protein was proposed to be directly recruited to phagosomes because small fluorescent vesicles that could indicate vesicular delivery of TtVps13A-GFP were not detected.[264] The

deletion of *TtVps13A* resulted in reduced phagosome formation and delayed phagocytic digestion of decorated fluorescent *Bacillus subtilis* spores. Consistently, the growth dependent on *Klebsiella pneumoniae* phagocytosis, but not that on rich-medium, was reduced.[264]

D. melanogaster

In *D. melanogaster,* the knockdown of the VPS13A/C counterpart in S2 cells (CG2093) resulted in reduced endocytosis.[148] Although this role was not further explored, it is in agreement with the very recent demonstration of the protein cofractionation with the endosomal proteins Rab5 and Rab7 and its immunoisolation with Rab7-containing membrane fractions.[317] An homozygous mutant in which this homologue is truncated has been generated and shown to have impaired brain proteostasis and neurodegeneration.[317] In that line, the absence of the VPS13A/C homologue in the retina of *D. melanogaster* has been found to increase α-synuclein-mediated neurodegeneration.[126]

Mammals (mice and humans)

VPS13A

A mouse model for ChAc was generated by deletion of a part of the VPS13A gene. It showed similarities with the human disease at old ages including the appearance of acanthocytes, the striatum degeneration, and behavior and motor function disturbances (but not involuntary movements). These mice had an hybrid genetic background which lead to heterogeneous phenotypes.[300] Inbred ChAc mice have been originated later which confirm differences in ChAc phenotypes depending on the mouse background.[263] At the molecular level, increased striatal expression of a gamma amino butyric acid ($GABA_A$) receptor subunit and gephyrin (a $GABA_A$ receptor anchoring protein) was detected in the ChAc mice,[151] but no differences in GABA or monoamines levels were found in different brain regions apart from homovalinic acid, a dopamine metabolite, which showed reduced concentration in the midbrain.[300] Endogenous mouse VPS13A in the brain fractionates with microsomes and synaptosomes[152] and was observed with a reticular pattern at perinuclear regions in striatum neurons.[152] It was visualized as granular in spermatocytes, and more cytoplasmic in other cell types.[152]

Some clue about the function of VPS13A can be gleaned from knowing the alterations leading to the aberrant acanthocytic shape of erythrocytes. Abnormal lipid composition is the cause of acanthocyte appearance in other pathologies. However, this may not be the case in ChAc as reports analyzing lipids are contradictory.[102,219,221,262,315] Therefore, abnormalities on the proteins associated to the membrane might be the cause of the acanthocyte phenotype.

Changes in band 3 (the major protein at the membrane of RBCs) stability and functionality have been found, but they were not always consistent.[13,33,137] Band 3 is a substrate of the cross-linking enzyme tissue transglutaminase (tTGase) and more tTGase products were observed in erythrocytes and muscles from ChAc patients,[181] which indicated that anchoring abnormalities could be related to the erythrocyte and muscular alterations of the disease. Increased tyrosine phosphorylation of many proteins was found in ChAc RBCs.[34,82,219] Those include band 3, β-spectrin and β-adducin, which are part of the complexes that anchor the plasma membrane with the cytoskeleton. Band 3 phosphorylation was found to be dependent on Lyn, a non-receptor tyrosine kinase present at higher levels in an active form in ChAc RBCs.[82,169] Phosphorylation diminishes the interaction of the anchoring proteins with the cytoskeleton, which could cause the aberrant morphology of erythrocytes.[82]

Not only anchoring but cytoskeleton organization is altered in the absence of VPS13A. First, electron microscopy visualization of ChAc acanthocytes membranes have shown an irregular distribution of the cytoskeleton.[298] Second, decreased actin polymerization has been observed in *VPS13A* siRNA treated cells,[6,80] and in RBCs,[79] fibroblasts,[112] platelets,[272] and medium spiny neurons derived from fibroblasts of ChAc patients.[289] And last, disarrangement and diminished staining of microtubules and intermediate filaments have been reported in ChAc fibroblasts.[112]

A form of endocytosis known as drug-induced endovesiculation has been shown to be strongly reduced in ChAc RBCs.[216,286] This might be a consequence of the cytoskeleton and anchorage alterations and/or of Lyn activation, as Lyn has been associated with vesicles.[82] In addition, abnormal higher concentrations of members of the small G-protein family, which participate in vesicle generation and trafficking, were found in ChAc RBCs membranes,[82] supporting the alteration of these processes in ChAc RBCs.

The presence of acanthocytes might also be related to a PIP dysregulation as $PI(4,5)P_2$ has been shown to influence binding of band 4.1 to membranes,[9] and actin polymerization.[155] In mammalian cells, a PIPs connection with VPS13 proteins has been indicated by the reduced PI4P at the plasma membrane that was observed in a population of VPS13A-depleted PC12 cells.[229] However, other PIPs at the plasma membrane seemed unaltered.[229]

Other phenotypes observed upon *VPS13A* knockdown are reduced platelet secretion, that could be related to a diminished amount of VAMP8 (a SNARE protein involved in fusion processes);[111,272] an altered Ca^{2+} entry dependent on Orai1 (a subunit of a Ca^{2+} channel), whose levels are also reduced upon VPS13A depletion;[340] and an increased apoptosis.[113] However, the mechanisms by which VPS13A absence lead to these and the above described

phenotypes, and their relative importance regarding the appearance of ChAc have not been clearly elucidated yet.

VPS13B

VPS13B was proposed to have a role in the maintenance of Golgi apparatus as its structure was disrupted in VPS13B-depleted HeLa cells and in fibroblasts of patients with CS.[277] VPS13B peripheral association with membranes was demonstrated and its partial localization at the *cis*-Golgi was visualized and found to be dependent on the C terminus of the protein,[277] and on the interaction of VPS13B with active RAB6.[276]

In addition, alterations of endolysosomal components have been observed in VPS13B deficient cells. In particular, less EEA1-positive early endosomes, glycosylation defects of LAMP2, and larger LAMP2-positive lysosomes.[69] These phenotypes may be related to the Golgi apparatus as its fragmentation has been associated to reduced EEA1 and glycosylation of proteins occurs at the Golgi.[63] Alternatively, VPS13B could participate more directly in the endolysosomal pathways and the authors speculate about a role in fission processess.[69]

VPS13C

VPS13C has been detected in phagosomes of mice cells.[250,285,304] VPS13C is probably involved in endocytic traffic too as its silencing in a high-throughput screen was found to decrease FcRn receptor-mediated transcytosis of IgG.[210] In addition, VPS13C was described in HEK293T cells to interact with RAB7, a protein of late endosomes, and specially with the constitutive active form of RAB7 and with two mutated RAB7 variants causing a disease called Charcot-Marie-Tooth type 2B, characterized by axonal degeneration of peripheral nerves.[179]

Other reports associated VPS13C to maintenance of mitochondria. Although the majority of VPS13C was present in low-density fractions by subcellular fractionation of HEK293T cells, some VPS13C cofractionated with the Golgi apparatus, ER and mitochondrial proteins. In addition, an outer mitochondrial membrane (OMM) localization was reported for VPS13C, which was found to be reduced upon addition of the protonophore CCCP (carbonyl cyanide *m*-chlorophenyl hydrazine).[161] CCCP induces degradation of mitochondria by mitophagy and PINK1 and Parkin, which are involved in this process, showed enhanced accumulation in mitochondria when VPS13C was absent; for which reason, a role of VPS13C as a negative regulator of PINK1 was suggested.[161] In addition, VPS13C absence in COS-7 cells led to fragmentation and clustering of mitochondria, changes in their morphology, decreased mitochondrial transmembrane potential and to an increase in maximal respiration and reserve capacity.[161] In BE(2)-M17 neuroblastoma cells, axial length ratio of mitochondria was reduced in the absence of VPS13C.[126]

In another research work, overexpression of C-terminal tagged VPS13C in HeLa cells did not show colocalization with mitochondria or the ER. Instead, colocalization with LAMP1 and Galectin-12, markers of lysosomes and lipid droplets (LD), respectively, was observed.[335] Endogenous VPS13C was present in LD fractions and was shown to interact with Galectin-12 and to protect it from lysosomal degradation.[335]

VPS13D

A hypothetical role in endosomal sorting has been proposed for VPS13D based on the predicted UBA (ubiquitin associated) domains in the VPS13D sequence and the presence of those domains in many endolysosomal proteins.[311] However, no experimental proof has been reported yet about VPS13D molecular functions.

1.2 | Autophagy

As described in previous sections and by the time that this research work started, VPS13 proteins had been mostly implicated in membrane-dependent processes such as vesicular trafficking in *S. cerevisiae* and maintenance of Golgi integrity in humans, phagocytosis in *T. thermophila* and endocytosis in *D. melanogaster.* Macroautophagy is another process highly dependent on membrane dynamics. However, the potential relationship between VPS13 proteins and autophagy had never been experimentally addressed.

1.2.1 | Types of autophagy

Macroautophagy is a degradative process by which double membrane vesicles nucleate from diverse origins, elongate to engulf cytoplasmic constituents, close, and fuse with lysosomes for the degradation of their content by acid hydrolases. The obtained molecular constituents are then transported back to the cytoplasm and used in the synthesis of new cellular components or for energy production.[185]

The double membrane vesicles are called autophagosomes and are the hallmark of macroautophagy. Other types of autophagy, meaning 'self digestion', have been described. They differ in the way that the cellular content destined for degradation is delivered to the lysosome.[234] In microautophagy, such material is directly captured by invaginations of the lysosomal membrane, which forms vesicles inside the lysosome that are later degraded.[163] In chaperone-mediated autophagy (CMA), proteins containing the KFERQ sequence are recognized and transported by the chaperone HSC70 to the lysosome-associated membrane protein 2A (LAMP2A) and then translocated across the membrane to the lysosome.[11] The general term autophagy will be used throughout this thesis to name macroautophagy because it is the only type of autophagy addressed in this study.

Cell's components can be enwrapped in autophagosomes in a non-selective way and, in that case, the process is called bulk autophagy (or, simply, autophagy). On the contrary, specific content is surrounded by autophagosomes in selective autophagy.[293] Depending on whether such content are particular organelles, protein aggregates or intracellular pathogens, the process is called reticulophagy,[46] ribophagy,[46] mitophagy,[61] pexophagy,[173] lysophagy,[117] nucleophagy,[208] lipophagy,[325] aggrephagy,[332] or xenophagy.[145]

1.2.2 | The autophagic machinery

Autophagosomes were first described in the 60's by electron microscopy studies. However, it was not until the 90's that the knowledge about the molecular machinery involved in their formation started. If interested in the progression of discoveries on the field, the reader is guided to a very detailed historical review.[217]

ATG proteins

The pioneering studies of Ohsumi (for which he has been recently awarded the Nobel Prize) in *S. cerevisiae* lead to the identification of many *ATG* (autophagy related) genes,[305] required for autophagosome formation and thus considered the core autophagy machinery. Since then, an increasing vast number of studies on this machinery have been reported and comprehensively reviewed countless times.[28,76,193,215,232,281] A simplified description of the role of ATG proteins (yellow-colored in FIG. 2), organized in functional complexes, is provided in the following lines.

The induction of autophagosome formation is controlled by two kinase complexes. The Atg1-complex, constituted in mammals by the serine-threonine kinase ULK1 (unc-51 like autophagy activated kinase 1) — homologue of yeast Atg1— and other proteins, whose phosphorylation regulates the initiation of autophagosome formation.

The other complex contains the class III phosphatidylinositol 3-kinase (PI3K) VPS34 that is essential for the synthesis of PI3P, a signaling lipid that favors the recruitment of ATG proteins to the isolation membrane. Besides VPS34, Beclin1 and VPS15 are constant members of the complex. In addition, the complex has ATG14 or UVRAG (UV radiation resistance associated gene) depending on the pathway where it is functioning: autophagy or endocytosis, respectively. During autophagosome formation, WIPI (WD repeat domain phosphoinositide interacting) proteins — homologues of yeast Atg18 — and ATG2 interact with the produced PI3P.

In mammalian cells, the autophagosome emerge from specialized regions of the ER, the omegasomes, which are often in close proximity with other organelles such as mitochondria, endosomes and lipid droplets.[30] These ER microdomains contain the transmembrane protein

VMP1 (vacuolar membrane protein 1) that regulates the omegasome and MCS between the ER and other organelles.[296] Then, membranes of multiple origins, contribute to the enlargement of the isolation membrane (which originally was called phagophore).[30,153,175] ATG9, a multimembrane-spanning protein, marks specific vesicles that also supply membranes for the growing autophagosome.

The process of elongation and closure of the autophagosome membrane depends on two ubiquitin-like conjugations. In the first one, ATG12 is covalently bound to ATG5 with the aid of ATG7 and ATG10. Subsequently, ATG16 joins the ATG12—ATG5 proteins forming a complex that localizes at the autophagosome membrane and regulates the second conjugation reaction. That reaction attaches LC3 (microtubule-associated protein 1 light chain 3), homologue of yeast Atg8, to phosphatidylethanolamine (PE). LC3 must first be processed by the ATG4 protease, which cleaves proLC3 soon after its translation producing cytosolic LC3-I. Conjugation of LC3 to PE forms the so-called LC3-II, that remains attached to the inner and outer membranes of autophagosomes and hence it is widely used as an autophagosome marker. Upon fusion with the lysosome, the inner-membrane bound LC3-II is degraded into the autophagolysosome whereas the outer-membrane LC3-II is cleaved again by ATG4 and recycled back to the cytoplasm.

As already mentioned, the presented hierarchy of ATG proteins is a simplified description of the autophagic process, but the picture is far more complicated. An increasing number of studies reveal that many ATGs are involved in the regulation of other ATGs at different steps of the process, thus having a role at more than one stage during autophagosome formation and with complex feedback regulations, such as those described for proteins of the ULK1 complex.[86,149,225] Another example is ATG14, which functions at the fusion step besides its role in autophagosome biogenesis.[60] Moreover, noncanonical pathways have been described where not all the ATG proteins are needed for autophagosome formation.[70,150,282] In addition, some ATG proteins have extra roles in different cellular processes,[29,150,177,268] as well as other non-ATG proteins — considered or known to belong to other pathways — have a role in autophagy.[153]

Non-ATG proteins and intersection of autophagy with other pathways

As our understanding of the cell biology increases, an important interplay of autophagy with many cellular processes has been described. Some of them are involved in maintaining cell's homeostasis (unfolded protein response, ubiquitin-proteasome system and CMA)[278,50,331] and survival (apoptosis and necrosis)[198,213]. A particular close connection is the one between autophagy and endocytosis as, besides direct fusion with lysosomes, autophagosomes can fuse with endosomes to form amphisomes that will later fuse with lysosomes (FIG. 2).[302]

Endocytosis is the process of internalization of extracellular material mediated by vesicles derived from the plasma membrane. These vesicles are trafficked through the cell and undergo fission and fusion events to sort the internalized cargo. Part of the cargo, such as some plasma membrane receptors, can be recycled back to the cell surface soon after their internalization. The rest of the cargo is trafficked through the cell in early endosomes (EE) that mature into late endosomes (LE). Intraluminal vesicles (ILV) are formed during this process and thus LE are also called multivesicular bodies (MVB). The fusion of LE with acid lysosomes results in fully mature endolysosomes, where the cargo of endosomes is degraded. Alternatively, endocytosed proteins can be trafficked from EE and LE to the TGN or to the plasma membrane through recycling endosomes (RE). The transport from endosomes to the TGN is necessary for the recycling of acid-hydrolase receptors, which participate in the delivery of acid-hydrolases from the TGN to endosomes and lysosomes.[118] Therefore, a continuous bidirectional vesicle trafficking occurs between endosomes and the TGN (FIG. 2).

The interaction of endocytosis and autophagy is not limited to the described fusion of autophagosomes with endosomes. Endocytosis and their players influence autophagy progression at additional steps of the process: they can modulate initiation signaling, provide membranes for expansion of autophagosomes, regulate PI3P production or guide the movement of autophagosomes.[302] Indeed, among the non-ATG proteins having an impact on autophagy,[153] those belonging to the endocytic pathway have an important, non-negligible role. In a reciprocal manner, ATG proteins have a role in endocytosis too.[201]

Key participants in the endocytic traffic but having also an impact in autophagy are RAB (Ras genes from rat brain) GTPases (the non-colored proteins in FIG. 2). They are a group of proteins of the Ras superfamily of small-G proteins. More than 60 RAB proteins have been identified and many are at the surface of endosomes, giving them a particular identity that assures the well-functioning of the endocytic traffic. As far as autophagy is concerned, the most well-known functions are found for RAB1 and RAB11 in autophagosome formation, RAB5 in PI3K regulation and RAB7 in trafficking and fusion processes; but additional roles of these and other RAB proteins have been described regarding autophagy.[10,125,294]

1.2.3 | Relevance of autophagy for human health

Autophagy is induced and essential for the cell survival to a variety of stress situations such as starvation or infection. Equally important is the function of basal autophagy, which is essential to maintain cellular homeostasis by degrading non-functional organelles and protein aggregates. This process is especially important in neurons, since they are long-lived cells no longer undergoing mitosis and therefore unable to dilute their detrimental

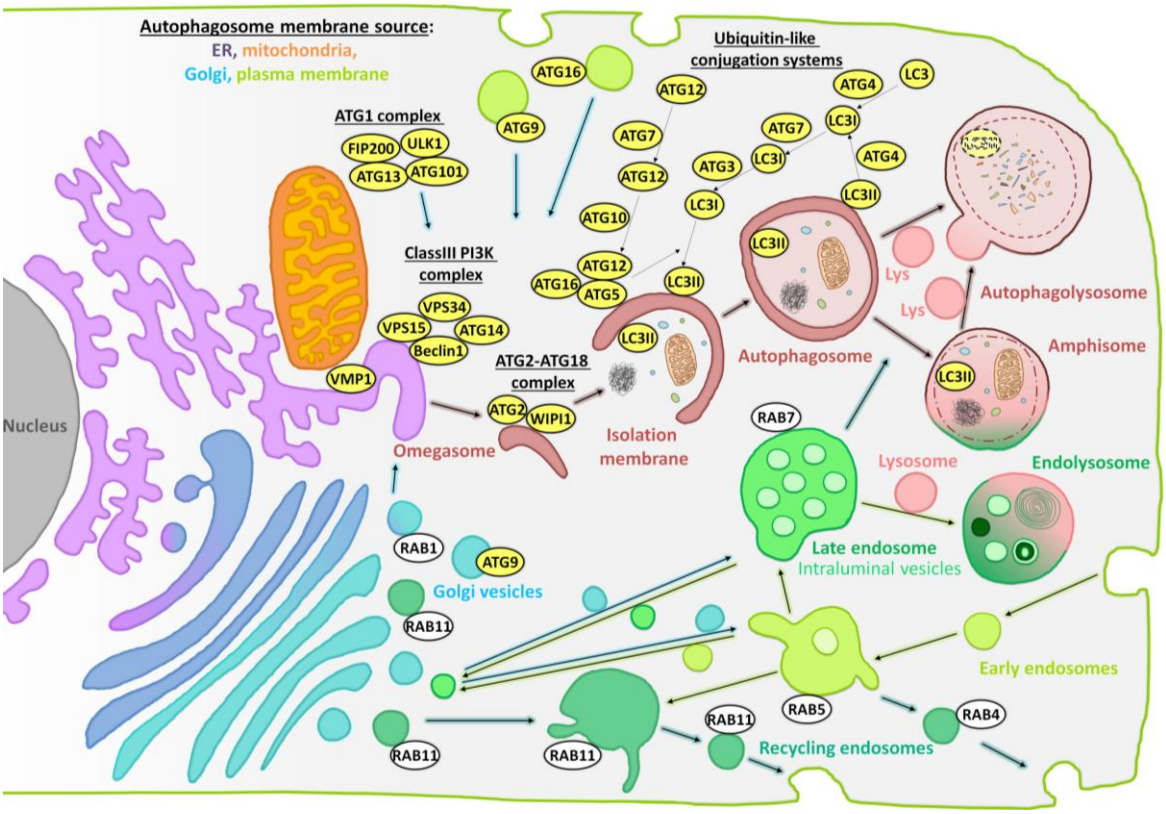

FIG. 2 | Autophagic and endocytic pathways. Autophagosomes usually form in structures at the ER called omegasomes because of its resemblance to the Greek letter. Besides de ER, membranes from many sources contribute to the autophagosome elongation. The proteins of the autophagic machinery (yellow) act in complexes to aid in the formation of autophagosomes. Once formed, they fuse with lysosomes and degrade their cargo and inner membrane. Autophagosomes can also fuse with endosomes, especially late endosomes, which originate from maturation of early endosomes. Autophagy and endocytosis converge at the lysosome. Early and recycling endosomes play a role in autophagy too, particularly described at the formation of autophagosomes. Different RAB proteins (white) are at the membranes of distinct types of endosomes. Continuous vesicular traffic between the TGN, endosomes and lysosomes is also required for targeting specific proteins at different locations.

components by cell division.[214] As autophagy effectiveness seems to be reduced with aging,[247] this process is associated with many aging-related disorders. Autophagy dysregulation and malfunctioning participate in cancer,[72] heart,[284] liver,[211] pulmonary,[191] metabolic,[257] infectious,[280] and neurodegenerative diseases,[140] among other diverse pathologies.[128,273] Therefore, for the development of treatments for these diseases, autophagy has become a powerful target to modulate, either towards its reduction or its enhancement, dependent on the disorder.[256,303]

Autophagy also plays a fundamental role during cell differentiation, when cells' components that are not longer needed are degraded. A clear example is erythropoiesis, in which RBCs' mitochondria and other organelles are removed by autophagy to generate erythrocytes.[314]

1.2.4 | An hypothetic role of VPS13 proteins in autophagy

Taken into account VPS13 functions in membrane traffic-related pathways, which share machinery with autophagy, and the importance of autophagy in the cell types most affected

by the loss of VPS13A (neurons and erythrocytes), it is reasonable to hypothesize that VPS13 proteins have a role in autophagy. An additional clue about a potential participation of VPS13 proteins in autophagy came from a peculiar model organism: *D. discoideum.*

1.3 | *Dictyostelium discoideum*

D. discoideum is a simple eukaryote that belongs to the amoebozoa group, which evolved after the divergence of plants but before that of fungi and metazoa.[252]

1.3.1 | Life cycle of *D. discoideum*

D. discoideum lives in the soil as solitary cells during vegetative growth, when they phagocyte bacteria and proliferate by binary fission and long as feeding is not compromised. However, when bacteria are scarce, the vegetative cells secrete pulses of cAMP that are sensed by other cells and a developmental cycle starts. Thousands of cells are attracted chemotactically to the cAMP and form streams that move towards the same point, where they converge and aggregate into multicellular loose mounds that will become tight structures later. At that point, cells start to differentiate in spore and stalk cells and move to distinct regions of the multicellular structure, which acquires characteristic shapes along the process. First, a structure known as 'finger', and presenting a single tip, is observed. This structure can move somewhere else, and hence called 'migrating slug', before continuing its development. It then collapses in a structure named 'mexican hat' and raises again to eventually culminate in what is called 'fruiting body'. This final structure is composed by a stalk of vacuolated dead cells and a head filled of spores able to germinate into vegetative cells when the conditions are favorable again **(FIG. 3)**.[75]

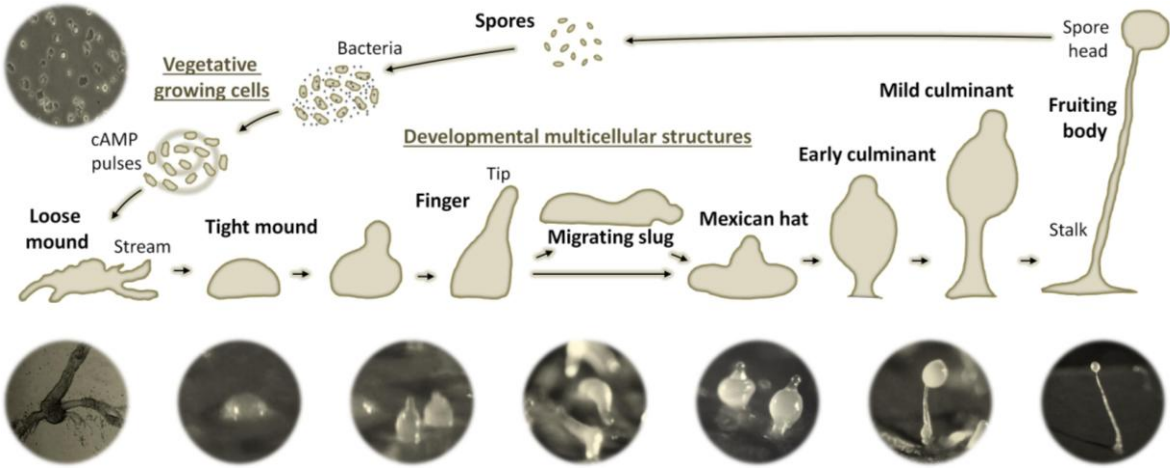

FIG. 3| Life cycle of *D. discoideum*. *D. discoideum* enters a developmental process when the feeding bacteria are absent. cAMP pulses function as a chemotactic signal that allows the cells to aggregate. They form diverse developmental structures and finally culminate in a fruiting body that contains spores to start a new cycle when conditions are favorable for growing.

1.3.2 | General advantages of *D. discoideum* as a simple model

There are many reasons for the convenience of using *D. discoideum* as a model organism in biomedical research. Consequently, it is increasingly being used to study many genes and processes, their related disorders and potential drug treatments. A detailed review has been written and it is annexed to this thesis,[204] but only a brief summary is provided here.

To begin with the advantages of *D. discoideum* as a model organism, *D. discoideum* is easy to grow at the laboratory, especially after the isolation of some strains able to feed by macropinocytosis and hence to grow in liquid medium in the absence of bacteria. It has a short doubling time (about 8-10 hours) so large amounts of cells can be quickly obtained. In addition, the genetic manipulation of *D. discoideum* is easily performed by electroporation, and targeted modification of its haploid (and sequenced)[71] genome by homologous recombination facilitates the generation of desired mutants.

This organism is more similar to human cells than the commonly used yeast model *S. cerevisiae.* For example, the absence of cell walls makes *D. discoideum* more appropriate to study processes dependent on the remodeling and movement of the plasma membrane (phagocytosis, macropinocytosis, pseudopods formation and motility). Moreover, although most components of cellular processes are conserved in many organisms, more similarities exist between humans and *D. discoideum* than between those and *S. cerevisiae*, in which ancestor proteins could have been diverged or even lost during evolution. In this line, some cellular processes, such as autophagy, are more similar in *D. discoideum* than in yeast in comparison to humans.[183]

1.3.3 | *D. discoideum* to study autophagy

From the structural point of view, autophagosomes originate from multiple locations in the cell both in mammals and *D. discoideum*, whereas they have a unique origin in *S. cerevisiae*, called phagohore assembly site (PAS), located near the vacuole (the equivalent of lysosomes in yeast).[138] Moreover, similarities can be found regarding the close interplay of autophagy with the endocytic pathway. Instead of a single vacuole present in yeast,[143] *D. discoideum* cells possess many lysosomes and those are similar to the mammalian ones, despite certain differences. For instance, lysosomes are more acidic in *D. discoideum* (pH<3.5)[174] than in human cells such as HeLa cells (pH≃4.7).[212] Endosome maturation and lysosome fate are also somehow different. In *D. discoideum,* lysosomes mature into postlysosomes that are secreted,[164,171] whereas in mammals, lysosomes are reformed (although they can also be secreted in specialized cell types).[49,95]

From the molecular point of view, the autophagic machinery shares also more similarities between mammals and *D. discoideum*. Some proteins that participate in the process are present in the amoeba while they are absent in yeast.[183] One of those proteins is VMP1 a protein participating in many cellular processes besides autophagy.[40,42,43,296]

Like in other organisms, autophagy in *D. discoideum* is crucial for the homeostasis and survival of cells, and also for development.[162] As already explained, *D. discoideum* development occurs when food is no longer available. Yet, this process requires the synthesis of new proteins with essential roles during the differentiation and patterning of the cells that will constitute the culminant fruiting bodies. Therefore, the energy and molecular constituents needed for protein synthesis in starving conditions must be obtained from within cells, by the autophagic degradation and recycling of cells own material. It is hence easy to understand that an impairment of autophagy has a negative impact in the developmental process. Indeed, *D. discoideum* autophagy mutants do not culminate in normal fruiting bodies but instead show aberrant developmental phenotypes, whose severity depends on the disrupted gene. Some mutants form aberrant mounds with multiple tips such as *atg101*$^{-}$,[184] *atg6*$^{-}$,[222] *atg5*$^{-}$,[223] *atg7*$^{-}$,[223] *atg8*$^{-}$,[222] or *atg9*$^{-}$;[306] and others, like *atg1*$^{-}$,[222] *atg13*$^{-}$[184] or *vmp1*$^{-}$,[40] are even unable to aggregate.

Many developmental mutants have been isolated in *D. discoideum* affecting different developmental stages. Four of them were named *tip*$^{-}$ mutants (*tipA*$^{-}$, *tipB*$^{-}$, *tipC*$^{-}$ and *tipD*$^{-}$) since they formed aberrant mounds with multiple tips.[290] TipC is highly homologue to VPS13 proteins and, because of its autophagic-mutant resembling phenotype, we considered that assessment of autophagy in the *tipC*$^{-}$ mutant was a good starting point to evaluate the role of VPS13 proteins in autophagy.

2 | OBJECTIVES

2 | OBJECTIVES

- **Evaluation of the involvement in autophagy of the *D. discoideum* VPS13 proteins.**
  - Analysis of the autophagic activity of all *vps13*$^-$ mutants.
  - Visualization of autophagic markers in the *tipC*$^-$ mutant.
  - Assessment of the functional complementation of the *tipC*$^-$ phenotypes by the overexpression of conserved regions of TipC.

- **Evaluation of the involvement in autophagy of human VPS13A.**
  - Analysis of the autophagic activity in VPS13A-depleted HeLa cells.
  - Visualization of several autophagic markers in VPS13A-depleted HeLa cells.

- **Search for VPS13 proteins interactors.**
  - Identification by immunoprecipitation and mass-spectrometry of possible interactors of GFP-tagged conserved regions of *D. discoideum* Vps13 proteins.
  - Evaluation of the interaction of *D. discoideum* Rab7 and TipC by immunoprecipitation.
  - Evaluation of the interaction of human RAB7 and VPS13A by immunoprecipitation.

- **Study of the subcellular location of human VPS13A.**
  - Assessment of the subcellular location of overexpressed and endogenous VPS13A.

- **Study of the endocytic traffic in VPS13A-depleted human cells.**
  - Visualization of several markers of endosomes and lysosomes.
  - Evaluation of the processing of a lysosomal protease.

- **Study of VPS13A-depleted human cells at the ultrastructural level.**
  - Classification and quantification of distinct vesicles of the endolysosomal system.
  - Assessment of the structure of mitochondria and of the MCS between mitochondria and other organelles.

3 | MATERIALS AND METHODS

3 | MATERIALS AND METHODS

This chapter comprises a description of the protocols followed during the experimental work of this thesis, as well as the products used for their performance. Only specific information is included for commonly used methods in molecular biology. Step by step protocols of cell culture transfection, western blot and immunofluorescence procedures were described in a published chapter annexed to this thesis.[203]

3.1 | DNA constructs

3.1.1 | PCR products for *vps13*- mutants production in *D. discoideum*

Mutants were generated by the interruption of the genes by homologous recombination using DNA constructs (KO-constructs) in which a cassette containing the blasticidin resistance gene (Bsr) was flanked by two genomic sequences of the 5' end of the coding region of *vps13* genes (to disrupt the protein as near the N terminus as possible), separated approximately 1000 pb. The oligonucleotides used for the amplification of the Bsr cassette were: Bsr-F (GAGGTCGACGGTATCGATAAGC) and Bsr-R (GGGCTGCAGGAATTAACCATGC); an those used for the amplification of the *vps13* sequences by polymerase chain reaction (PCR) were: Vps13A-KO-1F (TAAGTCGACCCCATTACAGTGAAGAAGG), Vps13A-KO-1R (TAAAAGCTTCTTGACCAACATATCTCCACC), Vps13A-KO-2F (TAACTGCAGACCTTCTTCAGTTTCACC), Vps13A-KO-2R (TCCACTAGTACCTTGAACCAACATACG), Vps13B-KO-1F (GATTAATGTATTCTCAGGAAATGTAG), Vps13B-KO-1R (CCCGGGAAGCTTATCGATACCGTCGACCTCCTCTGATACTGATTCTCCTCG), Vps13B-KO-2F (CATATGCCGCATGGTTAATTCCTGCAGCCCGCAACACATTCACAAGATTGG), Vps13B-KO-2R (GAAAAATCGACCAAAGTATCAACAAG), Vps13D-KO-1F (GGGAACAAAAGCTGGGTACCGGGCCCCCCCTAGGATCATTTTTACAAGAAGTTGG), Vps13D-KO-1R (CCCGGGAAGCTTATCGATACCGTCGACCTCATGCTTGACATAAATCTTTAGTTG), Vps13D-KO-2F (CATATGCCGCATGGTTAATTCCTGCAGCCCCATCATCATCGTCATCACAACCACC), Vps13D-KO-2R (AATTGGAGCTCCACCGCGGTGGCGGCCGCTCATTTTCTTTTCCTATTCCTATTCC), Vps13E-KO-1F (GGGAACAAAAGCTGGGTACCGGGCCCCCCCGGATACATTGTCAATACCATGGTGG), Vps13E-KO-1R (CCCGGGAAGCTTATCGATACCGTCGACCTCCCTAATGGTTGTTGTTGTTGTTGTTGC), Vps13E-KO-2F (CATATGCCGCATGGTTAATTCCTGCAGCCCCTCAACCACACAACAGTGAATGGG), Vps13E-KO-2R (AATTGGAGCTCCACCGCGGTGGCGGCCGCTCTAAACTTCTACAACGAATTTGATCC), Vps13F-KO-1F (GGGAACAAAAGCTGGGTACCGGGCCCCCCCCTAAATATTAGTATTTGGAGTGGAAATG), Vps13F-KO-1R (CCCGGGAAGCTTATCGATACCGTCGACCTCGCAAATGATGATGAATCAATTAAACCACC), Vps13F-KO-2F (CATATGCCGCATGGTTAATTCCTGCAGCCCCAACCATTGAATATGATGAACATC) and Vps13F-KO-2R (AATTGGAGCTCCACCGCGGTGGCGGCCGCTCTCCTTTAATGTATCAGAGGGTGC).

Different approaches were used for the generation of the KO-constructs. For *vps13A*, the flanked regions were amplified by PCR from *D. discoideum* genomic DNA and cloned in a vector pBlueScript SK containing the Bsr cassette, which was previously inserted between EcoRI and HindIII.[1] Enzyme restriction sites were included in the oligonucleotides sequences to allow conventional cloning. That work was performed by Beatriz Núñez-Corcuera. For *vps13B,* the KO construct was obtained by nested PCR. Briefly, both flanking regions and the Bsr cassette were amplified by PCR using the indicated oligonucleotides containing overlapping regions. A final PCR product was obtained by mixing the three fragments in a single PCR reaction. That work was performed by María Magro-Sáez. *vps13D, vps13E* and *vps13F* KO constructs were obtained by a gap-repair approach (described later for the generation of the VPS13A^EGFP plasmid) so the oligonucleotides contain 30 bases extra, corresponding to the Bsr cassette or the cloning vector, to allow homologous recombination.

Regardless of the used method for the generation of the KO construct, the final PCR products containing the flanking regions of each specific gene surrounding the Bsr cassette were transformed in *D. discoideum* cells by electroporation (see section below). After clonal isolation of transformants resistant to blasticidin selection (see section below), clones were chosen for further analysis. DNA from each clone was extracted with QuickExtract™ DNA Extraction Solution (Epicentre, QE09050) according to manufacturer's instructions. The disruption of the genome at the desired position in the genome, and not somewhere else, was verified by PCR (as exemplified in the figure 5 in the results section). The oligonucleotides used to verify homologous recombination were: Vps13A-test (TACTCTAGAAAAATGGTATTT GAAGGATTAGTATCAGATG), Vps13A-WT (GGAATGTATGCTAATCTTGCGCGACG), Vps13B-test (CGCCGGTACCCATTAGTAGCCGATATTATAGC), Vps13B-WT (CGATTCACGTACCACATCACC), Vps13D-test (ATGGTATTTGAAAGTGTAGTAGC), Vps13D-WT (AACATATGATGAGATAGGG), Vps13E-test (ATGGTATCAAAAATATTACCAGG), Vps13E-WT (CCATATCTTCTGGTGTTACC), VPS13F-test (ATGTTTGAATCGATAGTATCAAATTTATTG), Vps13F-WT (TAGGGTGTTGTCGGA TTGG) and Bsr-test-KO (GTATGCTATACGAAGTTATCCGTGG).

3.1.2 | DNA plasmids

The DNA sequences coding the N- and C-terminal regions of TipC were amplified from genomic DNA by PCR using the following oligonucleotides: TipC-Nt-F (CGCGCTCGAGGGATCC AAAATGGTTTCACATATTGCAGC), TipC-Nt-R (CGGGGATCCCTGAACTAGATGGTGTTGTTGGAC), TipC-Ct-F (CGGGGATCCAAAATGGCTCAAACCATTGATCCTGCAGGTC) and TipC-Ct-R (CCGGGA TCCATCTAAATTATTACCAAATCTTTTTTCC). The PCR products were cloned into the BamHI site of the integrative pDV-CGFP-CTAP vector (GenBank Accession Number EF028672)

because constructs were not stable in bacteria in extrachromosomal vectors. The correct orientation of the fragments in the plasmid was confirmed by restriction enzyme digestion.

Similarly, the DNA sequences coding the N- and C-terminal regions of Vps13A were amplified using the following oligonucleotides: Vps13A-Nt-F (TACTCTAGAAAAATGGTATTTGAAGGATTAGTATCAGATG), Vps13A-Nt-R (TACTCTAGATAATTGATAAATGGTTGATGG), Vps13A-Ct-F (TACAGATCTAAAAATGCTCTCAATCCCAGGTAC), Vps13A-Ct-R (GGCACTAGTATATTTAATAGAGGAAGAATTTGAATTTG). The PCR products were cloned into XbaI site (the N-terminal region) or into the BglII and SpeI (the C-terminal region) in the pDM323 extrachromosomal vector (previously described)[313].

HA-Rab7 plasmid was generated by PCR amplification of *D. discoideum* cDNA using the oligonucleotides HA-Rab7A-F (GCAAGATCTAAAATGTATCCATATGATGTTCCAGATTATGCAGCCACAAAGAAAAAGGTT) and Rab7A-R (CGTACTAGTTTAACAACAACCTGATTTAGC) and cloned into the pDM359 (GenBank Accession Number EU912542).

The sequence of every DNA plasmid was confirmed by Sanger sequencing.

Other plasmids used during this thesis were: GFP-PgkA and GFP-Tkt-1 (plasmids previously generated in the laboratory),[41] GFP-Atg18 and GFP-Atg8 (a gift from Jason King),[139] GFP-WIPI-1 (Addgene, 38272), BFP-RAB5 (Addgene, 49147), mCherry-RAB7A (Addgene, 61804), GFP-RAB7A (a gift from Patricia Boya), and mTagRFP-mWasabi-LC3 (a gift from Cuihong Zhou).[345]

The generation of the VPS13^EGFP plasmid, which was performed thanks to the aid of Olivier Vincent, was particularly complex and thus deserves its own section.

VPS13$^{476\text{^}EGFP}$ plasmid

We constructed a plasmid for the expression of the complete VPS13A protein tagged with GFP after alanine 476. Different overlapping fragments of *VPS13A* transcript variant A (NM_033305) were obtained by PCR amplification of cDNA from HeLa cells.

GFP was amplified from the pEGFP-C3 plasmid. The ori (2micron) and URA3 elements, necessary for plasmid selection and amplification in yeast cells, were amplified from the pRS426 plasmid. The oligonucleotides used for such amplifications were: yeast-gr-F (TTCTGTGGATAACCGTATTACCGCCATGCATTAGTTATGGTTCCGCGCACATTTCCCCG), yeast-gr-R (TATGAACTAATGACCCCGTAATTGATTACTATTAGTGAGTTTAGTATACATGCATTTAC), EGFP-gr-F (CTTTACTCTATGAAGCAATTGGCTATAGTGAAACAGCAGTGAGCAAGGGCGAGGAGC), EGFP-gr-R (TCAAGGCTTCAAATGTTTTTAGTAAAGTTGGATCAACCTTGTACAGCTCGTCCATGCCG), VPS13A-gr-1 (TCAGATCCGCTAGCGCTACCGGACTCAGATCGCCACCATGGTTTTCGAGTCGGTGGTCG), VPS13A-gr-2 (ACCACCCCGGTGAACAGCTCCTCGCCCTTGCTCACTGCTGTTTCACTATAGCCA

ATTGC), VPS13A-gr-3 (GATCACTCTCGGCATGGACGAGCTGTACAAGGTTGATCCAACTTTACTAA AAACATTTG), VPS13A-gr-5 (CCACAACCTCAAGATTTAATGGCAGG), VPS13A-gr-6 (GGATCTAC TCCTGCCATTAAATCTTGAGG), VPS13A-gr-7 (CAGACTGTAGATCGGATGTTGTATGG), VPS13A-gr-8 (GTGAAATAGAAGATTCCCTCCCTCC) and VPS13A-gr-4 (CGTCGACTGCAGAATTCGAAGCT TGAGCTCGATCAGAGGCTCGGAGAAGGTTCTCTTGC).

The pEGFP-C3 plasmid without the GFP (excised by ScaI and AgeI) was used as a backbone in which the amplified PCR products were next assembled by gap repair. A scheme of the assembly strategy to generate the plasmid is depicted in the figure 23 in the results section.

The vector fragments and PCR products were transformed in the *Saccharomyces cerevisiae* strain FY250. For that, yeast cells were grown in YPAD medium and 20 ml were harvested at the log phase (OD=1.5) by centrifugation at 2000 g for 5 minutes, resuspended in sterile water for washing and centrifuged again at 2000 g for 5 min. The cell pellet was resuspended in 400 µl TeLiAc solution (100 mM LiAc, TE 1X) and 50 µl of competent cells were added to 2 µl of previously prepared carrier DNA, which is sonicated salmon sperm DNA (Sigma, D1626) denatured at 100°C for 5 min and cooled on ice, with the mixture of DNA (approximately 1 µg of each DNA fragment, all precipitated to reduce the total volume to 10 µl of sterile water). TeLiPEG solution (100 mM LiAc, 40% PEG, TE 1X) was added and the mixture was vortexed, incubated at 30 ºC for 30 min and 42 ºC during 15 min and centrifuged. Yeast cells were allowed to grow in YPAD for 2 h and then centrifuged, resuspended in sterile water, plated in YNB-agar plates without uracil for selection and incubated at 30 ºC until visible colonies appear. The plasmidic DNA of those colonies was isolated and transformed in DH5α *Escherichia coli* by a conventional heat shock procedure. After amplification in bacteria, by growing bacteria in the presence of kanamycin, the plasmid DNA was isolated and the whole sequence of VPS13A^EGFP was verified by Sanger sequencing.

3.2 | Specific *D. discoideum* techniques

3.2.1 | Strains, cell culture and development

All *D. discoideum* strains used in this thesis are originated from AX4 cells. The original *tip*$^-$ mutants,[290] which had been kindly deposited by William F. Loomis in the Dicty-stock center, were acquired from that repository. The identity of the *tip*$^-$ mutants was further confirmed by PCR using diagnostic amplifications of the disrupted genes.

The other *vps13*$^-$ mutants were generated as part of this thesis as described in the previous section. The parent AX4 cells used for generation of each mutant were used as wild type for an accurate comparison of phenotypes.

Axenic culture

For cell culture maintenance, cells were grown in liquid non-defined complete medium (HL-5, Formedium, HLB0102) in an incubator at 22ºC. In general, cells were grown in plastic plates. Alternatively, they were grown in suspension on a rotatory shaker at 160 r.p.m. when it was required.

Culture on bacterial lawns and development

Cells were grown in an incubator at 22ºC in association with bacteria on SM-agar plates. *Klebsiella aerogenes* has been used unless otherwise indicated. The cells grow by phagocytosis of bacteria and form plaques. Development was visualized at the center of the plaque, where the bacteria have been phagocytosed. Alternatively, and in order to visualize a synchronous development, 5 x 10^7 axenically and exponentially growing cells (at 1-3 x 10^6 cells/ml) were centrifuged, washed with PDF buffer (20 mM KCl, 9 mM K_2HPO_4, 13 mM KH_2PO_4, 1 mM $CaCl_2$, 1 mM $MgSO_4$, pH 6.4) and deposited on 47 mm nitrocellulose filters (Millipore, HABP04700) above a cellulosic absorbent pad (Millipore, AP1004700) moistened with PDF buffer and put in an humid chamber at 22ºC in the dark. After approximately 24 h development was visualized using a Nikon SMZ800 binocular and photographed with a camera Nikon DS-Fi1.

Sporulation assay

After 40h of development on nitrocellulose filters, to assure the complete development of structures and formation of spores, the structures were resuspended in spore buffer (0.3% cemusol, 20 mM KPO_4, 20 mM EDTA pH 6.2). Spores were counted and 100 spores were plated on a SM-agar plate in association with bacteria. Each viable spore forms a plaque, so the viability of spores can be measured by simple counting. In addition, efficiency of production of viable spores can be calculated. It is defined as the percentage of cells (the number of cells used for development) that form viable spores (the number of plaques after spore plating), normalized by the percentage obtained in the wild-type strain.

Calcofluor staining

Developed structures were put on a coverslip and stained with 0.1 mg/ml calcofluor (Sigma, F3543) protected from light during 5 minutes and then extensively washed with water. The coverslip was placed on top of a mounting slide and sealed with a nail polish. Images were taken immediately after using an inverted Zeiss LSM710 laser confocal microscope with a 63x/1.40 Plan-Apochromatic oil immersion objective.

3.2.2 | Generation of new *D. discoideum* strains

Electroporation

Cells were transformed by electroporation. For that, 5 x 10^6 axenically and exponentially growing cells were washed twice with ice-cold H50 buffer (19.98 mM HEPES, 50.03 mM KCl, 9.93 mM NaCl, 1 mM $MgSO_4$, 5 mM $NaHCO_3$, 1.3 mM NaH_2PO_4, pH 7.0) and then mixed with 1-10 µg DNA (depending on the efficiency of transfection of each plasmid or PCR product) in a total volume of 100 µl with H50 buffer. The mixture was added to the electroporation cuvette (Bio-Rad, 1652089) and electroporated with one or two pulses (0.85 kV/25 µF). Electroporated cells were then plated in HL5 medium.

Selection and clonal isolation

Transformed cells were selected with the pertinent antibiotics, depending on the antibiotic resistance conferred by the extracellular DNA. The concentration used for each antibiotic in the growing medium was 5 µg/ml blasticidin S hydrohloride (Calbiochem, 203350), 10 µg/ml G418 (Gibco, 11811023), 25 µg/ml hygromycin B (Calbiochem, 400051). Selection was carried out from 24h after electroporation until resistant colonies appear.

For clonal isolation, the antibiotic-resistant cells were harvested, plated in SM-agar plates in association with *Klebsiella* and incubated until lysis plaques form (no more than 150 cells/plate have been used to assure the generation of lysis plaques from individual cells).

3.2.3 | Autophagy assays

For autophagy assays, cells were kept at low cellular density, less than 10^6 cells/ml, to avoid the induction of autophagy at higher cellular concentrations.

The autophagic degradation in *D. discoideum* cells was measured by the proteolytic cleavage of cytosolic GFP tagged proteins.[41] Briefly, 10^6 cells previously transformed with GFP-Tkt-1 or GFP-PgkA were incubated in HL5 (as a control) or HL5 supplemented with NH_4Cl to reach a 100 mM concentration during 2 h. The same amount of NH_4Cl was added again and the cells incubated for 2 additional hours. Cells were then lysed with 50 µl of RIPA lysis buffer (50 mM Tris–HCl pH 8, 1 % NP-40, 0.1 % SDS, 0.5 % sodium deoxycholate, 150 mM NaCl, 2 mM EDTA) supplemented with 1:100 protease inhibitor cocktail (Sigma-Aldrich, P8340).

The amount of GFP fusion protein and cleaved GFP in 10 µg of total protein lysate were assessed after protein electrophoresis in a standard 12% acrylamide SDS-PAGE, transference, antibody incubation and development according to the western blot section.

Autophagic markers in *D. discoideum* were visualized by *in vivo* confocal microscopy of cells previously transformed with GFP-Atg8 or GFP-Atg18. For basal conditions, cells were kept in

HL5 or SIH complete medium (Formedium, SIH0102), and for starvation, cells were incubated with PDF or SIH without arginine and lysine (Formedium, SIH0102) 1 h prior to visualization. When SIH was used, cells were changed to SIH complete medium 24h in advance. Ubiquitin was visualized by immunofluorescence (see the protocol below).

3.2.4 | Phagocytosis assay

Axenically growing cells in suspension at 10^6 cells/ml were placed in fresh HL5 medium and incubated with fluorescent latex beads (Polysciences, 18860) on a rotatory shaker (50µl of latex beads / 5 ml cell culture). Samples of culture were collected at different times (time 0 collected just after addition of beads) and put in ice. Cold Soerensen buffer (2 mM Na_2HPO_4, 14.6 mM KH_2PO_4, pH 6) was added. The samples were then placed in ice-cold 20% Polyethylene Glycol (PEG) 8000 and centrifuged through it in order to separate extracellular and intracellular (phagocytosed) beads. The pellet was washed twice with ice-cold Soerensen buffer and resuspended in lysis buffer (0.2 % triton X-100; 50 mM Na_2HPO_4, pH 9.3). Fluorescence of each lysate was determined in triplicate using a PerkinElmer LS50B fluorescence spectrometer and corrected by taking into account fluorescence at time 0 and protein concentration in each sample. Protein concentration in cell lysates was determined by a Pierce BCA Protein Assay Kit (Thermo Scientific, 23227).

3.3 | Specific techniques for human cell lines

3.3.1 | Cell culture

HeLa and HeLa cells stably expressing GFP-LC3 were a gift from Alberto Muñoz and Aviva M. Tolkovsky, respectively. HeLa cells stably expressing GFP-LC3 had already been used to study autophagy.[20] Cells were grown in complete Dulbecco's modified Eagle's medium (DMEM; Sigma-Aldrich, D5648) supplemented with 10 % fetal bovine serum (FBS) (Gibco, 10270-106) and 1X penicillin-streptomycin (Gibco, 15140-122) at standard culture conditions (37ºC, 5% CO_2). During cell splitting, cells were detached from the plate using TrypLE Express Enzyme (Gibco, 12604-039).

3.3.2 | DNA and siRNA transfection and qPCR

DNA transfection was performed using Lipofectamine 2000 (Invitrogen, 11668019) according to the manufacturer's instructions. Briefly, Lipofectamine 2000 and DNA were mixed in Opti-MEM reduced serum medium (Life Technologies, 31985062) and DNA-Lipofectamine 2000 complexes were added to the cells. After 6 h, the medium was changed to fresh DMEM. Transfected cells were visualized 24 h after transfection with the exception of

WIPI-1 transfected cells, which were visualized at 48 h to avoid the observation of the transient induced autophagy after plasmid transfection.

For *VPS13A* and *VPS13C* knockdown, silencer select negative control siRNA (Ambion, ID No. 2 4390843) and validated *VPS13A* siRNA (siRNA 1: s23340; siRNA2: s23342) and *VPS13C* siRNA (s29543) were reverse transfected to cells using Lipofectamine RNAiMAX (Invitrogen, 13778030) according to the manufacturer's protocol. Briefly, siRNA and Lipofectamine RNAiMAX were mixed in Opti-MEM and cells were added to the mixture. Cells were transfected again with the same siRNAs 48 h after the first transfection and the experiments were carried out 72 h after the second transfection.

Knockdown efficiency was evaluated by quantitative real time PCR (q-PCR). For that, total RNA was isolated 48 h after siRNA transfection using TRIzol reagent (Ambion, 15596018) and 1 μg was used for reverse transcription (RT-PCR) into cDNA. The iScript cDNA Synthesis Kit (BioRad, 1708890) was used for RT-PCR. Conventional q-PCR assay was applied using a TaqMan Universal Master Mix (Applied Biosystems, 4304437) and predesigned TaqMan Assays (Applied Biosystems, Hs00362891_m1 and Hs00419559_m1 for *VPS13A* and *VPS13C,* respectively) according to the manufacturer's instructions and in a 7300 real-time PCR System (Applied Biosystems). Each sample was analyzed in triplicate. The mRNA levels of *VPS13A* and *VPS13C* were calculated according to the comparative Ct method and using *IPO8* as internal reference for normalization.

3.3.3 | Autophagy assays

Only subconfluent cells, at about 70% confluence, were used to avoid induction of autophagy in growing conditions.[135] To induce autophagy by starvation, cells were washed twice with prewarmed phosphate-buffered saline (PBS) 1X (133 mM NaCl, 8 mM Na_2HPO_4, 2mM KH_2PO_4; pH 7.4) and once again with prewarmed starvation Earle's Balanced Salt Solution (EBSS; Sigma-Aldrich, E2888) and then incubated in EBSS during the indicated hours. Cells to be analyzed in basal conditions in the same experiment were similarly washed and then incubated with fresh DMEM. In every case, they were incubated at standard culture conditions.

The autophagic degradation in HeLa cells was measured by the accumulation of LC3II and cleaved GFP when chloroquine (CQ) at 5 μM was added to the growth or starvation medium for 4 h. A detailed explanation of this optimized method is provided in a published chapter which is annexed to this thesis.[203]

Visualization of autophagic markers by confocal microscopy was done using cells in growing conditions or starved for 2 h.

3.4 | Common methods

3.4.1 | Western blot and band densitometry

For protein extraction, cells were generally lysed with RIPA buffer supplemented with 1:100 protease inhibitor cocktail. 10 µg of total protein were prepared in SDS sample loading buffer, with the exception of VPS13A detection and overexpressed GFP-TipC tagged ends, for which 20-30 µg of total protein were used. In general, conventional handcast SDS-polyacrilamide gels were used (BioRad) at different polyacrilamide concentrations according to the molecular size of proteins to be detected. A 14% polyacrilamide concentration was used to resolve LC3I and LC3II bands. For human VPS13 proteins detection, precast NuPage Tris-Acetate 3-8% polyacrylamide gradient gels (Invitrogen, EA0375) were used. For VPS13A and VPS13C separation, electrophoresis was performed at least until the 31kDa band of the HiMark Pre-Stained Protein Standard (Novex, LC5699) reached the bottom of the gel. Electrotransference on PVDF (polyvinylidene fluoride) membranes (Millipore, IPVH00010) was performed by tank blotting and membranes were blocked in 5% skimmed milk in TBS-T buffer for at least 1h at room temperature (RT). Membranes were then incubated with primary antibodies in 5% skim milk in TBS-T overnight at 4ºC, washed with TBS-T, incubated with the appropriate secondary antibodies and washed before antibody detection.

Primary antibodies were used at the following concentrations: anti-CTSB (1:1000; RyD Systems, AF953), anti-GAPDH (Enzo LifeSciences, ADI-CSA-335), anti-GFP (1:4000; Sigma-Aldrich, G1544), anti-HA (1:1000, Sigma-Aldrich, 12CA5), anti-LC3 (1:1000; Cell Signaling, 2775), anti-RAB7 (1:1000; Cell Signaling, 9367) and anti-VPS13A (1:500; Sigma-Aldrich, HPA021662). Horseradish peroxidase-conjugated secondary antibodies were used at 1:5000 (Santa Cruz Biotechnology).

Antibody binding was detected by Amersham ECL Western Blotting Detection Reagents (GE Healthcare Life Sciences, RPN2134) or Clarity Western ECL Substrate (BioRad, 1705060) and the resulting chemiluminescent signal was captured using CURIX RP2 Plus films (Agfa). Films were introduced in a X-ray film processing machine and scanned. Protein amount of each band was quantified by densitometry using ImageJ software. Importantly, for a correct comparison of bands, films should not be overexposed,[26] although when differences on protein amount between samples are very pronounced (due, for example, to CQ treatment), this is not easy and a compromise of acceptable weak and strong signals has to be found.[203]

3.4.2 | Immunoprecipitation assays

D. discoideum or HeLa cells expressing a GFP tagged protein were washed and harvested. Lysis was performed using protein lysis buffer (10 mM TrisHCl pH 7.5, 150 mM NaCl, 0.5 mM

EDTA, 0.5% NP-40, 2.5 mM NaF, 0.2mM Na_3VO_4) supplemented with 1:100 protease inhibitor cocktail. Cell lysates were centrifuged (13500 g for 15 min at 4 °C) and the supernatant transferred to a microcentrifuge tube with washed GFP-Trap A beads (Chromoteck, gtak-20) in dilution/washing buffer (10 mM TrisHCl pH 7.5, 150 mM NaCl, 0.5 mM EDTA, 2.5 mM NaF, 0.2mM Na_3VO_4) supplemented with protease inhibitors according to the manufacturer's protocol. Incubation with beads was performed for 4h and then the beads were washed five times with washing buffer and prepared in loading buffer for mass-spectrometry or western-blot analysis.

3.4.3 | Mass-spectrometry

Sample preparation

Mass spectrometry was performed at the proteomic facility of Centro Nacional de Biotecnología (Madrid). The protein extract samples were resuspended in a volume up to 100 µl of Laemmli sample buffer and applied onto a conventional 4% stacking and 12% resolving SDS-PAGE gel. Electrophoresis was stopped as soon as the front entered 1 cm into the resolving gel in order to concentrate the whole proteome in the stacking/resolving gel interface. The unresolved protein bands were visualized by Coomassie staining and each gel lane was excised, cut into cubes (1 mm^2), deposited in 96-well plates and automatically processed in a Proteineer DP digestor (Bruker Daltonics). Digestion was performed according to a previously described protocol,[279] with the following minor modifications: gel plugs were washed first with 50 mM NH_4HCO_3 and then with ACN (acetonitrile) prior to reduction with 10 mM DTT in 25 mM NH_4HCO_3 solution, and alkylation was carried out with 55 mM IAA (iodoacetamide) in 50 mM NH_4HCO_3 solution. Gel pieces were rinsed with 50 mM NH_4HCO_3, then with ACN and dried under a stream of nitrogen. Proteomics Grade Trypsin (Sigma Aldrich, T6567) at a final concentration of 16 ng/µl in 25% ACN/50 mM NH_4HCO_3 solution was added and digestion took place at 37°C for 4 h. The reaction was stopped by adding 50% ACN/0.5% TFA (trifluoroacetic acid) for peptide extraction and the tryptic eluted peptides were dried by speed-vacuum centrifugation.

Protein identification by nano LC–MS/MS QTof (Triple Tof) analysis

The peptide samples were analyzed on a nano liquid chromatography (LC) system (Eksigent Technologies nanoLC Ultra 1D plus, AB SCIEX) coupled to 5600 Triple TOF mass spectrometer (AB SCIEX) with a nanoelectrospray ion source. Samples were injected on a C18 PepMap trap column (5 µm, 100 µm I.D. x 2 cm, Thermo Scientific) at 2 µL/min, in 0.1% formic acid in water, and the trap column was switched on-line to a C18 nanoAcquity BEH analytical column (1.7 µm, 100 Å, 75 µm I.D. x15 cm, Waters). Equilibration was done in

mobile phase A (0.1% formic acid in water) and peptide elution was achieved in a 60 min gradient from 5% - 40% B (0.1% formic acid in acetonitrile) at 250 nL/min. The mass spectrometer operated in data-dependent acquisition mode. For TOF scans, the accumulation time was set to 250 ms, and per cycle, up to 15 precursor ions were monitored.

MS and MS/MS data obtained for each sample were processed using Analyst TF 1.5.1 Software (AB SCIEX, Foster City, CA). Raw data were translated to mascot general file (mgf) format and searched against a composite target/decoy database built from the 8418 sequences in the *Dictyostelium discoideum* reference proteome at Uniprot Knowledgebase (as of July 2015), using an in-house Mascot Server v. 2.4 (Matrix Science, London, U.K.). Search parameters were set as follows: carbamidomethylcysteine as fixed modification and methionine oxidation as variable one. Peptide mass tolerance was set to 30 ppm and 0.05 Da, in MS and MS/MS mode, respectively and two missed cleavage sites were allowed. False Discovery Rates (FDR < 1%) for peptide identification were manually calculated.

3.4.4 | Confocal microscopy and immunocytochemistry

Cells grown on glass sterilized coverslips in 24-well plates were fixed with 3 % paraformaldehyde in PBS, pH 7.4, for 15 min at room temperature (RT) and then washed with PBS and incubated with 100 mM glycine in PBS for 30 min at RT to quench the possible fluorescence signal from free aldehyde groups in PFA. Permeabilization with cold methanol was subsequently performed at -20 ºC for 10 min. Coverslips were washed with PBS and incubated with blocking buffer, 3% BSA (Bovine serum albumin) 0.1% Triton X-100 in PBS for 1 h at RT. Primary antibodies were applied in 3% BSA 0.1% Triton X-100 in PBS for 3 h at RT in an humid chamber. Coverslips were washed with PBS and secondary antibodies were applied in 3% BSA 0.1% Triton X-100 in PBS for 1 h at RT in an humid chamber. Coverslips were then washed with PBS and mounted on slides using Prolong Diamond Antifade Mountant (Molecular Probes, P36970).

Primary antibodies were used at the following concentrations: anti-CTSB (1:150; RyD Systems, AF953), anti-calnexin (1:100; BD Transduction Laboratories, 610523), anti GM-130 (1:100; BD Transduction Laboratories, 610823), anti-LAMP1 (1:100; Cell Signaling, 15665), anti-LAMP1 (1:200; Cell Signaling, 9091), anti-LC3 (1:100; Nanotools, 0260-100/LC3-2G6), anti-LC3 (1:200; Cell Signaling, 3868), anti-RAB7 (1:100; Cell Signaling, 9367), anti-SQSTM1 (1:150; Abcam, ab109012), anti-ubiquitin (1:100; Cell Signaling, 3936) and anti-VPS13A (1:100; Sigma-Aldrich, HPA021662). Secondary antibodies were used at 1:500 (Invitrogen). For visualization of mitochondria, live cells were incubated with Mitotracker Red CMXRos (Molecular Probes, M7512) at 100nM in DMEM for 20 min at 37ºC.

Images were acquired using an inverted Zeiss LSM710 laser confocal microscope with a 63x/1.40 Plan-Apochromatic oil immersion objective. Samples corresponding to control or *VPS13A/C* siRNA treated cells of the same experiment were acquired under identical exposure conditions to allow subsequent comparison of images.

3.4.5 | Electron microscopy

Electron microscopy was performed at the microscopy facility of Centro de Biología Molecular Severo Ochoa (Madrid). Cells were fixed for 2 h at room temperature with 4% PFA and 2% glutaraldehyde solution in 0.1 M phosphate buffer (PB, pH 7.4). Post-fixation was performed with 1% OsO4 and 1.5% $K_3Fe(CN)_6$ in water at 4ºC for 1 h. Samples were dehydrated with acetone and in situ flat-embedded in Epoxy, TAAB 812 Resin (TAAB Laboratories) according to standard procedures. After polymerization, resin sheets containing the cell monolayers were detached from the substrate and mounted onto resin blocks to obtain 80 nm ultrathin sections, that were deposited onto slot grids, stained with saturated uranyl acetate and lead citrate. Visualization was done at 80 kV in a Jeol JEM-1010 electron microscope and images were recorded with a TemCam-F416 (4Kx4K) digital camera from TVIPS.

3.4.6 | Image analysis

Analysis of images was performed using ImageJ software. Fluorescent puncta in samples of *D. discoideum* cells was done manually due to technical difficulties for automatic puncta detection. For fluorescent puncta and puncta area quantification in samples of HeLa cells, ImageJ macros were used to create selection masks with identical background correction and threshold conditions for all the samples of the same experiment and to count puncta and measure areas. Colocalization was defined for pixels with fluorescent signal intensity above the applied threshold in both channels, corresponding to signal of different markers. Quantifications and area or length measurements from micrographs were done manually using ImageJ tools to select the elements to measure.

3.4.7 | Statistical analysis

Data was analyzed using Microsoft Excel and GraphPad Prism Software. Data are presented as means ± standard deviation (SD). Measurements in control and experimental groups were compared and statistical significance was determined by the two-tailed Student's *t* test and considered significant at $p < 0.05$ *, $p < 0.01$ **, $p < 0.001$ ***.

4 | RESULTS

4 | RESULTS

This chapter shows the experimental results obtained during this thesis. The discussion of those results is provided in the next chapter.

4.1 | Autophagic flux in *D. discoideum tip*$^-$ mutants

As described in the introduction, four multitipped mutants (*tipA*$^-$, *tipB*$^-$, *tipC*$^-$ and *tipD*$^-$) had been previously reported in *D. discoideum*,[290] and the multitipped phenotype is characteristic of some autophagy mutants.[184,222,223,306] Autophagy was not studied in the *tip*$^-$ mutants because by the time they were described, the multitipped phenotype had not been associated with autophagy deficiencies yet. However, autophagy could be impaired in these mutants.

With reference to this thesis, the interesting mutant was *tipC*$^-$ because the disrupted protein (TipC) was identified as a VPS13 homologue by sequence analysis. TipD was, at the moment, simply described as a protein containing a WD40 domain. It was later known to be homologue to ATG16, which reinforced our idea of an autophagic association of Tip proteins with autophagy. About TipA and TipB, little information can be obtained from their sequence. No functional domain is identified in TipB and, in TipA, only a PP2Cc (serine/threonine phosphatases, family 2C, catalytic) domain and a DEP (Dishevelled, Egl-10, and Pleckstrin) domain of unclear function are predicted. Neither TipA nor TipB have known homologues in other organisms that could aid in the elucidation of their functions.

In order to assess if the multitip phenotype of the *tipC*$^-$ mutant was due to a deficiency of autophagy, we compared the autophagic activity of all multitipped mutants with that of a wild-type strain.

The autophagic activity is commonly known as autophagic flux to give an idea of the dynamism of the process and it can be measured by the ability to degrade a cytosolic-GFP fusion protein within lysosomes (for that to happen, the protein has to be captured within autophagosomes and those have to fuse with lysosomes and be degraded).[41] The amount of autophagic degradation is proportional to the accumulation of the more degradation-resistant GFP when NH_4Cl, a lysosomotropic compound, is added at non-saturating concentrations, i.e. low enough to allow the cleavage of the GFP bound to the protein but sufficient to diminish the degradation capacity of lysosomes and provoke accumulation of free GFP.

Markedly reduced autophagic flux was detected in *tipC*$^-$ and *tipD*$^-$ mutants in comparison to the wild type, while the autophagic flux was not dramatically altered in the other two mutants **(FIG. 4)**.

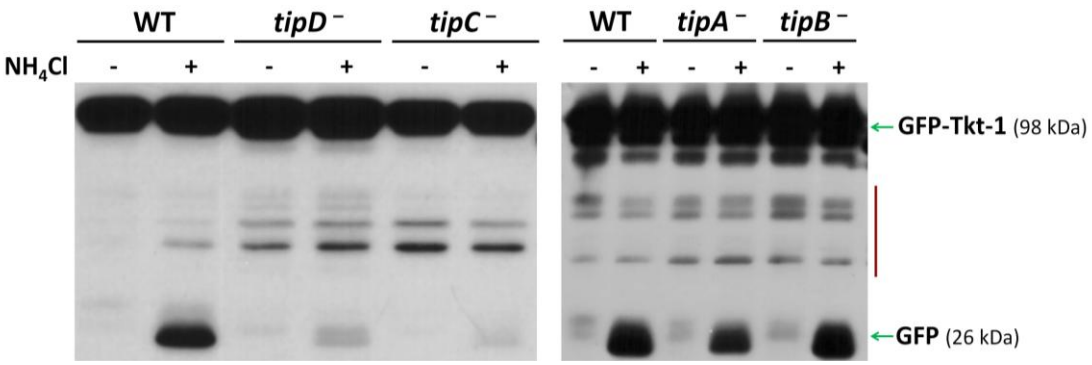

FIG. 4| *tipC*⁻ and *tipD*⁻ display reduced autophagic flux. *tip*⁻ mutants expressing GFP-Tkt-1 were incubated during 4 hours in the presence or absence of 100 mM NH_4Cl. Protein lysates were analyzed by western blot. Representative images of 3 independent experiments are shown. *tipC*⁻ and *tipD*⁻ accumulated less amount of free GFP cleaved fragments (green arrow) in comparison to the wild-type (WT). *tipA*⁻ and *tipB*⁻ GFP accumulation was similar to that of the wild-type. The red line indicates non-specific immunoreactive proteins.

4.2 | Autophagic flux in *D. discoideum vps13*⁻ mutants

Apart from TipC (also called Vps13C), other five VPS13 proteins are present in *D. discoideum*. To assess if their absence similarly leads to a decreased autophagic flux, we generated the mutant strains by homologous recombination and confirmed by PCR the disruption of the corresponding gene in each one of the five new *vps13*⁻ strains. As an example, the procedure for *vps13F* disruption is illustrated (FIG. 5).

B

Oligos pair	Well	Size WT (bp)	Size KO (bp)
1+2	1, 3	983	0
1+3	2, 4	0	950
4+5	1,2,3,4	1270	1270

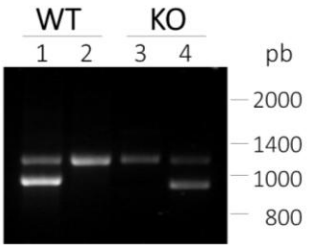

FIG. 5| Generation and PCR confirmation of *D. discoideum vps13F*⁻ mutant. (A) Schematic representation of the replacement of part of the genomic sequence (blue) of the gene by a Bsr cassette (purple). Small introns are represented by thin lines. Crosses represent homologous recombination. Colored arrows indicate the oligonucleotides used for gene disruption confirmation by PCR. Note that the oligonucleotide 1 sequence is upstream of the sequence used for homologous recombination. (B) Gene disruption was confirmed by positive or negative amplification of DNA fragments using distinct pairs of oligonucleotides; the predicted results are written in the table. An additional pair of oligonucleotides, flanking and independent genomic region which is longer than the two expected PCR products derived from the gene of interest, was used as a positive control of the PCR.

Contrary to *tipC*⁻, the other *vps13*⁻ mutants developed to form apparently normal fruiting bodies on *K. aerogenes* lawns (FIG. 6). Of note, however, was the extremely slow formation of

lysis plaques of the *vps13F*⁻ mutant and its development to form small fruiting bodies only at the edges of plaques and only after a very long time.

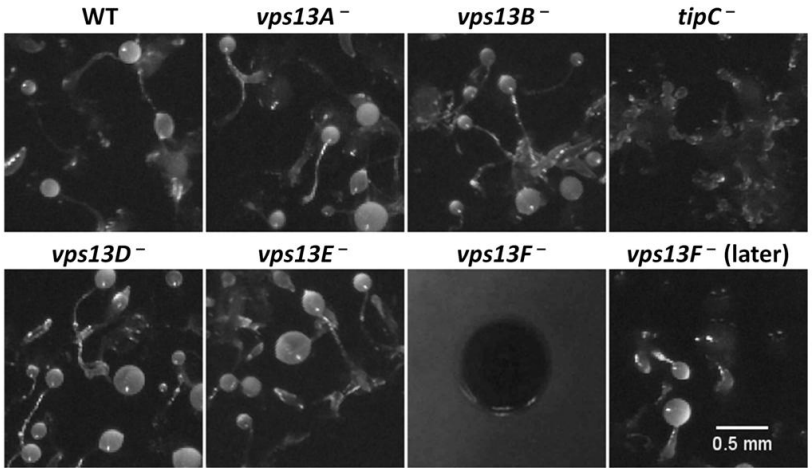

FIG. 6| Development of *D. discoideum vps13*⁻ mutants. Isolated *vps13*⁻ cells were grown on *K. aerogenes* and structures resulting from development of each colony were photographed. *vps13F*⁻ was imaged twice because of its slow growth: the same day as the other mutants (when no structures were visible in the small lysis plaques) and two weeks later, when structures were formed at the edges of the lysis plaque. All the mutants, but *tipC*⁻ (*vps13C*⁻), formed normal-looking fruiting bodies.

Despite the relationship between abnormal developmental phenotypes and deficient autophagy, it is possible that autophagy could be partially altered in the new strains. Therefore, the autophagic flux was assessed in the other *vps13*⁻ mutants. Modest differences might exist in autophagic flux for some of them, especially *vps13A*⁻, but none was comparable to the one observed in the *tipC*⁻ strain (FIG. 7), which was therefore chosen for a more detailed analysis.

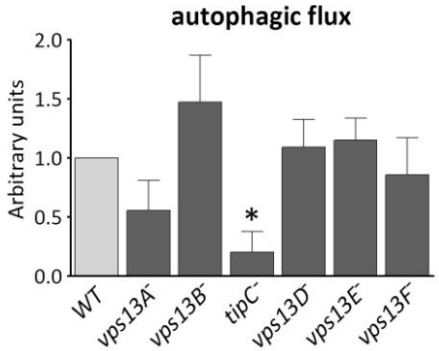

FIG. 7| Autophagic flux of *vps13*⁻ mutants. *vps13*⁻ cells expressing GFP-pgkA were incubated in the presence or absence of NH_4Cl in a similar procedure than in figure 4. Densitometric values of free GFP cleaved bands were normalized for those of the complete fusion protein as a measure of relative GFP accumulation and compared to the accumulation of GFP in the wild-type. Autophagic flux was only dramatically impaired the *tipC*⁻ mutant. Means and SD of at least three experiments are represented.

4.3 | Atg8 and Atg18 autophagic markers in the *tipC*⁻ mutant

The reduced autophagic flux of *tipC*⁻ indicated that the autophagic degradation is compromised in this mutant. However, it does not reveal at which step the autophagic process is impaired. A decrease in autophagic flux can be due to a reduced autophagosome

formation or also be the consequence of a defective autophagosome fusion to lysosomes and/or lysosomal degradation. Atg8 labels autophagosomes until this very late step, as it is bound to their outer and inner membranes until it is recycled to the cytoplasm or degraded, respectively. Strains expressing GFP-Atg8 were analyzed in growth and starvation conditions. In wild-type cells, GFP-Atg8 puncta appear during starvation. However, fewer GFP-Atg8 puncta were present in *tipC*⁻ starved cells in comparison to the wild type (FIG. 8A). Additionally to the small puncta, aberrant large GFP-Atg8 structures were observed in the mutant that were ubiquitin-positive and thus probably represent protein aggregates (FIG. 8B).

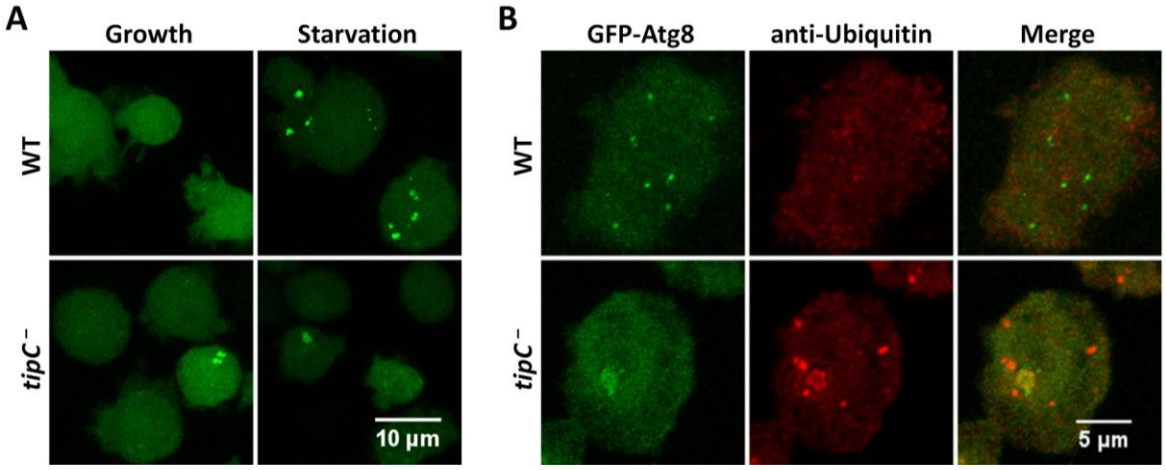

FIG. 8| **Aberrant Atg8 pattern in *tipC*⁻**. Confocal representative images of wild-type and *tipC*⁻ cells overexpressing GFP-Atg8. (A) Fewer GFP-Atg8 puncta were observed in the *tipC*⁻ strain by *in vivo* imaging of starved cells. (B) Ubiquitin-labeled protein aggregates colocalized with GFP-Atg8 aberrant structures in fixed *tipC*⁻ cells.

Because of the aggregation of GFP-Atg8, we used another autophagic marker, GFP-Atg18, which label the expanding autophagosome and allows a better quantification of puncta. The percentage of cells with puncta increased in the starved wild-type strain but starvation did not trigger such increase in *tipC*⁻ cells (FIG. 9).

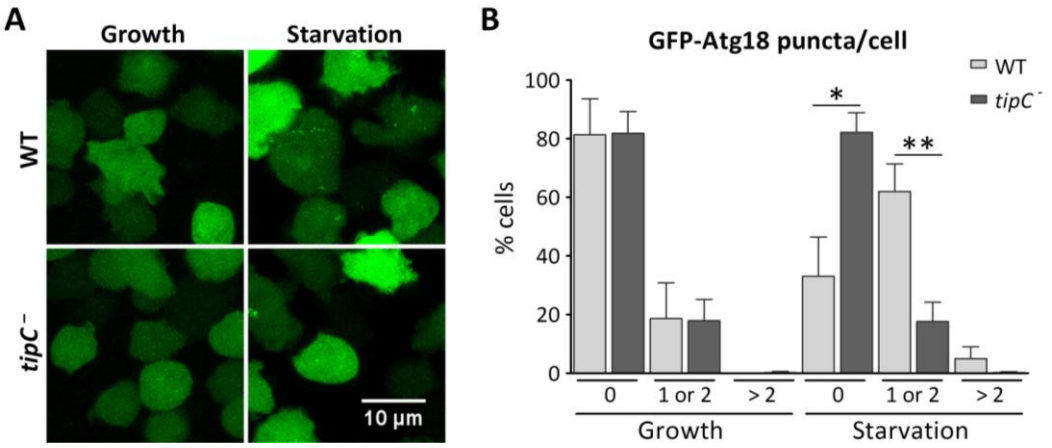

FIG. 9| **Abnormal Atg18 pattern in *tipC*⁻**. Wild-type and *tipC*⁻ cells overexpressing GFP-Atg18 were visualized and classified according to the number of puncta. (A) Fewer GFP-Atg18 puncta were observed in the *tipC*⁻ strain by *in vivo* confocal imaging of starved cells. (B) Representation of mean and SD of the percentage of cells (at least 100 cells per condition) showing 0, 1-2 or >2 puncta in three independent experiments. A large percentage of *tipC*⁻ cells did not show any puncta even in starvation.

4.4 | Expression of TipC N and C termini

To further characterize TipC, we aimed to visualize the subcellular localization of the protein by expressing TipC fused to GFP at the C terminus. Due to the long size of the protein, a strategy of serial cloning of fragments of the coding sequence, using its few unique restriction sites, was designed. Unfortunately, the plasmid containing the full TipC coding sequence was unstable in bacteria probably due to the high percentage of A/T in *D. discoideum*. As an alternative, the N- and C-terminal regions of TipC were chosen for overexpression since in those regions the homology of TipC to other VPS13 proteins is higher and it might be possible that those regions could harbor some of the protein's functions on their own (FIG. 10).

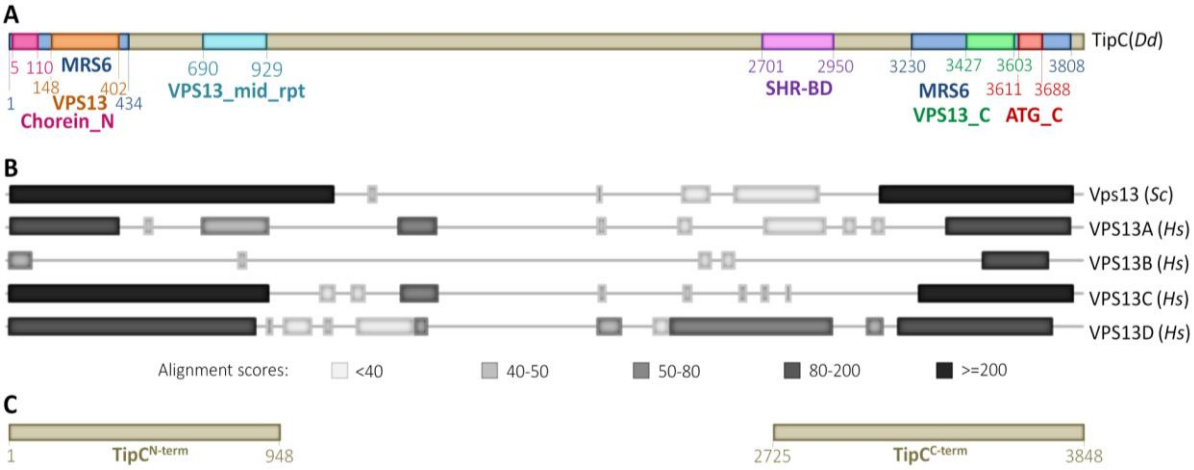

FIG. 10| TipC shares the greatest homology with other VPS13 proteins at the N- and C-terminal ends, which are therefore chosen for overexpression. (A) Schematic representation of the identified domains in the *D. discoideum* TipC protein (see introduction for description of the illustrated domains). (B) Alignment of *S.cerevisiae* and human VPS13 proteins with TipC shows higher homology at the end termini of the proteins. (C) Representation of the regions of TipC selected for overexpression.

Vectors expressing these regions of TipC fused to GFP were transformed in wild-type and *tipC*$^-$ cells and visualized by confocal microscopy. The subcellular localization of the overexpressed N- and C-terminal regions of TipC was mainly cytosolic although some brighter puncta could also, but very faintly, be distinguished (FIG. 11A). The correct size of the expressed polypeptides was confirmed by western blot (FIG. 11B).

Strikingly, the overexpression of the TipC C terminus sequence in the *tipC*$^-$ mutant resulted in the development of fruiting bodies similar to those of the wild type. On the contrary, the expression of the TipC N-terminal region barely modified the *tipC*$^-$ phenotype (FIG. 12A).

Few small and aberrant fruiting-body resembling structures emerge from the multitipped mound in the *tipC*$^-$ mutant. When these structures were stained with calcofluor (which labels the cellulose walls of the dead cells in the stalk and of spores), we observed disorganization of the cells in the stalk, a thinner cellulose accumulation in the stalk tube, and few round spores.

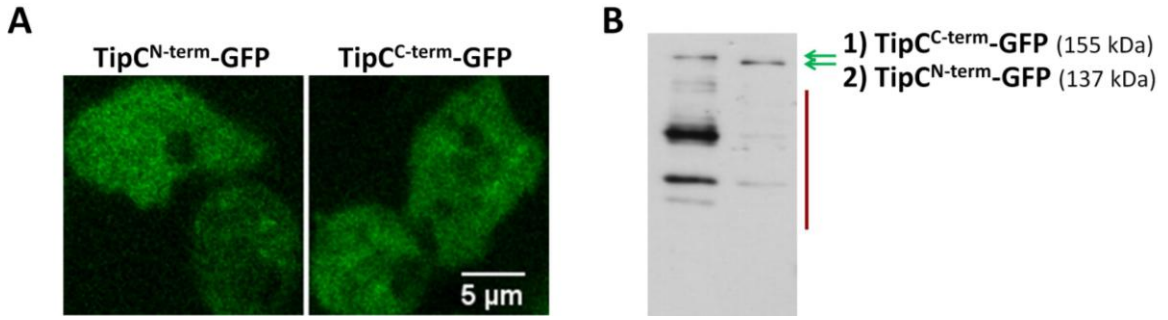

FIG. 11| Overexpression of the N- and C-terminal fragments of TipC. (A) *In vivo* confocal microscopy images of *D. discoideum* cells overexpressing the N and C terminus of TipC fused to GFP. (B) Western-blot confirmation of the correct size of the expressed fusion proteins (green arrows). The red line indicates degradation of the overexpressed proteins.

The rescue of the developmental phenotype by the expression of the C-terminal region of TipC was notable with this staining, which showed a more organized stalk and more spores with an ellipsoidal shape. Still, by comparison to the wild type, it was evident that the rescue was partial **(FIG. 12B)**.

The production of viable spores was measured as an additional parameter to quantify the developmental recovery. The spore efficiency in the *tipC*⁻ mutant was 1.70 ± 0.03% of that of the wild type and it was recovered to 56.94 ± 0.20% by expression of the C terminus.

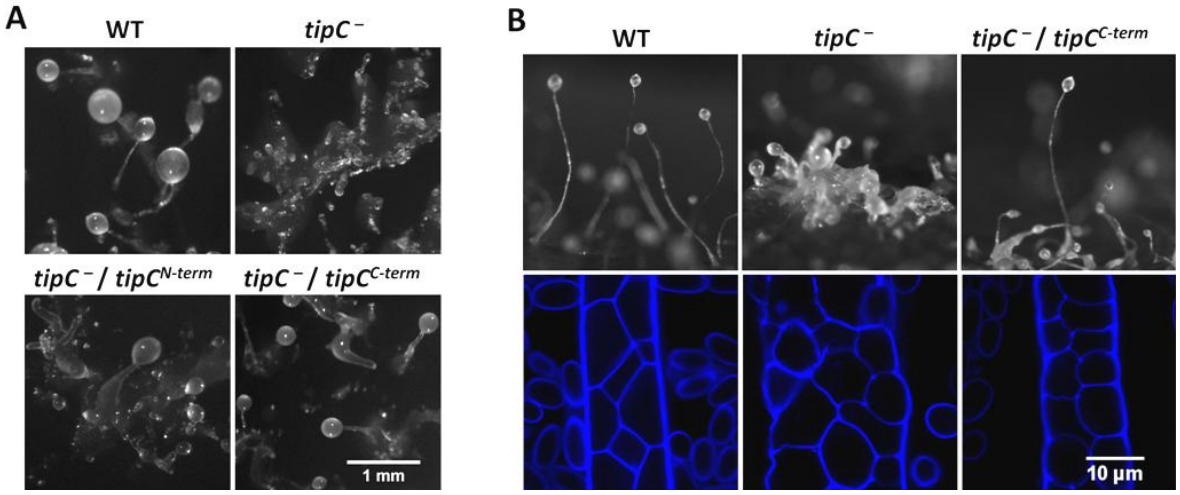

FIG. 12| Partial recovery of *tipC*⁻ development by overexpression of the C terminus of TipC. (A) The N- and C-terminal ends of TipC were overexpressed in the *tipC*⁻ background and the development of the transformed cells on *K. aerogenes* lawns was compared to that of the wild type and the original mutant. The expression of the C terminus largely recovered the formation of isolated fruiting bodies. (B) The recovery was evident after synchronous development of structures and their staining by calcofluor.

Because of the requirement of autophagy during *D. discoideum* development and the homology to Atg2 in the C terminus of TipC, we hypothesized that this region had a role in autophagy and that it could partly function independently of the rest of the protein. In order to evaluate this idea, we visualized RFP-Atg18 puncta formation in starvation. Again, the expression of the C terminus of TipC resulted in a partial recovery as more cells displayed

more puncta than in the *tipC*- mutant, but not as many as in the wild type (FIG. 13A). In summary, the partial recovery of the multitipped phenotype, which is associated to an autophagic block,[184,222,223,306] and the partial recovery of Atg18 puncta indicate that the isolated C-terminal region of the protein is able to restore autophagy to some extent.

Since connections between autophagy and phagocytosis had been reported,[285] and Vps13A was shown to be required for phagocytosis in *T.thermophila*,[264] we evaluated phagocytosis as another process being potentially dependent on TipC and, particularly, on the C terminus of the protein. Certainly, a modest decrease of phagocytosis rate, measured by the uptake of fluorescent beads, was observed in the *tipC*- mutant that was recovered when the C terminus of TipC was overexpressed (FIG. 13B).

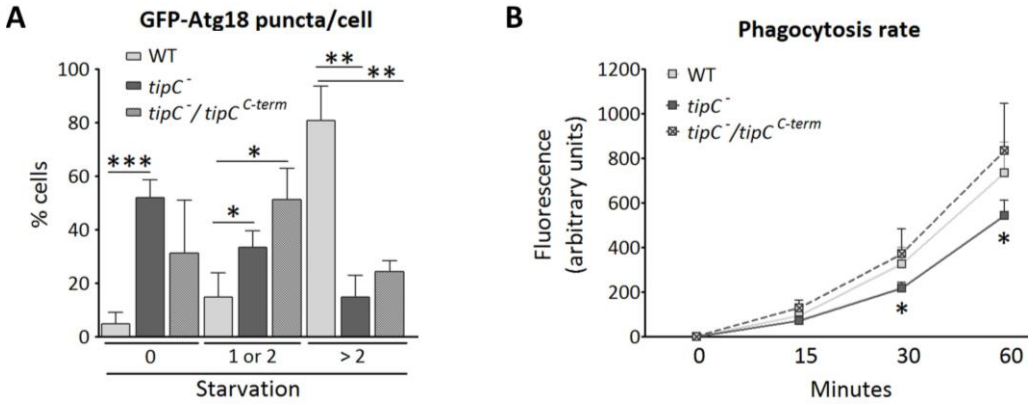

FIG. 13| **Partial recovery of *tipC*- functions by overexpression of the C terminus of TipC.** (A) Atg18 puncta formation in starvation was partially recovered in the complemented strain according to the percentage of cells displaying puncta. Mean and SD of three independent experiments are represented. Approximately 100 cells per condition were evaluated. (B) The complemented strain phagocytosed as many fluorescent beads as the wild type whereas in the original mutant the phagocytosis rate was moderately decreased (statistical significance with respect to the WT). Mean and SD of four independent experiments are represented.

4.5 | Autophagy flux in VPS13A-depleted human cells

VPS13 proteins and autophagic machinery are conserved during evolution. Therefore we decided to evaluate if a role in autophagy was conserved in human VPS13 proteins. Apart from the relevance that a role of human VPS13 proteins in autophagy would have concerning their related diseases, the study of the process in a different cell model could provide additional clues of the exact role of VPS13 proteins in autophagy.

The alignment of human VPS13 protein sequences with that of TipC showed that VPS13A and VPS13C are the more similar to TipC. These proteins are also the most similar ones to yeast Vps13 and probably to the common ancestral protein. Therefore, *VPS13A* and *VPS13C* were knocked down with specific siRNAs in HeLa cells. These cells were chosen because they had been already widely used for the study of autophagy,[20,212] and hence, from the technical point of view, the analysis of autophagy in these cells could be easier. Moreover, *VPS13A* expression in HeLa cells had been previously shown to be similar to that of other cell lines.[65]

The level of silencing of VPS13A was first assessed by RT-PCR and we found a reduction of 89.5 ± 2.9 % of *VPS13A* mRNA levels in *VPS13A* siRNA treated cells in comparison to control siRNA treated cells. We next evaluated the level of the protein by western-blot using a commercial anti-VPS13A antibody. We observed, as expected, that a band of 360 kDa disappeared upon silencing *VPS13A* expression; but that another one, with a higher molecular weight, remained present (FIG. 14). We evaluated the possibility that the higher molecular band corresponded to a cross-detection of the homologous VPS13C (422 kDa). This was indeed confirmed by inhibition of *VPS13C* expression using a siRNA that reduced the mRNA levels of *VPS13C* up to 71.6 ± 5.4 % in comparison to control siRNA treated cells (FIG. 14). The simultaneous treatment with both *VPS13A* and *VPS13C* siRNAs resulted in the clear reduction of both proteins (FIG. 14).

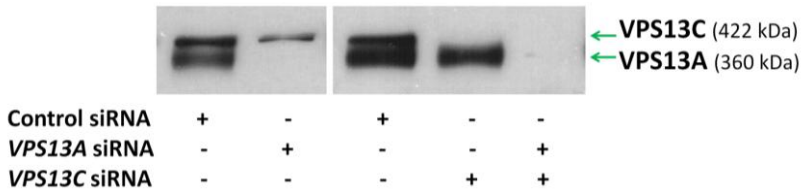

FIG. 14| Confirmation of *VPS13A* and *VPS13C* expression by specific siRNAs. HeLa cells were treated with control, *VPS13A* and/or *VPS13C* siRNAs and protein expression was assessed by western blot using an anti-VPS13A antibody that was also able to recognize VPS13C.

We silenced *VPS13A* gene expression by siRNA in stably expressing GFP-LC3 HeLa cells and incubated them in complete or starvation medium in the presence or absence of chloroquine (CQ) at non-saturating concentrations. Optimization of this technique is described in detail in the published chapter which is annexed to this thesis.[203] Briefly, we evaluated the levels of endogenous LC3-I and LC3-II and also of the expressed GFP-LC3 protein and the free GFP band, which is generated as a result of GFP-LC3 partial degradation.[212]

The comparison of these parameters between control and VPS13A-depleted cells indicated a partial block of autophagy. For example, the strong decrease of GFP-LC3 and free GFP levels upon starvation is due to the autophagic lysosomal degradation of the marker (note the accumulation upon CQ addition) and this degradation was largely prevented in the VPS13A-depleted cells (FIG. 15A-B). In growth, higher levels of both markers are observed, which are not further increased by CQ.

LC3I levels were increased in the absence of VPS13A in comparison to the control cells regardless the conditions, which is indicative of an alteration in the balance of LC3-I production or lipidation. In addition, the difference of LC3-II in the presence and absence of CQ is reduced in VPS13A-depleted cells in both growth and starvation conditions, which is a strong indication of altered autophagic flux (FIG. 15 A-B).

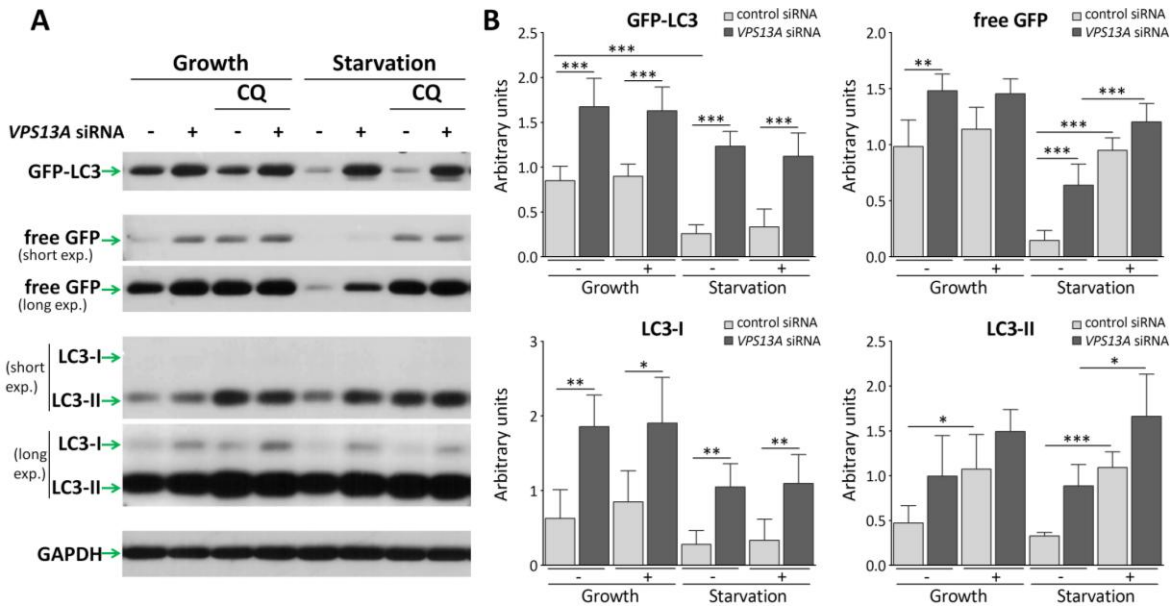

FIG. 15| Autophagic flux is impaired in VPS13A-depleted cells. (A) GFP-LC3, cleaved GFP, LC3-I and LC3-II in lysates of HeLa cells stably expressing GFP-LC3, treated with control or *VPS13A* siRNAs and incubated in complete or starvation medium in the absence or presence of 5 μM CQ during 4 h. A representative western blot of 5 independent experiments is shown (B) Protein bands were densitometred and normalized against GAPDH. Plots show mean values, SD and relevant significant differences.

The absence of VPS13C also resulted in some changes of these markers, indicating a probable partial impairment of autophagy, but less pronounced than those of VPS13A (not shown). VPS13A and VPS13C are very similar and it was possible that the loss of one protein could be partially compensated by the presence of the other. Therefore, we simultaneously silenced the expression of both genes, expecting to impair autophagic degradation to a higher degree. However, a functional redundancy of both proteins was not clear because some markers, such as LC3-II accumulation in basal conditions, showed a more severe change while others, such as LC3-I accumulation, showed an apparent alleviation (not shown). Such a complex outcome of the simultaneous silencing of *VPS13A* and *VPS13C* was similarly observed in further studies of autophagic markers in which cells were treated with both siRNAs. This suggested that VPS13A and VPS13C could have somehow related but not redundant roles. For simplicity, only the study of VPS13A, which has a stronger contribution to autophagy according to the assessment of autophagic flux, is included in this thesis.

4.6 | Further study of autophagy in VPS13A-depleted cells

To further characterize the role of VPS13A in autophagy, we visualized by confocal microscopy HeLa cells stably expressing GFP-LC3 and treated with control or *VPS13A* siRNA in complete and starvation medium. An increase in GFP-LC3 puncta was observed upon knockdown of *VPS13A* expression and, contrary to what it was observed in the siRNA control treated cells, the number of puncta did not increase upon starvation. Moreover, a difference of the pattern was noted. VPS13A silencing provoked the clustering of puncta in a

juxtanuclear localization while puncta in the control cells were more distributed. In addition, normal GFP-LC3 translocation from the nucleus to the cytoplasm upon starvation,[142] observed in the control cells, was impaired in VPS13A-depleted cells (FIG. 16) . Accumulation of LC3 was also observed in HeLa cells using antibodies against the endogenous protein in HeLa cells treated with the same and other siRNAs targeting *VPS13A* expression (not shown).

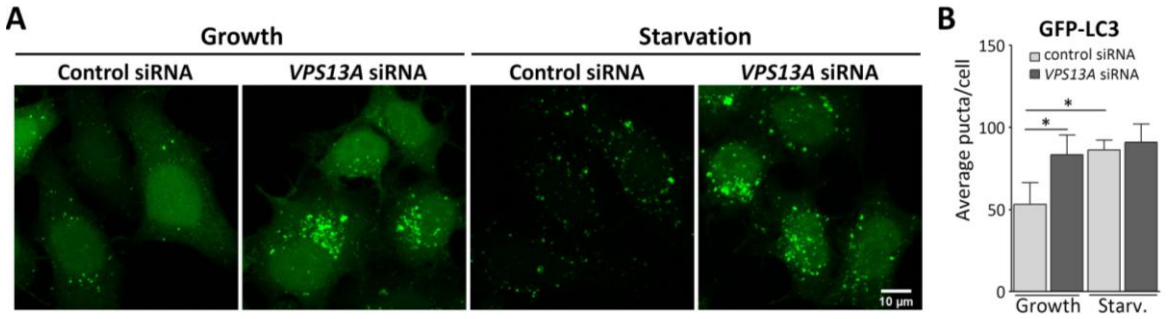

FIG. 16| LC3 is accumulated in VPS13A-depleted cells. (A) HeLa cells stably expressing GFP-LC3 were treated with control or *VPS13A* siRNAs, incubated in complete or starvation medium during 2 h and observed by confocal microscopy. Representative images are shown. (B) Quantification of an average of 36 cells per condition and per experiment of 3 independent experiments. Means and SD are plotted.

As we did when studying autophagy in *D. discoideum*, we used a homologue of Atg18, WIPI-1, to visualize the autophagic process with a different marker. We chose this protein because, although it is supposed to function at early stages of the process, its accumulation had been described as a consequence of defects in degradation.[239] WIPI-1 was transiently transfected in HeLa cells and observed in complete and starvation medium. When VPS13A was absent, WIPI-1 was accumulated and the number of puncta did not change upon starvation. Similarly to LC3, WIPI-1 also tended to cluster in a juxtanuclear region (FIG. 17).

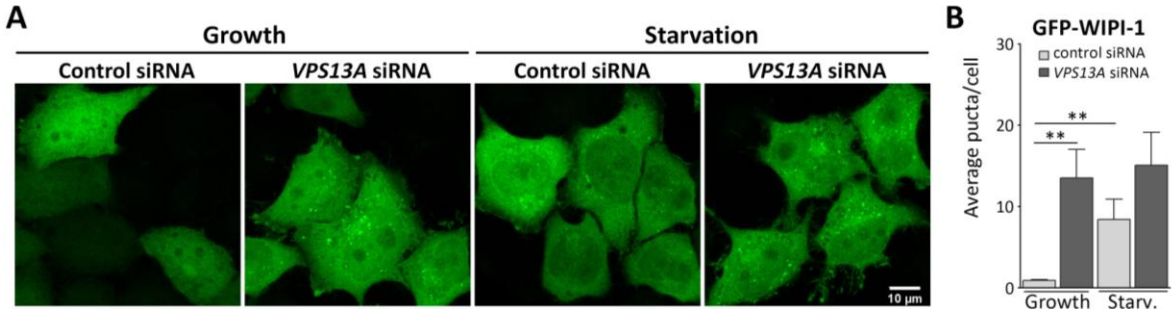

FIG. 17| WIPI-1 is accumulated in VPS13A-depleted cells. (A) HeLa cells were treated with control or *VPS13A* siRNAs, transiently transfected with GFP-WIPI-1, incubated in complete or starvation medium during 2 h and observed by confocal microscopy. (B) Quantification of an average of 30 cells per condition and per experiment of 3 independent experiments. Means and SD are plotted.

The autophagic flux measurements and the accumulation of LC3 and WIPI-1 indicated that autophagic degradation was partially impaired in the absence of VPS13A. A commonly used marker to analyze such phenotype is SQSTM1/p62, which is a protein that binds to ubiquitinated cargo for degradation and to LC3 and it is thus degraded by autophagy. As

expected, upon silencing of VPS13A expression, we found a severe accumulation of SQSTM1 (FIG. 18). This phenotype was observed using different *VPS13A* siRNAs (not shown).

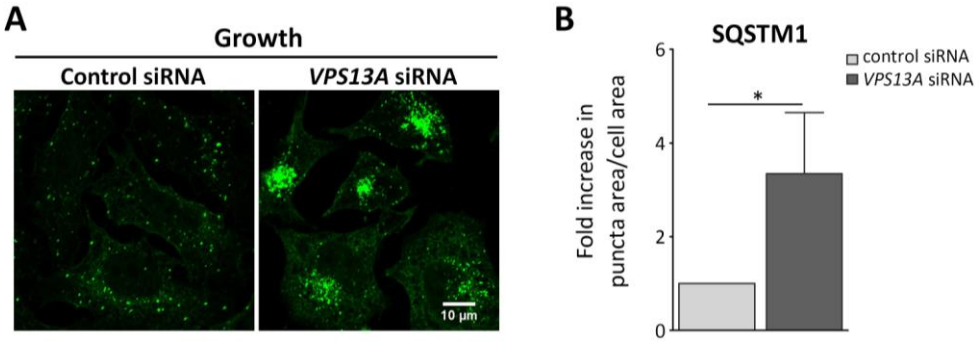

FIG. 18| SQSTM1/p62 is accumulated in VPS13A-depleted cells. (A) HeLa cells were treated with control or *VPS13A* siRNAs and endogenous SQSTM1 was observed by confocal microscopy. (B) Quantification of an average of 58 cells per condition and per experiment of 4 independent experiments. Means and SD are plotted.

Impairment of autophagic degradation can occur because of a blockage at the closure, fusion or degradation steps. To know if the defect in VPS13A-depleted cells occurred before or after fusion of autophagosomes with the degradative compartments, we used another marker, mTagRFP-mWasabi-LC3.[345] This tandem-fluorescent LC3 (tf-LC3) is informative of fusion with acidic vesicles because green fluorescence of mWasabi ($pK_a = 6.5$)[345] is quenched inside the acidic lysosomes (pH≃4.7 in HeLa cells)[212] while mTagRFP red fluorescence ($pK_a < 4$)[345] is not sensitive to this pH. Consequently, autophagosomes and autolysosomes are seen as yellow and red puncta, respectively.[345] Therefore, an increase of yellow puncta indicates impairment of fusion and an increase of red puncta is representative of a defect of lysosomal degradation, and thus this marker would show at which step was autophagy impaired in the absence of VPS13A. However, we did not find changes in the proportion of colors despite the increase in total puncta and their accumulation at a juxtanuclear area. (FIG. 19).

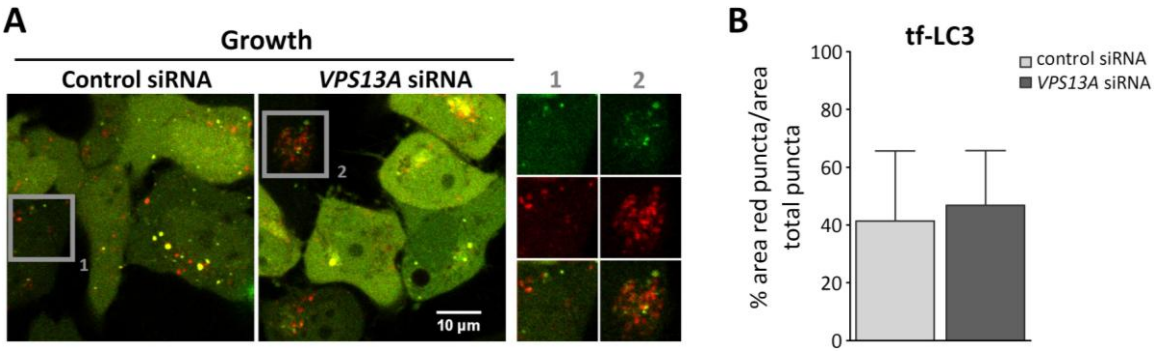

FIG. 19|Non-acidic and acidic autophagosome derived vesicles are accumulated in VPS13A-depleted cells. (A) HeLa cells were treated with control or *VPS13A* siRNAs, transiently transfected with mTagRFP-mWasabi-LC3 and observed by confocal microscopy. Insets show green and red channels separately in selected areas in order to better visualize red puncta in which green fluorescence is absent. (B) Quantification of an average of 22 cells per condition and per experiment of 4 independent experiments. Means and SD are plotted.

Such an effect is usually interpreted as an induction of autophagy consistent with an increase of generation of autophagosomes (more yellow puncta) and of their degradation (more red

autophagolysosomes). As we knew from the previous experiments that autophagic flux was impaired in VPS13A depleted cells, we reasoned that fusion with acidic compartments when VPS13A is absent does not necessarily mean that fusion with lysosomes and degradation capacity are completely functional. A proportion of the observed puncta could correspond to amphisomes, which would be labeled in yellow or red depending on their pH (5.9-6.8 in EE; 5.4-5.6 in LE),[297] and the accumulation could be due to a diminished fusion of amphisomes with lysosomes. Alternatively, it was also possible that autophagosomes and amphisomes fuse correctly with lysosomes but that the autophagolysosomes and endolysosomes have a higher pH and a hampered degradative activity. Taken together, these results suggest that the lack of VPS13A in HeLa cells affects the late stages of autophagosome degradation.

4.7 | Identification of *Dictyostelium* VPS13 proteins interactors

In order to shed light on the molecular function of VPS13 proteins in autophagy, we sought potential interactors of VPS13 proteins with a role in autophagy.

We showed above that the C terminus of TipC was able to function on its own to some extent, at least regarding some autophagy-related roles. Consequently, we assumed that this region of the protein could potentially interact with proteins necessary for the execution or regulation of those functions. We also included in the analysis the N-terminal region of TipC because, given the strong conservation of this region in all VPS13 proteins, we considered that it could also be important for some VPS13 functions.

Protein extracts from the strains expressing *D. discoideum* TipC^{Cterm}-GFP or TipC^{Nterm}-GFP were used for pull down of the tagged polypeptides and identification of possible interactors by liquid chromatography coupled to tandem mass spectrometry (LC-MS/MS). The identification of proteins that co-immunoprecipitated with the tagged polypeptides was made by database searching of the detected peptides. Only the proteins not appearing in a control GFP pull-down sample and presenting a coverage above 10% were considered strong candidates for the interaction **(TABLE 1A-B)**. Due to their abundance, 60S and 40S ribosomal proteins were ignored even if meeting the cited criteria.

Assuming that the strong conservation of both regions in all VPS13 proteins could be related to their interaction with other proteins, we also included in this analysis the pull downs of the N- and C-terminal regions of *D. discoideum* Vps13A **(TABLE 1C-D)**. We chose this protein because it shows the highest similarity to the four human VPS13 proteins (followed by TipC); but specially because *vps13A*$^-$ strain is the only one, besides *tipC*$^-$, to have a reduced autophagy flux. The expression of the N- and C-terminal Vps13A polypeptides was verified by

fluorescence microscopy, which did not reveal a specific pattern but some bright puncta as in the case of TipC, and by western blot to confirm their correct molecular weight (not shown).

UniProt ID	Protein name	(A) TipC N-term	(B) TipC C-term	(C) Vps13A N-term	(D) Vps13A C-term
Q54GX7	Actin-10	41.8 (13)	46.0 (12)	31.9 (10)	32.4 (10)
P07828	Actin-18	10.8 (1)	15.0 (1)	15.0 (1)	15.0 (2)
Q55EU6	Putative actin-23	34.9 (1)		24.6 (1)	25.1 (1)
P0CT31	Elongation factor 1-alpha	28.0 (11)	28.0 (10)	12.6 (6)	14.8 (4)
P08799	Myosin-2 heavy chain				20.9 (37)
P13833	Myosin regulatory light chain				13.0 (2)
P15064	Ras-like protein RasG	18.0 (2)	30.2 (4)		
P32252	Ras-like protein RasB		11.2 (2)		
P34139	Ras-related protein Rab-1A	20.8 (2)	34.7 (4)		
Q54NU2	Ras-related protein Rab-1D	22.5 (2)	22.5 (2)		
P36411	Ras-related protein Rab-7A	22.2 (4)	15.3 (3)		10.3 (1)
P34144	Rho-related protein Rac1A	10.3 (2)	21.1 (4)		
P02599	Calmodulin	18.4 (2)			
P02887	Discoidin-1 subunit B/C	20.6 (4)		10.7 (2)	
Q76NW2	Histone H4				27.8 (3)
Q54J48	Probable pyridoxal 5'-phosphate synthase subunit pdx2		21.8 (3)		
Q54XE6	Probable H/ACA ribonucleoprotein complex subunit 1				18.7 (4)
Q8MPA5	Small heat shock protein hspG7		19.8 (1)		
Q550E9	Small heat shock protein hspG8				10.4 (1)
P14794	Ubiquitin/ribosomal protein L40	41.4 (4)	41.4 (4)		23.4 (2)

TABLE 1 | Strong candidates for the interaction with the N- and C-terminal regions of TipC and Vps13A *D. discoideum* proteins. The percent protein coverage is indicated in each case and the number of unique peptides passing a cutoff of false discovery rate (FDR) > 0.1% is written in brackets.

None of the identified proteins are direct players of the autophagic pathway. Nevertheless, some candidates have established roles in autophagy. This is the case of Rab proteins.[10,125,294] As mentioned in the introduction, VPS13B and VPS13C had already been described respectively as RAB6 and RAB7A interactors,[179,276] which suggests that RAB proteins could be relevant partners for VPS13 proteins and support the further study of the interaction of additional VPS13 proteins with RABs.

We intended to carry out a similar approach with the equivalent N- and C-terminal regions of the human VPS13A protein. This would have served to know if the interaction with RABs or other proteins was conserved and to identify additional potential interactors that could aid in the elucidation of VPS13A functions. Unfortunately, the expression of those fragments was not stable in different cell lines (barely any fluorescence was observed by confocal microscopy and only fragments of smaller molecular weight than the expected one were identified by western blot).

4.8 | Conserved interaction of TipC and VPS13A with RAB7

As RAB7A (herein called RAB7 for simplicity) has been described to participate in the fusion of LE or amphisomes with lysosomes,[124] we centered our efforts to confirm the RAB7-VPS13 interaction by coimmunoprecipitation. Protein extracts from *tipC*⁻ *D. discoideum* cells expressing TipC$^{C\text{-}term}$-GFP and Rab7 tagged with HA (HA-Rab7) were used for immunoprecipitation. The TipC polypeptide efficiently immunoprecipitated HA-Rab7 (FIG. 20).

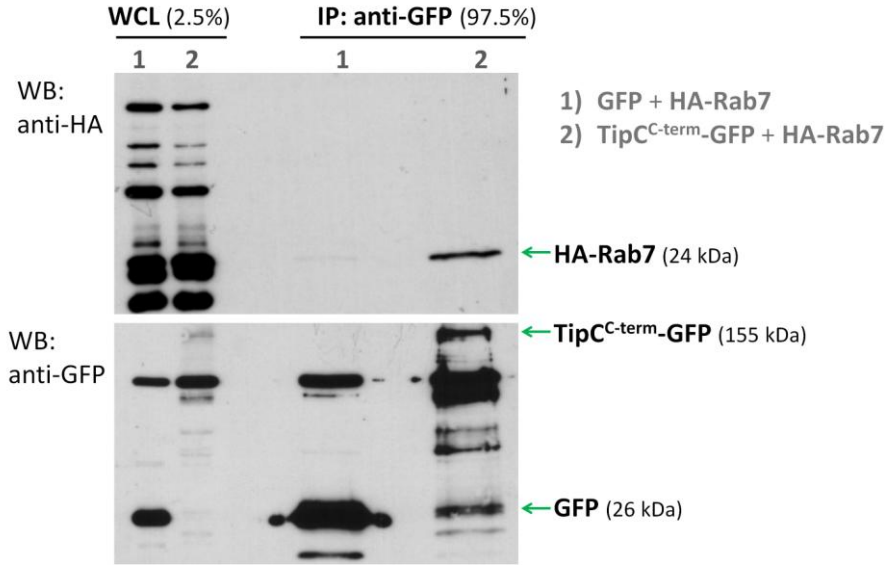

FIG. 20| **Rab7 coimmunoprecipitates with the C terminus of TipC.** The C terminus region of TipC was immunoprecipitated in lysates of the *tipC*⁻ mutant overexpressing this polypeptide and HA-Rab7. The immunoprecipitates were analyzed by western blot using an anti-HA antibody and an anti-GFP antibody. An immnoprecipitation of GFP was used as a control. Grey numbers above each lane indicate the sample loaded in the lane; the legend is shown in grey on the right. The percentage of sample loaded is indicated for WCL (whole cell lysates) and IP (immunoprecipates). Representative western-blot of 4 independent experiments.

Regarding human VPS13 proteins, the interaction of VPS13C with RAB7 had already been described.[179] In order to know if VPS13A also interacts with RAB7, and as we had observed that the VPS13A antibody was able to detect VPS13C, we inhibited by siRNA the expression of *VPS13A* or *VPS13C* before the immunoprecipitation of transiently transfected GFP-RAB7. Both endogenous VPS13A and VPS13C were immunoprecipitated by GFP-RAB7 at higher levels over the control GFP, although a high exposure is needed for their detection in the immunoprecipitates, suggesting that the interaction is labile or transient (FIG. 21).

4.9 | VPS13A subcellular localization

In order to determine the subcellular localization of VPS13A and the possible colocalization with RAB7, both endogenous VPS13A and an overexpressed GFP-tagged version were visualized by confocal microscopy.

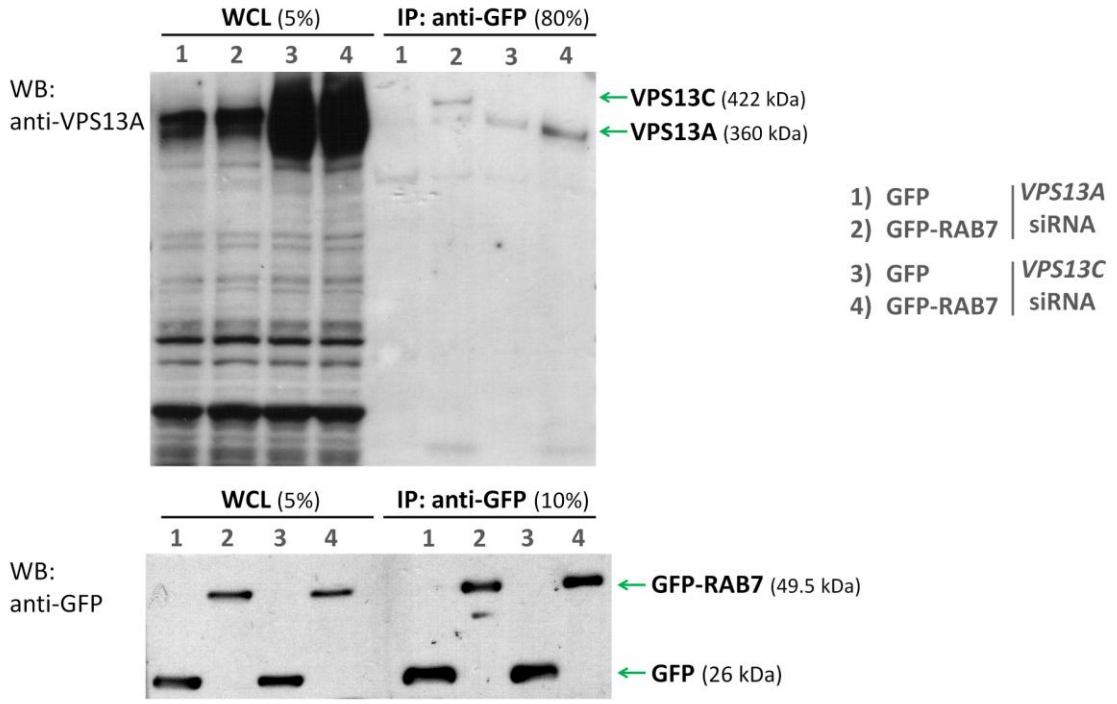

FIG. 21| VPS13A and VPS13C immunoprecipitate with RAB7. GFP-RAB7 was immunoprecipitated from lysates of HeLa cells treated with *VPS13A* or *VPS13C* siRNAs and transiently transfected with GFP-RAB7. The immunoprecipitates were analyzed by western blot using an anti-VPS13A antibody and a anti-GFP antibody in two different western blots. The electrophoresis of the samples in two gels with different acrylamide percentage was required in order to obtain a good separation of VPS13A and VPS13C bands and to visualize GFP. Grey numbers above each lane indicate the sample loaded in the lane; the legend is shown in grey on the right. The percentage of sample loaded is indicated for WCL (whole cell lysates) and IP (immunoprecipates).

We first performed an immunofluorescence against the endogenous VPS13A with the same antibody used for western-blot detection. As the antibody was able to recognize VPS13C by western-blot, we assessed its specificity by immunofluorescence using cells in which VPS13A and VPS13C had been depleted by siRNA. The antibody sensitivity was poor but, in spite of the high background signal, a characteristic pattern could be visualized in control cells that was lost specifically in VPS13A-depleted cells. This pattern consisted on many puncta distributed along a sort of network. Some disperse bright puncta were visualized but their specificity was dubious as a few scattered bright puncta were also observed in the absence of VPS13A. VPS13C depletion did not result in any obvious change of the fluorescent pattern and thus we believe that we can use this antibody to specifically study the subcellular localization of VPS13A (FIG. 22); specially because, among a set of many commercial antibodies tested by us, this was the only one labeling subcellular structures disappearing upon VPS13A inhibition (not shown).

As the signal obtained by immunofluorescence was very low, we decided to overexpress the protein fused to EGFP. By the time of starting this approach, a report was published showing that the N- and C-terminal tagging of yeast Vps13 render the protein non-functional, at least with respect to some phenotypes. However, when the EGFP was inserted into a specific

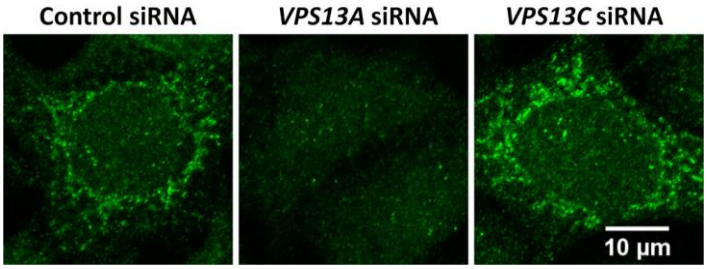

FIG. 22| VPS13A presents a distinct subcellular pattern. HeLa cells were treated with control, *VPS13A* or *VPS13C* siRNAs and the endogenous VPS13A protein was observed by immunofluorescence and confocal microscopy. The same VPS13A specific pattern was observed in COS-7 cells (not shown).

location inside the coding sequence of the gene, the protein became completely functional.[154] Another article with similar results but with the tag at other internal position was published later.[228] Therefore, we designed a plasmid in which EGFP was inserted in frame into the human *VPS13A* sequence in the equivalent position to that of yeast *VPS13* in the first reported article. To generate this complex construct, we performed a gap repair approach, which takes advantage of the efficient homologous recombination of yeast **(FIG. 23)**.[131]

The overexpressed tagged VPS13A had the expected molecular weight (confirmed by western blot, not shown) and was distributed in the cell in the characteristic pattern observed for the endogenous VPS13A **(FIG. 23)**. However, only a very small percentage of cells was transfected and the signal in the transfected cells had a very low intensity. The size of the plasmid (17kb) was probably the bottleneck hampering the transfection efficiency, which could not be enhanced despite our efforts using several different protocols and transfection methods. From that plasmid we have very recently generated a new one with a shorter size (14kb) that is more efficiently transfected and results in a better signal. This plasmid will be probably a valuable tool to study VPS13A localization and interactors in the future.

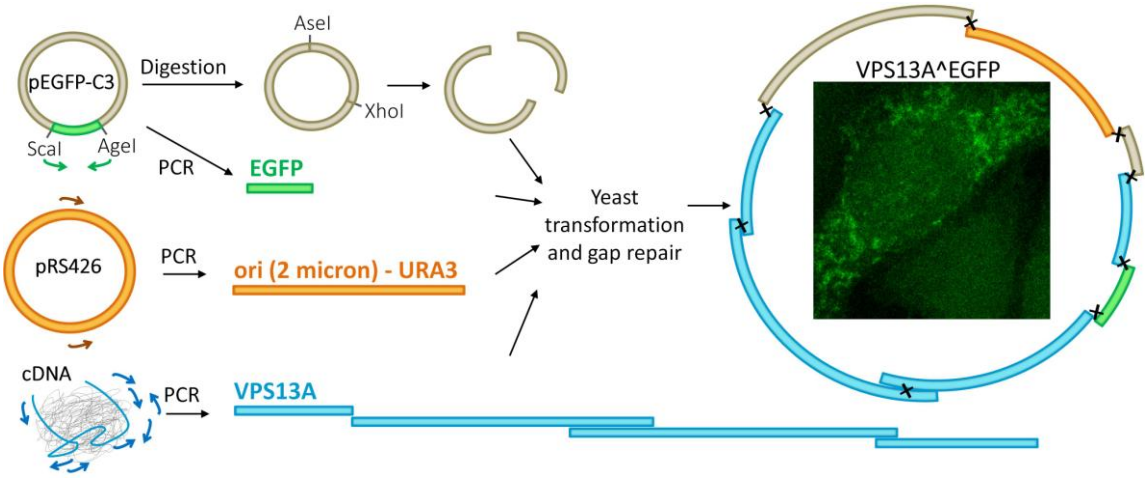

FIG. 23| Generation of a mammalian expression vector for VPS13A^EGFP by yeast GAP repair. PCR fragments corresponding to *VPS13A* cDNA, EGFP, all the elements necessary for plasmid selection and amplification in yeast cells and two fragments of a digested mammalian expression vector were introduced in yeast cells, where they were all assembled by homologous recombination. The plasmid was subsequently isolated from yeast cells, expanded and isolated in *E. coli* and transfected in HeLa cells. An example of a HeLa cell transiently transfected with the resulting plasmid and visualized by confocal microscopy is shown.

As the expression vector for VPS13A^EGFP still required further optimization in order to obtain an adequate signal, we started the subcellular localization analysis of endogenous VPS13A with the available antibody despite its low quality. We also evaluated VPS13A colocalization with autophagic markers and with RAB7, considering our interest in autophagy and the observed interaction of VPS13A with RAB7 by coimmunoprecipitation.

We used markers for different organelles. Poor or no colocalization was observed with the ER, the Golgi apparatus, endosomes, autophagosomes and lysosomes although, due to the low signal, we cannot rule out the possible presence of low levels of VPS13A in these organelles. In fact, occasional and partial colocalizations were observed in some puncta labeling these organelles. Interestingly, a clear proximity and partial colocalization was observed with mitochondria suggesting that VPS13A may have a role associated to this organelle **(FIG. 24)**.

4.10 | Endocytic traffic in VPS13A-depleted cells

We hypothesized that the role of VPS13A in autophagy was related to RAB7, a regulatory protein of the endocytic traffic. We therefore analyzed the pattern of RAB7 and other endosomal markers upon *VPS13A*-siRNA treatment. RAB7 was strongly accumulated in the same juxtanuclear region as it was previously observed for LC3 in the absence of VPS13A **(FIG. 25)**. The accumulation of endogenous RAB7 was also noticed by western blot and after treatment with distinct *VPS13A* siRNAs (not shown).

The accumulation of RAB7, and hence LE, suggested that the endocytic pathway is altered by the loss of VPS13A. As another marker of the endocytic pathway, we visualized RAB5 (a protein at EE) and it was also accumulated and clustered in the same region as RAB7 and LC3 **(FIG. 25)**. Such a strong accumulation in the same region hampered the clear assessment of relative colocalization of markers that would serve to evaluate potential defects in endosomal maturation or in autophagosome-endosome fusion. A partial delay of both processes was suggested by the preliminary data but the results were not conclusive (and hence, not shown).

The perinuclear area is known to concentrate most lysosomes for degradation of both autophagosomes and LE/MVB and thus the accumulation of autophagy and endosomal markers suggest a defect at the level of degradation. This could be the result of abnormal maturation of endosomes and autophagosomes, defects in the fusion with lysosomes or even in the degradative activity in endolysosomes or autophagolysosomes.

Maturation of endosomes is characterized by a decrease of luminal pH among other changes such as conversion of PIPs and a switch of RAB proteins.[118]

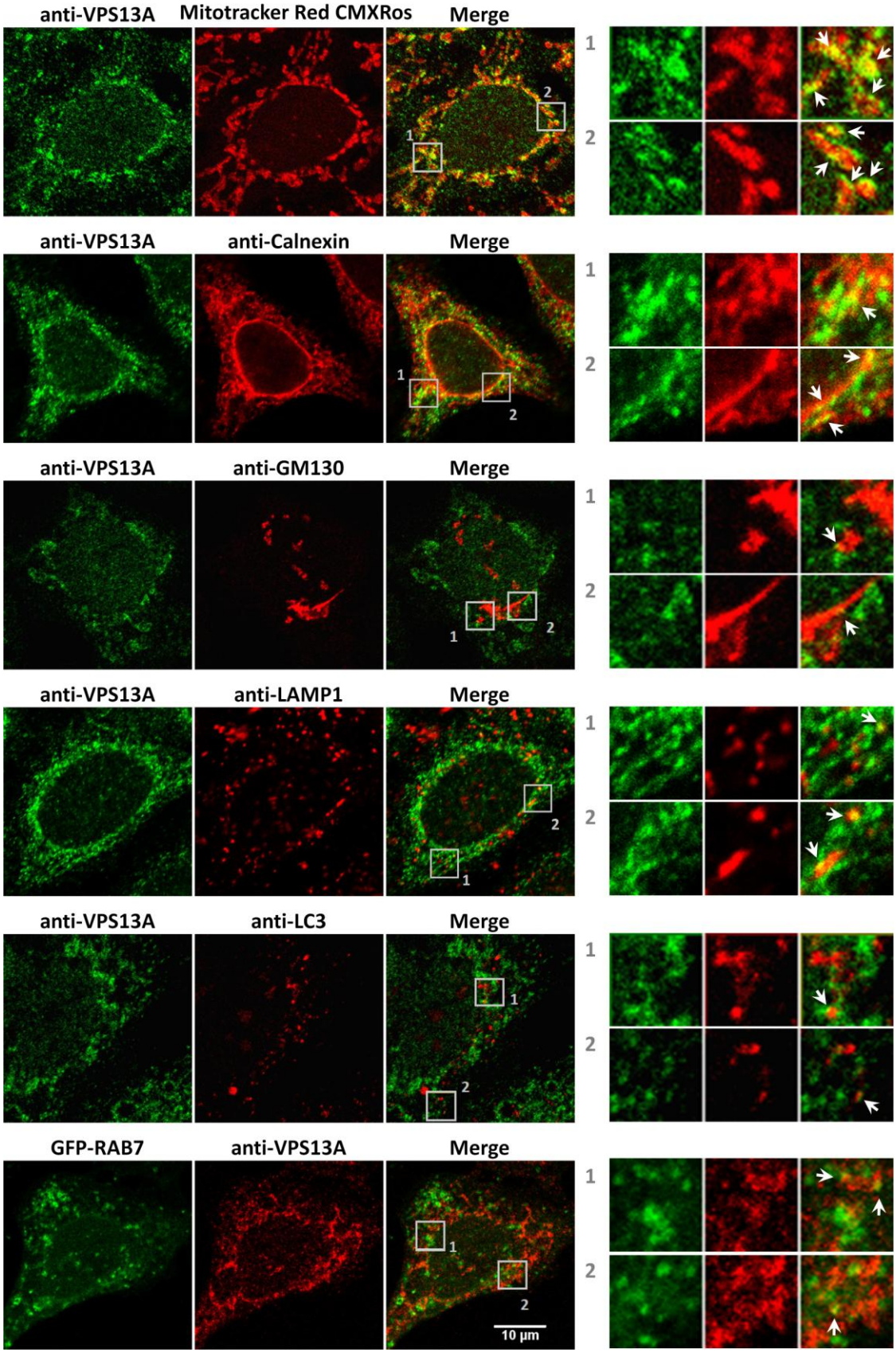

FIG. 24| VPS13A partially colocalizes with mitochondria. Endogenous VPS13A was labeled by immunofluorescence and visualized in HeLa cells stained with Mitotracker Red CMX ROS to stain mitochondria, transiently transfected with RAB7 to visualize LE or cells labeled with antibodies against GM130, calnexin, LAMP1 or LC3 (markers of the *cis*-Golgi, ER, lysosomes or autophagosomes, respectively). Examples of VPS13A puncta colocalizing with those markers are indicated by white arrows in the enlargements of selected areas.

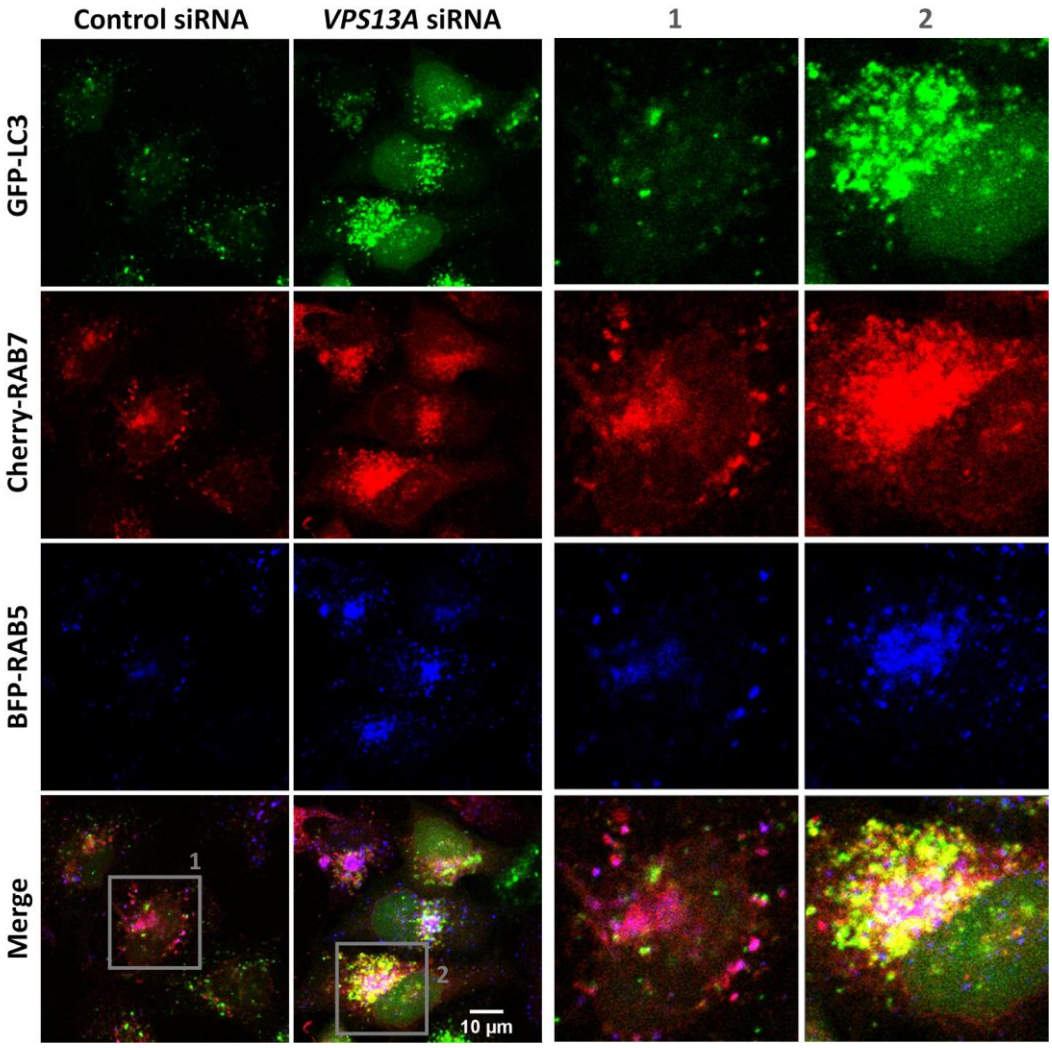

FIG. 25| Autophagosomes and endosomes are accumulated in VPS13A-depleted cells. HeLa cells stably expressing GFP-LC3, were treated with control or *VPS13A* siRNAs and transiently transfected with RAB7 and RAB5. Enlargements of selected areas are shown. Images are representative of three independent experiments.

A severe defect in acidification was not expected as we had observed quenching of mWasabi fluorescence and thus red puncta when we visualized the tf-LC3 in HeLa cells depleted of VPS13A.

We found that, in the absence of VPS13A, lysosomes visualized by immunodetection of LAMP1 (a glycoprotein at the membrane of lysosomes) and CTSB (cathepsin B; a lysosomal cysteine protease), accumulated in a juxtanuclear region, similarly to the accumulation observed of autophagic and endosomal markers (FIG. 26).

The evaluation of the colocalization of these two proteins could be useful to uncover a potential defect in the delivery of lysosomal hydrolases to lysosomes. The extensive colocalization of LAMP1 and CTSB indicates that there is not a dramatic impairment of this delivery, but a partial defect might exist that would lead to a decreased degradation capacity of lysosomes. Unfortunately, as in the case of endosomal markers, the severe accumulation of

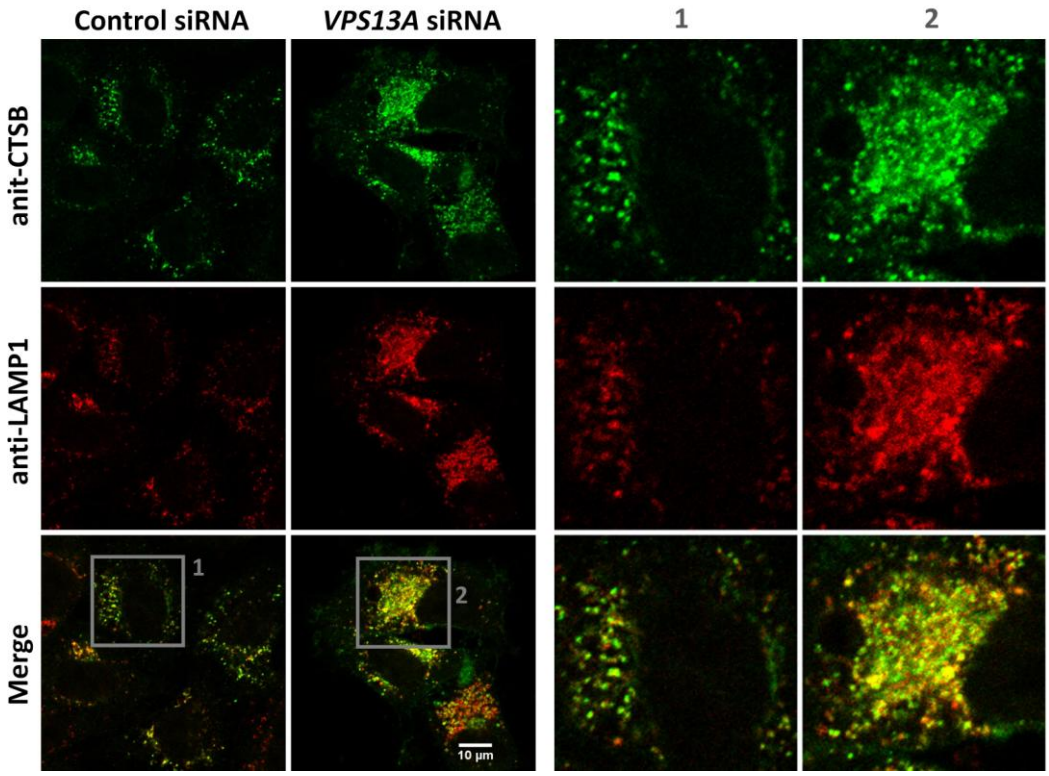

FIG. 26| Lysosomes are accumulated in VPS13A-depleted cells. HeLa cells were treated with control or *VPS13A* siRNAs and endogenous LAMP1 and CTSB were observed by immunofluorescence. Enlargements of selected areas are shown. Images are representative of three independent experiments.

both proteins in the absence of VPS13A hampers a precise analysis of the relative colocalization of the proteins with each other and a clear conclusion was not reached.

Lysosomal hydrolases such as CTSB might be correctly delivered to lysosomes but not be active, provoking a degradation defect. Lysosomal hydrolases are synthesized as proenzymes and delivered in such form to the lysosomes. There, the acidic environment allows the proenzymes release from their receptors (which cycle back to the TGN) and the proteolytic cleavage of proenzymes to form active acid hydrolases. CTSB cleavage of its propeptide generates an active single chain protease. In the case of CTSB, this mature form can be further processed into a double chain form by an additional cleavage that generates a heavy chain and a light chain.[2,32,308]

As an indicator of protease activity, we evaluated the processing of CTSB and we found it was diminished in the absence of VPS13A (FIG. 27). This could indicate a slight defect in the delivery of CTSB to lysosomes or in acidification of lysosomes. A precise measure of lysosomal pH would be necessary to know if the defect of CTSB processing is due to a reduced acidification of lysosomes or to the delivery to lysosomes. Taken into account the described role of yeast Vps13 in TGN to PVC trafficking, the later could be the case, but further research is needed to determine if that is the defect in the absence of human VPS13A.

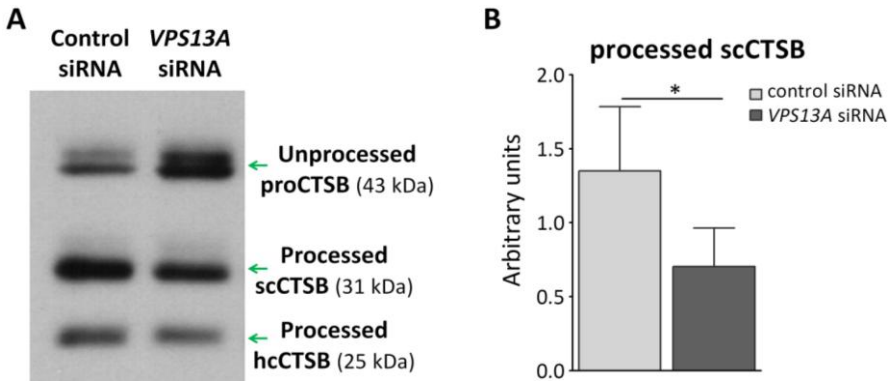

FIG. 27| **CTSB processing is reduced in VPS13A-depleted cells.** (A) CTSB unprocessed (proCTSB) and processed single chain (scCTSB) and heavy chain (hcCTSB) forms of cathepsin B in lysates of HeLa cells treated with control or *VPS13A* siRNAs were analyzed by western blot. A representative experiment of 4 independent experiments is shown. (B) The unprocessed inmature proCTSB and the proteolytically cleaved mature scCTSB were densitometred and the ratio was calculated. Plots show mean values and SD.

4.11 | Ultrastructural analysis of VPS13A-depleted cells

From the previous experiments, lysosomal degradation capacity might be impaired in the absence of VPS13A and that would provoke a delay in autophagolysosome and endolysosome degradation. However, a defective fusion of autophagosomes, amphisomes and endosomes with lysosomes could also be the cause of the observed accumulation of non-degraded autophagosomes and endosomes. Relative colocalization of autophagosomes and LE with lysosomes was attempted to be analyzed by confocal microcopy (not shown) but, similar to what was already mentioned regarding colocalization with other markers, the severe accumulation in the absence of VPS13A hampers an accurate evaluation of the relative colocalization of markers and hence modest defects in fusion processes could have been neglected by conventional confocal microscopy, which has a limited spatial resolution (only cellular elements separated by more than approximately 250nm can be individually visualized).[135] Visualization by transmission electron microscopy (TEM) can better define the identity of the accumulated structures. Therefore, control and *VPS13A* siRNAs were transfected in HeLa cells and processed for TEM visualization.

EE are usually visualized by TEM as fairly electron lucent vacuoles with an approximate diameter of 100-500 nm and very heterogeneous morphology. Tubules usually emerge from EE but their visualization together with the vacuole is not frequent in thin sections. LE (250 to 1000 nm) are defined as such by the presence of ILV, with a typical size of 40-100 nm. ILV already form at EE but many more are present in LE, which are thus also called MVB. In our analysis we have considered an endosome is a LE when at least 5 ILV can be observed. When, apart from ILV, electron dense material is part of the heterogeneous LE content, we assume that the LE has been fused with lysosomes and therefore it is an endolysosome. Their size ranges from 200 to more than 1 μm. Within this endolysosome feature we cannot distinguish

those vesicles derived from LE, autophagosomes or amphisomes fused to lysosomes, the later defined as vesicles whose lumen is more homogeneous and electron dense.[118,144]

Taking these criteria into account, we classified the endocytic vesicles observed upon VPS13A depletion in HeLa cells. The size of different types of endosomes was not significantly altered but we observed a higher number of endolysosomes, indicating that the blockage in the endosomal pathway is at the level of endosomal degradation rather that at endosomal maturation or fusion of endosomes with lysosomes. The blockage in degradation is probably the cause of LC3 accumulation because few autophagosomes, distinguished by an intact double membrane, are observed, suggesting that the LC3 accumulation is not due to a defect of autophagosome fusion with endosomes or lysosomes but to an impaired amphisome and autophagolysosome degradation. Similar results were observed using two different *VPS13A* siRNA sequences to knock down *VPS13A* expression **(FIG. 28)**.

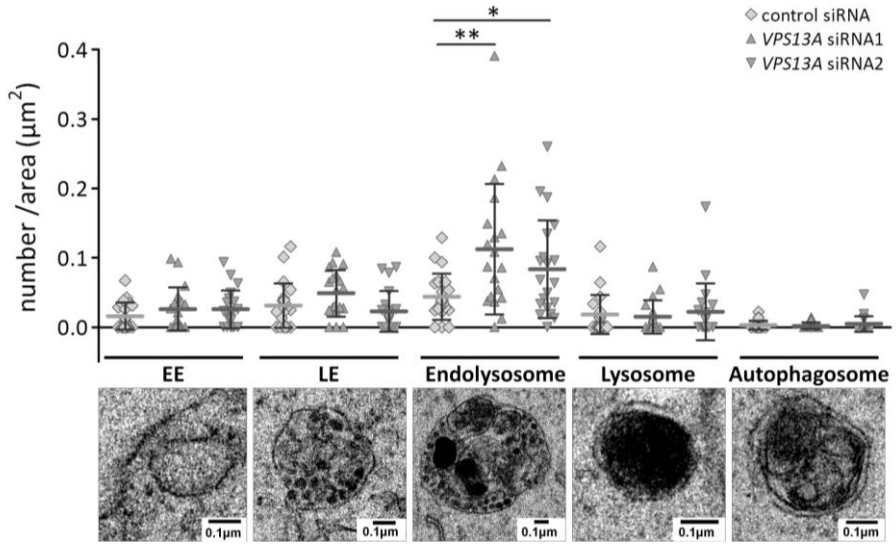

FIG. 28| Endolysosomes are accumulated in VPS13A-depeleted cells. HeLa cells treated with control or *VPS13A* siRNAs were observed by TEM. The number of endocytic and autophagic vesicles and lysosomes (an example of each is shown) were quantified in 19 electron micrographs of random cell sections per sample.

TEM spatial resolution allows the correct visualization of MCS, which are very interesting in the study of VPS13A according to the described localization of yeast Vps13 at vCLAMPs and NVJ and the ability of Vps13 localization at vCLAMPs to compensate ERMES deficiency.[154,228] It has been demonstrated that, in yeast, the absence of both ERMES and vCLAMPs is lethal but that an increase of vCLAMPS can compensate the deficiency of ERMES and *vice versa*.[73,114] As the lack of ERMES can be compensated by yeast Vps13 localization at vCLAMPs and the inability of Vps13 to localize at vCLAMPs leads to lethality when ERMES is also lost,[154,228] we hypothesized that MCS could be altered in the absence of VPS13A in mammalian cells.

In metazoans, no contacts between endosomes or lysosomes and mitochondria have been characterized yet. However, such contacts and their potential alteration in the absence of

VPS13A would be an attractive way to connect our observations: the partial localization of VPS13A at the mitochondria and the effects of VPS13A loss on the endocytic pathway. Supporting the existence of MCS between mitochondria and the endocytic pathway, contacts between mitochondria and melanosomes, a lysosome-related organelle, have been described.[56] The membranes of both organelles at those contacts have been described to be at 20-30 nm. Interestingly, this distance matches the longitude reported for the Vps13 protein (20 nm). We visualized endocytic vesicles occasionally being at such distance (below 30 nm) of mitochondria in our TEM analysis. However, neither the mean number of those contacts per mitochondria and nor the length of those contacts were significantly different between control and VPS13A-depleted cells **(FIG. 29A)**. Similarly, no differences were found considering a distance between mitochondria and endosomes below 100 nm (not shown).

We have also analyzed the MCS between the ER and mitochondria in our samples. The proteins that constitute the ERMES are not conserved in metazoans, but different MCS between the ER and mitochondria have been described and called MAMs (Mitochondrial Associated Membranes).[309] MAMs have been demonstrated to be altered by the absence of specific proteins such as VMP1,[296] and we wanted to know if VPS13A loss could have an impact on MAMs. According to the previous literature, a distance below 30 nm was defined to consider the closeness of the two organelles as a MAM. We found that the average number of MAM per mitochondria was similar in all the samples. The length of MAMs was significantly smaller upon knockdown of *VPS13A* expression with one of the *VPS13A*-siRNAs (siRNA-1) but not with the other (siRNA-2), and therefore, the importance of VPS13A regarding MAMs length is uncertain **(FIG. 29B)**.

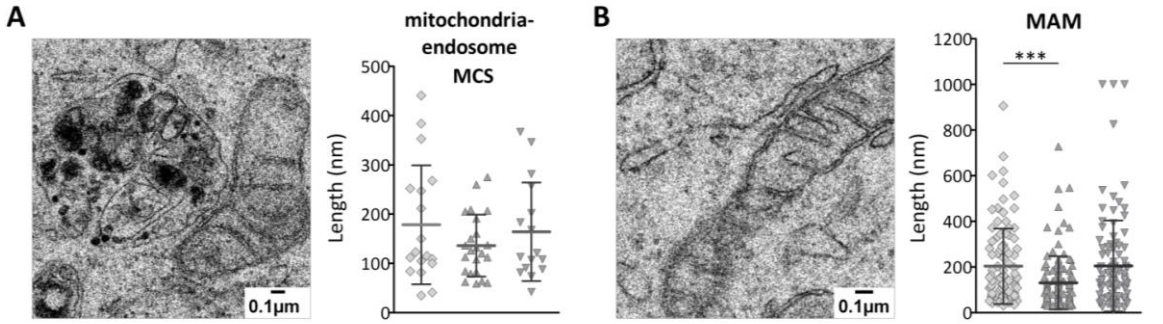

	mitochondria (total)	M-E MCS (total)	M-E MCS/mitochondria (mean ± SD; n=19)
◆ control siRNA	249	18	0.072 ± 0.260
▲ VPS13A siRNA1	317	23	0.073 ± 0.305
▼ VPS13A siRNA2	300	16	0.053 ± 0.225

	mitochondria (total)	MAMs (total)	MAMs/mitochondria (mean ± SD; n=19)
◆ control siRNA	249	102	0.430 ± 0.699
▲ VPS13A siRNA1	317	115	0.366 ± 0.683
▼ VPS13A siRNA2	300	103	0.343 ± 0.664

FIG. 29| VPS13A-depletion does not modify the number of MCS but it might alter their length. HeLa cells treated with control or *VPS13A* siRNAs were observed by TEM. MCS between the mitochondria and endosomes (A) and between the mitochondria and the ER (B) were evaluated. An example of each type of MCS is shown. The tables include the number of total mitochondria and total MCS quantified in 19 electron micrographs of random cell sections per sample and the calculated number of MCS per mitochondria. The length of each MCS was measured and plotted in the graphs. Means and SD are shown.

The mitochondrial localization of VPS13A, together with the reported functions of yeast Vps13 and human VPS13C related to suppression of mitophagy,[161,228] and the fragmentation and modifications of their morphology observed in the absence of VPS13C,[126,161] lead us to analyze mitochondrial levels and morphology. No differences were found in the number of mitochondria in VPS13A-depleted cells observed by TEM. In addition, levels of mitochondrial proteins, analyzed by western blot, are not modified upon inhibition of *VPS13A* expression (not shown). Both observations suggest that mitophagy is not being largely altered in these conditions.

Several morphometric parameters of mitochondria morphology were analyzed by TEM. We found modest changes in mitochondria only when cells were treated with the specific *VPS13A* siRNA-1. They comprise decreases mitochondrial size and decreased length of cristae per mitochondrial area. Mitochondrial size is unaltered upon knockdown of *VPS13A* expression using the alternative siRNA-2, but the length of cristae per mitochondrial area does show a tendency to decrease (albeit non significant) (FIG. 30). Other parameters such as axial length ratio did not show any significant differences upon treatment with any of the two used *VPS13A* siRNAs. Consequently, no gross defects were observed in mitochondrial morphology in the absence of VPS13A, however further studies aimed to asses mitochondrial functions should be performed.

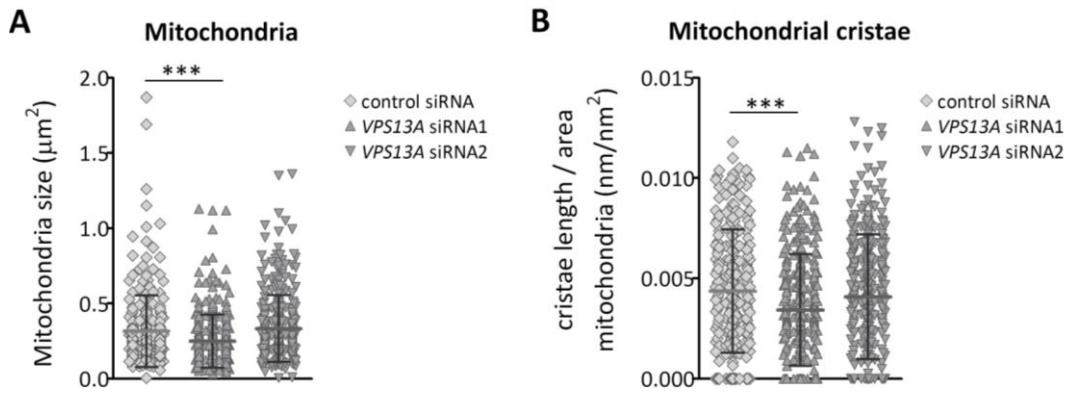

FIG. 30| Some mitochondria features might be altered in VPS13A-depleted cells. HeLa cells treated with control or *VPS13A* siRNAs were observed by TEM. Mitochondrial area (A) and the length of cristae per mitochondrial area (B) were measured in the mitochondria (n=249, n=317 and n=300 for control siRNA, *VPS13A* siRNA-1 and *VPS13A* siRNA-2 treated cells, respectively) of 19 electron micrographs of random cell sections per sample.

5 | DISCUSSION

5 | DISCUSSION

In this chapter, our results on VPS13 roles, interactor partners and subcellular localization are discussed taking into account the related literature. Future research to unveil the exact molecular role of VPS13A and to consider autophagy and lysosomal dysfunction as possible targets for the treatment of ChAc will be also discussed.

5.1 | Role of VPS13 proteins in autophagy and endocytic traffic

The first evidence of the relationship of VPS13 proteins with autophagy has been our description of a deficient autophagic flux in the absence of the *D. discoideum* protein TipC, a member of the VPS13 family. Autophagy in the *tipC*$^-$ mutant was assessed based on its observed multitipped phenotype, which is a typical developmental phenotype of autophagy mutants.[184,222,223,306] We also evaluated autophagic flux of the other non *vps13*$^-$ multitipped mutants described at the same time than *tipC*$^-$. We found that *tipC*$^-$ and *tipD*$^-$, showed a clear impairment of autophagy, which was confirmed by the aberrant pattern of two autophagic markers, Atg18 and Atg8, and the colocalization of the later with ubiquitin. Only the characterization of the *tipC*$^-$ mutant has been included in this thesis; that of *tipD*$^-$ can be read, if desired, in the annexed article.[202]

Before discussing VPS13 roles in autophagy, it is worthwhile mentioning that we have demonstrated the value of the multitipped phenotype as a helpful clue to identify autophagy mutants in *D. discoideum*. We now consider that the alleviation of this phenotype in the *tipC*$^-$ mutant might be similarly a very convenient tool for the screening of drugs that could mitigate the defects caused by the absence of VPS13 proteins.

The *tipC*$^-$ mutant is the only *vps13*$^-$ mutant with a multitipped phenotype and the one with the most severe defect in autophagy. The lack of Vps13A also led to a diminished autophagic flux but the reduction was less severe. The contribution to autophagy of the other four *D. discoideum* VPS13 proteins, if any, was not large enough to be detected by the current assay to monitor autophagic flux in this organism because this method cannot easily detect slight defects. More sophisticated approaches would be necessary to evaluate a potential requirement of these VPS13 proteins for a total functionality of autophagy.

Phagocytosis is a process that has been related to autophagy,[285] and, as already described in the introduction, to VPS13 proteins in *T. thermophila* and in mice.[264122250,285,304] We have observed that this process is partially impaired in the *tipC*$^-$ mutant and probably strongly defective in the *vps13F*$^-$ mutant as suggested by the delayed growth and development of *vps13F*$^-$ mutant on *K. pneumoniae* lawns. Vps13F requirement in phagocytosis has been

reported very recently by the observation that *vps13F*- cells kill *K. pneumoniae* modestly slower than wild-type cells.[160] The stronger severity of the defect in our *vps13F*- mutant is probably due to the different background: AX4 *versus* DH-1 in the reported work.

Defects in intracellular killing could be the result of impaired degradation of the internalized phagosome, which may be in agreement with our observed defects in the endocytic pathway of VPS13A-depleted HeLa cells. However, no significant defects in the phagocytic and endocytic internalization nor in the morphology or acidity of vesicles were found when Vps13F was disrupted in DH1 cells.[160] It would be interesting to verify the lack of defects in these features in our AX4 *vps13F*- cells because, like the phagocytic defect, minor alterations might be more evident in this background.

A relationship of VPS13 proteins with autophagy has been very recently suggested in another model organism, *D. melanogaster*. The SQSTM1/p62 homologue, Ref(2)P, was shown to accumulate and partially colocalize with a larger number of ubiquitin-positive protein aggregates present in a *Vps13* mutant.[317] Because of its similarity to autophagy mutants, this phenotype suggests an impairment of autophagy, which was not directly addressed in that report.

We have demonstrated that VPS13A is required for a fully-functional autophagy in human HeLa cells, similarly to *D. discoideum* TipC and Vps13A. It is probable that *D. discoideum* and human VPS13 proteins have similar roles regarding autophagy-related functions, but some differences were observed upon their depletion. For example, the reduction of Atg18 puncta in the absence of TipC *versus* the accumulation of WIPI-1, a mammalian Atg18 homologue, in the absence of human VPS13A irrespective of the growing conditions. Apart from differences in the exact roles of the *D. discoideum* and human VPS13 proteins, the discrepancies between organisms might be due to distinct features of the autophagic or endolysosomal pathway and their regulation.

The involvement of VPS13A in autophagy is further supported by recently published observations. Overexpression of VPS13A in HEK293 cells was reported to improve cell viability upon starvation.[266] Based on this, together with the observation of an increased LC3II/LC3I ratio in starvation in comparison to mock-transfected cells, it was claimed that autophagic flux was upregulated when VPS13A was overexpressed.[266] Overexpression of VPS13A had an effect on SQSTM1/p62 levels too, further supporting some influence of VPS13A in autophagy.[266] However, in the striatum of ChAc mice, no difference was observed regarding LC3 and SQSTM1/p62 signal.[266]

The importance of VPS13A in autophagy and the possible implication of autophagy in ChAc development are suggested by the visualization of remnants of vesicles, mitochondria and lysosomes, and also SQSTM1/p62 positive aggregates, in ChAc red blood cells. This suggested a delayed autophagic clearance during erythroid maturation in patients.[169] At the molecular level, more Ulk1, Atg13, Atg7 and LC3-I were noticed in lysates of ChAc erythrocytes.[169]

To date, no experimental evidence has been published about the role of autophagy in the other cell type most affected by ChAc: striatal medium spiny neurons (MSN). They cannot be directly studied from patients for obvious reasons but protocols to generate them from fibroblasts have been developed.[289] We attempted to study autophagy in patients' fibroblasts and in midbrain dopaminergic neurons (mDAN). mDAN are obtained upon differentiation of induced pluripotent stem cells (iPSC) derived from fibroblasts of patients and are easier to generate than MSN. This work was done in collaboration with PD Dr. Dr. Andreas Hermann at Dresden University. Unfortunately, we did not obtain conclusive results from these preliminary experiments due to the reduced number of samples and their large variability among individuals, and perhaps also due to the probable lesser requirement of VPS13A for autophagy in these cells. Similarly, in a recent report none or a lesser difference has been found on mDAN with respect to diminished actin polymerization rates or increased Lyn activation, [289] phenotypes largely associated with the absence of VPS13A. [6,80,82,112,272]

VPS13C might also be involved in autophagy but the autophagic alterations that we have observed upon *VPS13C* depletion were not as evident as those upon *VPS13A* loss. We have observed an accumulation of LC3-II in basal conditions as the most pronounced autophagic phenotype in the absence of VPS13C. As VPS13A and VPS13C could have redundant roles in autophagy, we simultaneously knocked down their expression. This resulted in a phenotype not compatible with a mere aggravation of the autophagic blockade, suggesting that both proteins, although very likely related, do not seem to have redundant functions in autophagy. Distinct functions of VPS13A and VPS13C, at least regarding some roles, are actually expected by the different human diseases caused by mutations in their coding genes.

VPS13C participation in autophagy has been recently assessed in 3T3-L1 cells, in which no difference was found upon *VPS13C* expression silencing.[335] In that work, autophagic flux was evaluated in starvation but the requirement of VPS13C in autophagy could be different in basal conditions. Moreover, VPS13C contribution to autophagy could be dependent on the cell type and it is possible that it is particularly important in HeLa cells.

Using HeLa cells, we have observed an altered endocytic pathway in the absence of VPS13A. In this cell type, autophagosomes fuse primarily with LE (forming amphisomes) before fusing with lysosomes.[79,172] Therefore, if VPS13 proteins participation in autophagy is related to

endocytosis, its impact on autophagy would be larger in HeLa cells and other cell types relying on amphisomes, in which autophagy would be hence more vulnerable to defects in the endocytic pathway.

Because no relationship has been reported for yeast Vps13 and bulk autophagy so far, we speculate that human VPS13 proteins could have gained the autophagy-related functions during evolution; or, in contrast, that yeast Vps13 might have not such an impact in autophagic degradation in the yeast cells. Remarkably, yeast cells have the peculiarity of presenting one giant vacuole instead of multiple small lysosomes,[143] and the interplay between endocytic and autophagic pathways may have profound differences. We think that precisely this interplay is at the cause of the autophagic impairment observed upon VPS13A depletion in HeLa cells and that could explain the lack of association of bulk autophagy with yeast Vps13 in the literature. However, yeast Vps13 might be somehow related with vacuolar degradation as deleted *vps13* intensified the toxicity derived from the presence of an expanded polyglutamine (polyQ) domain.[182]

The observations that somehow relate the other members of the VPS13 human family with the endosomal pathway have been already mentioned in the introduction.[69,210,311] However, this relationship should be further addressed by a detailed study of endosomal makers as only EEA1 and LAMP2, and only upon VPS13B depletion, have been analyzed.[69] In preliminary experiments, we have observed an accumulation of endocytic and lysosomal proteins in the absence of VPS13C and that was intensified by the simultaneous absence of VPS13A in some cases but not in others (not shown). Again, a complex relationship of both proteins and their roles is suggested but much more work is needed for its elucidation.

The autophagic pathway and the endocytic pathway converge into the lysosomes for degradation of autophagosomes and LE/MVB. Alterations in the degradative capacity of lysosomes could potentially explain the phenotypes that we have observed in VPS13A-depleted HeLa cells such as the compromised autophagic capacity of the cells to degrade cargo, resulting in partial autophagy flux defects and accumulation of certain proteins such as SQSTM1/p62. The clustering of autophagic, endosomal and lysosomal markers at the juxtanuclear area is also indicative of a blockade in degradation. TEM analysis showed the accumulation of endolysosomes but not intact autophagosomes, EE, LE or lysosomes, suggesting again that the defect is at a late stage of degradation. Moreover the partial defect of cathepsin B processing suggests that the lysosomal competency for degradation is compromised. Further studies are needed to fully characterize lysosomal function.

Contrary to bulk autophagy, mitophagy (a selective form of autophagy) has been associated to yeast Vps13, which has been reported to function in maintenance of mitochondrial

integrity.[228] In accordance, mitophagy was enhanced in the absence of the protein.[228] Similarly, reduction of mitophagy has been proposed as a function of human VPS13C.[161]

We have not evaluated VPS13A roles in selective forms of autophagy, including mitophagy, although we have not found differences in the number of mitochondria and the levels of mitochondrial proteins in VPS13A-depleted cells. In spite of this, the differences between yeast and human cell biology and the possible distinct functions of VPS13A and VPS13C, a role in mitochondrial function and mitophagy should be explored further for VPS13A, specially taking into account that we have observed VPS13A to localize at mitochondria. In addition, two mitochondria-related phenotypes have been reported in the absence of VPS13A. First, the presence of swollen mitochondria in muscles from ChAc patients.[181] And second, the modest increase of cells with depolarized mitochondria observed in K562 and ZF cells upon *VPS13A* knockdown.[80,113]

5.2 | VPS13 proteins localization and function

Subcellular localization of VPS13 proteins is challenging due to their size, low abundance and poor antibody quality. With respect to mammalian VPS13 proteins, a cytoplasmic but vesicular appearance in some cells was reported.[310] In ZF and $CaCO_2$ cells, endogenous VPS13A was claimed to be cytoplasmic.[113] In PC12 cells, the endogenous protein was observed to be partially colocalizing and fractionating with synaptotagmin I and GM130, markers of dense core vesicles and *cis*-Golgi, respectively.[103] In our hands, a remarkable colocalization of VPS13A with GM130 was not detected. In HEK293 cells, a punctate pattern colocalizating with β-adducin and partially with β-actin was attributed to overexpressed C-terminal tagged VPS13A.[283]

This thesis is the first study to demonstrate a mitochondrial localization of the human VPS13A in HeLa and COS-7 cells, although we cannot rule out the presence of the protein in other organelles. We do not know if the discrepancies with other reported localizations are due to the different cell types used or to possible technical issues derived from antibody specificity or misslocalization of the overexpressed protein. However, the disappearance of the mitochondrial network pattern upon VPS13A silencing and the observation of the same pattern upon overexpression of the VPS13^EGFP protein strongly support the validity of the localization of VPS13A in the mitochondrial network.

A mitochondrial localization is unlikely exclusive of VPS13A. Endogenous VPS13C was reported to be associated with the OMM,[161] although no colocalization with mitochondria was visualized for overexpressed C-terminal tagged VPS13C in HeLa cells in another study.[335] In that report, the VPS13C tagged version was showed to colocalize with lysosomes and lipid

droplets and the endogenous VPS13C was detected in cellular fractions enriched for lipid droplets.[335] A partial mitochondrial localization is supported by proteomic analysis in which human VPS13C and mouse VPS13C, VPS13A and VPS13D have been detected in the MAMs fraction.[236,341] Interestingly, in the proteome analysis of lipid droplets from mouse skeletal muscle, many mitochondrial proteins (and VPS13A, VPS13C and VPS13D) were identified and the closeness of LD and mitochondria was shown.[343] Although this proteomic data should be individually validated by other experimental approaches, it indicates that VPS13 proteins could be localized at the sites of contact of mitochondria with ER and, possibly, with lipid droplets in mammalian cells.

The MCS between the mitochondria and the ER (MAMs) are important in the transport of some small molecules and lipids. Similarly, the closeness between mitochondria, LD and lysosomes can favor the hydrolysis of stored lipids and the transport of the resulting fatty acids to the mitochondria for their oxidation; alternatively, fatty acids resulting from degradation can be stored in LD for being used when necessary. In fact, mitochondria and LD contacts are stimulated during starvation. Less described is the interaction of mitochondria with endosomes, although it has been shown to be related to iron transfer in erythroid and epithelial cells.[57,99]

So far, a localization of a VPS13 protein at mitochondrial contacts has been only demonstrated for the yeast Vps13, localized at vCLAMPs (and, additionally at NVJs).[154,228] Contacts between the mitochondria and the endosomes or lysosomes have been barely described and only in yeast.[73,114] The potential existence of MCS between mitochondria and endosomes and lysosomes in humans raises the attractive hypothesis that VPS13A may function at these MCS and makes VPS13A localization at the mitochondria compatible with the defects observed upon VPS13A depletion in the endocytic pathway. However, as indicated above, VPS13A could be playing roles in other subcellular locations besides mitochondria, such as endosomes or lysosomes and, in fact, VPS13A puncta was observed to occasionally colocalize with these organelles.

We have observed, by electron microscopy, mitochondria being occasionally in contact with endosomes. However, we have not found differences in the number of these MCS in the absence of VPS13A, although their length tends to be reduced. Similar results were obtained for the analysis of MAMs. This does not imply that VPS13A is not functioning at these contacts because VPS13A is not necessarily involved in the formation of contacts or in their stability, but it could be involved in their functionality by performing, for instance, some transport function between organelles.

In yeast, the localization of Vps13 at vCLAMPs is able to compensate the absence of ERMES, but not in the absence of Mcp1 (Mdm10 complementing protein 1), a mitochondrial protein involved in lipid homeostasis which can rescue, when overexpressed, defects of ERMES mutants.[154] Vps13 localization at vCLAMPs is also unable to compensate ERMES deficiency if Vps39 is loss too.[154] This protein, like Vps13, is essential in the absence of ERMES.[73,114] Vps39 is a member of the HOPS (homotypic fusion and vacuole protein sorting) complex, involved in the fusion of late endosomes with lysosomes, but it has been found to localize at vCLAMPs independently of the other proteins that form the HOPS complex. Vps39 overexpression increases vCLAMPs and, interestingly, in a proteomic approach of mitochondria enriched fractions, Vps13 was identified to a greater extent in the GFP pull-down when GFP-Vps39 was overexpressed,[73] supporting the presence of Vps13 at those vCLAMPs and a potential interaction with Vps39.[114] Vps39 association to membranes is dependent on the RAB7 homologue in yeast, Ypt7, both in solitary, at vCLAMPs,[114] and when Vps39 is associated with the other members of the HOPS complex to participate in fusion of late endosomes to the vacuole.[36,108] Intriguingly, VPS13 proteins interact with RAB7 (see discussion below) and negatively stained Vps13 visualized by electron microscopy,[58] has an appearance resembling the architecture of the HOPS complex.[36] These observations might point to a possible role of Vps13 in vesicle fusion, similar to that of the HOPS complex.

The visualization of VPS13A by electron microscopy would be helpful to determine if VPS13A localizes at mitochondria uniquely at the sites of contact with other organelles. However, to date, the poor quality of the antibody and the low transfection efficiency of the overexpressed protein make this task challenging.

Alternatively to a direct contact of mitochondria with endosomes or lysosomes, a mitochondrial localization of VPS13A and the endocytic defects observed when the protein is lost could be connected by signaling pathways. Direct or not, a crosstalk between these organelles might be important for each other functions,[241] as exemplified by importance of mitochondria for the fusion and function of lysosomes in different cell types.[19,59,248]

5.3 | VPS13 partners and related functions

By a proteomic approach, we have identified potential interactors with the N- and C-terminal regions of *D. discoideum* TipC and Vps13A proteins. As expected, a few proteins interacted with both TipC and Vps13A, although the fact that some of them apparently interact with both ends of the proteins may suggest that immunoprecipitation was not specific. However, given their absence in the GFP control sample, we cannot discard the possibility that both ends of the proteins can interact with the same partners. Moreover, as the detected

interactions are not necessarily direct, it is theoretically possible that some proteins could be immunoprecipitated with both termini of the same protein if the interactors with each termini formed a complex.

Among the identified protein candidates for the interaction with the terminal regions of *D. discoideum* Vps13 proteins, we paid special attention to Rab7 because it had already been described to participate in autophagy and it had been related to VPS13 proteins before.[179] We confirmed the interaction of Rab7 with the overexpressed C terminus of TipC in *D. discoideum* and with endogenous human VPS13A and VPS13C in HeLa cells. VPS13C had already been described as an interactor of Rab7;[179] however, this is the first time that an interaction of RAB7 has been observed with VP13A and other members of the VPS13 family in *D. discoideum*, indicating the conservation of this interaction in other species. In support of this, *D. melanogaster* homologue of human VPS13A and Rab7 have been recently shown to be present in the same subcellular fractions and in immuno-isolated membranes positive for each other.[317] In other organisms, indirect evidence could support a probable interaction of VPS13 proteins with Rab7. For example, Rab7 was also identified in the *T. thermophila* phagosome.[122] In *S. cerevisiae*, the *ypt7* (Rab7) mutant showed negative genetic interaction with the *vps13* mutant,[115] also displayed sporulation defects,[74] and suppressed defective targeting of mutated Pma1.[168] Moreover, as already mentioned, Ypt7 (Rab7) has been found to localize at vCLAMPs, where it is necessary for the recruitment of Vsp39 to those MCS.[114]

The interaction of Rab7 with VPS13 proteins might be transient because only a partial amount of protein immunoprecipitated with each other. Assuming the hypothesis that VPS13A could be at the sites of interaction between mitochondria and Rab7-containing endosomes, a very short-lived interaction between these organelles could explain why MCS between them are difficult to detect in metazoans. A transient 'kiss and run' interaction between endosomes and mitochondria supports this idea.[57,99] The interaction might be brief but necessary for some functions. A comprehensive and recent review of Rab7 roles has been published elsewhere.[98] Here, only some of the functions (especially those than can be associated with VPS13 phenotypes) are briefly discussed.

Rab7 is involved in the trafficking of endosomes and autophagosomes on microtubules in the minus-end or plus-end direction (towards the nucleus or towards the plasma membrane) through its interaction with RILP or FYCO, respectively.[129,224] It could be possible that the observed accumulation of autophagosomes and endosomes in the juxtanuclear region upon VPS13A silencing is in part related to this traffic function besides the described defect in degradation.

Although we have not observed accumulation of lysosomes by TEM in VPS13A-depleted cells, it is still possible that a subtle defect in their fusion efficiency with autophagosomes and endosomes affects the degradative competency of the endolysosomes. It is known that Rab7 bound to vesicles recruits Vps39 and Vps41 as components of the tethering HOPS complex, and facilitate the fusion of two vesicles.[235,346] However, our data do not support a prominent defect in fusion with lysosomes.

Another explanation to the observed impaired degradation could be that lysosomes were not completely functional in the VPS13A-depleted cells. Lysosomal biogenesis and maintenance depend on a correct endosomal trafficking,[123] involved in the delivery of hydrolases to lysosomes, which are active only at an acidic environment.[118] We have shown CTSB colocalizing with lysosomes (although the amount of relative colocalization could not be accurately determined), but CTSB processing was reduced. RAB7 influences lysosome position and acidification[37,130,167] and CTSB processing is inefficient when the endolysosomal pathway is blocked.[271] In addition, RAB7 regulates autophagic lysosome reformation (ALR), a process where non-acid tubules emerge from autolysosomes for the recycling of lysosomal membrane proteins.[253,339,344]

Other roles described for RAB7 in the endocytic pathway are the sorting of some specific proteins from early to late endosomes,[90] recycling of RAB5 (an early endosomal marker)[244], or the regulation of the retromer,[12,165,238,251] involved the transport of proteins from endosomes to the TGN. Particularly in relation to the functions of RAB7 and the retromer, RAB7 has been shown to be regulated by Parkin,[287] and LRRK2,[25,91,170] proteins that, like RAB7 and VPS35 (a component of the retromer), have been associated with Parkinson's disease.[121] Loss of VPS13C has been recently linked to a variant of PD by increasing Parkin protein levels, increasing PINK1 and Parkin accumulation at mitochondria, and promoting mitophagy.[161] RAB7 functions during mitophagy as well, in the expansion of mitochondria surrounding isolating membranes.[333] Altogether, the analysis of VPS13C interaction with Rab7 might provide some clue about VPS13C functions in the context of PD.

As a RAB7 interacting protein, VPS13A could be a protein regulating the GDP/GTP cycle and RAB7 activity or participating in its functions if it is a RAB7 effector. Alternatively, VPS13A could be involved in RAB7 recruitment to membranes. Interestingly, PIPs play fundamental roles in controlling the localization and functions of RABs and RAB-related proteins and VPS13 proteins have been shown to bind PIPs and influence their presence at some membranes.[58,227,229,258]

Specific PIPs are present at different cellular membranes and they determine the binding of proteins to those membranes, regulating functions such as endocytic internalization, sorting,

transport, maturation and fusion processes.[270] For example, during maturation of EE to LE, RAB5 switch to RAB7 is mediated by PI3P.[270] PI4P has been related to the binding and activity of RABs on secretory vesicles,[270] but PI4P has also been visualized at EE, in which it has been shown to be essential for the sorting of receptors,[105] and in RAB7 positive LE,[100] in which it probably participates in fusion with lysosomes. In accordance, acidic lipids such as PIPs, DAG and sterols are involved in fusion processes as they promote the concentration of the fusion machinery at the sites of fusion and might also control actin remodeling at those locations.[83,188,220] PI3P and PI4P are required for phagosome-lysosome fusion,[127] and PI4P production on autophagosomes is involved in autophagosome-lysosome fusion.[326] In addition, an interplay between Rho GTPases involved in actin polymerization, such as RAC1, and PIPs has been described.[52]

Apart from Rab7, Rab1 has been identified as a potential partner of *D. discoideum* TipC. Rab1 participates in trafficking from the ER to the Golgi but also in the sorting of early endosomes,[197] and in autophagosome formation and α-synuclein clearance.[294]

The association of different RAB GTPases and VPS13 proteins has been reported in different proteomic approaches. *D. melanogaster* VPS13 proteins were isolated by affinity chromatography using different GTP-RABs.[89] The study of the human interactome has revealed interactions between VPS13C and RAB1A, RAB9A and RAB30.[120] Of note, RAB30 originated from RAB1 and RAB9 from RAB7 and have some similar functions.[89] VPS13C has been reported to interact with RAB24,[24] involved in the maturation of autophagosomes,[338] and in endosomal degradation through the interaction with RAB7 and RILP.[7] Not by proteomics but in more focused studies, the interaction of VPS13B and RAB6,[276] and VPS13C with RAB7,[179] have been demonstrated. Taken into account this and our own experimental evidence, we propose that Rab GTPases are closely related to VPS13 functions.

RAB proteins constitute a family of proteins within the Ras superfamily of GTPases, which also includes the Rho and Ras families. Interestingly, members of these families also were identified as potential interactors of TipC in our mass spectrometry assay. Rac1A (ras-related C3 botunlinum toxin substrate 1) is one of them, belonging to the Rho family. Interestingly, decreased RAC1A activity has been reported in K562 cells upon VPS13A silencing.[80] The reduction of RAC1A activity could be mediated by RAB7 as it interacts with RAC1 and induces its activity.[176,292] In exchange, a RAC1 effector, Armus, inactivates RAB7. Such an interplay of RAC1, RAB7 and Armus has been shown to be essential for an efficient autophagic flux in starvation.[44] Reduced RAC1 activity decreases PAK1 phosphorylation, a phenotype that has also been observed in the absence of VPS13A.[80,272] RAC1 activity (and the activity of some RAB proteins too) can be regulated by the p85α regulatory subunit of PI3K,[47] and p85α has

been shown to be less phosphorylated in K562 cells upon silencing of *VPS13A* expression.[80] Notably, PI3Ks interact with rasG,[109] which potentially interacts with TipC. Another member of the Ras family potentially interacting with TipC is RasB.

Both RasB and RasG have been shown to have roles in endocytosis and phagocytosis and, similar to PI3K, RAC1A and PAK1, they have functions in actin polymerization.[132] This is probably related to the observation that some actins, and myosin-2 heavy chain, which is a component of the actin-based molecular motor myosin, were also immunoprecipitated with the *D. discoideum* VPS13 proteins. In addition, overexpressed VPS13A has been shown to interact with β-actin and β-adducin (a protein that binds actin filaments).[283] Actin polymerization can regulate chemotaxis, phagocytosis, endocytosis and other cellular processes including autophagosome fusion with lysosomes.[52] Therefore, the decreased actin polymerization reported in the absence of VPS13A might have consequences on these processes beyond the aberrant morphology of erythrocytes.

Another protein regulating the actin-cytoskeleton is EF-1a.[97] It was identified in our mass spectrometry assay in the four VPS13 samples but not in the GFP sample. While this non-specificity is suspicious, this interaction has also been reported as part of a macromolecular complex[324] and was also identified in the phagosome of *T. thermophila*.[122]

EF-1a is a calmodulin-binding protein and the Ca^{2+}/calmodulin binding is necessary for phagosome formation.[92] β-adducin activity is regulated by calmodulin too.[283] Interestingly, we have identified calmodulin as an interactor partner of TipC, which suggests a connection of calcium with VPS13 proteins functions. Calcium levels regulate TGN fusion processes,[58] vesicle fusion processes and lysosomal reformation,[87,118,178] and actin dynamics.[240] Calcium-related proteins associated with VPS13 proteins are Cdc31, which is required for some yeast Vps13 functions,[58] and the Ca^{2+} channel subunit Orai1, whose levels are reduced in the absence of human VPS13A.[340]

Again related to the Ras proteins, they are activated during intracellular signaling. For example, during phagocytosis signaling, which is mediated by the folate receptor.[132] This receptor can interact with Lyn,[189] and VPS13A was observed in Lyn immunoprecipitates,[169] suggesting a role of VPS13A in signaling. Interestingly, the intracellular signaling triggered by the presence of *K. pneumoniae* is hampered in *D. discoideum Vps13F*$^{-}$ cells, which also present a diminished response to extracellular stimuli.[160] Addition of folate was able to restore the killing defect of phagocytosed *K. pneumoniae* in *Vps13F*$^{-}$ *D. discoideum* cells,[160] which suggests the possibility to compensate some VPS13 phenotypes by an increased signaling.

Histone H4 was identified in our mass spectrometry analysis as an interactor of *D. discoideum* Vps13A and it was detected in the *T. thermophila* phagosome proteome too.[122] H4 is deacetylated by HDAC6, which was shown to interact with overexpressed VPS13A.[266] α-tubulin is also deacetylated by HDAC6 and also interacts with overexpressed VPS13A.[266] Tubulin acetylation is a typical feature of stable microtubules and its modification could be at the cause of the alterations observed of microtubule cytoskeleton in the absence of VPS13A.[112] No difference was observed in acetylated tubulin in ChAc mice in comparison to controls, but overexpression of VPS13A decreased α-tubulin acetylation and protected cells from nocodazole (a microtubule de-polimerizing agent) or tubacin (an HDAC6 inhibitor) induced cell death, thus indicating some functional relationship between HDAC6, α-tubulin and VPS13A.[266] Importantly, the correct transport along microtubules is required for endosome sorting and maturation,[118] and for fusion with autophagosomes.[146]

Back to HDA6 and H4, cortactin, which is a protein involved in actin polymerization, can be recruited by HDAC6. HDAC6 binds ubiquitinated proteins and damaged mitochondria for their aggregation and promotes the actin polymerization necessary for fusion of quality control autophagosomes with lysosomes.[157,159] Another substrate of HDAC6, Hsp90, participates in actin-remodeling and clathrin-independent endocytic processes such as macropinocitosis.[88] H4 has been shown to influence phagocytosis of apoptotic cells and platelet aggregation,[84] and to be involved in OMM permeabilization and apoptosis.[45] Therefore, VPS13A interaction with these proteins might be related to actin depolymerization and other phenotypes observed in the absence of VPS13A.

D. discoideum Vps13A was identified as a Sec7 binding partner.[200] The reciprocal identification was not found in our analysis but it should be taken into account that only the N- and C-terminal regions of the protein were immunoprecipitated and thus, interactors with other regions would have been missed in our approach.

We have not found any ATG protein as potential interactor of *D. discoideum* Vps13A or TipC but human VPS13A was shown in ATG7 immunoprecipitates.[169] It was proposed that VPS13A interacts with ATG7 and Lyn and for the autophagic degradation of active Lyn, which is sequestered by Hsp90 in complexes and interacts with ULK1 and ATG7. We could have missed such interaction with Atg7 because of the lack of a part of the protein. It is possible that this ATG7 interaction could be related to the higher non-lipidated LC3I levels that we have observed in VPS13A-depeleted cells.

5.4 | Concluding remarks and Future perspective

The current literature and the results presented in this thesis raise the hypothesis that VPS13 proteins may regulate multiple cellular processes by the interplay with members of the Ras superfamily of small GTPases. As these proteins, for example RAB7, are often involved in multiple membrane-traffic-dependent processes, their dysregulation may lead to the complex defects observed in the absence of the VPS13 proteins.

RAB7 has been proposed as a target to treat PD as its overexpression in HEK293 cells and *D. melanogaster* enhances the autophagic degradation of α-synuclein aggregates,[62] and other PD phenotypes.[171] More feasible as a therapeutic approach would be the use of small molecules to modulate RAB7 GTPase activity, although few have been designed to date and they are mostly inhibitors.[3,110] RAB7 has been also associated to other neurodegenerative diseases to which it could be considered a potential target.[328] Taken into account VPS13A interaction with RAB7, RAB7 could be considered as a target to treat ChAc too. However, in order to do that, the functional relationship of VPS13A interaction with RAB7 has to be elucidated first.

Independently of the roles and molecular mechanisms of VPS13A functions, our results, and those obtained by others,[169,317] suggest that lysosomal degradation may be one of the pathways affected in ChAc. A diminished capacity of degradation would undoubtedly impact on autophagy and endocytic traffic and should be considered as a possible therapeutic target in future studies.

The induction of autophagic degradation could be therefore useful in the treatment of ChAc. Compounds to induce autophagy at its first steps are known and even used in clinical practice; however, according to our results, the induction of autophagosome formation would be probably detrimental as it would mean further material for degradation in already overwhelmed lysosomes. Few compounds are known that can enhance the later steps of the process.[195] PADK (Z-Phe-Ala-diazomethylketone) and derived nonpeptidic modulators of cathepsins have been designed that could be useful.[18,316] They also influence RAB proteins levels.[39] It would be helpful to clarify if the major defect blocking degradation is an impaired fusion, acidification or hydrolase activity prior to consider these or other compounds. However, defects in one process could lead to defects in others as, for example, cathepsin inhibitors have been suggested to impair fusion of autophagosomes with lysosomes.[134] As an alternative approach, we speculate that in order to alleviate lysosomes from material for degradation, instead of an induction of autophagosome formation, its inhibition, with already existing compounds, could be potentially useful. That would not favor the degradation of possible damaged material but could alleviate the accumulation of endosomes that could also

be at the cause of some ChAc associated phenotypes as endosomes are central organelles in many cell signaling processes.

In conclusion, this thesis demonstrates the role of VPS13 proteins in autophagy as part of a more general role of vesicle trafficking processes and highlights the potential importance of lysosomal degradation in the etiology of ChAc.

6 | CONCLUSIONS

6 | CONCLUSIONS

1. The VPS13 protein TipC is required for autophagy in *D. discoideum*. It is the first time that the VPS13 family of proteins has been implicated in autophagy.

2. The conserved C terminus of TipC is able to largely complement the mutant phenotypes connected to autophagy: aberrant multicellular development, spore production, autophagic puncta formation and partial phagocytosis defect.

3. In human HeLa cells, VPS13A, the protein whose mutations cause chorea-acanthocytosis, is also involved in autophagy as its absence leads to a reduced autophagic degradation and the accumulation of autophagic markers.

4. Rab7, a protein of the endocytic pathway with roles in autophagy is an interactor of *D. discoideum* TipC and human VPS13A.

5. The lack of VPS13A in HeLa cells leads to the accumulation of endosomal and lysosomal markers, primarily corresponding to endolysosomes as observed by transmission electron microscopy.

6. The processing of cathepsin B is reduced in the absence of VPS13A in HeLa cells, suggesting a defective lysosomal degradation as the possible cause of the observed autophagic and endocytic phenotypes.

7. Confocal microscopy analyses indicate that VPS13A mainly colocalizes with mitochondria and, to a lesser extent, with other organelles including endoplasmic reticulum, autophagosomes, endosomes and lysosomes.

8. We did not detect consistent alterations in the mitochondrial structure or in the number and size of the membrane contact sites of mitochondria with endosomes and the endoplasmic reticulum.

9. The autophagic and endocytic pathways, converging at lysosomal degradation, are altered in the absence of VPS13A and therefore they must be considered as possible therapeutic targets for chorea-acanthocytosis.

7 | CONCLUSIONES

7 | CONCLUSIONES

1. La proteína VPS13 TipC es necesaria para la autofagia en *D. discoideum.* Esta es la primera vez que la familia de proteínas VPS13 se ha implicado en autofagia.

2. El extremo C terminal conservado de TipC es capaz complementar en gran medida los fenotipos mutantes asociados con autofagia: el desarrollo multicelular aberrante, la producción de esporas, la formación de autofagosomas y el defecto parcial de fagocitosis.

3. En la células humanas HeLa, VPS13A, la proteína cuyas mutaciones causan corea-acantocitosis, está también involucrada en autofagia ya que su ausencia conlleva una reducción de la degradación autofágica y la acumulación de marcadores autofágicos.

4. Rab7, una proteína de la ruta endocítica con funciones en autofagia, es un interactor de la proteína TipC de *D. discoideum* y de VPS13A de humanos.

5. La ausencia de VPS13A en células HeLa conlleva una acumulación de marcadores endosomales y lisosomales, principalmente correspondientes a endolisosomas según lo observado por microscopía electrónica de transmisión.

6. El procesamiento de la catepsina B es menor en ausencia de VPS13A en células HeLa, lo que sugiere una degradación lisosomal deficiente como la posible causa de los fenotipos observados respecto a autofagia y endocitosis.

7. Los análisis de microscopía confocal indican que VPS13A se encuentra principalmente colocalizando con la mitocondria y, en menor medida, con otros orgánulos incluyendo el retículo endoplasmático, autofagosomas, endosomas y lisosomas.

8. No detectamos alteraciones consistentes en la estructura mitocondrial o en el número y tamaño de los sitios de contacto de mitocondria con endosomas y con el retículo endoplasmático.

9. Las rutas autofágica y endocítica, que convergen en la degradación lisosomal, están alteradas en ausencia de VPS13A y por lo tanto deben ser consideradas como posibles dianas terapéuticas para la corea acantocitosis.

REFERENCES

8 | REFERENCES

1. Adachi H, Hasebe T, Yoshinaga K, Ohta T, Sutoh K. Isolation of Dictyostelium discoideum Cytokinesis Mutants by Restriction Enzyme-Mediated Integration of the Blasticidin S Resistance Marker. *Biochem Biophys Res Commun*. 1994;205(3):1808-1814. doi:10.1006/bbrc.1994.2880.
2. Aggarwal N, Sloane BF. Cathepsin B: Multiple roles in cancer. *Proteomics - Clin Appl*. 2014;8(5-6):427-437. doi:10.1002/prca.201300105.
3. Agola JO, Hong L, Surviladze Z, et al. A competitive nucleotide binding inhibitor: In vitro characterization of Rab7 GTPase inhibition. *ACS Chem Biol*. 2012;7(6):1095-1108. doi:10.1021/cb3001099.
4. Al-Asmi A, Jansen AC, Badhwar A, et al. Familial Temporal Lobe Epilepsy as a Presenting Feature of Choreoacanthocytosis. *Epilepsia*. 2005;46(8):1256-1263. doi:10.1111/j.1528-1167.2005.65804.x.
5. Al-Shali K, Hegele RA. Acanthocytes and Disorders of Lipoprotein Metabolism. In: *Neuroacanthocytosis Syndromes*. Berlin/Heidelberg: Springer-Verlag; 2004:21-30. doi:10.1007/1-4020-2898-9_3.
6. Alesutan I, Seifert J, Pakladok T, et al. Chorein sensitivity of actin polymerization, cell shape and mechanical stiffness of vascular endothelial cells. *Cell Physiol Biochem*. 2013;32(3):728-742. doi:10.1159/000354475.
7. Amaya C, Militello RD, Calligaris SD, Colombo MI. Rab24 interacts with the Rab7/Rab interacting lysosomal protein complex to regulate endosomal degradation. *Traffic*. 2016;17(11):1181-1196. doi:10.1111/tra.12431.
8. An CH, Kim YR, Kim HS, Kim SS, Yoo NJ, Lee SH. Frameshift mutations of vacuolar protein sorting genes in gastric and colorectal cancers with microsatellite instability. *Hum Pathol*. 2012;43(1):40-47. doi:10.1016/j.humpath.2010.03.015.
9. An X, Zhang X, Debnath G, Baines AJ, Mohandas N. Phosphatidylinositol-4,5-biphosphate (PIP2) differentially regulates the interaction of human erythrocyte protein 4.1 (4.1R) with membrane proteins. *Biochemistry*. 2006;45(18):5725-5732. doi:10.1021/bi060015v.
10. Ao X, Zou L, Wu Y. Regulation of autophagy by the Rab GTPase network. *Cell Death Differ*. 2014;21(3):348-358. doi:10.1038/cdd.2013.187.
11. Arias E, Cuervo AM. Chaperone-mediated autophagy in protein quality control. *Curr Opin Cell Biol*. 2011;23(2):184-189. doi:10.1016/j.ceb.2010.10.009.
12. Arlt H, Reggiori F, Ungermann C. Retromer and the dynamin Vps1 cooperate in the retrieval of transmembrane proteins from vacuoles. *J Cell Sci*. 2015;128(4):645-655. doi:10.1242/jcs.132720.
13. Asano K, Osawa Y, Yanagisawa N, Takahashi Y, Oshima M. Erythrocyte membrane abnormalities in patients with amyotrophic chorea with acanthocythosis: Part 2. Abnormal degradation of membrane proteins. *J Neurol Sci*. 1985;68(2):161-173. doi:10.1016/0022-510X(85)90097-8.
14. Bader B, Arzberger T, Heinsen H, Dobson-Stone C, Kretzschmar HA, Danek A. Neuropathology of Chorea-Acanthocytosis. In: *Neuroacanthocytosis Syndromes II*. Berlin, Heidelberg: Springer Berlin Heidelberg; 2008:187-195. doi:10.1007/978-3-540-71693-8_15.
15. Bader B, Velayos-Baeza A, Walker RH, Danek A. Dominant transmission of chorea-

acanthocytosis with VPS13A mutations remains speculative. *Acta Neuropathol*. 2009;117(1):95-96. doi:10.1007/s00401-008-0418-7.

16. Bader B, Vollmar C, Ackl N, et al. Bilateral temporal lobe epilepsy confirmed with intracranial EEG in chorea-acanthocytosis. *Seizure*. 2011;20(4):340-342. doi:10.1016/j.seizure.2010.12.007.

17. Bader B, Walker RH, Vogel M, Prosiegel M, McIntosh J, Danek A. Tongue protrusion and feeding dystonia: a hallmark of chorea-acanthocytosis. *Mov Disord*. 2010;25(1):127-129. doi:10.1002/mds.22863.

18. Bahr BA, Wisniewski ML, Butler D. Positive Lysosomal Modulation As a Unique Strategy to Treat Age-Related Protein Accumulation Diseases. *Rejuvenation Res*. 2012;15(2):189-197. doi:10.1089/rej.2011.1282.

19. Baixauli F, Acín-Pérez R, Villarroya-Beltrí C, et al. Mitochondrial respiration controls lysosomal function during inflammatory t cell responses. *Cell Metab*. 2015;22(3):485-498. doi:10.1016/j.cmet.2015.07.020.

20. Bampton ETW, Goemans CG, Niranjan D, Mizushima N, Tolkovsky AM. The dynamics of autophagy visualized in live cells: from autophagosome formation to fusion with endo/lysosomes. *Autophagy*. 2005;1(1):23-36. doi:10.4161/auto.1.1.1495.

21. Bankaitis V a, Johnson LM, Emr SD. Isolation of yeast mutants defective in protein targeting to the vacuole. *Proc Natl Acad Sci U S A*. 1986;83(23):9075-9079. doi:10.1073/pnas.83.23.9075.

22. Banta LM, Robinson JS, Klionsky DJ, Emr SD. Organelle assembly in yeast: characterization of yeast mutants defective in vacuolar biogenesis and protein sorting. *J Cell Biol*. 1988;107(4):1369-1383. doi:10.1083/jcb.107.4.1369.

23. Bayreuther C, Borg M, Ferrero-Vacher C, Chaussenot A, Lebrun C. Choréo-acanthocytose sans acanthocytes. *Rev Neurol (Paris)*. 2010;166(1):100-103. doi:10.1016/j.neurol.2009.03.005.

24. Behrends C, Sowa ME, Gygi SP, Harper JW. Network organization of the human autophagy system. *Nature*. 2010;466(7302):68-76. doi:10.1038/nature09204.

25. Beilina A, Rudenko IN, Kaganovich A, et al. Unbiased screen for interactors of leucine-rich repeat kinase 2 supports a common pathway for sporadic and familial Parkinson disease. *Proc Natl Acad Sci U S A*. 2014;111(7):2626-2631. doi:10.1073/pnas.1318306111.

26. Bell G. Quatifying western blots: none more black. *BMC Biol*. 2016;14:4-6. doi:10.1186/s12915-016-0339-1.

27. Benninger F, Afawi Z, Korczyn AD, et al. Seizures as presenting and prominent symptom in chorea-acanthocytosis with c.2343del VPS13A gene mutation. *Epilepsia*. 2016;57(4):549-556. doi:10.1111/epi.13318.

28. Bento CF, Renna M, Ghislat G, et al. Mammalian Autophagy: How Does It Work? *Annu Rev Biochem*. 2016;85(1):685-713. doi:10.1146/annurev-biochem-060815-014556.

29. Bestebroer J, V'kovski P, Mauthe M, Reggiori F. Hidden behind autophagy: The unconventional roles of ATG proteins. *Traffic*. 2013;14(10):1029-1041. doi:10.1111/tra.12091.

30. Biazik J, Ylä-Anttila P, Vihinen H, Jokitalo E, Eskelinen EL. Ultrastructural relationship of the phagophore with surrounding organelles. *Autophagy*. 2015;11(3):439-451. doi:10.1080/15548627.2015.1017178.

31. Bohlega S, Al-Jishi A, Dobson-Stone C, et al. Chorea-acanthocytosis: Clinical and genetic

findings in three families from the Arabian peninsula. *Mov Disord*. 2003;18(4):403-407. doi:10.1002/mds.10361.

32. Bonifacino JS, Rojas R. Retrograde transport from endosomes to the trans-Golgi network. *Nat Rev Mol Cell Biol*. 2006;7(8):568-579. doi:10.1038/nrm1985.

33. Bosman GJCGM, Bartholomeus IGP, De Grip WJ, Horstink MWIM. Erythrocyte anion transporter and antibrain immunoreactivity in chorea-acanthocytosis. A contribution to etiology, genetics, and diagnosis. *Brain Res Bull*. 1994;33(5):523-528. doi:10.1016/0361-9230(94)90078-7.

34. Bosman GJCGM, Franceschi L de. Neuroacanthocytosis-Related Changes in Erythrocyte Membrane Organization and Function. In: *Neuroacanthocytosis Syndromes II*. Berlin, Heidelberg: Springer Berlin Heidelberg; 2008:133-142. doi:10.1007/978-3-540-71693-8_10.

35. Brickner JH, Fuller RS. SOI1 encodes a novel, conserved protein that promotes TGN-endosomal cycling of Kex2p and other membrane proteins by modulating the function of two TGN localization signals. *J Cell Biol*. 1997;139(1):23-36. doi:10.1083/jcb.139.1.23.

36. Bröcker C, Kuhlee A, Gatsogiannis C, et al. Molecular architecture of the multisubunit homotypic fusion and vacuole protein sorting (HOPS) tethering complex. *Proc Natl Acad Sci U S A*. 2012;109(6):1991-1996. doi:10.1073/pnas.1117797109.

37. Bucci C, Thomsen P, Nicoziani P, et al. Rab7 : A Key to Lysosome Biogenesis. *Mol Biol Cell*. 2000;11(February):467-480. doi:10.1016/S0960-9822(01)00531-0.

38. Burbaud P, Rougier A, Ferrer X, et al. Improvement of severe trunk spasms by bilateral high-frequency stimulation of the motor thalamus in a patient with chorea-acanthocytosis. *Mov Disord*. 2002;17(1):204-207. doi:10.1002/mds.1260.

39. Butler D, Hwang J, Estick C, et al. Protective Effects of Positive Lysosomal Modulation in Alzheimer's Disease Transgenic Mouse Models. Ikezu T, ed. *PLoS One*. 2011;6(6):e20501. doi:10.1371/journal.pone.0020501.

40. Calvo-Garrido J, Carilla-Latorre S, Lázaro-Diéguez F, Egea G, Escalante R. Vacuole membrane protein 1 is an endoplasmic reticulum protein required for organelle biogenesis, protein secretion, and development. *Mol Biol Cell*. 2008;19(8):3442-3453. doi:10.1091/mbc.E08-01-0075.

41. Calvo-Garrido J, Carilla-Latorre S, Mesquita A, Escalante R. A proteolytic cleavage assay to monitor autophagy in Dictyostelium discoideum. *Autophagy*. 2011;7(9):1063-1068. doi:10.4161/auto.7.9.16629.

42. Calvo-Garrido J, Escalante R. Autophagy dysfunction and ubiquitin-positive protein aggregates in Dictyostelium cells lacking Vmp1. *Autophagy*. 2010;6(1):100-109. doi:10.4161/auto.6.1.10697.

43. Calvo-Garrido J, King JS, Muñoz-Braceras S, Escalante R. Vmp1 Regulates PtdIns3P Signaling During Autophagosome Formation in Dictyostelium discoideum. *Traffic*. 2014;15(11):1235-1246. doi:10.1111/tra.12210.

44. Carroll B, Mohd-Naim N, Maximiano F, et al. The TBC/RabGAP Armus Coordinates Rac1 and Rab7 Functions during Autophagy. *Dev Cell*. 2013;25(1):15-28. doi:10.1016/j.devcel.2013.03.005.

45. Cascone A, Bruelle C, Lindholm D, Bernardi P, Eriksson O. Destabilization of the outer and inner mitochondrial membranes by core and linker histones. *PLoS One*. 2012;7(4). doi:10.1371/journal.pone.0035357.

46. Cebollero E, Reggiori F, Kraft C. Reticulophagy and Ribophagy: Regulated Degradation

of Protein Production Factories. *Int J Cell Biol*. 2012;2012:1-9. doi:10.1155/2012/182834.

47. Chamberlain MD, Berry TR, Pastor MC, Anderson DH. The p85 alpha Subunit of Phosphatidylinositol 3 ¯ -Kinase Binds to and Stimulates the GTPase Activity of Rab Proteins. 2004;279(47):48607-48614. doi:10.1074/jbc.M409769200.

48. Chen C-M, Chen Y-C, Chiang M-C, et al. Association of GCH1 and MIR4697, but not SIPA1L2 and VPS13C polymorphisms, with Parkinson's disease in Taiwan. *Neurobiol Aging*. 2016;39:221.e1-221.e5. doi:10.1016/j.neurobiolaging.2015.12.016.

49. Chen Y, Yu L. Autophagic lysosome reformation. *Exp Cell Res*. 2013;319(2):142-146. doi:10.1016/j.yexcr.2012.09.004.

50. Cohen-Kaplan V, Livneh I, Avni N, Cohen-Rosenzweig C, Ciechanover A. The ubiquitin-proteasome system and autophagy: Coordinated and independent activities. *Int J Biochem Cell Biol*. 2016;79:403-418. doi:10.1016/j.biocel.2016.07.019.

51. Connolly BS, Hazrati L-N, Lang AE. Neuropathological findings in chorea-acanthocytosis: new insights into mechanisms underlying parkinsonism and seizures. *Acta Neuropathol*. 2014;127(4):613-615. doi:10.1007/s00401-013-1241-3.

52. Coutts AS, La Thangue NB. Regulation of actin nucleation and autophagosome formation. *Cell Mol Life Sci*. 2016;73(17):3249-3263. doi:10.1007/s00018-016-2224-z.

53. Danek A, Bader B, Velayos-Baeza A, Walker RH. Autosomal recessive transmission of chorea-acanthocytosis confirmed. *Acta Neuropathol*. 2012;123(6):905-906. doi:10.1007/s00401-012-0971-y.

54. Danek A, Jung HH, Melone MAB, Rampoldi L, Broccoli V, Walker RH. Neuroacanthocytosis: New developments in a neglected group of dementing disorders. *J Neurol Sci*. 2005;229-230:171-186. doi:10.1016/j.jns.2004.11.024.

55. Danek A, Sheesley L, Tierney M, Uttner I, Grafman J. Cognitive and Neuropsychiatric Findings in McLeod Syndrome and in Chorea-Acanthocytosis. In: *Neuroacanthocytosis Syndromes*. Berlin/Heidelberg: Springer-Verlag; 2004:95-115. doi:10.1007/1-4020-2898-9_12.

56. Daniele T, Hurbain I, Vago R, et al. Mitochondria and melanosomes establish physical contacts modulated by Mfn2 and involved in organelle biogenesis. *Curr Biol*. 2014;24(4):393-403. doi:10.1016/j.cub.2014.01.007.

57. Das A, Nag S, Mason AB, Barroso MM. Endosome-mitochondria interactions are modulated by iron release from transferrin. *J Cell Biol*. 2016;214(7). doi:10.1083/jcb.201602069.

58. De M, Oleskie AN, Ayyash M, et al. The Vps13p-Cdc31p complex is directly required for TGN late endosome transport and TGN homotypic fusion. *J Cell Biol*. January 2017:jcb.201606078. doi:10.1083/jcb.201606078.

59. Demers-Lamarche J, Guillebaud G, Tlili M, et al. Loss of mitochondrial function impairs Lysosomes. *J Biol Chem*. 2016;291(19):10263-10276. doi:10.1074/jbc.M115.695825.

60. Diao J, Liu R, Rong Y, et al. ATG14 promotes membrane tethering and fusion of autophagosomes to endolysosomes. *Nature*. 2015;520(7548):563-566. doi:10.1038/nature14147.

61. Ding WX, Yin XM. Mitophagy: Mechanisms, pathophysiological roles, and analysis. *Biol Chem*. 2012;393(7):547-564. doi:10.1515/hsz-2012-0119.

62. Dinter E, Saridaki T, Nippold M, et al. Rab7 induces clearance of α-synuclein aggregates. *J Neurochem*. 2016;138(5):758-774. doi:10.1111/jnc.13712.

63. van Dis V, Kuijpers M, Haasdijk ED, et al. Golgi fragmentation precedes neuromuscular denervation and is associated with endosome abnormalities in SOD1-ALS mouse motor neurons. *Acta Neuropathol Commun*. 2014;2(1):38. doi:10.1186/2051-5960-2-38.

64. Dobson-Stone C, Danek A, Rampoldi L, et al. Mutational spectrum of the CHAC gene in patients with chorea-acanthocytosis. *Eur J Hum Genet*. 2002;10(11):773-781. doi:10.1038/sj.ejhg.5200866.

65. Dobson-Stone C, Velayos-Baeza A, Filippone LA, et al. Chorein detection for the diagnosis of Chorea-acanthocytosis. *Ann Neurol*. 2004;56(2):299-302. doi:10.1002/ana.20200.

66. Douzgou S, Petersen M. Clinical variability of genetic isolates of Cohen syndrome. *Clin Genet*. 2011;79(6):501-506. doi:10.1111/j.1399-0004.2011.01669.x.

67. Drin G, Casella J-F, Gautier R, Boehmer T, Schwartz TU, Antonny B. A general amphipathic alpha-helical motif for sensing membrane curvature. *Nat Struct Mol Biol*. 2007;14(2):138-146. doi:10.1038/nsmb1194.

68. Dulski J, Sołtan W, Schinwelski M, et al. Clinical variability of neuroacanthocytosis syndromes-a series of six patients with long follow-up. *Clin Neurol Neurosurg*. 2016;147:78-83. doi:10.1016/j.clineuro.2016.05.028.

69. Duplomb L, Duvet S, Picot D, et al. Cohen syndrome is associated with major glycosylation defects. *Hum Mol Genet*. 2014;23(9):2391-2399. doi:10.1093/hmg/ddt630.

70. Dupont N, Nascimbeni AC, Morel E, Codogno P. *Molecular Mechanisms of Noncanonical Autophagy*. Vol 328. Elsevier Inc.; 2017. doi:10.1016/bs.ircmb.2016.08.001.

71. Eichinger L, Pachebat JA, Glöckner G, et al. The genome of the social amoeba Dictyostelium discoideum. *Nature*. 2005;435(7038):43-57. doi:10.1038/nature03481.

72. Eisenberg-Lerner A, Kimchi A. The paradox of autophagy and its implication in cancer etiology and therapy. *Apoptosis*. 2009;14(4):376-391. doi:10.1007/s10495-008-0307-5.

73. Elbaz-Alon Y, Rosenfeld-Gur E, Shinder V, Futerman AH, Geiger T, Schuldiner M. A dynamic interface between vacuoles and mitochondria in yeast. *Dev Cell*. 2014;30(1):95-102. doi:10.1016/j.devcel.2014.06.007.

74. Enyenihi AH, Saunders WS. Large-scale functional genomic analysis of sporulation and meiosis in Saccharomyces cerevisiae. *Genetics*. 2003;163(January):47-54.

75. Escalante R, Vicente JJ. Dictyostelium discoideum: A model system for differentiation and patterning. *Int J Dev Biol*. 2000;44(8):819-835.

76. Feng Y, He D, Yao Z, Klionsky DJ. The machinery of macroautophagy. *Cell Res*. 2014;24(1):24-41. doi:10.1038/cr.2013.168.

77. Fernández-Pajarín G, Sesar A, Ares B, et al. Deep brain bilateral pallidal stimulation in chorea-acanthocytosis caused by a homozygous VPS13A mutation. *Eur J Neurol*. 2016;23(1):e4-e5. doi:10.1111/ene.12833.

78. Fidler DR, Murphy SE, Courtis K, et al. Using HHsearch to tackle proteins of unknown function: A pilot study with PH domains. *Traffic*. 2016;17(11):1214-1226. doi:10.1111/tra.12432.

79. Filimonenko M, Stuffers S, Raiborg C, et al. Functional multivesicular bodies are required for autophagic clearance of protein aggregates associated with neurodegenerative disease. *J Cell Biol*. 2007;179(3):485-500.

doi:10.1083/jcb.200702115.

80. Foller M, Hermann A, Gu S, et al. Chorein-sensitive polymerization of cortical actin and suicidal cell death in chorea-acanthocytosis. *FASEB J*. 2012;26(4):1526-1534. doi:10.1096/fj.11-198317.

81. Foo JN, Tan LC, Irwan ID, et al. Genome-wide association study of Parkinson's disease in East Asians. *Hum Mol Genet*. 2016. doi:10.1093/hmg/ddw379.

82. De Franceschi L, Tomelleri C, Matte A, et al. Erythrocyte membrane changes of chorea-acanthocytosis are the result of altered Lyn kinase activity. *Blood*. 2011;118(20):5652-5663. doi:10.1182/blood-2011-05-355339.

83. Fratti RA, Jun Y, Merz AJ, Margolis N, Wickner W, Wickner B. Interdependent assembly of specific regulatory lipids and membrane fusion proteins into the vertex ring domain of docked vacuoles. *J Cell Biol*. 2004;167(6):1087-1098. doi:10.1083/jcb.200409068.

84. Friggeri A, Banerjee S, Xie N, et al. Extracellular histones inhibit efferocytosis. *Mol Med*. 2012;18(1):825-833. doi:10.2119/molmed.2012.00005.

85. Furukawa T, Kuboki Y, Tanji E, et al. Whole-exome sequencing uncovers frequent GNAS mutations in intraductal papillary mucinous neoplasms of the pancreas. *Sci Rep*. 2011;1:161. doi:10.1038/srep00161.

86. Gammoh N, Florey O, Overholtzer M, Jiang X. Interaction between FIP200 and ATG16L1 distinguishes ULK1 complex-dependent and -independent autophagy. *Nat Struct Mol Biol*. 2013;20(2):144-149. doi:10.1038/nsmb.2475.

87. Ganley IG, Wong PM, Gammoh N, Jiang X. Distinct Autophagosomal-Lysosomal Fusion Mechanism Revealed by Thapsigargin-Induced Autophagy Arrest. *Mol Cell*. 2011;42(6):731-743. doi:10.1016/j.molcel.2011.04.024.

88. Gao Y, Hubbert CC, Lu J, Lee Y, Lee J, Yao T. Histone Deacetylase 6 Regulates Growth Factor-Induced Actin Remodeling and Endocytosis. *Society*. 2007;27(24):8637-8647. doi:10.1128/MCB.00393-07.

89. Gillingham AK, Sinka R, Torres IL, Lilley KS, Munro S. Toward a comprehensive map of the effectors of rab GTPases. *Dev Cell*. 2014;31(3):358-373. doi:10.1016/j.devcel.2014.10.007.

90. Girard E, Chmiest D, Fournier N, et al. Rab7 Is Functionally Required for Selective Cargo Sorting at the Early Endosome. *Traffic*. 2014;15(3):309-326. doi:10.1111/tra.12143.

91. Gómez-Suaga P, Rivero-Ríos P, Fdez E, et al. LRRK2 delays degradative receptor trafficking by impeding late endosomal budding through decreasing Rab7 activity. *Hum Mol Genet*. 2014;23(25):6779-6796. doi:10.1093/hmg/ddu395.

92. Gonda K, Komatsu M, Numata O. Calmodulin and Ca2+/Calmodulin-Binding Proteins are Involved in Tetrahymena thermophila Phagocytosis. *Cell Struct Funct*. 2000;25(4):243-251. doi:10.1247/csf.25.243.

93. Gooneratne IK, Weeratunga PN, Gamage R. Teaching video neuroimages: orofacial dyskinesia and oral ulceration due to involuntary biting in neuroacanthocytosis. *Neurology*. 2014;82(8):e70. doi:10.1212/WNL.0000000000000144.

94. Grarup N, Overvad M, Sparsø T, et al. The diabetogenic VPS13C/C2CD4A/C2CD4B rs7172432 variant impairs glucose-stimulated insulin response in 5,722 non-diabetic Danish individuals. *Diabetologia*. 2011;54(4):789-794. doi:10.1007/s00125-010-2031-2.

95. Griffiths GM. Secretion from Myeloid Cells: Secretory Lysosomes. *Microbiol Spectr*.

2016;4(4). doi:10.1128/microbiolspec.MCHD-0030-2016.

96. Grippa A, Buxó L, Mora G, et al. The seipin complex Fld1/Ldb16 stabilizes ER-lipid droplet contact sites. *J Cell Biol*. 2015;211(4):829-844. doi:10.1083/jcb.201502070.

97. Gross SR, Kinzy TG. Translation elongation factor 1A is essential for regulation of the actin cytoskeleton and cell morphology. *Nat Struct Mol Biol*. 2005;12(9):772-778. doi:10.1038/nsmb979.

98. Guerra F, Bucci C. Multiple Roles of the Small GTPase Rab7. *Cells*. 2016;5(3):34. doi:10.3390/cells5030034.

99. Hamdi A, Roshan TM, Kahawita TM, Mason AB, Sheftel AD, Ponka P. Erythroid cell mitochondria receive endosomal iron by a "kiss-and-run" mechanism. *Biochim Biophys Acta - Mol Cell Res*. 2016;1863(12):2859-2867. doi:10.1016/j.bbamcr.2016.09.008.

100. Hammond GR V, Machner MP, Balla T. A novel probe for phosphatidylinositol 4-phosphate reveals multiple pools beyond the Golgi. *J Cell Biol*. 2014;205(1):113-126. doi:10.1083/jcb.201312072.

101. Hancock LC, Behta RP, Lopes JM. Genomic analysis of the Opi- phenotype. *Genetics*. 2006;173(2):621-634. doi:10.1534/genetics.106.057489.

102. Hardie RJ, Pullon HW, Harding AE, et al. Neuroacanthocytosis. A clinical, haematological and pathological study of 19 cases. *Brain*. 1991:13-49.

103. Hayashi T, Kishida M, Nishizawa Y, et al. Subcellular localization and putative role of VPS13A/chorein in dopaminergic neuronal cells. *Biochem Biophys Res Commun*. 2012;419(3):511-516. doi:10.1016/j.bbrc.2012.02.047.

104. Henkel K, Danek A, Grafman J, Butman J, Kassubek J. Head of the caudate nucleus is most vulnerable in chorea–acanthocytosis: A voxel-based morphometry study. *Mov Disord*. 2006;21(10):1728-1731. doi:10.1002/mds.21046.

105. Henmi Y, Morikawa Y, Oe N, et al. *PtdIns4KIIalpha Generates Endosomal PtdIns(4)P and Is Required for Receptor Sorting at Early Endosomes*. Vol 27.; 2016. doi:10.1091/mbc.E15-08-0564.

106. Hermann A, Walker RH. Diagnosis and treatment of chorea syndromes. *Curr Neurol Neurosci Rep*. 2015;15(2):1. doi:10.1007/s11910-014-0514-0.

107. Hirose G. Neuroacanthocytosis in Japan — Review of the Literature and Cases. In: *Neuroacanthocytosis Syndromes II*. Berlin, Heidelberg: Springer Berlin Heidelberg; 2008:75-84. doi:10.1007/978-3-540-71693-8_6.

108. Ho R, Stroupe C. The HOPS/Class C Vps Complex Tethers High-Curvature Membranes via a Direct Protein-Membrane Interaction. *Traffic*. 2016;17(10):1078-1090. doi:10.1111/tra.12421.

109. Hoeller O, Bolourani P, Clark J, et al. Two distinct functions for PI3-kinases in macropinocytosis. *J Cell Sci*. 2013;126:4296-4307. doi:10.1242/jcs.134015.

110. Hong L, Simons P, Waller A, et al. *A Small Molecule Pan-Inhibitor of Ras-Superfamily GTPases with High Efficacy towards Rab7*. National Center for Biotechnology Information (US); 2010.

111. Honisch S, Fehrenbacher B, Lebedeva A, et al. Chorein Sensitive Dopamine Release from Pheochromocytoma (PC12) Cells. *NeuroSignals*. 2015;23(1):1-10. doi:10.1159/000442599.

112. Honisch S, Gu S, Vom Hagen JM, et al. Chorein sensitive arrangement of cytoskeletal architecture. *Cell Physiol Biochem*. 2015;37(1):399-408. doi:10.1159/000430363.

113. Honisch S, Yu W, Liu G, et al. Chorein addiction in VPS13A overexpressing rhabdomyosarcoma cells. *Oncotarget*. 2015;6(12):10309-10319. doi:10.18632/oncotarget.3582.

114. Hönscher C, Mari M, Auffarth K, et al. Cellular metabolism regulates contact sites between vacuoles and mitochondria. *Dev Cell*. 2014;30(1):86-94. doi:10.1016/j.devcel.2014.06.006.

115. Hoppins S, Collins SR, Cassidy-Stone A, et al. A mitochondrial-focused genetic interaction map reveals a scaffold-like complex required for inner membrane organization in mitochondria. *J Cell Biol*. 2011;195(2):323-340. doi:10.1083/jcb.201107053.

116. Huh W-K, Falvo J V., Gerke LC, et al. Global analysis of protein localization in budding yeast. *Nature*. 2003;425(6959):686-691. doi:10.1038/nature02026.

117. Hung Y-H, Chen LM-W, Yang J-Y, Yuan Yang W. Spatiotemporally controlled induction of autophagy-mediated lysosome turnover. *Nat Commun*. 2013;4:2111. doi:10.1038/ncomms3111.

118. Huotari J, Helenius A. Endosome maturation. *EMBO J*. 2011;30(17):3481-3500. doi:10.1038/emboj.2011.286.

119. Huppertz H-J, Kröll-Seger J, Danek A, Weber B, Dorn T, Kassubek J. Automatic striatal volumetry allows for identification of patients with chorea-acanthocytosis at single subject level. *J Neural Transm*. 2008;115(10):1393-1400. doi:10.1007/s00702-008-0094-8.

120. Huttlin EL, Ting L, Bruckner RJ, et al. The BioPlex Network: A Systematic Exploration of the Human Interactome. *Cell*. 2015;162(2):425-440. doi:10.1016/j.cell.2015.06.043.

121. Inoshita T, Imai Y. Regulation of vesicular trafficking by Parkinson's disease-associated genes. *AIMS Mol Sci*. 2015;2(4):461-475. doi:10.3934/molsci.2015.4.461.

122. Jacobs ME, DeSouza L V., Samaranayake H, Pearlman RE, Siu KWM, Klobutcher LA. The Tetrahymena thermophila phagosome proteome. *Eukaryot Cell*. 2006;5(12):1990-2000. doi:10.1128/EC.00195-06.

123. Jacomin A-C, Fauvarque M-O, Taillebourg E. A functional endosomal pathway is necessary for lysosome biogenesis in Drosophila. *BMC Cell Biol*. 2016;17(1):36. doi:10.1186/s12860-016-0115-7.

124. Jäger S, Bucci C, Tanida I, et al. Role for Rab7 in maturation of late autophagic vacuoles. *J Cell Sci*. 2004;117(Pt 20):4837-4848. doi:10.1242/jcs.01370.

125. Jain N, Ganesh S. Emerging nexus between RAB GTPases, autophagy and neurodegeneration. *Autophagy*. 2016;12(5):900-904. doi:10.1080/15548627.2016.1147673.

126. Jansen IE, Ye H, Heetveld S, et al. *Discovery and Functional Prioritization of Parkinson's Disease Candidate Genes from Large-Scale Whole Exome Sequencing*. Vol 18.; 2017. doi:10.1186/s13059-017-1147-9.

127. Jeschke A, Zehethofer N, Lindner B, et al. Phosphatidylinositol 4-phosphate and phosphatidylinositol 3-phosphate regulate phagolysosome biogenesis. *Proc Natl Acad Sci*. 2015;112(15):201423456. doi:10.1073/pnas.1423456112.

128. Jiang P, Mizushima N. Autophagy and human diseases. *Cell Res*. 2014;24(1):69-79. doi:10.1038/cr.2013.161.

129. Johansson M, Rocha N, Zwart W, et al. Activation of endosomal dynein motors by stepwise assembly of Rab7–RILP–p150Glued, ORP1L, and the receptor βlll spectrin. *J*

Cell Biol. 2007;176(4):459-471. doi:10.1083/jcb.200606077.

130. Johnson DE, Ostrowski P, Jaumouillé V, Grinstein S. The position of lysosomes within the cell determines their luminal pH. *J Cell Biol*. 2016;212(6):677-692. doi:10.1083/jcb.201507112.

131. Joska TM, Mashruwala A, Boyd JM, Belden WJ. A universal cloning method based on yeast homologous recombination that is simple, efficient, and versatile. *J Microbiol Methods*. 2014;100:46-51. doi:10.1016/j.mimet.2013.11.013.

132. Junemann A, Filić V, Winterhoff M, et al. A *Diaphanous* -related formin links Ras signaling directly to actin assembly in macropinocytosis and phagocytosis. *Proc Natl Acad Sci*. 2016;113(47):E7464-E7473. doi:10.1073/pnas.1611024113.

133. Jung HH, Danek A, Walker RH. Neuroacanthocytosis Syndromes. *Orphanet J Rare Dis*. 2011;6:68. doi:10.1007/1-4020-2898-9.

134. Jung M, Lee J, Seo HY, Lim JS, Kim EK. Cathepsin inhibition-induced lysosomal dysfunction enhances pancreatic beta-cell apoptosis in high glucose. *PLoS One*. 2015;10(1):1-18. doi:10.1371/journal.pone.0116972.

135. Karanasios E, Stapleton E, Manifava M, Ktistakis NT. Imaging autophagy. *Curr Protoc Cytom*. 2014;(SUPPL.69):1-16. doi:10.1002/0471142956.cy1234s69.

136. Kaul B, Goyal V, Shukla G, et al. Mineral deposition on magnetic resonance imaging in chorea-acanthocytosis: a pathogenic link with pantothenate kinase-associated neurodegeneration? *Neurol India*. 2013;61(2):169-170. doi:10.4103/0028-3886.111129.

137. Kay MM, Goodman J, Goodman S, Lawrence C. Membrane protein band 3 alteration associated with neurologic disease and tissue-reactive antibodies. *Exp Clin Immunogenet*. 1990;7(3):181-199.

138. King JS. Autophagy across the eukaryotes: is S. cerevisiae the odd one out? *Autophagy*. 2012;8(7):1159-1162. doi:10.4161/auto.20527.

139. King JS, Veltman DM, Insall RH. The induction of autophagy by mechanical stress. *Autophagy*. 2011;7(12):1490-1499. doi:10.4161/auto.7.12.17924.

140. Kiriyama Y, Nochi H. The Function of Autophagy in Neurodegenerative Diseases. *Int J Mol Sci*. 2015;16(11):26797-26812. doi:10.3390/ijms161125990.

141. Kivitie-Kallio S, Norio R. Cohen Syndrome: Essential features, natural history, and heterogeneity. *Am J Med Genet*. 2001;102(2):125-135. doi:10.1002/1096-8628(20010801)102:2<125::AID-AJMG1439>3.0.CO;2-0.

142. Klionsky DJ, Abdalla FC, Abeliovich H, et al. Guidelines for the use and interpretation of assays for monitoring autophagy. *Autophagy*. 2012;8(4):445. doi:10.4161/auto.19496.

143. Klionsky DJ, Eskelinen E-L. The vacuole versus the lysosome: when size matters. *Autophagy*. 2014;10(2):185-187. doi:10.4161/auto.27367.

144. Klumperman J, Raposo G. The complex ultrastructure of the endolysosomal system. *Cold Spring Harb Perspect Biol*. 2014;6(10). doi:10.1101/cshperspect.a016857.

145. Knodler LA, Celli J. Eating the strangers within: host control of intracellular bacteria via xenophagy. *Cell Microbiol*. 2011;13(9):1319-1327. doi:10.1111/j.1462-5822.2011.01632.x.

146. Köchl R, Hu XW, Chan EYW, Tooze SA. Microtubules facilitate autophagosome formation and fusion of autophagosomes with endosomes. *Traffic*. 2006;7(2):129-145. doi:10.1111/j.1600-0854.2005.00368.x.

147. Kolehmainen J, Black GCM, Saarinen A, et al. Cohen syndrome is caused by mutations in a novel gene, COH1, encoding a transmembrane protein with a presumed role in vesicle-mediated sorting and intracellular protein transport. *Am J Hum Genet*. 2003;72(6):1359-1369. doi:10.1086/375454.

148. Korolchuk VI, Schütz MM, Gómez-Llorente C, et al. Drosophila Vps35 function is necessary for normal endocytic trafficking and actin cytoskeleton organisation. *J Cell Sci*. 2007;120(Pt 24):4367-4376. doi:10.1242/jcs.012336.

149. Kraft C, Kijanska M, Kalie E, et al. Binding of the Atg1/ULK1 kinase to the ubiquitin-like protein Atg8 regulates autophagy. *EMBO J*. 2012;31(18):3691-3703. doi:10.1038/emboj.2012.225.

150. Ktistakis NT, Tooze SA. Digesting the Expanding Mechanisms of Autophagy. *Trends Cell Biol*. 2016;26(8):624-635. doi:10.1016/j.tcb.2016.03.006.

151. Kurano Y, Nakamura M, Ichiba M, et al. Chorein deficiency leads to upregulation of gephyrin and GABAA receptor. *Biochem Biophys Res Commun*. 2006;351(2):438-442. doi:10.1016/j.bbrc.2006.10.070.

152. Kurano Y, Nakamura M, Ichiba M, et al. In vivo distribution and localization of chorein. *Biochem Biophys Res Commun*. 2007;353(2):431-435. doi:10.1016/j.bbrc.2006.12.059.

153. Lamb CA, Yoshimori T, Tooze SA. The autophagosome: origins unknown, biogenesis complex. *Nat Rev Mol Cell Biol*. 2013;14(12):759-774. doi:10.1038/nrm3696.

154. Lang AB, John Peter ATAT, Walter P, Kornmann B. ER-mitochondrial junctions can be bypassed by dominant mutations in the endosomal protein Vps13. *J Cell Biol*. 2015;210(6):883-890. doi:10.1083/jcb.201502105.

155. Lassing I, Lindberg U. Specific interaction between phosphatidylinositol 4,5-bisphosphate and profilactin. *Nature*. 1985;314(6010):472-474. doi:10.1038/314472a0.

156. Lee J-H, Lee S-M, Baik S-K. Demonstration of striatopallidal iron deposition in chorea-acanthocytosis by susceptibility-weighted imaging. *J Neurol*. 2011;258(2):321-322. doi:10.1007/s00415-010-5725-y.

157. Lee J-Y, Koga H, Kawaguchi Y, et al. HDAC6 controls autophagosome maturation essential for ubiquitin-selective quality-control autophagy. *EMBO J*. 2010;29(5):969-980. doi:10.1038/emboj.2009.405.

158. Lee JH, Cho WH, Cha SH, Kang DW. Globus pallidus interna deep brain stimulation for chorea-acanthocytosis. *J Korean Neurosurg Soc*. 2015;57(2):143-146. doi:10.3340/jkns.2015.57.2.143.

159. Lee JY, Nagano Y, Taylor JP, Lim KL, Yao TP. Disease-causing mutations in Parkin impair mitochondrial ubiquitination, aggregation, and HDAC6-dependent mitophagy. *J Cell Biol*. 2010;189(4):671-679. doi:10.1083/jcb.201001039.

160. Leiba J, Sabra A, Bodinier R, et al. Vps13F links bacterial recognition and intracellular killing in *Dictyostelium*. *Cell Microbiol*. 2017:e12722. doi:10.1111/cmi.12722.

161. Lesage S, Drouet V, Majounie E, et al. Loss of VPS13C Function in Autosomal-Recessive Parkinsonism Causes Mitochondrial Dysfunction and Increases PINK1/Parkin-Dependent Mitophagy. *Am J Hum Genet*. 2016;98(3):500-513. doi:10.1016/j.ajhg.2016.01.014.

162. Levine B, Klionsky DJ. Development by self-digestion: Molecular mechanisms and biological functions of autophagy. *Dev Cell*. 2004;6(4):463-477. doi:10.1016/S1534-5807(04)00099-1.

163. Li W, Li J, Bao J. Microautophagy: lesser-known self-eating. *Cell Mol Life Sci*. 2012;69(7):1125-1136. doi:10.1007/s00018-011-0865-5.

164. Lima WC, Cosson P. Secretory Lysosomes in Dictyostelium: Visualization, Characterization, and Dynamics. In: ; 2013:445-459. doi:10.1007/978-1-62703-302-2_25.

165. Liu T-TT, Gomez TS, Sackey BK, Billadeau DD, Burd CG. Rab GTPase regulation of retromer-mediated cargo export during endosome maturation. *Mol Biol Cell*. 2012;23(13):2505-2515. doi:10.1091/mbc.E11-11-0915.

166. Lossos A, Dobson-Stone C, Monaco AP, et al. Early clinical heterogeneity in choreoacanthocytosis. *Arch Neurol*. 2005;62(4):611-614. doi:62/4/611 [pii]\r10.1001/archneur.62.4.611.

167. De Luca M, Cogli L, Progida C, et al. RILP regulates vacuolar ATPase through interaction with the V1G1 subunit. *J Cell Sci*. 2014;127(12):2697-2708. doi:10.1242/jcs.142604.

168. Luo WJ, Chang A. Novel genes involved in endosomal traffic in yeast revealed by suppression of a targeting-defective plasma membrane ATPase mutant. *J Cell Biol*. 1997;138(4):731-746. doi:10.1083/jcb.138.4.731.

169. Lupo F, Tibaldi E, Matte A, et al. A new molecular link between defective autophagy and erythroid abnormalities in chorea-acanthocytosis. *Blood*. 2016;128(25):2976-2987. doi:10.1182/blood-2016-07-727321.

170. MacLeod DA, Rhinn H, Kuwahara T, et al. RAB7L1 Interacts with LRRK2 to Modify Intraneuronal Protein Sorting and Parkinson's Disease Risk. *Neuron*. 2013;77(3):425-439. doi:10.1016/j.neuron.2012.11.033.

171. Maniak M. Fusion and fission events in the endocytic pathway of Dictyostelium. *Traffic*. 2003;4(1):1-5. doi:10.1034/j.1600-0854.2003.40101.x.

172. Manil-Segalen M, Lefebvre C, Culetto E, Legouis R. Need an ESCRT for autophagosomal maturation? *Commun Integr Biol*. 2012;5(6):566-571. doi:10.4161/cib.21522.

173. Manjithaya R, Nazarko TY, Farré J-C, Subramani S. Molecular mechanism and physiological role of pexophagy. *FEBS Lett*. 2010;584(7):1367-1373. doi:10.1016/j.febslet.2010.01.019.

174. Marchetti A, Lelong E, Cosson P. A measure of endosomal pH by flow cytometry in Dictyostelium. *BMC Res Notes*. 2009;2(1):7. doi:10.1186/1756-0500-2-7.

175. Mari M, Tooze SA, Reggiori F. The puzzling origin of the autophagosomal membrane. *F1000 Biol Rep*. 2011;3:25. doi:10.3410/B3-25.

176. Mascia A, Gentile F, Izzo A, et al. Rab7 Regulates CDH1 Endocytosis, Circular Dorsal Ruffles Genesis, and Thyroglobulin Internalization in a Thyroid Cell Line. *J Cell Physiol*. 2016;231(8):1695-1708. doi:10.1002/jcp.25267.

177. Maskey D, Yousefi S, Schmid I, et al. ATG5 is induced by DNA-damaging agents and promotes mitotic catastrophe independent of autophagy. *Nat Commun*. 2013;4:748-762. doi:10.1038/ncomms3130.

178. Mauvezin C, Nagy P, Juhász G, Neufeld TP, Patel S. Autophagosome–lysosome fusion is independent of V-ATPase-mediated acidification. *Nat Commun*. 2015;6:7007. doi:10.1038/ncomms8007.

179. McCray BA, Skordalakes E, Taylor JP. Disease mutations in Rab7 result in unregulated nucleotide exchange and inappropriate activation. *Hum Mol Genet*. 2010;19(6):1033-1047. doi:10.1093/hmg/ddp567.

180. Meda SA, Narayanan B, Liu J, et al. A large scale multivariate parallel ICA method reveals novel imaging-genetic relationships for Alzheimer's disease in the ADNI cohort. *Neuroimage*. 2012;60(3):1608-1621. doi:10.1016/j.neuroimage.2011.12.076.

181. Melone MAB, Di Fede G, Peluso G, et al. Abnormal accumulation of tTGase products in muscle and erythrocytes of chorea-acanthocytosis patients. *J Neuropathol Exp Neurol*. 2002;61(10):841-848.

182. Meriin AB, Zhang X, Miliaras NB, et al. Aggregation of expanded polyglutamine domain in yeast leads to defects in endocytosis. *Mol Cell Biol*. 2003;23(21):7554-7565. doi:10.1128/MCB.23.21.7554-7565.2003.

183. Mesquita A, Cardenal-Muñoz E, Dominguez E, et al. Autophagy in Dictyostelium: Mechanisms, regulation and disease in a simple biomedical model. *Autophagy*. 2016;13(1):1-17. doi:10.1080/15548627.2016.1226737.

184. Mesquita A, Tábara LC, Martinez-Costa O, Santos-Rodrigo N, Vincent O, Escalante R. Dissecting the function of Atg1 complex in Dictyostelium autophagy reveals a connection with the pentose phosphate pathway enzyme transketolase. *Open Biol*. 2015;5(8):150088. doi:10.1098/rsob.150088.

185. Mijaljica D, Prescott M, Devenish RJ. The intriguing life of Autophagosomes. *Int J Mol Sci*. 2012;13(3):3618-3635. doi:10.3390/ijms13033618.

186. Miki Y, Nishie M, Ichiba M, et al. Chorea-acanthocytosis with upper motor neuron degeneration and 3419_3420 delCA and 3970_3973 delAGTC VPS13A mutations. *Acta Neuropathol*. 2010;119(2):271-273. doi:10.1007/s00401-009-0617-x.

187. Mikitova V, Levine TP. Analysis of the key elements of FFAT-like motifs identifies new proteins that potentially bind VAP on the ER, including two AKAPs and FAPP2. *PLoS One*. 2012;7(1). doi:10.1371/journal.pone.0030455.

188. Mima J, Hickey C, Xu H, Jun Y, Wickner W. Reconstituted membrane fusion requires regulatory lipids, {SNAREs} and synergistic {SNARE} chaperones. *{Embo} J*. 2008;27(15):2031-2042. doi:10.1038/emboj.2008.139.

189. Miotti S, Bagnoli M, Tomassetti A, Colnaghi MI, Canevari S. Interaction of folate receptor with signaling molecules lyn and G(alpha)(i-3) in detergent-resistant complexes from the ovary carcinoma cell line IGROV1. *J Cell Sci*. 2000;113 Pt 2:349-357.

190. Miquel M, Spampinato U, Latxague C, et al. Short and long term outcome of bilateral pallidal stimulation in chorea-acanthocytosis. *PLoS One*. 2013;8(11):1-11. doi:10.1371/journal.pone.0079241.

191. Mizumura K, Cloonan SM, Haspel JA, Choi AMK. The Emerging Importance of Autophagy in Pulmonary Diseases. *Chest*. 2012;142(5):1289-1299. doi:10.1378/chest.12-0809.

192. Mizuno E, Nakamura M, Agemura A, et al. Brain-specific transcript variants of 5' and 3' ends of mouse VPS13A and VPS13C. *Biochem Biophys Res Commun*. 2007;353(4):902-907. doi:10.1016/j.bbrc.2006.12.122.

193. Mizushima N, Yoshimori T, Ohsumi Y. The Role of Atg Proteins in Autophagosome Formation. *Annu Rev Cell Dev Biol*. 2011;27(1):107-132. doi:10.1146/annurev-cellbio-092910-154005.

194. Mochida GH, Rajab A, Eyaid W, et al. Broader geographical spectrum of Cohen syndrome due to COH1 mutations. *J Med Genet*. 2004;41(6):e87. doi:10.1136/JMG.2003.014779.

195. Morel E, Mehrpour M, Botti J, et al. Autophagy: A Druggable Process. *Annu Rev*

Pharmacol Toxicol. 2017;57(1):375-398. doi:10.1146/annurev-pharmtox-010716-104936.

196. Morisaki T, Yashiro M, Kakehashi A, et al. Comparative proteomics analysis of gastric cancer stem cells. *PLoS One*. 2014;9(11):e110736. doi:10.1371/journal.pone.0110736.

197. Mukhopadhyay A, Quiroz JA, Wolkoff AW. Rab1a regulates sorting of early endocytic vesicles. *Am J Physiol Gastrointest Liver Physiol*. 2014;306(5):412-424. doi:10.1152/ajpgi.00118.2013.

198. Mukhopadhyay S, Panda PK, Sinha N, Das DN, Bhutia SK. Autophagy and apoptosis: where do they meet? *Apoptosis*. 2014;19(4):555-566. doi:10.1007/s10495-014-0967-2.

199. Müller-Vahl KR, Berding G, Emrich HM, Peschel T. Chorea-acanthocytosis in monozygotic twins: clinical findings and neuropathological changes as detected by diffusion tensor imaging, FDG-PET and 123I-β-CIT-SPECT. *J Neurol*. 2007;254(8):1081-1088. doi:10.1007/s00415-006-0492-5.

200. Müller R, Herr C, Sukumaran SK, et al. The cytohesin paralog Sec7 of Dictyostelium discoideum is required for phagocytosis and cell motility. *Cell Commun Signal*. 2013;11:54. doi:10.1186/1478-811X-11-54.

201. Münz C. The Macroautophagy Machinery in Endo- and Exocytosis. *J Mol Biol*. December 2016. doi:10.1016/j.jmb.2016.11.028.

202. Muñoz-Braceras S, Calvo R, Escalante R. TipC and the chorea-acanthocytosis protein VPS13A regulate autophagy in *Dictyostelium* and human HeLa cells. *Autophagy*. 2015;11(6):918-927. doi:10.1080/15548627.2015.1034413.

203. Muñoz-Braceras S, Escalante R. Analysis of Relevant Parameters for Autophagic Flux Using HeLa Cells Expressing EGFP-LC3. *Methods Mol Biol*. 2016;1449:313-329. doi:10.1007/978-1-4939-3756-1_20.

204. Muñoz-Braceras S, Mesquita A, Escalante R. Dictyostelium discoideum as a Model in Biomedical Research. In: *Dictyostelids*. Berlin, Heidelberg: Springer Berlin Heidelberg; 2013:1-34. doi:10.1007/978-3-642-38487-5_1.

205. Nagy A, Noyce A, Velayos-Baeza A, Lees AJ, Warner TT, Ling H. Late Emergence of Parkinsonian Phenotype and Abnormal Dopamine Transporter Scan in Chorea-Acanthocytosis. *Mov Disord Clin Pract*. 2015;2(2):182-186. doi:10.1002/mdc3.12138.

206. Nakada T, Boyd JH, Russell JA, et al. VPS13D Gene Variant Is Associated with Altered IL-6 Production and Mortality in Septic Shock. *J Innate Immun*. 2015;7(5):545-553. doi:10.1159/000381265.

207. Nakanishi H, Suda Y, Neiman AM. Erv14 family cargo receptors are necessary for ER exit during sporulation in Saccharomyces cerevisiae. *J Cell Sci*. 2007;120(5):908-916. doi:10.1242/jcs.03405.

208. Nakatogawa H, Mochida K. Reticulophagy and nucleophagy: New findings and unsolved issues. *Autophagy*. 2015;11(12):2377-2378. doi:10.1080/15548627.2015.1106665.

209. Nalls MA, Pankratz N, Lill CM, et al. Large-scale meta-analysis of genome-wide association data identifies six new risk loci for Parkinson's disease. *Nat Genet*. 2014;46(9):989-993. doi:10.1038/ng.3043.

210. Nelms B, Dalomba NF, Lencer W. A targeted RNAi screen identifies factors affecting diverse stages of receptor-mediated transcytosis. *J Cell Biol*. 2017;216(2):511-525. doi:10.1083/jcb.201609035.

211. Ni H-M, Williams JA, Yang H, Shi Y-H, Fan J, Ding W-X. Targeting autophagy for the treatment of liver diseases. *Pharmacol Res*. 2012;66(6):463-474. doi:10.1016/j.phrs.2012.07.003.

212. Ni HM, Bockus A, Wozniak AL, et al. Dissecting the dynamic turnover of GFP-LC3 in the autolysosome. *Autophagy*. 2011;7(2):188-204. doi:10.4161/auto.7.2.14181.

213. Nikoletopoulou V, Markaki M, Palikaras K, Tavernarakis N. Crosstalk between apoptosis, necrosis and autophagy. *Biochim Biophys Acta - Mol Cell Res*. 2013;1833(12):3448-3459. doi:10.1016/j.bbamcr.2013.06.001.

214. Nikoletopoulou V, Papandreou M-E, Tavernarakis N. Autophagy in the physiology and pathology of the central nervous system. *Cell Death Differ*. 2015;22(3):398-407. doi:10.1038/cdd.2014.204.

215. Noda NN, Inagaki F. Mechanisms of Autophagy. *Annu Rev Biophys*. 2015;44(1):101-122. doi:10.1146/annurev-biophys-060414-034248.

216. Oberwagner W, Sauer T, Hermann A, Prohaska R, Müllner EW, Salzer U. Drug-induced endovesiculation of erythrocytes is modulated by the dynamics in the cytoskeleton/membrane interaction. *Blood Cells, Mol Dis*. 2017;64:15-22. doi:10.1016/j.bcmd.2017.03.004.

217. Ohsumi Y. Historical landmarks of autophagy research. *Cell Res*. 2014;24(1):9-23. doi:10.1038/cr.2013.169.

218. Okumura Y, Nakamura TS, Tanaka T, et al. The Dysferlin Domain-Only Protein, Spo73, Is Required for Prospore Membrane Extension in Saccharomyces cerevisiae. *mSphere*. 2015;1(1):1-14. doi:10.1128/mSphere.00038-15.Editor.

219. Olivieri O, De Franceschi L, Bordin L, et al. Increased membrane protein phosphorylation and anion transport activity in chorea-acanthocytosis. *Haematologica*. 1997;82(6):648-653.

220. Orr A, Wickner W, Rusin SF, Kettenbach AN, Zick M. Yeast vacuolar HOPS, regulated by its kinase, exploits affinities for acidic lipids and Rab:GTP for membrane binding and to catalyze tethering and fusion. *Mol Biol Cell*. 2015;26(2):305-315. doi:10.1091/mbc.E14-08-1298.

221. Oshima M, Osawa Y, Asano K, Saito T. Erythrocyte membrane abnormalities in patients with amyotrophic chorea with acanthocytosis. Part 1. Spin labeling studies and lipid analyses. *J Neurol Sci*. 1985;68(2-3):147-160.

222. Otto GP, Wu MY, Kazgan N, Anderson OR, Kessin RH. Dictyostelium Macroautophagy Mutants Vary in the Severity of Their Developmental Defects. *J Biol Chem*. 2004;279(15):15621-15629. doi:10.1074/jbc.M311139200.

223. Otto GP, Wu MY, Kazgan N, Anderson OR, Kessin RH. Macroautophagy is required for multicellular development of the social amoeba Dictyostelium discoideum. *J Biol Chem*. 2003;278(20):17636-17645. doi:10.1074/jbc.M212467200.

224. Pankiv S, Alemu EA, Brech A, et al. FYCO1 is a Rab7 effector that binds to LC3 and PI3P to mediate microtubule plus end - Directed vesicle transport. *J Cell Biol*. 2010;188(2):253-269. doi:10.1083/jcb.200907015.

225. Papinski D, Schuschnig M, Reiter W, et al. Early steps in autophagy depend on direct phosphorylation of Atg9 by the Atg1 kinase. *Mol Cell*. 2014;53(3):471-483. doi:10.1016/j.molcel.2013.12.011.

226. Park HY, Lee S-B, Yoo H-Y, et al. Whole-exome and transcriptome sequencing of refractory diffuse large B-cell lymphoma. *Oncotarget*. 2016;7(52):86433-86445. doi:10.18632/oncotarget.13239.

227. Park J-S, Neiman AM. VPS13 regulates membrane morphogenesis during sporulation in Saccharomyces cerevisiae. *J Cell Sci*. 2012;125(Pt 12):3004-3011. doi:10.1242/jcs.105114.

228. Park J-S, Thorsness MK, Policastro R, et al. *Yeast Vps13 Promotes Mitochondrial Function and Is Localized at Membrane Contact Sites*. Vol 1543.; 2016. doi:10.1091/mbc.E16-02-0112.

229. Park JS, Halegoua S, Kishida S, Neiman AM. A conserved function in phosphatidylinositol metabolism for mammalian Vps13 family proteins. *PLoS One*. 2015;10(4):1-13. doi:10.1371/journal.pone.0124836.

230. Park JS, Okumura Y, Tachikawa H, Neiman AM. SPO71 encodes a developmental stage-specific partner for Vps13 in Saccharomyces cerevisiae. *Eukaryot Cell*. 2013;12(11):1530-1537. doi:10.1128/EC.00239-13.

231. Parodi EM, Roesner JM, Huang LS. SPO73 and SPO71 Function cooperatively in prospore membrane elongation during sporulation in saccharomyces cerevisiae. *PLoS One*. 2015;10(11):1-12. doi:10.1371/journal.pone.0143571.

232. Parzych KR, Klionsky DJ. An overview of autophagy: morphology, mechanism, and regulation. *Antioxid Redox Signal*. 2014;20(3):460-473. doi:10.1089/ars.2013.5371.

233. Paucar M, Lindestad PÅ, Walker RH, Svenningsson P. Teaching video neuroimages: feeding dystonia in chorea-acanthocytosis. *Neurology*. 2015;85(19):e143-e144. doi:10.1212/WNL.0000000000002108.

234. Pereira L, Girardi JP, Bakovic M. Forms, crosstalks, and the role of phospholipid biosynthesis in autophagy. *Int J Cell Biol*. 2012;2012. doi:10.1155/2012/931956.

235. Plemel RL, Lobingier BT, Brett CL, et al. Subunit organization and Rab interactions of Vps-C protein complexes that control endolysosomal membrane traffic. *Mol Biol Cell*. 2011;22(8):1353-1363. doi:10.1091/mbc.E10-03-0260.

236. Poston CN, Krishnan SC, Bazemore-Walker CR. In-depth proteomic analysis of mammalian mitochondria-associated membranes (MAM). *J Proteomics*. 2013;79:219-230. doi:10.1016/j.jprot.2012.12.018.

237. Privitera G, Meli G. An unusual cause of anemia in cirrhosis: spur cell anemia, a case report with review of literature. *Gastroenterol Hepatol from bed to bench*. 2016;9(4):335-339.

238. Priya A, Kalaidzidis I V, Kalaidzidis Y, Lambright D, Datta S. Molecular insights into Rab7-mediated endosomal recruitment of core retromer: deciphering the role of Vps26 and Vps35. *Traffic*. 2015;16(1):68-84. doi:10.1111/tra.12237.

239. Proikas-Cezanne T, Pfisterer SG. Assessing Mammalian Autophagy by WIPI-1/Atg18 Puncta Formation. *Methods Enzymol*. 2009;451(C):247-260. doi:10.1016/S0076-6879(08)03616-1.

240. Prudent J, Popgeorgiev N, Gadet R, Deygas M, Rimokh R, Gillet G. Mitochondrial Ca2+ uptake controls actin cytoskeleton dynamics during cell migration. *Sci Rep*. 2016;6:36570. doi:10.1038/srep36570.

241. Raimundo N, Fernández-Mosquera L, Yambire KF, Diogo C V. Mechanisms of communication between mitochondria and lysosomes. *Int J Biochem Cell Biol*. 2016;79:345-349. doi:10.1016/j.biocel.2016.08.020.

242. Rampoldi L, Danek A, Monaco AP. Clinical features and molecular bases of neuroacanthocytosis. *J Mol Med*. 2002;80(8):475-491. doi:10.1007/s00109-002-0349-z.

243. Rampoldi L, Dobson-Stone C, Rubio JP, et al. A conserved sorting-associated protein is mutant in chorea-acanthocytosis. *Nat Genet*. 2001;28(2):119-120. doi:10.1038/88821.

244. Rana M, Lachmann J, Ungermann C. Identification of a Rab GAP cascade that controls recycling of the Rab5 GTPase Vps21 from the vacuole. *Mol Biol Cell*. 2015;26(13):2535-2549. doi:10.1091/mbc.E15-02-0062.

245. Raymond CK, I H-S, Vater CA, Stevens TH. Morphological classification of the yeast vacuolar protein sorting mutants: evidence for a prevacuolar compartment in class E vps mutants. *Mol Biol Cell*. 1992;3(12):1389-1402. doi:10.1091/mbc.E12-03-0184.

246. Redding K, Brickner JH, Marschall LG, Nichols JW, Fuller RS. Allele-specific suppression of a defective trans-Golgi network (TGN) localization signal in Kex2p identifies three genes involved in localization of TGN transmembrane proteins. *Mol Cell Biol*. 1996;16(11):6208-6217. doi:10.1128/MCB.16.11.6208.

247. Rezzani R, Stacchiotti A, Rodella LF. Morphological and biochemical studies on aging and autophagy. *Ageing Res Rev*. 2012;11(1):10-31. doi:10.1016/j.arr.2011.09.001.

248. Riquelme SA, Pogu J, Anegon I, Bueno SM, Kalergis AM. Carbon monoxide impairs mitochondria-dependent endosomal maturation and antigen presentation in dendritic cells. *Eur J Immunol*. 2015;45(12):3269-3288. doi:10.1002/eji.201545671.

249. Robinson JS, Klionsky DJ, Banta LM, Emr SD. Protein sorting in Saccharomyces cerevisiae: isolation of mutants defective in the delivery and processing of multiple vacuolar hydrolases. *Mol Cell Biol*. 1988;8(11):4936-4948. doi:10.1128/MCB.8.11.4936.

250. Rogers LD, Foster LJ. The dynamic phagosomal proteome and the contribution of the endoplasmic reticulum. *Proc Natl Acad Sci*. 2007;104(47):18520-18525. doi:10.1073/pnas.0705801104.

251. Rojas R, Van Vlijmen T, Mardones GA, et al. Regulation of retromer recruitment to endosomes by sequential action of Rab5 and Rab7. *J Cell Biol*. 2008;183(3):513-526. doi:10.1083/jcb.200804048.

252. Romeralo M, Escalante R, Baldauf SL. Evolution and Diversity of Dictyostelid Social Amoebae. *Protist*. 2012;163(3):327-343. doi:10.1016/j.protis.2011.09.004.

253. Rong Y, McPhee CK, McPhee C, et al. Spinster is required for autophagic lysosome reformation and mTOR reactivation following starvation. *Proc Natl Acad Sci U S A*. 2011;108(19):7826-7831. doi:10.1073/pnas.1013800108.

254. Rothman JH, Howald I, Stevens TH. Characterization of genes required for protein sorting and vacuolar function in the yeast Saccharomyces cerevisiae. *EMBO J*. 1989;8(7):2057-2065.

255. Rothman JH, Stevens TH. Protein sorting in yeast: Mutants defective in vacuole biogenesis mislocalize vacuolar proteins into the late secretory pathway. *Cell*. 1986;47(6):1041-1051. doi:10.1016/0092-8674(86)90819-6.

256. Rubinsztein DC, Codogno P, Levine B. Autophagy modulation as a potential therapeutic target for diverse diseases. *Nat Rev Drug Discov*. 2012;11(9):709-730. doi:10.1038/nrd3802.

257. Ryter SW, Koo JK, Choi AMK. Molecular regulation of autophagy and its implications for metabolic diseases. *Curr Opin Clin Nutr Metab Care*. 2014;17(4):329-337. doi:10.1097/MCO.0000000000000068.

258. Rzepnikowska W, Flis K, Kaminska J, et al. Amino acid substitution equivalent to human chorea-acanthocytosis I2771R in yeast Vps13 protein affects its binding to phosphatidylinositol 3-phosphate. *Hum Mol Genet*. 2017;122:19-27.

doi:10.1093/hmg/ddx054.

259. Safaralizadeh T, Jamshidi J, Esmaili Shandiz E, et al. SIPA1L2, MIR4697, GCH1 and VPS13C loci and risk of Parkinson's diseases in Iranian population: A case-control study. *J Neurol Sci*. 2016;369:1-4. doi:10.1016/j.jns.2016.08.001.

260. Saiki S, Sakai K, Kitagawa Y, Saiki M, Kataoka S, Hirose G. Mutation in the CHAC gene in a family of autosomal dominant chorea-acanthocytosis. *Neurology*. 2003;61(11):1614-1616. doi:10.1212/01.wnl.0000416389.94466.01.

261. Saiki S, Tamura Y. Muscular Aspects of Chorea-Acanthocytosis. In: *Neuroacanthocytosis Syndromes II*. Berlin, Heidelberg: Springer Berlin Heidelberg; 2008:225-237. doi:10.1007/978-3-540-71693-8_19.

262. Sakai T, Antoku Y, Iwashita H, Goto I, Nagamatsu K, Shii H. Chorea-acanthocytosis: Abnormal composition of covalently bound fatty acids of erythrocyte membrane proteins. *Ann Neurol*. 1991;29(6):664-669. doi:10.1002/ana.410290615.

263. Sakimoto H, Nakamura M, Nagata O, Yokoyama I, Sano A. Phenotypic abnormalities in a chorea-acanthocytosis mouse model are modulated by strain background. *Biochem Biophys Res Commun*. 2016;472(1):118-124. doi:10.1016/j.bbrc.2016.02.077.

264. Samaranayake HS, Cowan AE, Klobutcher LA. Vacuolar protein sorting protein 13A, TtVPS13A, localizes to the Tetrahymena thermophila phagosome membrane and is required for efficient phagocytosis. *Eukaryot Cell*. 2011;10(9):1207-1218. doi:10.1128/EC.05089-11.

265. Sano A. Psychiatric Morbidity in Neuroacanthocytosis. In: *Neuroacanthocytosis Syndromes II*. Berlin, Heidelberg: Springer Berlin Heidelberg; 2008:219-223. doi:10.1007/978-3-540-71693-8_18.

266. Sasaki N, Nakamura M, Kodama A, et al. Chorein interacts with a-Tubulin and histone deacetylase 6, and overexpression preserves cell viability during nutrient deprivation in human embryonic kidney 293 cells. *FASEB J*. 2016;30(11):3726-3732. doi:10.1096/fj.201500191RR.

267. Saxena R, Hivert M-F, Langenberg C, et al. Genetic variation in GIPR influences the glucose and insulin responses to an oral glucose challenge. *Nat Genet*. 2010;42(2):142-148. doi:10.1038/ng.521.

268. Schaaf MBE, Keulers TG, Vooijs MA, Rouschop KMA. LC3/GABARAP family proteins: autophagy-(un)related functions. *FASEB J*. 2016;30(12):3961-3978. doi:10.1096/fj.201600698R.

269. Scheid R, Bader B, Ott D V., Merkenschlager A, Danek A. Development of mesial temporal lobe epilepsy in chorea-acanthocytosis. *Neurology*. 2009;73(17):1419-1422. doi:10.1212/WNL.0b013e3181bd80d4.

270. Schink KO, Tan K-W, Stenmark H. Phosphoinositides in Control of Membrane Dynamics. *Annu Rev Cell Dev Biol*. 2016;322429(1):1-24. doi:10.1146/annurev-cellbio-111315-125349.

271. Schmid JA, Mach L, Paschke E, Glössl J. Accumulation of sialic acid in endocytic compartments interferes with the formation of mature lysosomes. Impaired proteolytic processing of cathepsin B in fibroblasts of patients with lysosomal sialic acid storage disease. *J Biol Chem*. 1999;274(27):19063-19071. doi:10.1074/jbc.274.27.19063.

272. Schmidt EM, Schmid E, Münzer P, et al. Chorein sensitivity of cytoskeletal organization and degranulation of platelets. *FASEB J*. 2013;27(7):2799-2806. doi:10.1096/fj.13-229286.

273. Schneider JL, Cuervo AM. Autophagy and human disease: emerging themes. *Curr Opin Genet Dev*. 2014;26:16-23. doi:10.1016/j.gde.2014.04.003.

274. Schneider SA, Lang AE, Moro E, Bader B, Danek A, Bhatia KP. Characteristic head drops and axial extension in advanced chorea-acanthocytosis. *Mov Disord*. 2010;25(10):1487-1491. doi:10.1002/mds.23052.

275. Seifert W, Holder-Espinasse M, Kühnisch J, et al. Expanded mutational spectrum in Cohen syndrome, tissue expression, and transcript variants of COH1. *Hum Mutat*. 2009;30(2):E404-E420. doi:10.1002/humu.20886.

276. Seifert W, Kühnisch J, Maritzen T, et al. Cohen syndrome-associated protein COH1 physically and functionally interacts with the small GTPase RAB6 at the Golgi complex and directs neurite outgrowth. *J Biol Chem*. 2015;290(6):3349-3358. doi:10.1074/jbc.M114.608174.

277. Seifert W, Kühnisch J, Maritzen T, Horn D, Haucke V, Hennies HC. Cohen syndrome-associated protein, COH1, is a novel, giant Golgi matrix protein required for Golgi integrity. *J Biol Chem*. 2011;286(43):37665-37675. doi:10.1074/jbc.M111.267971.

278. Senft D, Ronai ZA. UPR, autophagy, and mitochondria crosstalk underlies the ER stress response. *Trends Biochem Sci*. 2015;40(3):141-148. doi:10.1016/j.tibs.2015.01.002.

279. Shevchenko A, Wilm M, Vorm O, Mann M. Mass spectrometric sequencing of proteins silver-stained polyacrylamide gels. *Anal Chem*. 1996;68(5):850-858. doi:10.1021/ac950914h.

280. Shibutani ST, Saitoh T, Nowag H, Münz C, Yoshimori T. Autophagy and autophagy-related proteins in the immune system. *Nat Immunol*. 2015;16(10):1014-1024. doi:10.1038/ni.3273.

281. Shibutani ST, Yoshimori T. A current perspective of autophagosome biogenesis. *Cell Res*. 2014;24(1):58-68. doi:10.1038/cr.2013.159.

282. Shimizu S, Honda S, Arakawa S, Yamaguchi H. Alternative macroautophagy and mitophagy. *Int J Biochem Cell Biol*. 2014;50(1):64-66. doi:10.1016/j.biocel.2014.02.016.

283. Shiokawa N, Nakamura M, Sameshima M, et al. Chorein, the protein responsible for chorea-acanthocytosis, interacts with β-adducin and β-actin. *Biochem Biophys Res Commun*. 2013;441(1):96-101. doi:10.1016/j.bbrc.2013.10.011.

284. Shirakabe A, Ikeda Y, Sciarretta S, Zablocki DK, Sadoshima J. Aging and Autophagy in the Heart. *Circ Res*. 2016;118(10):1563-1576. doi:10.1161/CIRCRESAHA.116.307474.

285. Shui W, Sheu L, Liu J, et al. Membrane proteomics of phagosomes suggests a connection to autophagy. *Proc Natl Acad Sci U S A*. 2008;105(44):16952-16957. doi:10.1073/pnas.0809218105.

286. Siegl C, Hamminger P, Jank H, et al. Alterations of Red Cell Membrane Properties in Nneuroacanthocytosis. *PLoS One*. 2013;8(10):1-13. doi:10.1371/journal.pone.0076715.

287. Song P, Trajkovic K, Tsunemi T, Krainc D. Parkin Modulates Endosomal Organization and Function of the Endo-Lysosomal Pathway. *J Neurosci*. 2016;36(8):2425-2437. doi:10.1523/JNEUROSCI.2569-15.2016.

288. Sorrentino G, De Renzo A, Miniello S, Nori O, Bonavita V. *Late Appearance of Acanthocytes during the Course of Chorea-Acanthocytosis*. Vol 163.; 1999. doi:10.1016/S0022-510X(99)00005-2.

289. Stanslowsky N, Reinhardt P, Glass H, et al. Neuronal Dysfunction in iPSC-Derived

Medium Spiny Neurons from Chorea-Acanthocytosis Patients Is Reversed by Src Kinase Inhibition and F-Actin Stabilization. *J Neurosci*. 2016;36(47):12027-12043. doi:10.1523/JNEUROSCI.0456-16.2016.

290. Stege JT, Laub MT, Loomis WF. Tip genes act in parallel pathways of early Dictyostelium development. *Dev Genet*. 1999;25(1):64-77. doi:10.1002/(SICI)1520-6408(1999)25:1<64::AID-DVG7>3.0.CO;2-1.

291. Strawbridge RJ, Dupuis J, Prokopenko I, et al. Genome-wide association identifies nine common variants associated with fasting proinsulin levels and provides new insights into the pathophysiology of type 2 diabetes. *Diabetes*. 2011;60(10):2624-2634. doi:10.2337/db11-0415.

292. Sun Y, Büki KG, Ettala O, Vääräniemi JP, Väänänen HK. Possible role of direct Rac1-Rab7 interaction in ruffled border formation of osteoclasts. *J Biol Chem*. 2005;280(37):32356-32361. doi:10.1074/jbc.M414213200.

293. Svenning S, Johansen T. Selective autophagy. *Essays Biochem*. 2013;55:79-92. doi:10.1042/bse0550079.

294. Szatmári Z, Sass M. The autophagic roles of Rab small GTPases and their upstream regulators: A review. *Autophagy*. 2014;10(7):1154-1166. doi:10.4161/auto.29395.

295. Taban M, Memoracion-Peralta DSA, Wang H, Al-Gazali LI, Traboulsi EI. Cohen syndrome: Report of nine cases and review of the literature, with emphasis on ophthalmic features. *J Am Assoc Pediatr Ophthalmol Strabismus*. 2007;11(5):431-437. doi:10.1016/j.jaapos.2007.01.118.

296. Tabara LC, Escalante R. VMP1 establishes ER-microdomains that regulate membrane contact sites and autophagy. *PLoS One*. 2016;11(11):1-20. doi:10.1371/journal.pone.0166499.

297. Tanida I, Ueno T, Uchiyama Y. A super-ecliptic, phluorin-mkate2, tandem fluorescent protein-tagged human LC3 for the monitoring of mammalian autophagy. *PLoS One*. 2014;9(10):3-10. doi:10.1371/journal.pone.0110600.

298. Terada N, Fujii Y, Ueda H, et al. Ultrastructural Changes of Erythrocyte Membrane Skeletons in Chorea-Acanthocytosis and McLeod Syndrome Revealed by the Quick-Freezing and Deep-Etching Method. *Acta Haematol*. 1999;101(1):25-31. doi:10.1159/000040917.

299. Tiftikcioglu BI, Dericioglu N, Saygi S. Focal Seizures Originating from the Left Temporal Lobe in a Case with Chorea-Acanthocytosis. *Clin EEG Neurosci*. 2006;37(1):46-49. doi:10.1177/155005940603700110.

300. Tomemori Y, Ichiba M, Kusumoto A, et al. A gene-targeted mouse model for chorea-acanthocytosis. *J Neurochem*. 2005;92(4):759-766. doi:10.1111/j.1471-4159.2004.02924.x.

301. Tomiyasu A, Nakamura M, Ichiba M, et al. Novel pathogenic mutations and copy number variations in the VPS13A Gene in patients with chorea-acanthocytosis. *Am J Med Genet Part B Neuropsychiatr Genet*. 2011;156(5):620-631. doi:10.1002/ajmg.b.31206.

302. Tooze SA, Abada A, Elazar Z. Endocytosis and autophagy: Exploitation or cooperation? *Cold Spring Harb Perspect Biol*. 2014;6(5). doi:10.1101/cshperspect.a018358.

303. Towers CG, Thorburn A. Therapeutic Targeting of Autophagy. *EBioMedicine*. 2016;14:15-23. doi:10.1016/j.ebiom.2016.10.034.

304. Trost M, English L, Lemieux S, Courcelles M, Desjardins M, Thibault P. The Phagosomal Proteome in Interferon-γ-Activated Macrophages. *Immunity*. 2009;30(1):143-154.

doi:10.1016/j.immuni.2008.11.006.

305. Tsukada M, Ohsumi Y. Isolation and characterization of autophagy-defective mutants of Saccharomyces cerevisiae. *FEBS Lett*. 1993;333(1-2):169-174. doi:10.1016/0014-5793(93)80398-E.

306. Tung SM, Ünal C, Ley A, et al. Loss of Dictyostelium ATG9 results in a pleiotropic phenotype affecting growth, development, phagocytosis and clearance and replication of Legionella pneumophila. *Cell Microbiol*. 2010;12(6):765-780. doi:10.1111/j.1462-5822.2010.01432.x.

307. Ueno S, Maruki Y, Nakamura M, et al. The gene encoding a newly discovered protein, chorein, is mutated in chorea-acanthocytosis. *Nat Genet*. 2001;28(2):121-122. doi:10.1038/88825.

308. Urbanelli L, Trivelli F, Ercolani L, et al. Cathepsin L increased level upon Ras mutants expression: The role of p38 and p44/42 MAPK signaling pathways. *Mol Cell Biochem*. 2010;343(1-2):49-57. doi:10.1007/s11010-010-0497-3.

309. Vance JE. MAM (mitochondria-associated membranes) in mammalian cells: Lipids and beyond. *Biochim Biophys Acta - Mol Cell Biol Lipids*. 2014;1841(4):595-609. doi:10.1016/j.bbalip.2013.11.014.

310. Velayos-Baeza A, Lévecque C, Dobson-Stone C, Monaco AP. The Function of Chorein. In: *Neuroacanthocytosis Syndromes II*. Berlin, Heidelberg: Springer Berlin Heidelberg; 2008:87-105. doi:10.1007/978-3-540-71693-8_7.

311. Velayos-Baeza A, Vettori A, Copley RR, Dobson-Stone C, Monaco AP. Analysis of the human VPS13 gene family. *Genomics*. 2004;84(3):536-549. doi:10.1016/j.ygeno.2004.04.012.

312. Velikkakath AK, Nishimura T, Oita E, Ishihara N, Mizushima N. Mammalian Atg2 proteins are essential for autophagosome formation and important for regulation of size and distribution of lipid droplets. *Mol Biol Cell*. 2012;23(5):896-909. doi:10.1091/mbc.E11-09-0785\rmbc.E11-09-0785 [pii].

313. Veltman DM, Akar G, Bosgraaf L, Van Haastert PJM. A new set of small, extrachromosomal expression vectors for Dictyostelium discoideum. *Plasmid*. 2009;61(2):110-118. doi:10.1016/j.plasmid.2008.11.003.

314. Vessoni AT, Muotri AR, Okamoto OK. Autophagy in Stem Cell Maintenance and Differentiation. *Stem Cells Dev*. 2012;21(4):513-520. doi:10.1089/scd.2011.0526.

315. Villegas A, Moscat J, Vazquez A, et al. A new family with hereditary choreo-acanthocytosis. *Acta Haematol*. 1987;77(4):215-219. doi:10.1159/000205998.

316. Viswanathan K, Hoover DJ, Hwang J, et al. Nonpeptidic Lysosomal Modulators Derived from Z-Phe-Ala-Diazomethylketone for Treating Protein Accumulation Diseases. *ACS Med Chem Lett*. 2012;3(11):920-924. doi:10.1021/ml300197h.

317. Vonk JJ, Yeshaw WM, Pinto F, et al. Drosophila Vps13 Is Required for Protein Homeostasis in the Brain. Missirlis F, ed. *PLoS One*. 2017;12(1):e0170106. doi:10.1371/journal.pone.0170106.

318. Walker RH. Management of Neuroacanthocytosis Syndromes. *Tremor Other Hyperkinet Mov (N Y)*. 2015;5:346. doi:10.7916/D8W66K48.

319. Walker RH. Untangling the Thorns: Advances in the Neuroacanthocytosis Syndromes. *J Mov Disord*. 2015;8(2):41-54. doi:10.14802/jmd.15009.

320. Walker RH, Danek A, DobsonStone C, et al. Developments in neuroacanthocytosis: Expanding the spectrum of choreatic syndromes. *Mov Disord*. 2006;21(11):1794-1805.

doi:10.1002/mds.21108.

321. Walker RH, Liu Q, Ichiba M, et al. Self-mutilation in chorea–acanthocytosis: Manifestation of movement disorder or psychopathology? *Mov Disord*. 2006;21(12):2268-2269. doi:10.1002/mds.21156.

322. Walterfang M, Looi JCL, Styner M, et al. Shape alterations in the striatum in chorea-acanthocytosis. *Psychiatry Res - Neuroimaging*. 2011;192(1):29-36. doi:10.1016/j.pscychresns.2010.10.006.

323. Walterfang M, Yucel M, Walker R, et al. Adolescent obsessive compulsive disorder heralding chorea-acanthocytosis. *Mov Disord*. 2008;23(3):422-425. doi:10.1002/mds.21725.

324. Wan C, Borgeson B, Phanse S, et al. Panorama of ancient metazoan macromolecular complexes. *Nature*. 2015;525(7569):339-344. doi:10.1038/nature14877.

325. Wang C-W. Lipid droplets, lipophagy, and beyond. *Biochim Biophys Acta - Mol Cell Biol Lipids*. 2016;1861(8):793-805. doi:10.1016/j.bbalip.2015.12.010.

326. Wang H, Sun H, Zhu X, et al. GABARAPs regulate PI4P-dependent autophagosome : lysosome fusion. 2015;112(22). doi:10.1073/pnas.1507263112.

327. Wang L, Cheng L, Li N-N, Yu W-J, Sun X-Y, Peng R. Association of four new candidate genetic variants with Parkinson's disease in a Han Chinese population. *Am J Med Genet Part B Neuropsychiatr Genet*. 2016;171(3):342-347. doi:10.1002/ajmg.b.32410.

328. Wen H, Zhan L, Chen S, Long L, Xu E. Rab7 may be a novel therapeutic target for neurologic diseases as a key regulator in autophagy. *J Neurosci Res*. 2017;0(July 2016). doi:10.1002/jnr.24034.

329. Wihl G, Volkmann J, Allert N, Lehrke R, Sturm V, Freund H-J. Deep brain stimulation of the internal pallidum did not improve chorea in a patient with neuro-acanthocytosis. *Mov Disord*. 2001;16(3):572-575. doi:10.1002/mds.1109.

330. Windholz J, Kovacs P, Tönjes A, et al. Effects of genetic variants in ADCY5, GIPR, GCKR and VPS13C on early impairment of glucose and insulin metabolism in children. *PLoS One*. 2011;6(7). doi:10.1371/journal.pone.0022101.

331. Wu H, Chen S, Ammar A-B, et al. Crosstalk Between Macroautophagy and Chaperone-Mediated Autophagy: Implications for the Treatment of Neurological Diseases. *Mol Neurobiol*. 2015;52(3):1284-1296. doi:10.1007/s12035-014-8933-0.

332. Yamamoto A, Simonsen A. The elimination of accumulated and aggregated proteins: A role for aggrephagy in neurodegeneration. *Neurobiol Dis*. 2011;43(1):17-28. doi:10.1016/j.nbd.2010.08.015.

333. Yamano K, Fogel AI, Wang C, van der Bliek AM, Youle RJ. Mitochondrial Rab GAPs govern autophagosome biogenesis during mitophagy. *Elife*. 2014;3:e01612. doi:10.7554/eLife.01612.

334. Yamauchi T, Hara K, Maeda S, et al. A genome-wide association study in the Japanese population identifies susceptibility loci for type 2 diabetes at UBE2E2 and C2CD4A-C2CD4B. *Nat Genet*. 2010;42(10):864-868. doi:10.1038/ng.660.

335. Yang RY, Xue H, Yu L, Velayos-Baeza A, Monaco AP, Liu FT. Identification of VPS13C as a galectin-12- binding protein that regulates galectin-12 protein stability and adipogenesis. *PLoS One*. 2016;11(4):1-16. doi:10.1371/journal.pone.0153534.

336. Yang X, Zheng J, An R, et al. Polymorphism in MIR4697 but not VPS13C, GCH1, or SIPA1L2 is associated with risk of Parkinson's disease in a Han Chinese population. *Neurosci Lett*. April 2017. doi:10.1016/j.neulet.2017.04.003.

337. Yang Y, Zhang Y, Qu X, et al. Identification of differentially expressed genes in the development of osteosarcoma using RNA-seq. *Oncotarget*. 2016;7(52):87194-87205. doi:10.18632/oncotarget.13554.

338. Ylä-Anttila P, Mikkonen E, Happonen KE, et al. RAB24 facilitates clearance of autophagic compartments during basal conditions. *Autophagy*. 2015;11(10):1833-1848. doi:10.1080/15548627.2015.1086522.

339. Yu L, McPhee CK, Zheng L, et al. Autophagy termination and lysosome reformation regulated by mTOR. *Nature*. 2010;465(7300):942-946. doi:10.1038/nature09076.Autophagy.

340. Yu W, Honisch S, Schmidt S, et al. Chorein Sensitive Orai1 Expression and Store Operated Ca2+ Entry in Rhabdomyosarcoma Cells. *Cell Physiol Biochem*. 2016;40(5):1141-1152. doi:10.1159/000453168.

341. Zhang A, Williamson CD, Wong DS, et al. Quantitative proteomic analyses of human cytomegalovirus-induced restructuring of endoplasmic reticulum-mitochondrial contacts at late times of infection. *Mol Cell Proteomics*. 2011;10(10):M111 009936. doi:10.1074/mcp.M111.009936.

342. Zhang BY, Chang A, Kjeldsen TB, Arvan P. Intracellular retention of newly synthesized insulin in yeast is caused by endoproteolytic processing in the golgi complex. *J Cell Biol*. 2001;153(6):1187-1197. doi:10.1083/jcb.153.6.1187.

343. Zhang H, Wang Y, Li J, et al. Proteome of Skeletal Muscle Lipid Droplet Reveals Association with Mitochondria and Apolipoprotein A-I. *J Proteome Res*. 2011;10(10):4757-4768. doi:10.1021/pr200553c.

344. Zhang J, Zhou W, Lin J, et al. Autophagic lysosomal reformation depends on mTOR reactivation in H2O2-induced autophagy. *Int J Biochem Cell Biol*. 2016;70:76-81. doi:10.1016/j.biocel.2015.11.009.

345. Zhou C, Zhong W, Zhou J, et al. Monitoring autophagic flux by an improved tandem fluorescent-tagged LC3 (mTagRFP-mWasabi-LC3) reveals that high-dose rapamycin impairs autophagic flux in cancer cells. *Autophagy*. 2012;8(8):1215-1226. doi:10.4161/auto.20284.

346. Zick M, Wickner W. Improved reconstitution of yeast vacuole fusion with physiological SNARE concentrations reveals an asymmetric Rab(GTP) requirement. *Mol Biol Cell*. 2016;27(16):2590-2597. doi:10.1091/mbc.E16-04-0230.

ANNEX: PUBLICATIONS

ANNEX: PUBLICATIONS

PUBLICATIONS RELATED TO THE THESIS WORK (and included in the following pages):

Muñoz-Braceras S, Mesquita A, Escalante R. ***Dictyostelium discoideum* as a Model in Biomedical Research**. In: Dictyostelids. Berlin, Heidelberg: Springer Berlin Heidelberg; 2013:1-34. doi:10.1007/978-3-642-38487-5_1.

Muñoz-Braceras S, Calvo R, Escalante R. **TipC and the chorea-acanthocytosis protein VPS13A regulate autophagy in *Dictyostelium* and human HeLa cells**. Autophagy. 2015;11(6):918-927. doi:10.1080/15548627.2015.1034413.

Muñoz-Braceras S, Escalante R. **Analysis of Relevant Parameters for Autophagic Flux Using HeLa Cells Expressing EGFP-LC3.** Methods Mol Biol. 2016;1449:313-329. doi:10.1007/978-1-4939-3756-1_20.

Mesquita A, Cardenal-Muñoz E, Dominguez E, et al. **Autophagy in *Dictyostelium*: Mechanisms, regulation and disease in a simple biomedical model**. Autophagy. 2016;13(1):1-17. doi:10.1080/15548627.2016.1226737.

OTHER PUBLICATIONS:

Carilla-Latorre S, Annesley SJ, Munoz-Braceras S, Fisher PR, Escalante R. **Ndufaf5 deficiency in the *Dictyostelium* model: new roles in autophagy and development**. Mol Biol Cell. 2013;24(10):1519-1528. doi:10.1091/mbc.E12-11-0796.

Calvo-Garrido J, King JS, Muñoz-Braceras S, Escalante R. **Vmp1 Regulates PtdIns3P Signaling During Autophagosome Formation in *Dictyostelium discoideum***. Traffic. 2014;15(11):1235-1246. doi:10.1111/tra.12210.

Dictyostelium discoideum as a Model in Biomedical Research

Sandra Muñoz-Braceras, Ana Mesquita and Ricardo Escalante

Abstract The simple eukaryote *Dictyostelium discoideum* has been traditionally used to understand basic principles of cell and developmental biology and now has also become a useful system in biomedical research. What are the similarities and differences between *D. discoideum* and other simple microbial models such as *Saccharomyces cerevisiae*? Which aspects are more advantageous to address in *D. discoideum*? Are there any processes or specific proteins present in *D. discoideum* that are difficult or impossible to study in other systems? Does it make sense to use such a simple organism in biomedicine? These and other questions will be addressed in this chapter, together with some specific examples in which *D. discoideum* has proved its potential to model human disease.

Keywords *Dictyostelium discoideum* · Model organisms · Biomedical research · Human disease · Pathogens · *Pseudomonas* · *Legionella* · Chemotaxis · Development · Cell motility · Autophagy · Molecular pharmacology · Mitochondrial disease · Sphingolipids · Cisplatin · Bipolar disorder

1 Introduction

A model organism is used in experimental biology to understand particular biological processes with the expectation that the knowledge obtained is applicable in other organisms, often especially in humans. Regarding the study of human disease, a model organism is chosen on the basis of being simple and amenable to experimental manipulations, but also, and obviously, for its similarity to humans. These two aspects usually run in opposite directions as exemplified by microbial

S. Muñoz-Braceras · A. Mesquita · R. Escalante (✉)
Instituto de Investigaciones Biomédicas Alberto Sols CSIC-UAM,
Arturo Duperier 4, 28029 Madrid, Spain
e-mail: rescalante@iib.uam.es

M. Romeralo et al. (eds.), *Dictyostelids*,
DOI: 10.1007/978-3-642-38487-5_1,

models, which are the best suited for genetic manipulations but are distantly related to mammals. Fortunately, many processes affected in human diseases, such as those concerning basic cellular functions, are well conserved in evolution and thus can be addressed in simple but powerful microbial models. Historically, fungal models have been the most widely used non-metazoan eukaryotic organisms for their simplicity, genetic manipulability, and the profound knowledge of their biology. However, the fungal lifestyle has specific characteristics that make them different from animal cells. The social amoeba *Dictyostelium discoideum* is not a fungus and lacks the complexity of simple metazoan models such as the nematode *Caenorhabditis elegans* and the insect *Drosophila melanogaster* but it shares with them many cellular properties and a simple developmental cycle that can be used to model some basic aspects of human diseases.

Dictyostelid social amoebae are a group of eukaryotic soil microbes that prey on bacteria and yeast. Taxonomically, they belong to the Amoebozoa, a sister group of animals and fungi. Individual amoebas are highly motile cells and multiply by binary fission while nutrients are available. When food is scarce the cells become chemotactic and aggregate to form a simple multicellular organism. Cell motility is regulated by complex signaling pathways that render the cells responsive to an extracellular chemotactic molecule, which is produced and secreted by the cells themselves. Eventually, the cells become polarized and form streams, which converge into aggregative centers forming a mound. At this point, a developmental program involving cell movement and cell differentiation leads to the formation of a fruiting body formed by a stalk of vacuolated cells supporting the spores. There are around 150 known dictyostelid species and the latest studies group them into 8 divisions based on molecular phylogenic analyses (Romeralo et al. 2011). The best-studied species is *D. discoideum*, which has become a model organism in many different laboratories (Fig. 1).

2 What Makes Social Amoebas Different?

As mention above, a number of the model systems belong to the fungus kingdom and as such have specific characteristics, which are different from animal cells or *D. discoideum* cells. One of these fungal traits is the presence of rigid cell walls made of chitin which, like the cellulose walls present in plants, provide structural support and protection. In contrast, vegetative *D. discoideum* cells do not have cell walls and this allows the flexible plasma membrane to perform processes typically present in animal cells. These processes include phagocytosis (uptake of solid particles), macropinocytosis (uptake of liquid), cell motility and chemotaxis, which are accomplished by the formation of pseudopods (protrusions of the cell membrane generated by the mechanical force exerted by the cytoskeleton). The formation of the multicellular structure involves well-defined morphogenetic movements and cell differentiation processes that also share more similarities with animal development than with fungal mycelia (Escalante and Vicente 2000).

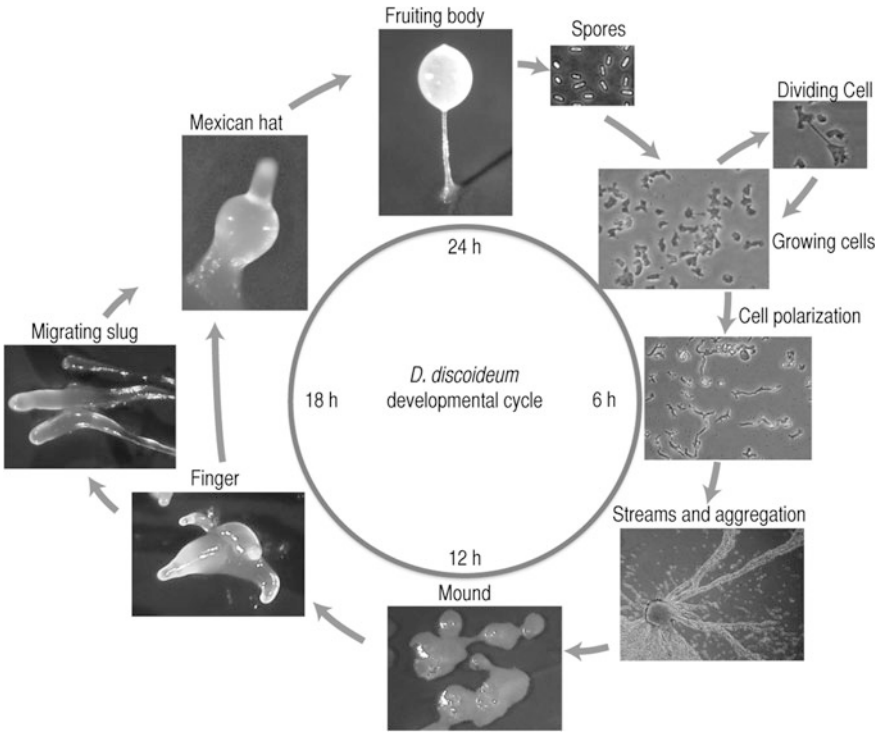

Fig. 1 *Dictyostelium discoideum* life cycle. Representative pictures of vegetative and developmental stages

All these parallelisms with animal cells have their reflection in the encoded proteins. Although social amoebas diverged before fungi, *D. discoideum* has many more proteins in common with animals than does the yeast model *S. cerevisiae* (Fig. 2). It is believed that many proteins present in the common ancestor of fungi, animals, and amoebas have been lost during fungal evolution. The similarities at the cellular level between amoebas and animal cells must have been the driving force for maintaining most of these proteins. Obviously, this has a profound impact on the utility of *D. discoideum* as a model system, since the function of many proteins and certain molecular pathways cannot be studied in fungal models.

One good example of this principle is the group of SH2 domain-containing proteins. These domains mediate protein–protein interactions and were thought to be present exclusively in animal cells. Surprisingly, *D. discoideum* possesses 13 SH2 proteins and 4 of them (STATa-d proteins, Signal Transducer and Activator of Transcription) have been characterized and found to be involved in development and cell type differentiation (Williams 2003; Langenick et al. 2008; Kawata 2011). The mammalian STATs are phosphorylated at specific tyrosine residues by JAK receptors and this phosphorylation creates sites for interaction with SH2 domains of other STATs, mediating their dimerization. The active dimers are then

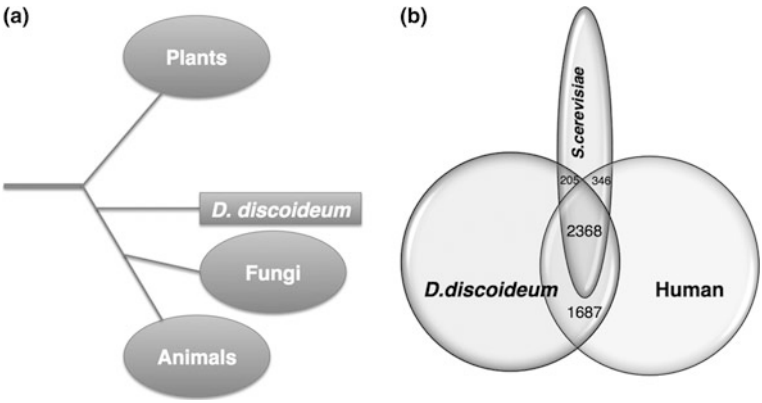

Fig. 2 Comparative genomics in *D. discoideum*. **a** A simplified representation of the evolutionary relationships of *D. discoideum* with plants, fungi and animals. **b** Proteome comparison between *D. discoideum*, human and *S. cerevisiae* using the on-line program PROCOM (http://procom.wustl.edu/). The intersections show the number of similar proteins with an E-value $<10^{-20}$. *D. discoideum* shows more conserved proteins in common with human than the yeast model does. Specifically, 1,687 proteins are present in human and *D. discoideum* but absent in *S. cerevisiae*, which makes the social amoeba a suitable system to study the function of new human proteins

translocated to the nucleus where they regulate the expression of developmental genes. As occurs in the worm *C. elegans*, which also possesses a STAT homolog (Wang and Levy 2006), no canonical JAK kinases have been found in *D. discoideum*, suggesting the presence of other tyrosine kinases involved in STAT activation. A recent study identified the kinase that activates STAT in *D. discoideum*. This kinase belongs to a group of kinases known as tyrosine-like kinases (TKLs) suggesting an atypical and possible ancestral regulation of STAT proteins (Araki et al. 2012). The study of this class of proteins in the *Dictyostelium* model is shedding light on their function and evolution (Soler-Lopez et al. 2004).

Another example of animal-like proteins in *D. discoideum* is illustrated by the recent discovery of the first lamin-like protein in a non-metazoan organism. Lamins are involved in severe inheritable diseases, including muscular dystrophy, cardiomyopathy, lipodystrophy, and progeria (Batsios et al. 2012), and are required for chromatin organization, gene expression, and cell cycle progression.

Along these lines, a comparative and functional genomic study aimed at characterizing proteins of unknown function conserved between *D. discoideum* and humans, but absent in the fungi *S. cerevisiae* and *S. pombe*. Of the total number of proteins, 41 were identified fulfilling these criteria and 28 were successfully disrupted by homologous recombination (Torija et al. 2006a, b). The sequences of the encoded proteins did not show recognizable functional motifs that would allow a prediction of their function. Two of these proteins turned out to be fundamental for cell function. One of them is Vacuole membrane protein 1 (Vmp1), whose disruption in *D. discoideum* leads to defects in autophagy and

other membrane traffic processes (Calvo-Garrido et al. 2008; Calvo-Garrido and Escalante 2010). The other protein is Mitochondrial dysfunction protein A (MidA), which is involved in *D. discoideum* and human cells in mitochondrial bioenergetics acting as an assembly factor of Complex I of the oxidative phosphorylation chain (Carilla-Latorre et al. 2010).

3 From the Soil to the Laboratory: The Early Times of *D. Discoideum* Research

The species *D. discoideum* can be considered as a newcomer in science history, since it was discovered not so long ago by Raper in 1933 in the Craggy Mountains of Western North Carolina (Raper 1935, 1936). At that time, several fundamental characteristics of dictyostelids, such as the first description of phagocytosis phenomena, had already been studied in other species of this group. It was revolutionary when Vuillemin realized that *Dictyostelium mucoroides* engulfed and digested bacteria intracellularly (Vuillemin 1903), in a way totally different from fungi, which obtain their nutrients by extracellular digestion. Later on, Raper went beyond mere observation and applied experimental biology to these organisms. Once *D. discoideum* could be grown to large quantities using a lawn of bacteria (Raper 1936, 1939), Raper addressed fundamental questions of cell biology and development. He was the first to study systematically the capacity of *D. discoideum* cells to ingest and kill pathogenic bacteria, anticipating the great importance of this model for the study of infectious diseases (Raper and Smith 1939). He discovered that the proportion of stalk and spore cells is kept nearly constant irrespective of the size of the developing structure (Raper 1940b). Another important aspect of development concerns cell fate specification, and he addressed this with elegant grafting experiments showing that the front of the slug, upon culmination, gives rise to the stalk and that the rear gives rise to the spores (Raper 1940a, b). All these early studies showed the enormous potential of this organism for developmental biology (Escalante and Vicente 2000) and set the stage for its success as an experimental system.

One of the first observations of directional cell movement in eukaryotic cells was made by Leber in 1888, when he observed streams of leukocytes moving toward an injured retina in rabbit (Leber 1888). Although the underlying cause of the movement was suggested to be mediated by extracellular molecules, experimental proof of chemotaxis and the identification of these molecules had to wait for several decades (McCutcheon 1946). The groundbreaking studies in *D. discoideum* by Bonner in 1947 (Bonner 1947) definitively settled the chemotaxis hypothesis and convinced others that the aggregative movement of *D. discoideum* cells toward the aggregation centers was a wonderful opportunity to characterize this phenomenon. As described below, the opportunity was not wasted and now this organism has become a leading model in cell motility and chemotaxis research.

The mysterious chemotactic molecule in dictyostelid movement was named acrasin and its chemical nature was identified in 1968 (Konijn et al. 1968). Surprisingly, the molecule turned out to be cyclic adenosine monophosphate (cAMP), discovered only a few years earlier by Sutherland as an intracellular second messenger in hormonal action (Rall and Sutherland 1958). cAMP is not the only acrasin identified; other dictyostelid species use different molecules such as glorin or folate for the same purpose. The identification of the first leukocyte chemotactic molecule took another several years (Yoshimura et al. 1987; Walz et al. 1987). These mammalian chemotactic molecules (called chemokines) are small peptides, different from dictyostelid acrasin molecules but they act through conserved receptors and signaling pathways.

The ease with which an organism can be grown and handled in the laboratory is an important factor in the advancement of new experimental tools. Significant efforts were invested to grow *D. discoideum* in liquid media; first in association with live or dead bacteria (Gezelius 1962; Sussman 1961) and later, by the isolation of strains capable of growing in axenic liquid broth medium (Sussman and Sussman 1967; Loomis 1971). Two independent strains, AX1 (which later gave rise to AX2) and AX3 (which later gave rise to AX4), were isolated from NC4 (a natural isolate of the species *D. discoideum*) in two different laboratories by clonal selection or mutagenesis. While the original NC4 isolate can only grow by phagocytizing bacteria, these strains were able to grow axenically by macropinocytosis, engulfing large amounts of liquid media. These new possibilities allowed the manipulation of large amounts of cells for diverse purposes and made it possible to synchronize development by washing off the nutrients and depositing the cells in a moist filter.

The isolation and study of mutants has been of central importance in the history of experimental biology. By studying the abnormal functioning of a given process, one might infer the mechanisms controlling the normal function. Sussman's group was the first to isolate *D. discoideum* mutants affected in growth and in different stages of development by exposing cells to UV-light. These mutants allowed the first synergistic studies and led to the realization of the complex networks underlying developmental processes, even in simple organisms (Sussman 1954; Sussman and Sussman 1953; Sonneborn et al. 1963). In many cases, a mixed population of two mutant strains could achieve normal development suggesting the presence of non-cell autonomous defects that can be mutually complemented in the mixed population. The particular genes affected in these mutants could not be identified at that moment, but these studies anticipated the future advances of developmental biology using this simple model.

Biochemical studies of enzyme activities in normal and mutant strains obtained by chemical mutagenesis opened new frontiers for the characterization of developmental processes, not only at the morphological but also at the biochemical level. An important example is the level and activity of enzymes involved in polysaccharide synthesis (Loomis et al. 1976; Loomis 1969a, b, 1970; Loomis and

Sussman 1966; Sussman 1965; Ashworth and Sussman 1967). The idea of a complex regulation of the level of expression of certain genes at transcriptional and translational levels during development was then clearly established (Roth et al. 1968; Newell et al. 1969).

4 The Advent of Molecular Genetics Propelled *D. discoideum* into the Post-genomic Era

In the 1970s, the development of recombinant DNA technology and DNA sequencing (Maxam and Gilbert 1977) allowed molecular genetics to flourish in several experimental systems. The first analyses of the *D. discoideum* genome were accomplished by Firtel and Sussman, who analyzed its size and realized its extreme AT-richness (Sussman and Rayner 1971; Firtel and Bonner 1972), and about a decade later, some *D. discoideum* genes were sequenced (Peffley and Sogin 1981; Hori et al. 1980; Poole et al. 1981). But the real breakthrough concerning the potential of *D. discoideum* as a genetic system came with the finding that *D. discoideum* cells could be transformed with exogenous DNA, which allows a direct manipulation of specific genes (Hirth et al. 1982). DNA is integrated randomly in the genome as tandem repeats of varying numbers of copies, but currently non-integrative extrachromosomal plasmids are also available (Gaudet et al. 2007; Veltman et al. 2009a, b; Firtel et al. 1985). This prompted the development of a wide array of techniques that have, nowadays, become routine in *D. discoideum* laboratories, including the expression of tagged proteins and reporter genes, gene inactivation by homologous recombination, insertional mutagenesis, and many other applications aimed at studying specific genes and their functions (Eichinger and Rivero 2006; Meima et al. 2007; Dubin and Nellen 2010; Levi et al. 2000).

Among these techniques, special attention must be paid to the generation of knock-out (KO) strains of specific genes by homologous recombination, which in *D. discoideum* is very efficient and since this organism is haploid, the consequences of the mutation can be determined directly in the clonal isolate without further manipulation. Myosin heavy chain and alpha-actinin were the first genes disrupted using homologous recombination in 1987 (De Lozanne and Spudich 1987; Witke et al. 1987), revealing the surprising finding that myosin is not essential for cell viability and that it is required for cytokinesis and development. Recent advances have facilitated the generation of large collections of strains carrying mutations in selected genes, opening the future possibility to achieve the systematic disruption of any single gene in this system (Torija et al. 2006a; Wiegand et al. 2011). Multiple KO mutants can now be obtained using the Cre-loxP system, and a remarkable example is the generation of a sextuple mutant lacking five type-1 phosphoinositide 3-kinases and the PTEN phosphatase; this mutant was used to investigate the role of phosphoinositide signaling in cell motility (Hoeller and Kay 2007).

A new step forward was the application in 1992 of another powerful technique: insertional mutagenesis by restriction enzyme-mediated integration (REMI) (Kuspa 2006; Kuspa and Loomis 1992). Briefly, a linearized plasmid containing a selection marker is electroporated together with a restriction enzyme into the cells. The restriction enzyme will create compatible integration sites in the genome, facilitating the integration of the plasmid. For example, the restriction enzyme *Dpn*II (which recognizes the 4-base sequence GATC and generates GATC overhangs) will allow the integration of a plasmid cut with the compatible restriction enzyme *Bam*HI (that recognizes the 6-base sequence GGATCC and generates GATC overhangs). The frequency of *Dpn*II-sites in the genome is much higher than that of *Bam*HI-sites, thus covering a wider spectrum of potential target genes. If the insertion interrupts a gene necessary for development, the resulting phenotype can be easily identified, and the strain isolated for further manipulation. This technique proved to be very efficient for generating mutants affecting diverse aspects of development. The difference with mutants generated by chemical mutagenesis or UV-light is that this technique enables the rapid identification of the disrupted gene. Identification of the mutated gene is accomplished by plasmid rescue and sequencing of the regions flanking the insertion (Fig. 3).

The potential of this technique was clearly illustrated by the work of Loomis, who isolated a collection of 80 REMI mutants affected in development (http://www-biology.ucsd.edu/labs/loomis/REMI/index.html). The study of some of these mutants has revealed essential signal transduction pathways controlling development and cell differentiation. The REMI technique also allows the identification of genes specifically involved in a given process using the appropriate phenotypic selection (Adachi et al. 1994; Nagasaki and Uyeda 2008).

The insertional mutagenesis has also been used in other screening strategies such as the powerful second-site suppressor analysis, which allows the identification of components of complex signal transduction pathways. It is based on the identification of a second mutation that overcomes the defect of a primary mutation. Second-site mutagenesis is performed on the mutant background using REMI, which later will allow the recovery of the gene acting as a suppressor. After antibiotic selection, transformants are screened for clones that display total or partial recovery of the phenotype. The disrupted gene is expected to act as a negative component downstream of the primary defect in a given signal transduction pathway (Shaulsky et al. 1996). For example, the mutation of *tagB*, which encodes a multidrug resistance transporter (MDR), blocked sporulation, and a second-site suppressor screening performed on the *tagB* mutant revealed several genes whose disruption partially bypassed the sporulation defect. One of these suppressors of *tagB* mutation was found to be a phosphodiesterase, which plays an essential role in the control of terminal differentiation (Shaulsky et al. 1996).

With all these new technical possibilities at hand, the next challenge was to obtain the whole sequence of the genome. This would allow comparative and functional genomic studies and fully exploit all the mentioned advantages.

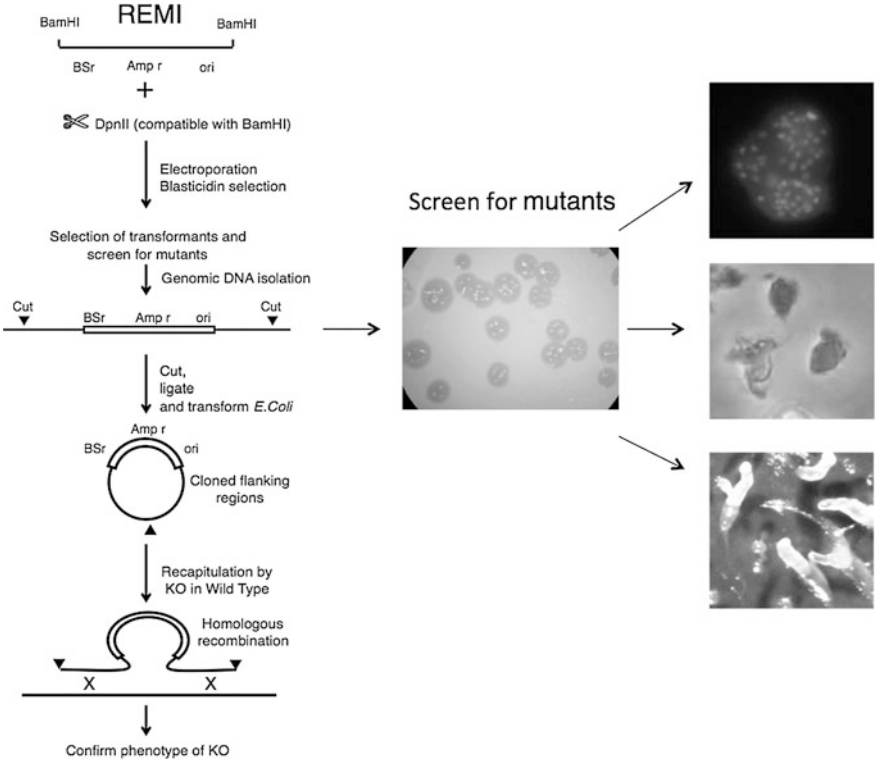

Fig. 3 Insertional mutagenesis in *D. discoideum* using REMI. A restriction enzyme (for example *Dpn*II) is used to create insertion sites in the genome for a plasmid containing compatible ends (in this case, cut with *Bam*HI). Transformants can be screened for abnormal cell morphology or developmental defects. Three mutants are shown as examples: multinucleated cells stained with DAPI, cells with aberrant polarization during aggregation and a mutant arrested at the slug stage. The disrupted gene can be identified by plasmid rescue of the genomic regions flanking the locus of insertion. Recreation of the mutant phenotype can be obtained by homologous recombination using the same construct

The sequence of the *D. discoideum* genome was published in 2005 (Eichinger et al. 2005). The genome is 34 megabases (Mb) in size, with six chromosomes encoding an estimated 12,500 proteins. This makes it quite small and compact, similar to the genome of the yeast model *S. cerevisiae*. The genome sequences of other dictyostelid species (*D. purpureum*, *D. fasciculatum,* and *Polysphondylium pallidum*) are now also available (Sucgang et al. 2011; Heidel et al. 2011). A central resource for dictyostelid genomics, dictyBase (http://www.dictybase.org/), provides invaluable tools, including full annotation, expression analysis, and associated bibliography.

5 A New Frontier in *D. discoideum* Research: Modeling Human Disease

Genome analyses have shown the presence of disease-related genes that are conserved between *D. discoideum* and human (Eichinger et al. 2005). Many of these genes are involved in processes that have been well conserved in evolution allowing their study in the social amoeba in a meaningful way, as has indeed been proved in many recent studies (Escalante 2011). In the past years, the number of studies in *D. discoideum* aimed at understanding genes or processes directly related to human disease has increased steadily as illustrated in the next sections of this chapter.

5.1 Pathogen–Host Interactions in D. discoideum

The bacterivore nature of dictyostelids and other protists imposes a strong selection pressure on the soil microbes. As a result, it is believed that some bacteria have developed during evolution strategies to survive the attack of these predatory amoebae. Pathogenic bacteria might have transformed these defense mechanisms into virulence traits to survive the attack of professional phagocytes in the human body: the macrophages and neutrophils. Since phagocytosis and endocytic traffic are highly conserved in evolution, it is not surprising that the essential mechanisms used by bacterial pathogens to evade and infect humans have been conserved in the interactions with *D. discoideum* and can be conveniently studied in this model (Lima et al. 2011; Steinert 2011).

D. discoideum cells can be easily co-cultured with pathogenic bacteria in agar plates. If the amoeba is able to ingest and kill the bacteria, clear plaques appear. Conversely, the absence of clear plaques reveals resistance to *D. discoideum* predation and might indicate the presence of virulence mechanisms (Fig. 4). This simple assay allows large-scale analysis of virulence levels among different isolates, or genetic screening to identify host or pathogen determinants. In 1978, an extensive study by Depraitere and Darmon (1978) tested up to 78 different gram-positive and gram-negative bacterial species for their capacity to support *D. discoideum* growth. They found that most of them were normally ingested and killed, but also found some species that showed different degrees of toxicity for the social amoeba. Since then, *D. discoideum* has been used as an infection model for a still growing list of human pathogens. Some of them are able to grow intracellularly and parasite the cell host, such as *Legionella* and *Mycobacterium* (Fig. 4); others are extracellular pathogens able to kill the host cells using a variety of toxins, such as *Pseudomonas aeruginosa*. The list of pathogens tested in the *Dictyostelium* model includes species such as *Salmonella typhimurium, Yersinia pseudotuberculosis, Burkholderia cenocepacia, Vibrio cholerae, Stenotrophomonas maltophilia*, *Acinetobacter baumannii,* and *Pseudomonas fluorescens* (Steinert 2011; Sperandio et al. 2012; Iwashkiw et al. 2012).

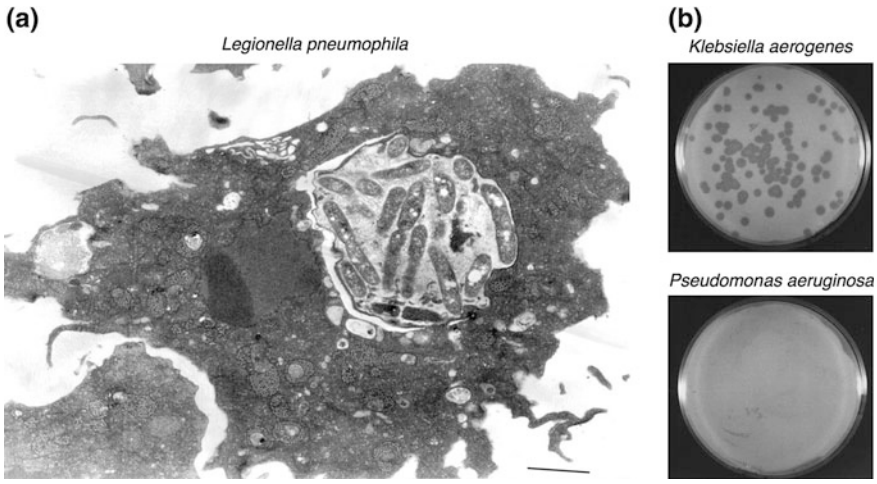

Fig. 4 *Dictyostelium discoideum* and bacterial pathogens. **a** Transmission electron micrograph of an *L. pneumophila*-infected *D. discoideum* cell. Bacteria are concentrated within a single vacuole. This photograph was reproduced with permission (Steinert 2011). **b** *Pseudomonas aeruginosa* virulence tested in a simple plating assay. *D. discoideum* cells are mixed with the non-pathogenic bacteria *K. aerogenes* or the pathogenic *P. aeruginosa* and plated on agar plates. *D. discoideum* is only able to feed on the non-pathogenic bacteria and, after a few days, clear plaques are formed

Pseudomonas aeruginosa is an opportunistic environmental bacterium that is particularly dangerous in patients with severe burns and compromised immunity, and it is one of the most common pathogens of nosocomial infections. It is also responsible for frequent chronic infections in patients suffering from cystic fibrosis. *Pseudomonas* is intrinsically resistant to antibiotics and it has developed a large array of virulence factors. Flagella and pili facilitate the contact of bacteria with their target cells and enhance their adhesion, which is a critical step in infection. After contact, the type III secretion system is capable of injecting into the cell cytoplasm an arsenal of cytotoxic molecules, which act at different levels and interfere with as yet unidentified host cofactors (Kipnis et al. 2006). Other products, such as elastase, alkaline phosphatase, and exotoxin A, are secreted into the extracellular space by secretion systems I and II. The expression of many of these systems is regulated in the bacterial population by a mechanism mediated by extracellular signals, the "quorum-sensing" (QS) (Van Delden and Iglewski 1998). Mutations affecting these virulence systems in *Pseudomonas* makes the bacteria more sensitive to *D. discoideum* predation and the correlation with data obtained in other virulence systems (worms, rats, and mice) is near-perfect, suggesting that the mechanisms of infection have been conserved (Lima et al. 2011; Cosson et al. 2002; Pukatzki et al. 2002).

Measuring the virulence of opportunistic bacteria in mammalian models is difficult since it requires immune-compromised mice or rats. This is very

expensive and even impractical when the number of tests is high such as those required for studies of clinical isolates or collections of mutated bacteria. The reproducibility of such assays is also questionable since the response of an individual to an infection depends on many different factors, which are often difficult to control. Consequently, the use of simple experimental systems such as the worm *C. elegans* and *D. discoideum* has become a reliable alternative in the research of *Pseudomonas* and other opportunistic pathogens.

A nice example of such use is the study of the evolution of *Pseudomonas* virulence within infected patients, as this requires massive testing of many isolates. Clinical populations of *P. aeruginosa* from acute infections show a wide range of virulence that can be conveniently tested in *D. discoideum* assays (Janjua et al. 2012). Another recent study has revealed that during the course of chronic infections in cystic fibrosis patients *Pseudomonas* accumulates mutations in virulence genes such as the *lasR* gene involved in QS response. *D. discoideum* was used to measure the virulence of hundreds of clinical isolates (Lelong et al. 2011; Bradbury et al. 2011). A decrease in virulence was observed over the time of infection, suggesting that the persistence of high virulence is not required to maintain a chronic infection. Interestingly, there was no correlation between the loss of lasR and the loss of virulence, indicating that other virulence traits must be affected.

A recent report analyzed the impact of the Crc protein, a global regulator of metabolism. A *P. aeruginosa* strain lacking Crc showed defects in type III secretion and motility and showed a less virulent phenotype in *D. discoideum*. These results suggest that Crc might be a good target in the search for new antibiotics (Linares et al. 2010).

Despite the functional and genomic similarities among different *P. aeruginosa* strains (Alonso et al. 1999; Morales et al. 2004), some differences in their pathogenicity have been observed (Lee et al. 2006). This is clearly exemplified by two clinical isolates commonly used as model strains, PAO1 and PA14. As occur in other models, *D. discoideum* is more sensitive to PA14 than to PAO1 (Carilla-Latorre et al. 2008). To investigate the origin of these differences, *D. discoideum* cells were exposed to either *P. aeruginosa* PAO1 or *P. aeruginosa* PA14 and after 4 h *D. discoideum* RNA was extracted. Transcriptome analyses by microarrays showed the existence of common and specific responses of *D. discoideum* cells to infection. The expression of 364 genes changed in a similar way upon infection with one or the other strain, whereas 169 genes were differentially regulated depending on whether the infecting strain was *P. aeruginosa* PAO1 or PA14. Effects on metabolism, signaling, stress response, and cell cycle can be inferred from the genes affected. These results indicate that the infective process of bacterial pathogens can be strain-specific and more complex than previously thought (Carilla-Latorre et al. 2008).

Intracellular pathogens interfere with the sequence of events leading to internalization by phagocytosis and intracellular digestion of the bacteria. In *D. discoideum* and mammalian cells, phagocytosis is initiated by bacterial adhesion to the cell surface. This triggers an actin cytoskeleton rearrangement at the site of

ingestion that plays an essential role in the internalization and transport of the phagosome vesicle into the cells. The signaling events involve heterotrimeric and monomeric G proteins, phospholipases, PI kinases, phosphatases, and calcium ions (Bozzaro et al. 2008). The following steps of maturation include acidification of the phagosome by fusion with acidic vesicles containing a V-H^+ATPase, and fusion with non-acidic vesicles containing Nramp1, a divalent metal transporter involved in the depletion of divalent metals that prevent bacterial growth (Peracino et al. 2006, 2010, 2012). Successive recruitment of lysosomal hydrolases eventually leads to bacterial digestion. Undigested material is then exocytosed to the exterior of the cell. The challenge is to understand how different pathogens interfere with this sequence of events.

Legionella pneumophila is a pathogenic gram-negative bacterium responsible for Legionnaires'disease, a severe life-threatening pneumonia. *Legionella* is common in the natural environment where it lives within different amoeba species. After ingestion, the bacteria are able to establish an intracellular niche evading lysosomal degradation. This *Legionella* replicative environment allows the bacteria to grow and replicate inside amoebae and human cells. The establishment of this intracellular niche is very complex and still poorly understood, but it is known to involve the recruitment of mitochondria, endoplasmic reticulum (ER), and smooth vesicles, and to block the fusion with lysosomes. The use of *D. discoideum* mutants has revealed that *Legionella* uptake takes place by conventional phagocytosis requiring heterotrimeric G proteins (Steinert 2011). *Legionella* expresses a number of effector proteins that are translocated to the cytoplasm by the secretion system Icm-Dot, interfering with diverse signaling pathways involved in membrane traffic. Some of these effectors include regulators of small GTPases (GEFs, guanine exchange factors, and GAPs, GTPase activating proteins), interactors of phosphatidylinositol 4-phosphate, a regulator of Arf1, and a protein involved in vesicle transport from the Golgi to the ER.

The expression in *D. discoideum* of another *Legionella* effector, LegC3, leads to the disruption of organelle trafficking by the accumulation of endosome-like structures containing undigested material (de Felipe et al. 2008). Ankyrin B (AnkB), another *Legionella* effector required for its replication, is essential for the recruitment of polyubiquitinated proteins to the *Legionella* vacuole. The AnkB effector achieves this by mimicking the action of host F-box proteins, thus hijacking the conserved SCF ubiquitin ligase complex in macrophages and *D. discoideum* (Price et al. 2009).

5.2 Pathobiology of Cell Motility and Chemotaxis

Cell motility and chemotaxis are essential for many aspects of the life cycle of eukaryotes. From the earliest stages of development, cell migration is necessary for the formation of the embryo. A paradigmatic example is that of the neural crest cells, a multipotent, migratory cell population. After gastrulation, these cells are

specified at the border of the neural plate. They move from there to colonize different regions of the embryo, and then give rise to different cell types such as connective tissue cells, cartilage, skeletal tissue, melanocytes, etc. (Trainor 2005). Their movement is regulated by extracellular signals that act as attractants and repellents of their migration (Jones and Trainor 2005). Cell migration is also essential in wound healing, where fibroblasts must move to repair the wound (Kole et al. 2005). The immune system is another example where white blood cells are attracted to sites of infection and inflammation by chemotaxis to exert their protective function (Parent 2004; Jin et al. 2008). Chemokines are extracellular molecules essential for guiding these immune cells to the site of infection. Abnormal secretion of chemokines may lead to excessive recruitment of leukocytes contributing to several inflammatory diseases such as chronic obstructive pulmonary disease (COPD), multiple sclerosis (MS), atherosclerosis, inflammatory bowel disease, and endocrine autoimmune disease. Another, no less important, motility-dependent pathological process is cancer, where the migratory capacity of transformed cells promotes their exit from the tissue of origin and the invasion of new areas (Roussos et al. 2011; Condeelis et al. 1992). It is therefore not surprising that many diseases are related with cell migration defects.

The motility behavior of leukocytes and *D. discoideum* cells is very similar in response to their chemoattractants (chemokines and cAMP, respectively). Cells elongate and polarize the cytoskeleton in the direction of the gradient. In both cell types, the signal is transmitted into the cells by G-protein coupled receptors (GPCRs) and the molecular parallelisms of signal transduction and the regulation of the chemotactic machinery are wonderfully conserved as described in other chapters of this book (Swaney et al. 2010; Wang et al. 2011a; King and Insall 2009; Jin et al. 2008).

The actin cytoskeleton is finely regulated during cell motility and chemotaxis since it is responsible for generating the forces necessary for cell movement. A number of diseases are associated with dysfunction of actin or its regulation, such as defects in immunity, neuronal development, degenerative diseases, cancer, and pathogen infection. *D. discoideum* has contributed to understanding the basic principles of some of these diseases. A relevant example is the Wiskott-Aldrich syndrome, an X-linked recessive immunodeficiency characterized by thrombocytopenia, eczema, and recurrent infections. The disease is caused by mutations in the *WAS* gene encoding WASP, a protein expressed preferentially in the hematopoietic system. This protein regulates the actin nucleation complex Arp2/3 and thus the formation of new actin filaments. Another member of the WASP family, the actin nucleation promoting protein SCAR/WAVE, which is essential for the generation of pseudopods, was first identified and characterized in *D. discoideum* (Bear et al. 1998; Veltman et al. 2012; Ura et al. 2012).

Lissencephaly, which literally means smooth brain, is a severe developmental brain defect caused by abnormal migration of neurons. This defect is caused by mutations in either one of the two proteins Lissencephaly 1 (LIS1) and Doublecortin (DCX), which interact with the microtubule and actin cytoskeleton. LIS1 and DCX have been characterized in *D. discoideum* and these studies have lead to

surprising results about the function of these important proteins (Meyer et al. 2011). Expression of a hypomorphic lissencephaly causing allele of LIS1 in *D. discoideum* led to severe abnormalities at the cellular level such as disruption of the microtubule cytoskeleton, disorganization of the Golgi apparatus, detachment of centrosomes from the nucleus, and reduced F-actin content. Moreover, a potential relationship with the actin cytoskeleton was suggested by the interaction with a potential actin regulator, Rac1A (Rehberg et al. 2005). DCX and LIS1 physically interact both in mammalian and in *D. discoideum* cells. Remarkably, ablation of DCX in the mutant strain expressing the hypomorphic LIS1 leads to an additional phenotype not present in the single mutants, a defect in the formation of streams during aggregation. These double mutants were able to respond normally when a few wild-type cells were added in the experiment, suggesting that the defect in aggregation is not due to abnormal cytoskeleton rearrangement but to defects in extracellular cAMP signaling. These and other additional experiments led to the conclusion that DCX and LIS1 cooperate in a cytoskeleton-independent manner to regulate cAMP signaling and open the question whether a similar cooperation might also be present during brain development (Meyer et al. 2011).

Shwachman-Bodian-Diamond syndrome (SDS) is a severe hereditary disease characterized by skeletal abnormalities, pancreatic insufficiency, bone marrow failure, and increased sensitivity to infections. The observation that leukocytes taken from SDS patients show abnormal orientation during chemotaxis led to the hypothesis that cell motility might play a role in the etiology of the disease. The function of the protein mutated in this syndrome (SBDS) is unknown and it has no primary sequence similarity to any other protein or structural domain that would indicate a possible function. Interestingly, the homologous *D. discoideum* protein fused to GFP showed an enrichment of the protein in the pseudopods during cell migration, suggesting a direct role in the chemotactic machinery (Wessels et al. 2006). However, recent work in *D. discoideum* led to unexpected results, since the SBDS protein was found to be directly involved in ribosome assembly. These results support the hypothesis that SDS is a ribosomopathy caused by abnormal ribosome maturation (Wong et al. 2011).

5.3 Autophagy and Protein Aggregation Disorders

Autophagy is a lysosomal degradation pathway of the cell's own material and is highly conserved in all eukaryotes. Three forms have been described: chaperone-mediated autophagy (CMA), microautophagy, and macroautophagy. They differ in their physiological functions and the mechanisms to carry out the degradative process. During CMA, specific proteins are recognized by chaperones and translocated through the lysosome membrane for degradation (Koga and Cuervo 2011; Arias and Cuervo 2011). Microautophagy is a poorly defined process involving invagination of the lysosome membrane; the resulting small vesicles containing cytoplasmic material are degraded inside the lysosome (Mijaljica et al. 2011).

The best known and the most conserved is the third type, macroautophagy (called 'autophagy' hereafter for simplicity) and it is the main cellular mechanism involved in protein and organelle degradation (Yang and Klionsky 2010; Calvo-Garrido et al. 2010).

Autophagy is triggered by starvation conditions such as nutrient or growth factor depletion, but it is also induced in circumstances requiring for example the elimination of protein aggregates and defective organelles, or in response to bacterial pathogens. A double-membrane vesicle called autophagosome is formed in the cytoplasm engulfing the cargo. This is followed by fusion of the autophagosome with lysosomes and the subsequent degradation of the vesicle and its content. The simple molecular constituents are released during this degradation process to be recycled or used for ATP production.

During aging and neurodegeneration, cells accumulate abnormal protein aggregates, misfolded proteins, and defective organelles that need to be removed by autophagy, since they would otherwise interfere with normal cell function and contribute to the increasing risk of suffering several disorders (Xilouri and Stefanis 2011). The enormous impact of autophagy on pathology and aging has just begun to be recognized and it has started to attract the interest of medical research. Its therapeutical manipulation might be of great importance to fight cancer and degenerative diseases, to mention just two of the most devastating illnesses affecting millions (Yang et al. 2011; Xie et al. 2011). Understanding the molecular mechanisms of the autophagy machinery and its regulation is essential for its potential use as a therapeutic target and we are still far from understanding it in sufficient detail.

The first autophagy proteins were identified in yeast (coined Atg, for "autophagy-related") and grouped into functional complexes that are required for the initiation, elongation, and completion of the autophagosomes, although the precise mechanism of action of many of these proteins and the way they are regulated are not completely understood. Three signaling complexes regulate the initial inductive stage: Tor 1 kinase, Atg1 kinase, and the class III PI3Kinase complex. Vesicle expansion and completion require two ubiquitin-like conjugation systems. In the first conjugation reaction Atg12 is covalently bound to Atg5, a reaction catalyzed by the E1-type enzyme Atg7 and the E2 enzyme Atg10. After this, Atg16 interacts with the Atg12-Atg5 complex localized in the elongating membrane. This step facilitates the second conjugation reaction involving Atg8 (known as LC3 in mammals), which is attached to the expanding autophagosome membrane by conjugation to phosphatidylethanolamine (Fig. 5). Other proteins have been recognized to be involved in autophagy but their functions are still poorly defined. Examples are the membrane proteins Vmp1 and Atg9, which are believed to play a role in autophagosome membrane initiation. For further details see the following reviews (Inoue and Klionsky 2010; Yang and Klionsky 2010; Calvo-Garrido and Escalante 2010).

The origin and the mechanisms of formation of the autophagic double membrane are still open questions. It seems that different organelles including the ER and mitochondria can mediate the formation of the autophagosome membrane, but

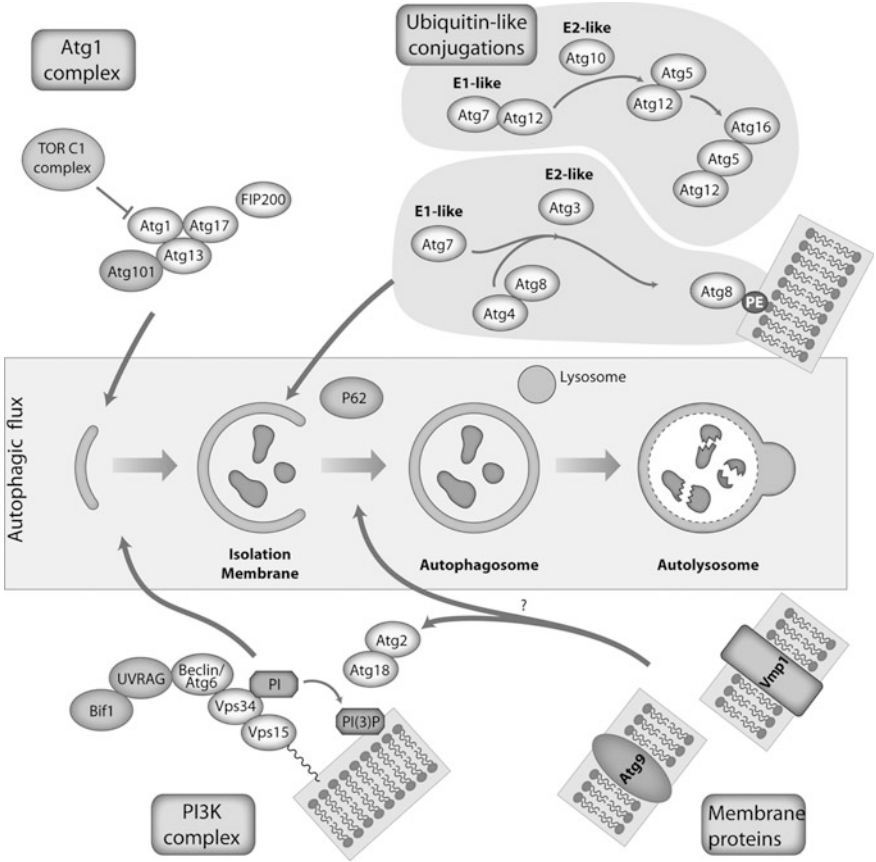

Fig. 5 Autophagic machinery in *D. discoideum*. The isolation membrane is a double membrane that enlarges and finally engulfs parts of the cytoplasm, aggregated proteins or organelles. After fusion with lysosomes, the content is degraded and recycled. The predicted *D. discoideum* autophagic proteins are organized into functional complexes using the information available from the yeast *S. cerevisiae* and mammalian cells. Some proteins such as Atg101, UVRAG, Bif 1 and Vmp1 are present in *Dictyostelium* and higher eukaryotes but seem to be absent in *S. cerevisiae*

how these membranes are recruited and specified to become an autophagosome is unknown (Reggiori 2006; Hailey et al. 2010). The PI3Kinase complex generates phosphatidylinositol 3-phosphate (PtdIns3P) at the site of autophagosome formation and this signaling is essential for the recruitment of autophagic proteins. Many other issues remain to be characterized, such as the mechanisms of membrane elongation and completion, the regulation of the fusion with lysosomes, and the link between the inductive signaling pathways, and the autophagic machinery. The autophagy process is so complex that other unknown autophagy-related proteins are expected to exist.

A number of studies in *D. discoideum* have revealed the similarities (both morphological and molecular) of its autophagic machinery with that of animal cells and, importantly, the presence of homologous autophagic proteins in *D. discoideum* and mammals that are absent in *S. cerevisiae* such as Atg101, FIP200, and Vmp1 (Calvo-Garrido et al. 2010; King et al. 2011; King 2012). In *D. discoideum*, as in mammalian cells, nascent autophagosomes originate in the cytoplasm from multiple origins and fuse with lysosomes, which are also animal-like. In contrast, in the yeast model *S. cerevisiae*, as in other fungi, these structures are concentrated and assembled in a single location of the cytoplasm near the single huge lysosome, the so-called vacuole.

Several markers have been optimized to study different stages of autophagosome formation as well as techniques to monitor autophagic flux (Calvo-Garrido et al. 2011; King et al. 2011), allowing a good level of molecular definition of the autophagic process in the *Dictyostelium* model. A number of mutants in *D. discoideum* have been generated affecting genes coding for at least one component of each of the referred functional complexes and the membrane proteins Atg9 and Vmp1 (Otto et al. 2003, 2004; Calvo-Garrido and Escalante 2010; Tung et al. 2010). A common phenotype in *D. discoideum* autophagy mutants is aberrant development and, interestingly, the severity of the phenotype depends on the mutated gene. The strongest phenotypes correspond to mutations in the kinase Atg1 and the transmembrane proteins Atg9 and Vmp1. Vmp1 is an ER protein that also co-localizes with autophagosomes, suggesting a role in the initial stages of autophagosome formation from the ER, modulating the spatial and temporal dynamics of PtdIns3P signaling (unpublished results). Apart from affecting autophagy, ablation of the protein causes defects in other membrane-dependent processes such as protein secretion and the functioning of the contractile vacuole, an organelle responsible for osmoregulation in social amoebas. Interestingly, Vmp1 has been proposed to have a role in pancreatitis and cancer (Ropolo et al. 2007; Grasso et al. 2011).

Another remarkable trait of autophagy mutants in *D. discoideum* is the presence of ubiquitinated protein aggregates, which are also common features in pathologies like Alzheimer's and Parkinson's disease, amyotrophic lateral sclerosis, Huntington's disease (HD), etc. The above-mentioned differences in the severity of the developmental phenotypes among autophagic mutants correlate quite well with the size and number of ubiquitin-positive protein aggregates (Calvo-Garrido and Escalante 2010). An attractive hypothesis is that the observed phenotypes are aggravated by the presence of these aggregates. The protein composition of the aggregates was partially analyzed in a mutant strain lacking Vmp1 and showed the presence of P62 (also known as Sequestosome 1), an adaptor protein involved in autophagic clearance of several substrates and also implicated in diverse protein aggregation disorders and infectious diseases (Zheng et al. 2011; Mostowy et al. 2011). The study of the formation and degradation of these aggregates is clinically important as it might provide opportunities for effective therapies.

It is still debated if protein aggregates in neurodegenerative diseases are the cause of the disease or a cell defense mechanism to accumulate and separate

abnormal proteins that otherwise would be toxic. Several studies in *D. discoideum* suggest that the protein aggregation phenotype might be deleterious for cell function, perhaps acting as a sink for other normal proteins that are attracted to the aggregate and thus lose their normal localization. This phenomenon was recently described in *D. discoideum* when VASP, an actin-binding protein, was expressed with an endosomal targeting signal. The mis-targeting of this protein leads to the formation of huge actin aggregates reminiscent of Hirano bodies, often present in neurodegenerative diseases. These actin aggregates were found to sequester a number of actin-binding and endosomal proteins promoting their disappearance from the cytoplasm, their normal location (Schmauch et al. 2009). Interestingly, the strong defect in the cytoskeleton observed in *D. discoideum* cells with Hirano bodies can be mimicked by disruption of these sequestered proteins, opening the possibility that protein sequestration might also contribute to neuronal malfunction in these pathologies. Hirano body-like aggregates can also be induced in *D. discoideum* by the overexpression of a truncated form of a 34 kDa actin-binding protein (Maselli et al. 2002). A recent report showed that both autophagy and the proteasome pathway contribute to the degradation of Hirano bodies in *D. discoideum*. Moreover, the autophagosome marker protein GFP-Atg8 co-localized with Hirano bodies in wild-type *D. discoideum* cells, but not in cells deficient in the autophagic proteins Atg5 or Atg1 (Kim et al. 2009).

D. discoideum is also a promising model to understand the normal physiological role of the presenilins, which are key proteins in Alzheimer's disease. Presenilins are the catalytic moiety of γ-secretase, a protease that cleaves a wide variety of integral membrane proteins. Inappropriate processing of amyloid precursor protein (APP) by this protease is associated with familial Alzheimer's disease. The analysis of null mutants indicates that presenilin complexes regulate cell differentiation and phagocytosis in *D. discoideum*. Remarkably, *D. discoideum* cells are able to process ectopically expressed human APP, and thus it might serve as a valuable model to understand the pathology and to apply high-throughput screening of new therapeutic drugs (McMains et al. 2010).

HD is a neurodegenerative genetic disorder caused by the presence of polyglutamine tracts in the protein huntingtin. *D. discoideum* has a huntingtin homolog whose disruption leads to pleiotropic defects in different cellular processes including cell motility, adhesion, and cytokinesis suggesting that huntingtin, as also suspected in human, is a complex multifunctional protein (Myre et al. 2011; Wang et al. 2011b).

Unexpected connections of human diseases with autophagy might arise from studies in *D. discoideum*. This is the case of the human *VCP* (p97) gene, whose mutations cause IBMPFD (inclusion body myopathy with early onset Paget's disease of bone and frontotemporal dementia), ALS14 (amyotrophic lateral sclerosis), and HSP (hereditary spastic paraplegia). This protein is conserved in *D. discoideum* and the expression of the most prevalent mutation leads to defects in growth, development, proteasomal activity, and autophagy. Interestingly, a novel relationship of VCP with the core autophagic protein Atg9 has been discovered, which is based on mutual inhibition (Arhzaouy et al. 2012).

5.4 The D. dictyostelium Model of Mitochondrial Disease

The mitochondrion is the organelle responsible for the generation of most cellular ATP through oxidative phosphorylation, and thus plays a key role in cellular bioenergetics. Similar to impaired autophagy, mitochondrial dysfunction affects the energy status of the cell and affects multicellular development. It should be noted that mitochondria are also involved in other important functions such as apoptosis, calcium homeostasis, lipid synthesis, generation of reactive oxygen species, aging, etc. (Sanz et al. 2006; Barja 2004; Satrustegui et al. 2007; Lopez-Lluch et al. 2008; Cadenas 2004; Fernandez-Moreno et al. 2007; Kompare and Rizzo 2008; Suen et al. 2008). Mitochondrial diseases are caused by genetic mutations in proteins encoded in the mitochondrial genome or in the nuclear genome. The pathological phenotypes of mitochondrial diseases are very complex and include blindness, deafness, epilepsy, heart disease, muscle, and neurological disorders, etc. Although many different associated mutations have been identified, the relationship between genotype and phenotype is still poorly understood. For example, the same genetic defect might result in different symptoms and the opposite is also true, similar outcomes might be originated by different genetic lesions (Debray et al. 2008; DiMauro and Schon 2008). Mitochondrial dysfunction is also believed to be involved in neurological disorders such as Parkinson's disease and Alzheimer's disease (Santos et al. 2011). The inefficient clearance of damaged mitochondria by mitophagy, a specific form of autophagy, is believed to be responsible for the accumulation of defects in mitochondria leading to cell malfunction and pathology during aging and neurodegenerative diseases (Xilouri and Stefanis 2011; Winslow and Rubinsztein 2011).

D. discoideum is a suitable model to study mitochondrial diseases for several reasons. It combines a powerful genetic tractability with a unique life cycle that provides a great variety of reproducible phenotypes associated with mitochondrial dysfunction (Francione et al. 2011). As occur in humans, mitochondrial disease in *D. discoideum* is characterized by what is known as pathological thresholds, so that some phenotypes appear more sensitive than others to the level of mitochondrial dysfunction. A number of different strategies are available in *D. discoideum* to generate sub-lethal mitochondrial defects such as RNAi (RNA interference) (Morita et al. 2005), antisense inhibition (Kotsifas et al. 2002), heteroplasmic disruption of mitochondrial genes (Francione and Fisher 2011), and disruption of nuclear genes encoding mitochondrial proteins (Torija et al. 2006b).

Traditionally, it has been assumed that low levels of ATP are the principal factor in mitochondrial diseases. However, recent studies in the *Dictyostelium* model suggest that some of the symptoms might be the consequence of abnormal regulation of signaling pathways. The relationship between the AMP-activated protein kinase (AMPK), a critical regulator of the energy status of the cell, and mitochondrial diseases has been clearly established in *D. discoideum* (Bokko et al. 2007). AMPK is highly sensitive to the AMP/ATP ratio and it is activated when ATP levels decrease as a consequence of mitochondrial dysfunction. Once

activated, AMPK tries to re-establish the cellular energy levels by activating pathways that generate ATP while inhibiting others that consume it (Hardie 2011). Antisense inhibition of the mitochondrial chaperonin 60 produces defective photo/thermotaxis at the slug stage and affects growth and morphogenesis in *D. discoideum*. Interestingly, these defective phenotypes are suppressed when AMPK expression is knocked-down in this mutant. Conversely, the expression of a constitutively active form of AMPK in wild-type cells mimics the observed phenotypes. These data strongly suggests that AMPK is chronically activated in *D. discoideum* cells with mitochondrial dysfunction (Bokko et al. 2007; Francione et al. 2009). Interestingly, recent reports indicate that abnormally activated AMPK is accumulated in cerebral neurons in Alzheimer's disease and other neurodegenerative disorders (Vingtdeux et al. 2011; Choi et al. 2010).

An added value of *D. discoideum* is the presence of complex I (CI), the largest complex of the respiratory chain that couples the oxidation of NADH to the reduction of ubiquinone and the transport of protons across the mitochondrial inner membrane. This complex is not present in some yeast models such as *S. cerevisiae* or *S. pombe*, although it is present in others such as *Yarrowia lipolytica*. CI has an enormous impact on human disease, since about 40 % of inherited mitochondrial disorders involve isolated or combined deficiencies in CI activity. CI contains 45 protein subunits in human and *D. discoideum* codes for most of these proteins (Francione et al. 2011). Despite its complexity, relatively few assembly factors have been described to assist in the correct assembly and stability of this huge complex. Studies in *D. discoideum* have led to the discovery of MidA (also known as PRO1853) and its role in CI function. Mutant *D. discoideum* cells where MidA has been ablated show a specific defect in CI activity that has also been confirmed in human HEK293T cells where MidA was down-regulated by RNAi. Moreover, both *D. discoideum* and human MidA interact with the essential CI subunit NDUFS2 (Carilla-Latorre et al. 2010). MidA deficiency not only causes the typical AMPK-dependent defects seen in other mitochondrial mutants, but also produces additional phenotypes related to phagocytosis and macropinocytosis that highlight the complexity of mitochondrial diseases even in this simple model. All these data suggest that MidA is a good candidate to be involved in human mitochondrial disease.

5.5 Molecular Pharmacology in D. dictyostelium

Understanding the mechanism of action of drugs and toxic compounds at the cellular and physiological levels is fundamental in clinical research. This difficult task is in part hampered by the use of complex models, for example mammalian cell lines, which are very different in origin and properties and often harbor mutations and chromosome duplications. Along the same line, and apart from the inherent ethical problems, the use of mammalian models (mice and rats) is

expensive and the necessity to use large numbers of animals (for example in drug screening) increases the costs even more.

But above all, in such complex models it is impossible to use unbiased genetic screening to clonally isolate mutant strains and the analysis of single and multiple KOs is far from simple. These problems can be partially circumvented by using simple and genetically tractable organisms such as *D. discoideum*. In spite of the evolutionary distance, recent research has shown an amazing conservation of the mechanisms of action of some drugs between the social amoeba and humans.

One example in which *D. discoideum* has proved useful is in deciphering the mechanisms underlying the resistance and sensitivity to chemotherapeutic drugs such as cisplatin. Only in Spain, approximately, 200,000 people are diagnosed with cancer every year and many of them are treated with chemotherapeutic drugs, which are cytotoxic molecules that are more efficient in killing rapidly dividing cancer cells than normal cells. However, one of the most important problems is that tumors often become resistant to the drugs. The mechanisms of such resistance are not completely understood and this knowledge is essential to design new anticancer drugs and new strategies. A blind genetic screening in *D. discoideum* for selection of mutants resistant to cisplatin opened new avenues for the research into the mechanisms of resistance (Alexander and Alexander 2011). Mutagenesis was performed by REMI to identify genes involved in cisplatin resistance. None of the identified genes were previously implicated in cisplatin action (Li et al. 2000). One of them was the gene encoding the enzyme sphingosine-1-phosphate (S-1-P) lyase, a highly conserved enzyme of the sphingolipid metabolic pathway (Li et al. 2001) (Fig. 6a). This discovery led to further characterization of this pathway using KOs and overexpression strains, which demonstrated that multiple enzymes of this biochemical pathway are involved in the mechanism of action of cisplatin and other chemotherapeutic drugs in the *Dictyostelium* model and, most importantly, also in human cells (Alexander and Alexander 2011). These studies suggest that the balance between the signaling sphingolipids ceramide and S-1-P determines whether a cell dies or lives in the presence of the drug. Thus, modulation of the activity of sphingolipid metabolizing enzymes is a potential new target for improving cancer therapy.

Bipolar disorders are complex pathological conditions leading to extreme changes in mood. Current treatments for bipolar disorder include, among others, valproic acid (VPA) and lithium (Li). The effects of these compounds are complex and seem to affect diverse signaling pathways, but their precise sites of action and the signaling pathways involved are largely unknown (Ketter 2010). In both *D. discoideum* and mammalian cells, VPA and Li acting at different levels are able to increase the level of activation of the MAP kinase ERK2 by increasing its phosphorylation (Einat et al. 2003). MAPK pathways are involved in neuronal differentiation and plasticity and thus are good candidates to be involved in the disease.

Extracellular signal-regulated kinases (ERKs) are a class of MAP kinases functioning in many different signaling pathways. In *D. discoideum* there are two ERK kinases (ERK1 and ERK2). ERK2 is involved in the chemotactic response to

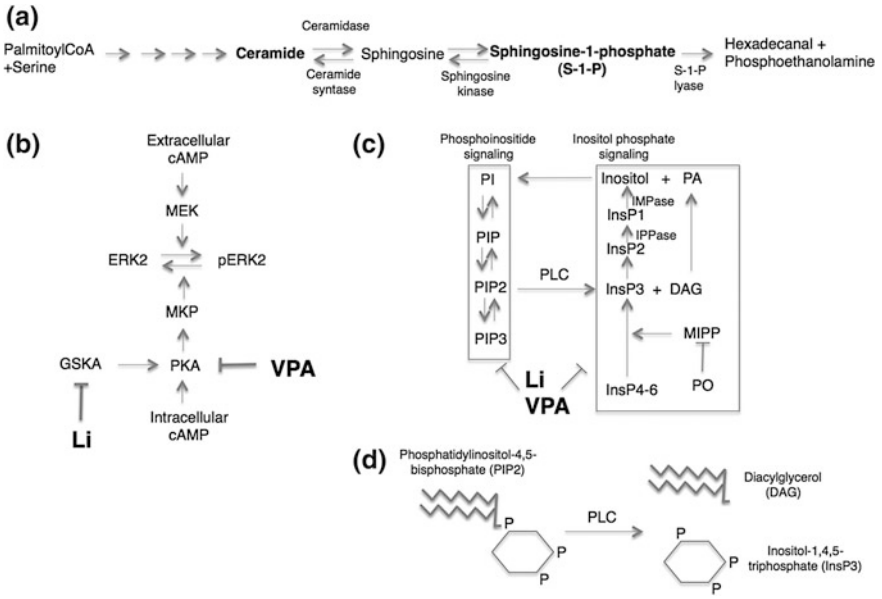

Fig. 6 Molecular pharmacology in *D. discoideum*. **a** Schematic representation of the sphingolipid metabolic pathway involved in cisplatin resistance. **b** MAPK regulation by VPA and Li, used to treat bipolar disorders. ERK2: extracellular regulated kinase 2; pERK2: phosphorylated ERK2; MKP: MAPK phosphatase; MEK: MAP kinase kinase; PKA: protein kinase A; GSK3: glycogen synthase kinase 3. **c** Inositol phosphate and phosphoinositide signaling regulation by bipolar disorder treatments. PO: prolyl oligopeptidase; MIPP: multiple inositol polyphosphate phosphatase; IPPase: inositol polyphosphate phosphatase; IMPase: inositol monophosphatase. **d** Schematic representation of the structure of PIP2 (phosphatidylinositol 4,5-biphosphate) and its cleavage by PLC (phospholipase C) to generate DAG (diacylglycerol) and InsP3 (Inositol 1,4,5-triphosphate). See the text for a complete description of the pathways

cAMP and cell differentiation during development (Nguyen et al. 2010). The use of KO strains and overexpressors suggests the model depicted in Fig. 6b (Ludtmann et al. 2011). Treatment of *D. discoideum* cells with cAMP gives rise to a transient phosphorylation of ERK2 and the use of Li or VPA induces a significant increase in this effect. However, they do so by affecting different pathways. VPA-induced ERK2 phosphorylation can be mimicked by decreasing intracellular cAMP or PKA activity and by pharmacological inhibition of phosphotyrosine phosphatase activity, suggesting that VPA acts by inhibiting the de-phosphorylation of ERK2 (Boeckeler et al. 2006). The precise mechanism and the crosstalk between the cAMP pathways and ERK2 are not fully defined and require further studies in *D. discoideum* and mammalian cells. The effect of Li is believed to involve inhibition of GSKA since GSKA ablation reduces the lithium effect on ERK2 phosphorylation, while VPA has an increased effect in this mutant suggesting that VPA acts through a GSKA-independent mechanism.

VPA and Li have also been shown to modulate another fundamental and well-conserved signaling pathway, the inositol phosphate pathway (Fig. 6c). Li attenuates inositol recycling by inhibiting the enzymes inositol monophosphatase (IMPase) and inositol polyphosphate 1-phosphatase (IPPase) (Williams et al. 2002; Allison et al. 1980; Hallcher and Sherman 1980; Berridge et al. 1989). Additional studies by REMI mutagenesis identified prolyl oligopeptidase (PO) as the gene disrupted in a mutant resistant to the block in development exerted by Li (Williams et al. 1999). PO mutants had elevated InsP3 levels, suggesting an effect on this signaling pathway. In agreement with this, the effect of Li, VPA and carbamazepine (another mood-stabilizing drug) on development was reversed by addition of exogenous inositol. A similar situation was also observed in mammalian neurons (Williams et al. 2002; Eickholt et al. 2005). Although PO is supposed to be involved in the cleavage of small peptides containing prolyl residues, a recent study established a clear link between PO and the enzyme multiple inositol polyphosphate phosphatase (MIPP) involved in the formation of InsP3 by the breakdown of InsP4, InsP5, and InsP6 (King et al. 2010). As expected, the ablation of MIPP results in reduced InsP3 levels and its overexpression leads to the opposite effect. Moreover, the PO-dependent effect on inositol signaling requires active MIPP. Taken together, these results suggest that PO is an inhibitor of MIPP activity. Importantly, a significant decrease in PO activity has been reported in bipolar disorder patients undergoing Li treatment (Breen et al. 2004).

Another layer of complexity is the presence in *D. discoideum* of a gene expression regulatory mechanism where the activation of MIPP induces the expression of inositol-regulatory genes including IMPase and IPPase, which are targets of Li, and inositol synthase 1 (INO1), involved in the synthesis of inositol. Interestingly, these observations have been reproduced in human cell culture (King et al. 2010).

A related signaling pathway, the phosphoinositide pathway, has also been implied in the mechanism of action of bipolar disorder drugs thanks to the work in *D. discoideum* (Xu et al. 2007; Chang et al. 2012). VPA treatment reduces phosphoinositide levels and this observation led for the first time to the suggestion that elevated phosphoinositol signaling might be an important factor in the development of the disease. Remarkably, this idea is supported by the observation of increased levels of phosphatidylinositol-4,5-bisphosphate (PIP2) in untreated patients and its down-regulation by the drugs (Soares et al. 1997, 2000). Further observations in *D. discoideum* implicate phosphoinositides as a target for Li treatment. Translocation of protein kinase B (PkbA) to the membrane is mediated by the interaction of its PH domain with PIP3, thus serving as a marker of PIP3 levels. Li was found to reduce PkbA translocation, suggesting a defect in PIP3 signaling. Once more, these observations were reproduced in human cells (King et al. 2009). In summary, the results in the *Dictyostelium* model support the hypothesis that Li and VPA exert their action through inositol depletion but also through attenuation of phosphoinositide signaling.

6 Concluding Remarks

The studies reviewed in this chapter justify the interest in *D. discoideum* as a model system to study several aspects of biomedical sciences and its potential to open new avenues in the study of mechanisms of human disease. A recent bibliometric analysis has shown that more than 75 % of research still focuses on the 10 % of proteins that were known before the human genome was sequenced (Edwards et al. 2011). This conservative tendency is still stronger for proteins of unknown function. Some of these proteins are highly conserved among evolutionarily distant species suggesting that they play relevant roles, perhaps related to human diseases. The inherent difficulty in the study of a disease-related protein of unknown function or the complexity of signaling networks in pathology can be partially overcome by the powerful genetics of simple models, as illustrated in this review. These models may serve to give us new and unexpected insights.

Acknowledgments This work was supported by grants BFU2009-09050 and BFU2012-32536 from the Spanish Ministerio de Ciencia e Innovación. Thanks to Dr. Ron Hartong for linguistic assistance and suggestions. A.M. is supported by a FPI fellowship from the Spanish Government. S.M.B. has been supported by "Obra Social Caja de Burgos y Fundación Gutiérrez Manrique".

References

Adachi H, Hasebe T, Yoshinaga K, Ohta T, Sutoh K (1994) Isolation of *Dictyostelium discoideum* cytokinesis mutants by restriction enzyme-mediated integration of the blasticidin S resistance marker. Biochem Biophys Res Commun 205:1808–1814

Alexander S, Alexander H (2011) Lead genetic studies in *Dictyostelium discoideum* and translational studies in human cells demonstrate that sphingolipids are key regulators of sensitivity to cisplatin and other anticancer drugs. Semin Cell Dev Biol 22(1):97–104. doi:10.1016/j.semcdb.2010.10.005

Allison JH, Boshans RL, Hallcher LM, Packman PM, Sherman WR (1980) The effects of lithium on myo-inositol levels in layers of frontal cerebral cortex, in cerebellum, and in corpus callosum of the rat. J Neurochem 34(2):456–458

Alonso A, Rojo F, Martinez JL (1999) Environmental and clinical isolates of *Pseudomonas aeruginosa* show pathogenic and biodegradative properties irrespective of their origin. Environ Microbiol 1(5):421–430

Araki T, Kawata T, Williams JG (2012) Identification of the kinase that activates a nonmetazoan STAT gives insights into the evolution of phosphotyrosine-SH2 domain signaling. Proc Natl Acad Sci USA 109(28):E1931–1937. doi:10.1073/pnas.1202715109

Arhzaouy K, Strucksberg KH, Tung SM, Tangavelou K, Stumpf M, Faix J, Schroder R, Clemen CS, Eichinger L (2012) Heteromeric p97/p97(R155C) complexes induce dominant negative changes in wild-type and autophagy 9-deficient Dictyostelium strains. PLoS ONE 7(10):e46879. doi:10.1371/journal.pone.0046879

Arias E, Cuervo AM (2011) Chaperone-mediated autophagy in protein quality control. Curr Opin Cell Biol 23(2):184–189. doi:10.1016/j.ceb.2010.10.009

Ashworth JM, Sussman M (1967) The appearance and disappearance of uridine diphosphate glucose pyrophosphorylase activity during differentiation of the cellular slime mold *Dictyostelium discoideum*. J Biol Chem 242:1696–1700

Barja G (2004) Free radicals and aging. Trends Neurosci 27(10):595–600. doi:10.1016/j.tins.2004.07.005

Batsios P, Peter T, Baumann O, Stick R, Meyer I, Graf R (2012) A lamin in lower eukaryotes? Nucleus 3(3):237–243. doi:10.4161/nucl.20149

Bear JE, Rawls JF, Saxe III CL (1998) SCAR, a WASP-related protein, isolated as a suppressor of receptor defects in late Dictyostelium development. J Cell Biol 142:1325–1335

Berridge MJ, Downes CP, Hanley MR (1989) Neural and developmental actions of lithium: a unifying hypothesis. Cell 59(3):411–419

Boeckeler K, Adley K, Xu X, Jenkins A, Jin T, Williams RS (2006) The neuroprotective agent, valproic acid, regulates the mitogen-activated protein kinase pathway through modulation of protein kinase A signalling in *Dictyostelium discoideum*. Eur J Cell Biol 85(9–10):1047–1057

Bokko PB, Francione L, Bandala-Sanchez E, Ahmed AU, Annesley SJ, Huang X, Khurana T, Kimmel AR, Fisher PR (2007) Diverse cytopathologies in mitochondrial disease are caused by AMP-activated protein kinase signaling. Mol Biol Cell 18(5):1874–1886

Bonner JT (1947) Evidence for the formation of cell aggregates by chemotaxis in the development of the slime mold *Dictyostelium discoideum*. J Exp Zool 106:1–26

Bozzaro S, Bucci C, Steinert M (2008) Phagocytosis and host–pathogen interactions in Dictyostelium with a look at macrophages. Int Rev Cell Mol Biol 271:253–300. doi:10.1016/S1937-6448(08)01206-9

Bradbury RS, Reid DW, Inglis TJ, Champion AC (2011) Decreased virulence of cystic fibrosis *Pseudomonas aeruginosa* in *Dictyostelium discoideum*. Microbiol Immunol 55(4):224–230. doi:10.1111/j.1348-0421.2011.00314.x

Breen G, Harwood AJ, Gregory K, Sinclair M, Collier D, St Clair D, Williams RS (2004) Two peptidase activities decrease in treated bipolar disorder not schizophrenic patients. Bipolar Disord 6(2):156–161

Cadenas E (2004) Mitochondrial free radical production and cell signaling. Mol Aspects Med 25(1–2):17–26. doi:10.1016/j.mam.2004.02.005

Calvo-Garrido J, Carilla-Latorre S, Kubohara Y, Santos-Rodrigo N, Mesquita A, Soldati T, Golstein P, Escalante R (2010) Autophagy in Dictyostelium: genes and pathways, cell death and infection. Autophagy 6(6):686–701 12513 [pii]

Calvo-Garrido J, Carilla-Latorre S, Lazaro-Dieguez F, Egea G, Escalante R (2008) Vacuole membrane protein 1 is an endoplasmic reticulum protein required for organelle biogenesis, protein secretion, and development. Mol Biol Cell 19(8):3442–3453. doi:10.1091/mbc.E08-01-0075

Calvo-Garrido J, Carilla-Latorre S, Mesquita A, Escalante R (2011) A proteolytic cleavage assay to monitor autophagy in *Dictyostelium discoideum*. Autophagy 7(9):1063–1068. doi:10.4161/auto.7.9.16629

Calvo-Garrido J, Escalante R (2010) Autophagy dysfunction and ubiquitin-positive protein aggregates in Dictyostelium cells lacking Vmp1. Autophagy 6(1):100–109

Carilla-Latorre S, Calvo-Garrido J, Bloomfield G, Skelton J, Kay RR, Ivens A, Martinez JL, Escalante R (2008) Dictyostelium transcriptional responses to *Pseudomonas aeruginosa*: common and specific effects from PAO1 and PA14 strains. BMC Microbiol 8:109. doi:10.1186/1471-2180-8-109

Carilla-Latorre S, Gallardo ME, Annesley SJ, Calvo-Garrido J, Grana O, Accari SL, Smith PK, Valencia A, Garesse R, Fisher PR, Escalante R (2010) MidA is a putative methyltransferase that is required for mitochondrial complex I function. J Cell Sci 123(Pt 10):1674–1683. doi:10.1242/jcs.066076

Chang P, Orabi B, Deranieh RM, Dham M, Hoeller O, Shimshoni JA, Yagen B, Bialer M, Greenberg ML, Walker MC, Williams RS (2012) The antiepileptic drug valproic acid and other medium-chain fatty acids acutely reduce phosphoinositide levels independently of inositol in Dictyostelium. Dis Model Mech 5(1):115–124. doi:10.1242/dmm.008029

Choi JS, Park C, Jeong JW (2010) AMP-activated protein kinase is activated in Parkinson's disease models mediated by 1-methyl-4-phenyl-1,2,3,6-tetrahydropyridine. Biochem Biophys Res Commun 391(1):147–151. doi:10.1016/j.bbrc.2009.11.022

Condeelis J, Jones J, Segall JE (1992) Chemotaxis of metastatic tumor cells: Clues to mechanisms from the Dictyostelium paradigm. Cancer Metastasis Rev 11:55–68

Cosson P, Zulianello L, Join-Lambert O, Faurisson F, Gebbie L, Benghezal M, van Delden C, Curty LK, Kohler T (2002) *Pseudomonas aeruginosa* virulence analyzed in a *Dictyostelium discoideum* host system. J Bact 184:3027–3033

de Felipe KS, Glover RT, Charpentier X, Anderson OR, Reyes M, Pericone CD, Shuman HA (2008) *Legionella* eukaryotic-like type IV substrates interfere with organelle trafficking. PLoS Pathog 4(8):e1000117. doi:10.1371/journal.ppat.1000117

De Lozanne A, Spudich JA (1987) Disruption of the Dictyostelium myosin heavy chain gene by homologous recombination. Science 236:1086–1091

Debray FG, Lambert M, Mitchell GA (2008) Disorders of mitochondrial function. Curr Opin Pediatr 20(4):471–482. doi:10.1097/MOP.0b013e328306ebb6

Depraitere C, Darmon M (1978) Croissance de l'amibe sociale *Dictyostelium discoideum* sur differentes especes bacteriennes. Ann Microbiol (Inst Pasteur) 129B:451–461

DiMauro S, Schon EA (2008) Mitochondrial disorders in the nervous system. Annu Rev Neurosci 31:91–123. doi:10.1146/annurev.neuro.30.051606.094302

Dubin M, Nellen W (2010) A versatile set of tagged expression vectors to monitor protein localisation and function in Dictyostelium. Gene 465(1–2):1–8. doi:10.1016/j.gene.2010.06.010 S0378-1119(10)00259-3 [pii]

Edwards AM, Isserlin R, Bader GD, Frye SV, Willson TM, Yu FH (2011) Too many roads not taken. Nature 470(7333):163–165. doi:10.1038/470163a

Eichinger L, Pachebat JA, Glockner G, Rajandream MA, Sucgang R, Berriman M, Song J, Olsen R, Szafranski K, Xu Q, Tunggal B, Kummerfeld S, Madera M, Konfortov BA, Rivero F, Bankier AT, Lehmann R, Hamlin N, Davies R, Gaudet P, Fey P, Pilcher K, Chen G, Saunders D, Sodergren E, Davis P, Kerhornou A, Nie X, Hall N, Anjard C, Hemphill L, Bason N, Farbrother P, Desany B, Just E, Morio T, Rost R, Churcher C, Cooper J, Haydock S, van Driessche N, Cronin A, Goodhead I, Muzny D, Mourier T, Pain A, Lu M, Harper D, Lindsay R, Hauser H, James K, Quiles M, Madan Babu M, Saito T, Buchrieser C, Wardroper A, Felder M, Thangavelu M, Johnson D, Knights A, Loulseged H, Mungall K, Oliver K, Price C, Quail MA, Urushihara H, Hernandez J, Rabbinowitsch E, Steffen D, Sanders M, Ma J, Kohara Y, Sharp S, Simmonds M, Spiegler S, Tivey A, Sugano S, White B, Walker D, Woodward J, Winckler T, Tanaka Y, Shaulsky G, Schleicher M, Weinstock G, Rosenthal A, Cox EC, Chisholm RL, Gibbs R, Loomis WF, Platzer M, Kay RR, Williams J, Dear PH, Noegel AA, Barrell B, Kuspa A (2005) The genome of the social amoeba *Dictyostelium discoideum*. Nature 435(7038):43–57

Eichinger L, Rivero F (2006) *Dictyostelium discoideum* protocols. Methods in molecular biology Humana Press, Totowa

Eickholt BJ, Towers GJ, Ryves WJ, Eikel D, Adley K, Ylinen LM, Chadborn NH, Harwood AJ, Nau H, Williams RS (2005) Effects of valproic acid derivatives on inositol trisphosphate depletion, teratogenicity, glycogen synthase kinase-3beta inhibition, and viral replication: a screening approach for new bipolar disorder drugs derived from the valproic acid core structure. Mol Pharmacol 67(5):1426–1433

Einat H, Yuan P, Gould TD, Li J, Du J, Zhang L, Manji HK, Chen G (2003) The role of the extracellular signal-regulated kinase signaling pathway in mood modulation. J Neurosci (Off J Soc Neurosci) 23(19):7311–7316

Escalante R (2011) Dictyostelium as a model for human disease. Semin Cell Dev Biol 22(1):69. doi:10.1016/j.semcdb.2010.12.001

Escalante R, Vicente JJ (2000) *Dictyostelium discoideum*: a model system for differentiation and patterning. Int J Dev Biol 44:819–835

Fernandez-Moreno MA, Farr CL, Kaguni LS, Garesse R (2007) *Drosophila melanogaster* as a model system to study mitochondrial biology. Methods Mol Biol 372:33–49

Firtel R, Bonner J (1972) Characterization of the genome of the cellular slime mold *Dictyostelium discoideum*. J Mol Biol 66:339–361

Firtel RA, Silan C, Ward TE, Howard P, Metz BA, Nellen W, Jacobson A (1985) Extrachromosomal replication of shuttle vectors in *Dictyostelium discoideum*. Mol Cell Biol 5:3241–3250

Francione L, Smith PK, Accari SL, Taylor PE, Bokko PB, Bozzaro S, Beech PL, Fisher PR (2009) *Legionella pneumophila* multiplication is enhanced by chronic AMPK signalling in mitochondrially diseased Dictyostelium cells. Dis Model Mech 2(9–10):479–489. doi:10.1242/dmm.003319

Francione LM, Annesley SJ, Carilla-Latorre S, Escalante R, Fisher PR (2011) The Dictyostelium model for mitochondrial disease. Semin Cell Dev Biol 22(1):120–130. doi:10.1016/j.semcdb.2010.11.004

Francione LM, Fisher PR (2011) Heteroplasmic mitochondrial disease in *Dictyostelium discoideum*. Biochem Pharmacol 82(10):1510–1520. doi:10.1016/j.bcp.2011.07.071

Gaudet P, Pilcher KE, Fey P, Chisholm RL (2007) Transformation of *Dictyostelium discoideum* with plasmid DNA. Nat Protoc 2(6):1317–1324

Gezelius K (1962) Growth of the cellular slime mold *Dictyostelium discoideum* on dead bacteria in liquid media. Physiologia Plantarum 15:587–592

Grasso D, Ropolo A, Lo Re A, Boggio V, Molejon MI, Iovanna JL, Gonzalez CD, Urrutia R, Vaccaro MI (2011) Zymophagy, a novel selective autophagy pathway mediated by VMP1-USP9x-p62, prevents pancreatic cell death. J Biol Chem 286(10):8308–8324. doi:10.1074/jbc.M110.197301

Hailey DW, Rambold AS, Satpute-Krishnan P, Mitra K, Sougrat R, Kim PK, Lippincott-Schwartz J (2010) Mitochondria supply membranes for autophagosome biogenesis during starvation. Cell 141(4):656–667. doi:10.1016/j.cell.2010.04.009 S0092-8674(10)00383-1 [pii]

Hallcher LM, Sherman WR (1980) The effects of lithium ion and other agents on the activity of myo-inositol-1-phosphatase from bovine brain. J Biol Chem 255(22):10896–10901

Hardie DG (2011) Sensing of energy and nutrients by AMP-activated protein kinase. Am J Clin Nutr 93(4):891S–896S. doi:10.3945/ajcn.110.001925

Heidel AJ, Lawal HM, Felder M, Schilde C, Helps NR, Tunggal B, Rivero F, John U, Schleicher M, Eichinger L, Platzer M, Noegel AA, Schaap P, Glockner G (2011) Phylogeny-wide analysis of social amoeba genomes highlights ancient origins for complex intercellular communication. Genome Res 21(11):1882–1891. doi:10.1101/gr.121137.111

Hirth KP, Edwards CA, Firtel RA (1982) A DNA-mediated transformation system for *Dictyostelium discoideum*. Proc Natl Acad Sci USA 79:7356–7360

Hoeller O, Kay RR (2007) Chemotaxis in the absence of PIP3 gradients. Curr Biol 17(9):813–817

Hori H, Osawa S, Iwabuchi M (1980) The nucleotide sequence of 5S rRNA from a cellular slime mold *Dictyostelium discoideum*. Nucl Acids Res 8:5535–5539

Inoue Y, Klionsky DJ (2010) Regulation of macroautophagy in *Saccharomyces cerevisiae*. Semin Cell Dev Biol 21(7):664–670. doi:10.1016/j.semcdb.2010.03.009 S1084-9521(10)00071-6 [pii]

Iwashkiw JA, Seper A, Weber BS, Scott NE, Vinogradov E, Stratilo C, Reiz B, Cordwell SJ, Whittal R, Schild S, Feldman MF (2012) Identification of a general O-linked protein glycosylation system in *Acinetobacter baumannii* and its role in virulence and biofilm formation. PLoS Pathog 8(6):e1002758. doi:10.1371/journal.ppat.1002758

Janjua HA, Segata N, Bernabo P, Tamburini S, Ellen A, Jousson O (2012) Clinical populations of *Pseudomonas aeruginosa* isolated from acute infections show a wide virulence range partially correlated with population structure and virulence gene expression. Microbiology 158(Pt 8):2089–2098. doi:10.1099/mic.0.056689-0

Jin T, Xu X, Hereld D (2008) Chemotaxis, chemokine receptors and human disease. Cytokine 44(1):1–8. doi:10.1016/j.cyto.2008.06.017

Jones NC, Trainor PA (2005) Role of morphogens in neural crest cell determination. J Neurobiol 64(4):388–404. doi:10.1002/neu.20162

Kawata T (2011) STAT signaling in Dictyostelium development. Dev Growth Differ 53(4):548–557. doi:10.1111/j.1440-169X.2010.01243.x

Ketter TA (2010) Diagnostic features, prevalence, and impact of bipolar disorder. J Clin Psychiatry 71(6):e14. doi:10.4088/JCP.8125tx11c

Kim DH, Davis RC, Furukawa R, Fechheimer M (2009) Autophagy contributes to degradation of Hirano bodies. Autophagy 5(1):44–51

King J, Keim M, Teo R, Weening KE, Kapur M, McQuillan K, Ryves J, Rogers B, Dalton E, Williams RS, Harwood AJ (2010) Genetic control of lithium sensitivity and regulation of inositol biosynthetic genes. PLoS ONE 5(6):e11151. doi:10.1371/journal.pone.0011151

King JS (2012) Autophagy across the eukaryotes: Is *S. cerevisiae* the odd one out? Autophagy 8(7):1159–1162

King JS, Insall RH (2009) Chemotaxis: finding the way forward with Dictyostelium. Trends Cell Biol 19(10):523–530. doi:10.1016/j.tcb.2009.07.004

King JS, Teo R, Ryves J, Reddy JV, Peters O, Orabi B, Hoeller O, Williams RS, Harwood AJ (2009) The mood stabiliser lithium suppresses PIP3 signalling in Dictyostelium and human cells. Dis Model Mech 2(5–6):306–312. doi:10.1242/dmm.001271

King JS, Veltman DM, Insall RH (2011) The induction of autophagy by mechanical stress. Autophagy 7(12):1490–1499

Kipnis E, Sawa T, Wiener-Kronish J (2006) Targeting mechanisms of *Pseudomonas aeruginosa* pathogenesis. Med Mal Infect 36(2):78–91

Koga H, Cuervo AM (2011) Chaperone-mediated autophagy dysfunction in the pathogenesis of neurodegeneration. Neurobiol Dis 43(1):29–37. doi:10.1016/j.nbd.2010.07.006

Kole TP, Tseng Y, Jiang I, Katz JL, Wirtz D (2005) Intracellular mechanics of migrating fibroblasts. Mol Biol Cell 16(1):328–338. doi:10.1091/mbc.E04-06-0485

Kompare M, Rizzo WB (2008) Mitochondrial fatty-acid oxidation disorders. Semin Pediatr Neurol 15(3):140–149. doi:10.1016/j.spen.2008.05.008

Konijn TM, Barkley DS, Chang YY, Bonner JT (1968) Cyclic AMP: a naturally occurring acrasin in the cellular slime molds. Am Nat 102:225–233

Kotsifas M, Barth C, De Lozanne A, Lay ST, Fisher PR (2002) Chaperonin 60 and mitochondrial disease in Dictyostelium. J Muscle Res Cell Motil 23:839–852

Kuspa A (2006) Restriction enzyme-mediated integration (REMI) mutagenesis. Methods Mol Biol 346:201–209

Kuspa A, Loomis WF (1992) Tagging developmental genes in Dictyostelium by restriction enzyme-mediated integration of plasmid DNA. Proc Natl Acad Sci USA 89:8803–8807

Langenick J, Araki T, Yamada Y, Williams JG (2008) A Dictyostelium homologue of the metazoan Cbl proteins regulates STAT signalling. J Cell Sci 121(Pt 21):3524–3530. doi:10.1242/jcs.036798

Leber T (1888) Über die Entstehung der Entzündung und die Wirkung der entzündungserregenden Schädlichkeiten. Fortschr Med 6:460–464

Lee DG, Urbach JM, Wu G, Liberati NT, Feinbaum RL, Miyata S, Diggins LT, He J, Saucier M, Deziel E, Friedman L, Li L, Grills G, Montgomery K, Kucherlapati R, Rahme LG, Ausubel FM (2006) Genomic analysis reveals that *Pseudomonas aeruginosa* virulence is combinatorial. Genome Biol 7(10):R90

Lelong E, Marchetti A, Simon M, Burns JL, van Delden C, Kohler T, Cosson P (2011) Evolution of *Pseudomonas aeruginosa* virulence in infected patients revealed in a *Dictyostelium discoideum* host model. Clin Microbiol Infect (Off Publ Eur Soc Clin Microbiol Infect Dis) 17(9):1415–1420. doi:10.1111/j.1469-0691.2010.03431.x

Levi S, Polyakov M, Egelhoff TT (2000) Green fluorescent protein and epitope tag fusion vectors for *Dictyostelium discoideum*. Plasmid 44:231–238

Li G, Alexander H, Schneider N, Alexander S (2000) Molecular basis for resistance to the anticancer drug cisplatin in Dictyostelium. Microbiology 146:2219–2227

Li GC, Foote C, Alexander S, Alexander H (2001) Sphingosine-1-phosphate lyase has a central role in the development of *Dictyostelium discoideum*. Development 128:3473–3483

Lima WC, Lelong E, Cosson P (2011) What can Dictyostelium bring to the study of *Pseudomonas* infections? Semin Cell Dev Biol 22(1):77–81. doi:10.1016/j.semcdb.2010.11.006

Linares JF, Moreno R, Fajardo A, Martinez-Solano L, Escalante R, Rojo F, Martinez JL (2010) The global regulator Crc modulates metabolism, susceptibility to antibiotics and virulence in *Pseudomonas aeruginosa*. Environ Microbiol 12(12):3196–3212. doi:10.1111/j.1462-2920.2010.02292.x EMI2292 [pii]

Loomis W, Sussman M (1966) Commitment to the synthesis of a specific enzyme during cellular slime mold development. J Mol Biol 22:401–404

Loomis WF (1969a) Acetyl-glucosaminidase, an early enzyme in the development of *Dictyostelium discoideum*. J Bacteriol 97:1149–1154

Loomis WF (1969b) Developmental regulation of alkaline phosphatase in *Dictyostelium discoideum*. J Bacteriol 100:417–422

Loomis WF (1970) Developmental regulation of alpha-mannosidase in *Dictyostelium discoideum*. J Bacteriol 103:375–381

Loomis WF (1971) Sensitivity of *Dictyostelium discoideum* to nucleic acid analogues. Exp Cell Res 64:484–486

Loomis WF, White S, Dimond RL (1976) A sequence of dependent stages in the development of *Dictyostelium discoideum*. Dev Biol 53:171–177

Lopez-Lluch G, Irusta PM, Navas P, de Cabo R (2008) Mitochondrial biogenesis and healthy aging. Exp Gerontol 43(9):813–819. doi:10.1016/j.exger.2008.06.014

Ludtmann MH, Boeckeler K, Williams RS (2011) Molecular pharmacology in a simple model system: implicating MAP kinase and phosphoinositide signalling in bipolar disorder. Semin Cell Dev Biol 22(1):105–113. doi:10.1016/j.semcdb.2010.11.002

Maselli AG, Davis R, Furukawa R, Fechheimer M (2002) Formation of Hirano bodies in Dictyostelium and mammalian cells induced by expression of a modified form of an actin-crosslinking protein. J Cell Sci 115:1939–1949

Maxam AM, Gilbert W (1977) A new method for sequencing DNA. Proc Natl Acad Sci USA 74(2):560–564

McCutcheon (1946) Chemotaxis in leukocytes. Physiol Rev 26(3):319–336

McMains VC, Myre M, Kreppel L, Kimmel AR (2010) Dictyostelium possesses highly diverged presenilin/gamma-secretase that regulates growth and cell-fate specification and can accurately process human APP: a system for functional studies of the presenilin/gamma-secretase complex. Dis Model Mech 3(9–10):581–594. doi:10.1242/dmm.004457 dmm.004457 [pii]

Meima ME, Weening KE, Schaap P (2007) Vectors for expression of proteins with single or combinatorial fluorescent protein and tandem affinity purification tags in Dictyostelium. Protein Expr Purif 53(2):283–288

Meyer I, Kuhnert O, Graf R (2011) Functional analyses of lissencephaly-related proteins in Dictyostelium. Semin Cell Dev Biol 22(1):89–96. doi:10.1016/j.semcdb.2010.10.007

Mijaljica D, Prescott M, Devenish RJ (2011) Microautophagy in mammalian cells: revisiting a 40-year-old conundrum. Autophagy 7(7):673–682

Morales G, Wiehlmann L, Gudowius P, van Delden C, Tummler B, Martinez JL, Rojo F (2004) Structure of *Pseudomonas aeruginosa* populations analyzed by single nucleotide polymorphism and pulsed-field gel electrophoresis genotyping. J Bacteriol 186(13):4228–4237. doi:10.1128/JB.186.13.4228-4237.2004

Morita T, Yamaguchi H, Amagai A, Maeda Y (2005) Involvement of the TRAP-1 homologue, Dd-TRAP1, in spore differentiation during Dictyostelium development. Exp Cell Res 303(2):425–431

Mostowy S, Sancho-Shimizu V, Hamon MA, Simeone R, Brosch R, Johansen T, Cossart P (2011) p62 and NDP52 proteins target intracytosolic *Shigella* and *Listeria* to different autophagy pathways. J Biol Chem 286(30):26987–26995. doi:10.1074/jbc.M111.223610

Myre MA, Lumsden AL, Thompson MN, Wasco W, Macdonald ME, Gusella JF (2011) Deficiency of huntingtin has pleiotropic effects in the social amoeba *Dictyostelium discoideum*. PLoS Genet 7(4):e1002052. doi:10.1371/journal.pgen.1002052

Nagasaki A, Uyeda TQ (2008) Screening of genes involved in cell migration in Dictyostelium. Exp Cell Res 314(5):1136–1146. doi:10.1016/j.yexcr.2007.12.002

Newell PC, Ellingson JS, Sussman M (1969) Synchrony of enzyme accumulation in a population of differentiating slime mold cells. Biochim Biophys Acta 177:610–614

Nguyen HN, Raisley B, Hadwiger JA (2010) MAP kinases have different functions in Dictyostelium G protein-mediated signaling. Cell Signal 22(5):836–847. doi:10.1016/j.cellsig.2010.01.008 S0898-6568(10)00014-8 [pii]

Otto GP, Wu MY, Kazgan N, Anderson OR, Kessin RH (2003) Macroautophagy is required for multicellular development of the social amoeba *Dictyostelium discoideum*. J Biol Chem 278(20):17636–17645. doi:10.1074/jbc.M212467200

Otto GP, Wu MY, Kazgan N, Anderson OR, Kessin RH (2004) Dictyostelium macroautophagy mutants vary in the severity of their developmental defects. J Biol Chem 279(15): 15621–15629. doi:10.1074/jbc.M311139200

Parent CA (2004) Making all the right moves: chemotaxis in neutrophils and Dictyostelium. Curr Opin Cell Biol 16:4–13

Peffley DM, Sogin ML (1981) A putative tRNA gene cloned from *Dictyostelium discoideum*: its nucleotide sequence and association with repetitive deoxyribonucleic acid. Biochem 20:4015–4021

Peracino B, Balest A, Bozzaro S (2010) Phosphoinositides differentially regulate bacterial uptake and Nramp1-induced resistance to Legionella infection in Dictyostelium. J Cell Sci 123(Pt 23):4039–4051. doi:10.1242/jcs.072124 jcs.072124 [pii]

Peracino B, Buracco S, Bozzaro S (2012) The Nramp (Slc11) proteins regulate development, resistance to pathogenic bacteria and iron homeostasis in *Dictyostelium discoideum*. J Cell Sci 126:301–311. doi:10.1242/jcs.116210

Peracino B, Wagner C, Balest A, Balbo A, Pergolizzi B, Noegel AA, Steinert M, Bozzaro S (2006) Function and mechanism of action of Dictyostelium Nramp1 (Slc11a1) in bacterial infection. Traffic 7(1):22–38

Poole S, Firtel RA, Lamar E, Rowekamp W (1981) Sequence and expression of the discoidin I gene family in *Dictyostelium discoideum*. J Mol Biol 153:273–289

Price CT, Al-Khodor S, Al-Quadan T, Santic M, Habyarimana F, Kalia A, Kwaik YA (2009) Molecular mimicry by an F-box effector of *Legionella pneumophila* hijacks a conserved polyubiquitination machinery within macrophages and protozoa. PLoS Pathog 5(12): e1000704. doi:10.1371/journal.ppat.1000704

Pukatzki S, Kessin RH, Mekalanos JJ (2002) The human pathogen *Pseudomonas aeruginosa* utilizes conserved virulence pathways to infect the social amoeba *Dictyostelium discoideum*. Proc Natl Acad Sci USA 99:3159–3164

Rall TW, Sutherland EW (1958) Formation of a cyclic adenine ribonucleotide by tissue particles. J Biol Chem 232(2):1065–1076

Raper KB (1935) *Dictyostelium discoideum*, a new species of slime mold from decaying forest leaves. J Agr Res 50:135–147

Raper KB (1936) The influence of the bacterial associate and of the medium upon the growth and development of *Dictyostelium discoideum*. Ph.D., Harvard University, Cambridge

Raper KB (1939) Influence of culture conditions upon the growth and development of *Dictyostelium discoideum*. J Agr Res 58:157–198

Raper KB (1940a) The communal nature of the fruiting process in the Acrasieae. Am J Bot 27:436–448

Raper KB (1940b) Pseudoplasmodium formation and organization in *Dictyostelium discoideum*. J Elisha Mitchell Sci Soc 56:241–282

Raper KB, Smith NR (1939) The growth of *Dictyostelium discoideum* on pathogenic bacteria. J Bacteriol 38:431–444

Reggiori F (2006) 1. Membrane origin for autophagy. Curr Top Dev Biol 74:1–30. doi:10.1016/S0070-2153(06)74001-7

Rehberg M, Kleylein-Sohn J, Faix J, Ho TH, Schulz I, Graf R (2005) Dictyostelium LIS1 is a centrosomal protein required for microtubule/cell cortex interactions, nucleus/centrosome linkage, and actin dynamics. Mol Biol Cell 16(6):2759–2771

Romeralo M, Escalante R, Baldauf SL (2011) Evolution and diversity of dictyostelid social Amoebae. Protist 163:327–343. doi:10.1016/j.protis.2011.09.004

Ropolo A, Grasso D, Pardo R, Sacchetti ML, Archange C, Lo Re A, Seux M, Nowak J, Gonzalez CD, Iovanna JL, Vaccaro MI (2007) The pancreatitis-induced vacuole membrane protein 1 triggers autophagy in mammalian cells. J Biol Chem 282(51):37124–37133. doi:10.1074/jbc.M706956200

Roth R, Ashworth J, Sussman M (1968) Periods of genetic transcription required for the synthesis of three enzymes during cellular slime mold development. Proc Natl Acad Sci USA 59:1235–1242

Roussos ET, Condeelis JS, Patsialou A (2011) Chemotaxis in cancer. Nat Rev Cancer 11(8):573–587. doi:10.1038/nrc3078

Santos RX, Correia SC, Carvalho C, Cardoso S, Santos MS, Moreira PI (2011) Mitophagy in neurodegeneration: an opportunity for therapy? Curr Drug Targ 12(6):790–799

Sanz A, Pamplona R, Barja G (2006) Is the mitochondrial free radical theory of aging intact? Antioxid Redox Signal 8(3–4):582–599. doi:10.1089/ars.2006.8.582

Satrustegui J, Pardo B, Del Arco A (2007) Mitochondrial transporters as novel targets for intracellular calcium signaling. Physiol Rev 87(1):29–67. doi:10.1152/physrev.00005.2006

Schmauch C, Claussner S, Zoltzer H, Maniak M (2009) Targeting the actin-binding protein VASP to late endosomes induces the formation of giant actin aggregates. Eur J Cell Biol 88(7):385–396. doi:10.1016/j.ejcb.2009.02.185

Shaulsky G, Escalante R, Loomis WF (1996) Developmental signal transduction pathways uncovered by genetic suppressors. Proc Natl Acad Sci USA 93(26):15260–15265

Soares JC, Dippold CS, Mallinger AG (1997) Platelet membrane phosphatidylinositol-4,5-bisphosphate alterations in bipolar disorder—evidence from a single case study. Psychiatry Res 69(2–3):197–202

Soares JC, Mallinger AG, Dippold CS, Forster Wells K, Frank E, Kupfer DJ (2000) Effects of lithium on platelet membrane phosphoinositides in bipolar disorder patients: a pilot study. Psychopharmacology (Berl) 149(1):12–16

Soler-Lopez M, Petosa C, Fukuzawa M, Ravelli R, Williams JG, Muller CW (2004) Structure of an activated Dictyostelium STAT in its DNA-unbound form. Mol Cell 13:791–804

Sonneborn DR, White GJ, Sussman M (1963) A mutation affecting both rate and pattern of morphogenesis in *Dictyostelium discoideum*. Dev Biol 7:79–93

Sperandio D, Decoin V, Latour X, Mijouin L, Hillion M, Feuilloley MG, Orange N, Merieau A (2012) Virulence of the *Pseudomonas fluorescens* clinical strain MFN1032 towards *Dictyostelium discoideum* and macrophages in relation with type III secretion system. BMC Microbiol 12(1):223. doi:10.1186/1471-2180-12-223

Steinert M (2011) Pathogen–host interactions in Dictyostelium, Legionella, Mycobacterium and other pathogens. Semin Cell Dev Biol 22(1):70–76. doi:10.1016/j.semcdb.2010.11.003

Sucgang R, Kuo A, Tian X, Salerno W, Parikh A, Feasley CL, Dalin E, Tu H, Huang E, Barry K, Lindquist E, Shapiro H, Bruce D, Schmutz J, Salamov A, Fey P, Gaudet P, Anjard C, Babu MM, Basu S, Bushmanova Y, van der Wel H, Katoh-Kurasawa M, Dinh C, Coutinho PM, Saito T, Elias M, Schaap P, Kay RR, Henrissat B, Eichinger L, Rivero F, Putnam NH, West CM, Loomis WF, Chisholm RL, Shaulsky G, Strassmann JE, Queller DC, Kuspa A, Grigoriev IV (2011) Comparative genomics of the social amoebae *Dictyostelium discoideum* and *Dictyostelium purpureum*. Genome Biol 12(2):R20. doi:10.1186/gb-2011-12-2-r20

Suen DF, Norris KL, Youle RJ (2008) Mitochondrial dynamics and apoptosis. Genes Dev 22(12):1577–1590. doi:10.1101/gad.1658508

Sussman M (1954) Synergistic and antagonistic interactions between morphogenetically deficient variants of the slime mould *Dictyostelium discoideum*. J Gen Microbiol 10:110–120

Sussman M (1961) Cultivation and serial transfer of the slime mold *Dictyostelium discoideum* in liquid nutrient medium. J Gen Microbiol 25:375–378

Sussman M (1965) Temporal, spatial, and quantitative control of enzyme activity during slime mold cytodifferentiation. Brookhaven Symp Biol 18:66–76

Sussman R, Rayner EP (1971) Physical characterization of deoxyribonucleic acids in *Dictyostelium discoideum*. Arch Biochem Biophys 144:127–137

Sussman R, Sussman M (1967) Cultivation of *Dictyostelium discoideum* in axenic culture. Biochem Biophys Res Commun 29:53–55

Sussman RR, Sussman M (1953) Cellular differentiation in Dictyosteliaceae: heritable modifications of the developmental pattern. Ann N Y Acad Sci 56:949–960

Swaney KF, Huang CH, Devreotes PN (2010) Eukaryotic chemotaxis: a network of signaling pathways controls motility, directional sensing, and polarity. Annu Rev Biophys 39:265–289. doi:10.1146/annurev.biophys.093008.131228

Torija P, Robles A, Escalante R (2006a) Optimization of a large-scale gene disruption protocol in Dictyostelium and analysis of conserved genes of unknown function. BMC Microbiol 6:75

Torija P, Vicente JJ, Rodrigues TB, Robles A, Cerdan S, Sastre L, Calvo RM, Escalante R (2006b) Functional genomics in Dictyostelium: MidA, a new conserved protein, is required for mitochondrial function and development. J Cell Sci 119(Pt 6):1154–1164

Trainor PA (2005) Specification of neural crest cell formation and migration in mouse embryos. Semin Cell Dev Biol 16(6):683–693. doi:10.1016/j.semcdb.2005.06.007

Tung SM, Unal C, Ley A, Pena C, Tunggal B, Noegel AA, Krut O, Steinert M, Eichinger L (2010) Loss of Dictyostelium ATG9 results in a pleiotropic phenotype affecting growth, development, phagocytosis and clearance and replication of *Legionella pneumophila*. Cell Microbiol 12:765–780. doi:10.1111/j.1462-5822.2010.01432.x

Ura S, Pollitt AY, Veltman DM, Morrice NA, Machesky LM, Insall RH (2012) Pseudopod growth and evolution during cell movement is controlled through SCAR/WAVE dephosphorylation. Curr Biol 22(7):553–561. doi:10.1016/j.cub.2012.02.020

Van Delden C, Iglewski BH (1998) Cell-to-cell signaling and *Pseudomonas aeruginosa* infections. Emerg Infect Dis 4(4):551–560

Veltman DM, Akar G, Bosgraaf L, Van Haastert PJ (2009a) A new set of small, extrachromosomal expression vectors for *Dictyostelium discoideum*. Plasmid 61(2):110–118. doi:10.1016/j.plasmid.2008.11.003

Veltman DM, Keizer-Gunnink I, Haastert PJ (2009b) An extrachromosomal, inducible expression system for *Dictyostelium discoideum*. Plasmid 61(2):119–125. doi:10.1016/j.plasmid.2008.11.002

Veltman DM, King JS, Machesky LM, Insall RH (2012) SCAR knockouts in Dictyostelium: WASP assumes SCAR's position and upstream regulators in pseudopods. J Cell Biol 198(4):501–508. doi:10.1083/jcb.201205058

Vingtdeux V, Davies P, Dickson DW, Marambaud P (2011) AMPK is abnormally activated in tangle- and pre-tangle-bearing neurons in Alzheimer's disease and other tauopathies. Acta Neuropathol 121(3):337–349. doi:10.1007/s00401-010-0759-x

Vuillemin P (1903) Une Acrasiee bacteriophage. CR Acad Sc Paris 137:387–389

Walz A, Peveri P, Aschauer H, Baggiolini M (1987) Purification and amino acid sequencing of NAF, a novel neutrophil-activating factor produced by monocytes. Biochem Biophys Res Commun 149(2):755–761

Wang Y, Chen CL, Iijima M (2011a) Signaling mechanisms for chemotaxis. Dev Growth Differ 53(4):495–502. doi:10.1111/j.1440-169X.2011.01265.x

Wang Y, Levy DE (2006) *C. elegans* STAT: evolution of a regulatory switch. Faseb J 20(10):1641–1652

Wang Y, Steimle PA, Ren Y, Ross CA, Robinson DN, Egelhoff TT, Sesaki H, Iijima M (2011b) Dictyostelium huntingtin controls chemotaxis and cytokinesis through the regulation of myosin II phosphorylation. Mol Biol Cell 22(13):2270–2281. doi:10.1091/mbc.E10-11-0926

Wessels D, Srikantha T, Yi S, Kuhl S, Aravind L, Soll DR (2006) The Shwachman-Bodian-Diamond syndrome gene encodes an RNA-binding protein that localizes to the pseudopod of Dictyostelium amoebae during chemotaxis. J Cell Sci 119(Pt 2):370–379

Wiegand S, Kruse J, Gronemann S, Hammann C (2011) Efficient generation of gene knockout plasmids for *Dictyostelium discoideum* using one-step cloning. Genomics 97(5):321–325. doi:10.1016/j.ygeno.2011.02.001

Williams JG (2003) The STAT proteins of Dictyostelium. In: Sehgal PB, Levy DE, Hirano T (eds) Signal transducers and activators of transcription (STATs) Activation and biology. Kluwer Academic Publishers, Boston, pp 105–121

Williams RSB, Cheng LL, Mudge AW, Harwood AJ (2002) A common mechanism of action for three mood-stabilizing drugs. Nature 417:292–295

Williams RSB, Eames M, Ryves WJ, Viggars J, Harwood AJ (1999) Loss of a prolyl oligopeptidase confers resistance to lithium by elevation of inositol (1,4,5) trisphosphate. EMBO J 18:2734–2745

Winslow AR, Rubinsztein DC (2011) The Parkinson disease protein alpha-synuclein inhibits autophagy. Autophagy 7(4):429–431

Witke W, Nellen W, Noegel A (1987) Homologous recombination in the Dictyostelium alpha-actinin gene leads to an altered mRNA and lack of the protein. EMBO J 6:4143–4148

Wong CC, Traynor D, Basse N, Kay RR, Warren AJ (2011) Defective ribosome assembly in Shwachman-Diamond syndrome. Blood 118(16):4305–4312. doi:10.1182/blood-2011-06-353938

Xie M, Morales CR, Lavandero S, Hill JA (2011) Tuning flux: autophagy as a target of heart disease therapy. Curr Opin Cardiol 26(3):216–222. doi:10.1097/HCO.0b013e328345980a

Xilouri M, Stefanis L (2011) Autophagic pathways in Parkinson disease and related disorders. Expert Rev Mol Med 13:e8. doi:10.1017/S1462399411001803

Xu X, Muller-Taubenberger A, Adley KE, Pawolleck N, Lee VW, Wiedemann C, Sihra TS, Maniak M, Jin T, Williams RS (2007) Attenuation of phospholipid signaling provides a novel mechanism for the action of valproic acid. Eukaryot Cell 6(6):899–906

Yang Z, Klionsky DJ (2010) Mammalian autophagy: core molecular machinery and signaling regulation. Curr Opin Cell Biol 22(2):124–131. doi:10.1016/j.ceb.2009.11.014 S0955-0674(09)00228-2 [pii]

Yang ZJ, Chee CE, Huang S, Sinicrope F (2011) Autophagy modulation for cancer therapy. Cancer Biol Ther 11(2):169–176. doi:10.4161/cbt.11.2.14663

Yoshimura T, Matsushima K, Tanaka S, Robinson EA, Appella E, Oppenheim JJ, Leonard EJ (1987) Purification of a human monocyte-derived neutrophil chemotactic factor that has peptide sequence similarity to other host defense cytokines. Proc Natl Acad Sci USA 84(24):9233–9237

Zheng Q, Su H, Ranek MJ, Wang X (2011) Autophagy and p62 in cardiac proteinopathy. Circ Res 109(3):296–308. doi:10.1161/CIRCRESAHA.111.244707

Autophagy
Publication details, including instructions for authors and subscription information:
http://www.tandfonline.com/loi/kaup20

TipC and the chorea-acanthocytosis protein VPS13A regulate autophagy in Dictyostelium and human HeLa cells

Sandra Muñoz-Braceras[a], Rosa Calvo[a] & Ricardo Escalante[a]
[a] Instituto de Investigaciones Biomedicas Alberto Sols; Consejo Superior de Investigaciones Científicas and Universidad Autónoma de Madrid; Madrid, Spain
Accepted author version posted online: 21 May 2015.

To cite this article: Sandra Muñoz-Braceras, Rosa Calvo & Ricardo Escalante (2015) TipC and the chorea-acanthocytosis protein VPS13A regulate autophagy in Dictyostelium and human HeLa cells, Autophagy, 11:6, 918-927, DOI: 10.1080/15548627.2015.1034413

To link to this article: http://dx.doi.org/10.1080/15548627.2015.1034413

Autophagy 11:6, 918–927; June 2015; © 2015 Taylor & Francis Group, LLC

TipC and the chorea-acanthocytosis protein VPS13A regulate autophagy in *Dictyostelium* and human HeLa cells

Sandra Muñoz-Braceras, Rosa Calvo, and Ricardo Escalante*

Instituto de Investigaciones Biomedicas Alberto Sols; Consejo Superior de Investigaciones Científicas and Universidad Autónoma de Madrid; Madrid, Spain

Keywords: autophagy, chorea-acanthocytosis, chorein, *Dictyostelium*, HeLa cells, TipC, VPS13, VPS13A

Abbreviations: *ATG*, autophagy related; AX4, axenic strain 4; DUF, domain of unknown function; GFP, green fluorescent protein; LC3, microtubule-associated protein 1 light chain 3; PtdIns3K, phosphatidylinositol 3-kinase; PtdIns3P, phosphatidylinositol 3-phosphate; VPS13, vacuolar protein sorting 13 homolog (*S. cerevisiae*); WIPI, WD repeat domain, phosphoinoside interacting

Deficient autophagy causes a distinct phenotype in *Dictyostelium discoideum*, characterized by the formation of multitips at the mound stage. This led us to analyze autophagy in a number of multitipped mutants described previously (*tipA*$^-$, *tipB*$^-$, *tipC*$^-$, and *tipD*$^-$). We found a clear autophagic dysfunction in *tipC*$^-$ and *tipD*$^-$ while the others showed no defects. *tipD* codes for a homolog of Atg16, which confirms the role of this protein in *Dictyostelium* autophagy and validates our approach. The *tipC*-encoded protein is highly similar to human VPS13A (also known as chorein), whose mutations cause the chorea-acanthocytosis syndrome. No member of the VPS13 protein family has been previously related to autophagy despite the presence of a region of similarity to Atg2 at the C terminus. This region also contains the conserved domain of unknown function DUF1162. Of interest, the expression of the TipC C-terminal coding sequence containing these 2 motifs largely complemented the mutant phenotype. *Dictyostelium* cells lacking TipC displayed a reduced number of autophagosomes visualized with the markers GFP-Atg18 and GFP-Atg8 and an impaired autophagic degradation as determined by a proteolytic cleavage assay. Downregulation of human *VPS13A* in HeLa cells by RNA interference confirmed the participation of the human protein in autophagy. VPS13A-depleted cells showed accumulation of autophagic markers and impaired autophagic flux.

Introduction

Dictyostelium discoideum is a social amoeba whose developmental process depends on macroautophagy (referred to as 'autophagy' hereafter for simplicity). This process is a highly conserved lysosomal degradation pathway and it is the main cellular mechanism for protein and organelle degradation in eukaryotes.[1,2] It is characterized by the formation of double-membrane vesicles, the autophagosomes, which engulf a variety of cargos including portions of the cytoplasm, protein aggregates or damaged organelles. The autophagosomes eventually fuse with lysosomes, where the cargo is degraded and simple biochemical compounds are released for recycling or energy production. At the molecular level, autophagy is controlled by different functional complexes, which are required for the origin, elongation, and maturation of the autophagosomes.[3] The hierarchical relationship among autophagic proteins allows a tight regulation of the process. At the initial step, the inductive complexes containing the serine/threonine kinase ULK1/Atg1 (unc-51 like autophagy activating kinase 1) and the class III phosphatidylinositol 3-kinase (PtdIns3K) PIK3C3/Vps34 (phosphatidylinositol 3-kinase, catalytic subunit type 3/vacuolar protein sorting 34) are recruited to specific sites of the endoplasmic reticulum and provide a platform for autophagosome biogenesis, the so-called omegasome.[4] The activity of PtdIns3K generates a PtdIns3P-enriched region to which the complex formed by Atg2 and WIPI/Atg18 (WD repeat domain, phosphoinoside interacting) is recruited. Later, the ATG12–ATG5-ATG16L1 complex and the lipidation of LC3/Atg8 (microtubule-associated protein 1 light chain 3) to the emerging membrane allow the elongation of the phagophore.[5]

A number of studies in *Dictyostelium* have revealed the similarities, both morphological and molecular, of its autophagic process with that of animal cells.[6] In addition, this organism possesses several autophagic proteins that are conserved in mammals but absent in *S. cerevisiae* such as ATG101 and VMP1.[2,6,7] *Dictyostelium* mutant strains lacking Atg proteins display deficient autophagy and developmental abnormalities.[8-11] The most common phenotype is the block of development at the mound stage and the formation of multiple tips instead of normal fruiting bodies. This feature can be used as a screening parameter that might help to identify new genes involved in autophagy. Four

*Correspondence to: Ricardo Escalante; Email: rescalante@iib.uam.es
Submitted: 07/28/2014; Revised: 02/20/2015; Accepted: 02/25/2015
http://dx.doi.org/10.1080/15548627.2015.1034413

multitipped mutants were described in the laboratory of William F. Loomis in 1999 and the proteins affected are named TipA, TipB, TipC, and TipD (DictyBase Gene IDs: DDB_G0281561, DDB_G0276333, DDB_G0267422, DDB_G0275323).[12,13] The 4 *tip* genes are expressed during vegetative growth and throughout development and have parallel but yet unknown functions during *Dictyostelium* development.[13] Sequence analysis reveals that *tipC* codes for a protein highly similar to the conserved VPS13 family. In humans, a member of this family, VPS13A, is the protein mutated in chorea-acanthocytosis.

Chorea-acanthocytosis (ChAc) (OMIM ID: 200150) is a rare autosomal recessive neurodegenerative disease. The most relevant symptoms are involuntary tensing of muscles (especially those in the face, mouth, and limbs), neurodegeneration, and erythrocyte acanthocytosis.[14-16] This disorder is caused by the loss of function of the 360-kDa protein VPS13A (also known as chorein), which is nearly absent in patients.[17-21] A mouse model of the disease has been reported.[22] It shows similarities to the human syndrome, such as brain pathology and red blood acanthocytosis, but displays a mild phenotype with late old-age onset.[22] In humans, VPS13A is expressed in a wide variety of tissues.[23] Defects in actin cytoskeleton regulation have been described in erythrocytes, platelets, and vascular endothelial cells in the absence of VPS13A.[24,25] In simpler organisms, null mutants in *Saccharomyces cerevisiae* and *Tetrahymena thermophila* suggest a role of Vps13 and VPS13A in membrane traffic and phagocytosis respectively but the precise VPS13 function is largely unknown.[26-28]

Here we describe how the VPS13-related protein TipC is required for efficient autophagy in *D. discoideum*. We extended our observations to human VPS13A by analyzing autophagy in RNA-interfered HeLa cells. Our results confirmed the role of VPS13A in autophagy and suggest the possibility that autophagy is involved in the etiology of chorea-acanthocytosis as described previously for other neurodegenerative diseases such as Parkinson, Alzheimer, and Huntington diseases.[29] This is relevant because, at present, no effective therapy for chorea-acanthocytosis is available and there is a growing interest of medical research in modulating autophagy as a therapeutic treatment.[29-31]

Results

Screening for autophagy defects in *Dictyostelium* multitipped mutants

Dictyostelium strains carrying gene disruptions in *tipA, tipB, tipC*, or *tipD* showed a similar phenotype in which large mounds split up to form multiple tips.[13] The similarity of this phenotype to the one observed in autophagy-deficient strains[2] led us to analyze autophagy in these mutants. To this end, autophagic flux was measured by a proteolytic cleavage assay described previously.[32] A large decrease in autophagic flux was detected in $tipC^-$ and $tipD^-$ strains (**Fig. 1A**) while $tipA^-$ and $tipB^-$ mutants showed similar levels than those of the wild type (**Fig. 1B**).

Analysis of the predicted protein sequences indicates that *tipD* (accession number EAL69727.1) codes for a protein similar to the yeast Atg16 and human ATG16L1. Of interest, the similarity of TipD to the homologous human protein is much higher (E-value: 2.2e-59) than it is to the yeast protein (E-value: 3.8e-4; E-values calculated with the LALIGN program from Biology WorkBench, http://workbench.sdsc.edu/) and the sequence also contains a large conserved WD-repeat region at the C terminus that is present in the human protein but absent in the yeast ortholog (**Fig. S1**). This domain might be involved in protein-protein interactions that have been conserved during evolution between *Dictyostelium* and mammalian cells. The identification of the *Dictyostelium* Atg16 ortholog and the confirmation of its role in autophagy validate our approach for the screening of new autophagic proteins using the mutitipped phenotypic feature.

tipC (EAL73163.1) encodes a large protein of 3848 amino acids highly similar to the VPS13 family of proteins (**Fig. S2**). The human VPS13 family has 4 members (VPS13A/B/C/D) and TipC shows the highest homology with VPS13A and VPS13C (**Fig. S3**). No previous connection with autophagy has been reported for any of these proteins. Since mutations in human VPS13A leads to chorea-acanthocytosis, a rare disease that causes neurodegeneration, we focused on the study of *Dictyostelium* TipC and human VPS13A.

The conserved C terminus of TipC is able to function independently to largely complement the mutant phenotype

TipC and VPS13A show 3 conserved regions at the N terminus and C terminus (**Fig. 2A–C**). Interestingly, the C terminus contains a small sequence similar to the C-terminal region of Atg2, as detected by the NCBI Conserved Domain Search using the Pfam database v27.0 (**Fig 2A and C**). This motif is depicted as ATG_C-terminal domain and it is detected in both *Dictyostelium* TipC and human VPS13A with a significant E-value (2.42e-6 and 2.59e-6 respectively). The same region is detected in the yeast protein, but with a much less significant score (E-value: 0.29). The C-terminal region also contains a conserved domain of unknown function DUF1162. In order to assess the functionality of the Tip C-terminal region, we cloned and expressed the coding sequence fused to GFP in the $tipC^-$ mutant strain. The expression of the C-terminal polypeptide was confirmed by western blot using an anti-GFP antibody (**Fig. 2D**) and by confocal analysis of GFP fluorescence, which showed a cytoplasmic localization (**Fig. 2E**). Remarkably, the expression of the fragment largely complemented the mutant developmental phenotype (**Fig. 2F**). The complemented strain no longer displayed the characteristic multitipped phenotype. It succeeded to pass the mound stage and form normal-looking fruiting bodies. Calcofluor staining, which labels the cellulose walls of stalk and spore cells, showed that the few stalks present in the original mutant were abnormal. The complemented strain, however, showed fairly differentiated stalks (**Fig. 2G**). Nevertheless, the recovery was not complete because some of the structures were smaller and had thick stalks. Spore differentiation was also complemented according to the ellipsoid morphology of spores that were stained with calcofluor (**Fig. 2G**) and the number and viability of the formed spores. Spore efficiency was quantified in comparison with the wild-type AX4 strain and it recovered from

1.70 ± 0.03% in the original mutant to 56.94 ± 0.20% in the complemented strain. All together, the full-length protein must be required for a total recovery, but the C-terminal region can function independently to some extent during development progression and stalk differentiation. Autophagy is required for these processes, and thus, the conserved C terminus of TipC probably has a critical function in autophagy.

Since autophagy and phagocytosis have been described as connected [33,34] and *Tetrahymena thermophila* VPS13A is required for efficient phagocytosis,[27] we have also analyzed this process in the AX4, *tipC*$^{-}$ and the complemented strains. The results indicated a modest defect in phagocytosis in the mutant that was clearly recovered in the complemented strain (**Fig. 2H**).

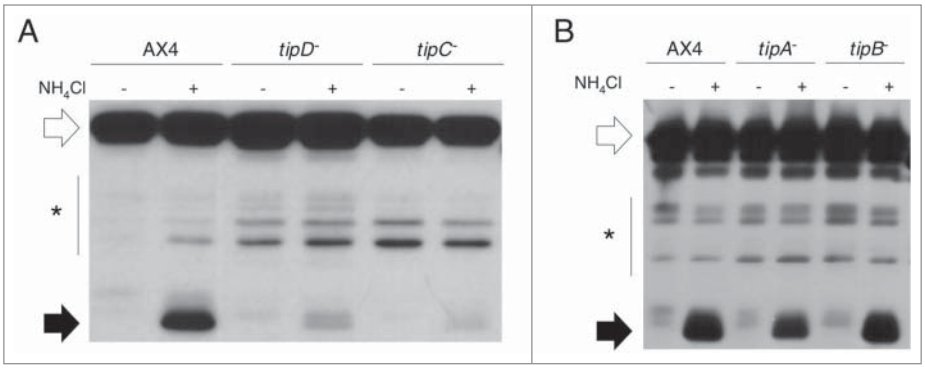

Figure 1. Autophagic flux is decreased in *tipC*$^{-}$ and *tipD*$^{-}$ cells. Proteolytic cleavage assay was performed in strains transfected with the marker GFP-Tkt-1. Protein extracts were analyzed by western blot using anti-GFP antibody. (**A**) The accumulation of cleaved GFP fragment (black arrows) in the presence of 100 mM NH_4Cl is reduced in *tipC*$^{-}$ and *tipD*$^{-}$ mutants compared to the wild-type AX4 strain. (**B**) *tipA*$^{-}$ and *tipB*$^{-}$ levels of cleaved GFP are similar to those of AX4. The complete GFP-Tkt-1fusion protein is marked by white arrows and the stars indicate nonspecific immunoreactive bands.

TipC and TipD regulate autophagy at different stages of autophagosome formation

To further characterize the role of TipC and TipD in autophagy and to determine which stage of autophagosome formation is affected, we expressed the autophagic markers GFP-Atg8 and GFP-Atg18 in *tipC*$^{-}$ and *tipD*$^{-}$ strains and visualized them by confocal microscopy. The number and the pattern of GFP-Atg8 puncta were altered in both strains. *tipC*$^{-}$ cells showed a reduced number of puncta and also some abnormally large structures absent in the wild-type strain. In the case of *tipD*$^{-}$ cells, they showed a much higher number of large structures, which appeared to be protein aggregates (**Fig. 3A**). GFP-Atg8 is an aggregate-prone marker and previous studies in *Dictyostelium* have shown a similar pattern in mutants of the autophagic proteins Atg1, Atg7, and Vmp1,[7,10] with the presence of large ubiquitinated protein aggregates containing GFP-Atg8. Therefore, we analyzed the presence of ubiquitin-positive aggregates by immunofluorescence. Both mutant strains contained ubiquitinated aggregates although they were larger in *tipD*$^{-}$ cells, where the colocalization with GFP-Atg8 was also more evident and demonstrates that these large structures are not real autophagosomes (**Fig. 3B**). These abnormal patterns and the presence of ubiquitinated aggregates are consistent with the observed block in autophagy flux.

Due to the GFP-Atg8 tendency to aggregate, we used another marker, GFP-Atg18, for quantitative analysis of puncta (**Fig. 4A and B**). GFP-Atg18 labels the initial stages of autophagosome formation and the puncta pattern is thinner than that of the GFP-Atg8. *tipC*$^{-}$, and *tipD*$^{-}$ cells showed a distinct GFP-Atg18 pattern. Puncta were accumulated in *tipD*$^{-}$ cells under growth and starvation conditions compared with the wild type. Since GFP-Atg18 is recruited to PtdIns3P-enriched endoplasmic reticulum-derived omegasomes,[35] this accumulation suggests that autophagosome formation is impaired at a stage posterior to the PtdIns3P signaling. This is consistent with the described role of Atg16 in the stage of autophagosome membrane elongation, downstream of Atg1 and PtdIns3K in the functional hierarchy.[5] Conversely, *tipC*$^{-}$ cells showed a significantly reduced number of GFP-Atg18 puncta. This is in agreement with an early blockade in autophagy, as observed in other *Dictyostelium* mutants lacking components that participate at the initial inductive signaling, such as the null mutant in Atg1.[7]

VPS13A depletion in human HeLa cells alters the pattern of autophagosome markers

We next studied the consequences of VPS13A depletion in human HeLa cells in order to determine if the role in autophagy is conserved. Cells were transfected with control or *VPS13A* siRNAs and the GFP-LC3 and GFP-WIPI1 pattern were observed in growth and starvation. Inhibition of *VPS13A* expression was determined by qRT-PCR. The *VPS13A* mRNA levels were reduced by 89.5 ± 2.9% compared to the levels in control-transfected cells. Depletion of VPS13A protein was also determined by western blot (**Fig. 5A**). In HeLa cells stably expressing GFP-LC3, a high proportion of VPS13A-depleted cells showed an accumulation of puncta at the perinuclear region regardless of the nutritional conditions. In starvation, besides the perinuclear accumulation, the *VPS13A* siRNA-treated cells showed less translocation of the marker from the nucleus to the cytoplasm as compared with the control-transfected cells (**Fig. 5B**). Puncta quantification shows that *VPS13A*-silenced cells had an increase of puncta in growth and this number did not increase during starvation as did occur in the control cells (**Fig. 5C**). In HeLa *VPS13A*-depleted cells transiently transfected with the GFP-WIPI1 marker, there were more GFP-WIPI1 puncta than in control cells in both conditions, and there was not a significant increase following starvation (**Fig. 5D and E**). These results suggest that the accumulation of puncta might be the result of a deficiency in autophagic flux.

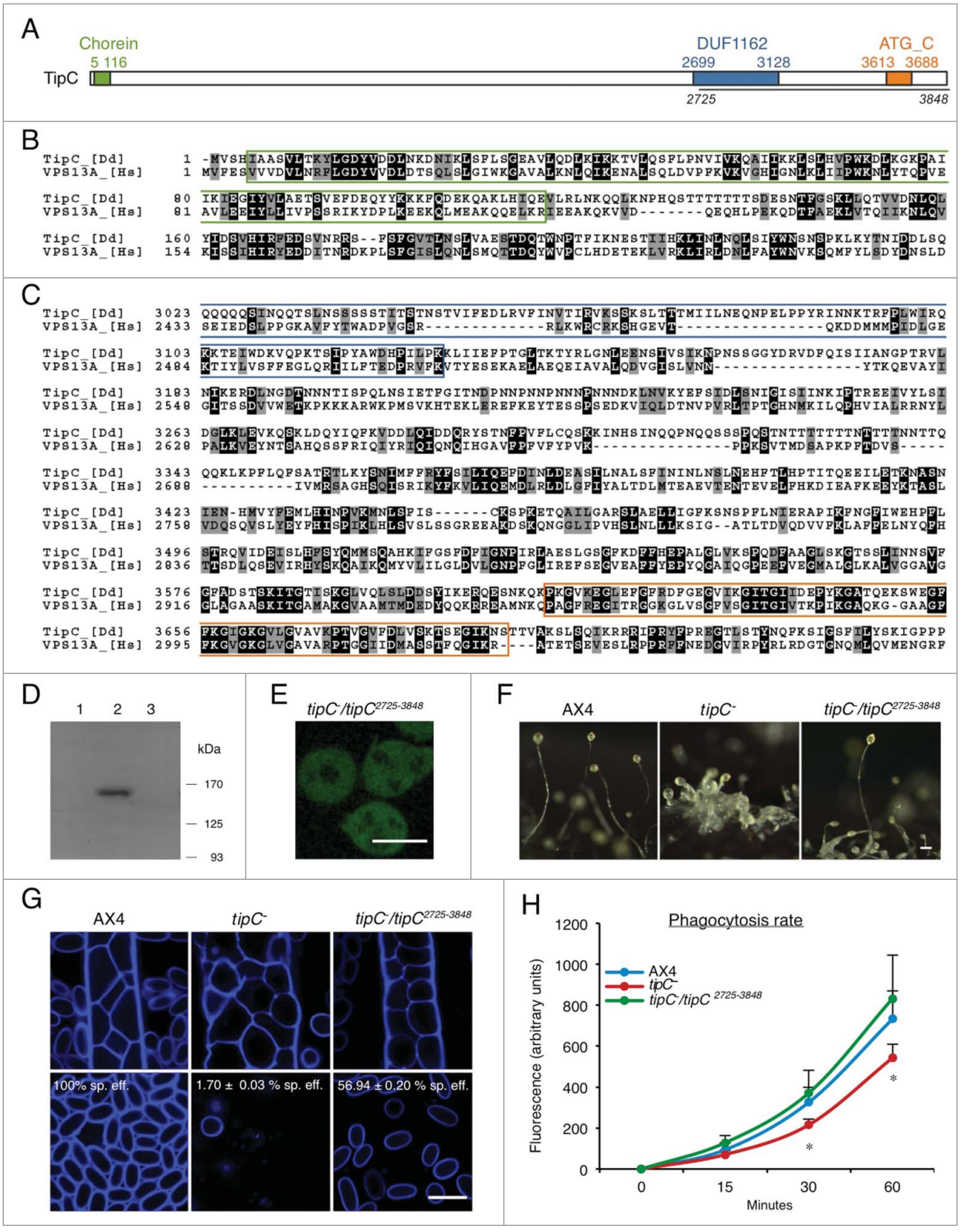

Figure 2. For figure legend, see page 922.

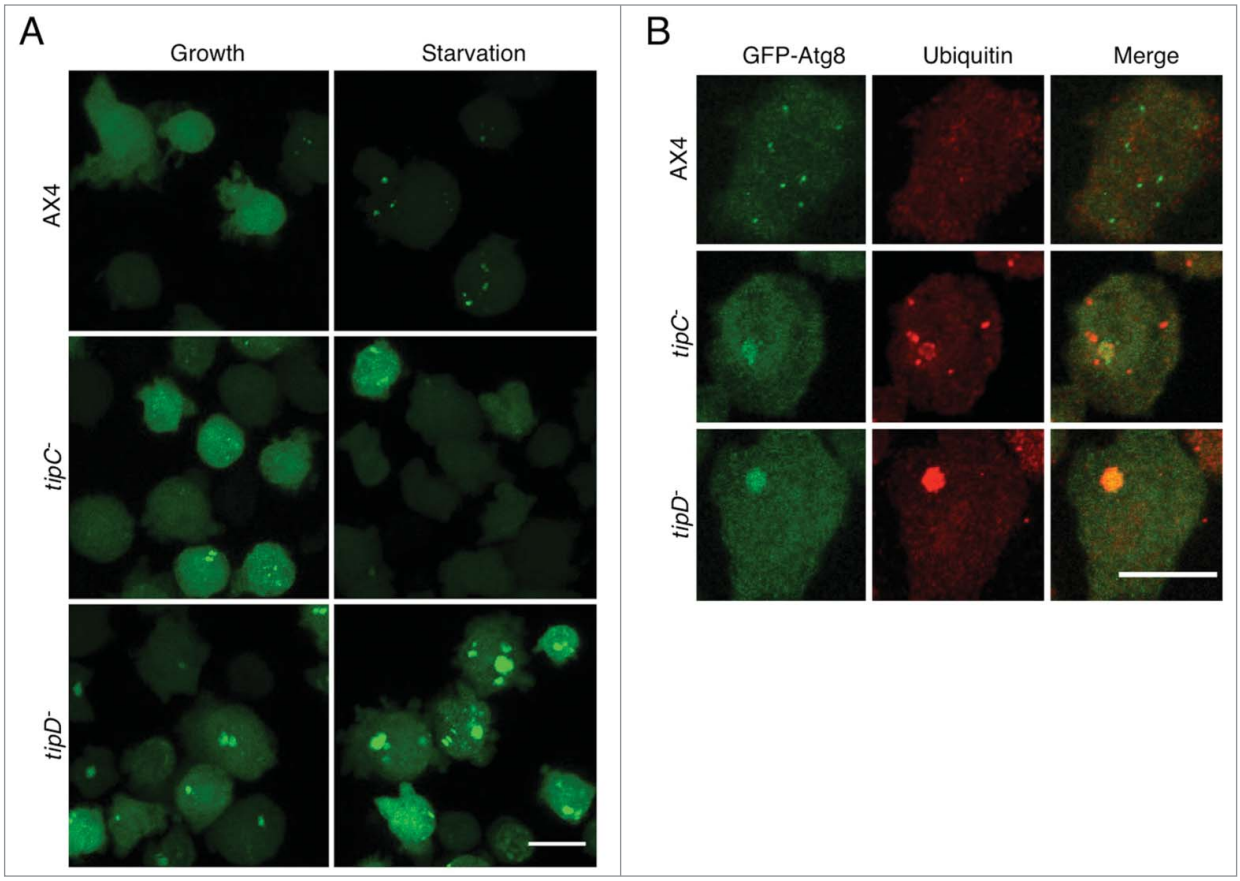

Figure 3. The pattern of GFP-Atg8 is altered in *tipC*$^{-}$ and *tipD*$^{-}$ cells. (**A**) In vivo confocal analysis of cells expressing GFP-Atg8 in growing and starvation conditions. Puncta formation is inhibited in starved *tipC*$^{-}$ cells compared with AX4. In contrast, large aggregates of the autophagosome marker are evident in *tipD*$^{-}$ cells in both growing conditions. (**B**) Immunofluorescence of ubiquitin in the cells expressing GFP-Atg8 demonstrates the presence of ubiquitin-positive protein aggregates in both mutants. The ubiquitin structures are smaller in *tipC*$^{-}$ cells and do not always colocalize with GFP-Atg8, while the autophagosome marker is clearly contained in the large *tipD*$^{-}$ ubiquitinated aggregates. Scale bar: 10 μm.

VPS13A is required for autophagic flux

In order to analyze autophagic flux, siRNA-treated HeLa cells stably expressing GFP-LC3 were incubated in complete or starvation medium in the presence or absence of the lysosome inhibitor chloroquine. Protein extracts of at least 3 independent experiments were analyzed by western blot to detect GFP-LC3, cleaved GFP, and endogenous LC3-I/-II levels (**Fig. 6**). Since GFP-LC3 is degraded by autophagy, the level of GFP-LC3 has been previously shown to decrease during starvation.[36-38] As expected, this was the case for the control cells; however, high levels of the marker were present in the *VPS13A* siRNA-treated cells irrespective of the nutritional conditions (**Fig. 6A, B**). Another marker of autophagic flux is the cleaved GFP band, which is generated in part by autophagic degradation, as demonstrated by the GFP accumulation in chloroquine-treated cells. Once more, cleaved GFP accumulation was evident, together with a smaller increase

Figure 2 (See previous page). The conserved C terminus of TipC largely complements the *tipC*$^{-}$ phenotype. (**A**) Scheme of the 3848-amino acid TipC protein and the conserved domains (colored boxes). The line under the scheme depicts the fragment expressed in the complementation experiments. Alignment of the N-terminal (**B**) and C-terminal (**C**) regions of *D. discoideum* TipC (EAL73163.1) and the human VPS13A (NP_150648.2) proteins using the ClustalW algorithm and shaded using the Boxshade tool at the SDSC Biology WorkBench server (http://workbench.sdsc.edu/). Identical residues are *shaded black*, and similar residues are *shaded gray*. Colored boxes frame the conserved domains. (**D**) Western blot using anti-GFP antibody confirmed the presence of a unique band of 150 kDa in the transformed strain with the C-terminal region of TipC (amino acids 2725 to 3848) fused to GFP. Lanes 1 and 3 correspond to protein extracts of AX4 and *tipC*$^{-}$ that do not express the fused proteins and were used as controls of antibody specificity. (**E**) The C-terminal TipC polypeptide fused to GFP is localized in the cytoplasm according to in vivo confocal microscopy visualization of transformed cells. (**F**) The complemented strain rescues fruiting body development. Scale bar: 10 μm. (**G**) Calcofluor staining shows details of stalk differentiation and spore shape of the different strains. For *tipC*$^{-}$ mainly cell debris could be visualized. Scale bar: 10 μm. Spore efficiency of each strain (sp. eff.) is indicated. (**H**) Phagocytosis rate of the wild-type, the mutant, and the complemented strain was measured through the internalized fluorescent signal of cells that were previously incubated with fluorescent beads during the indicated times.

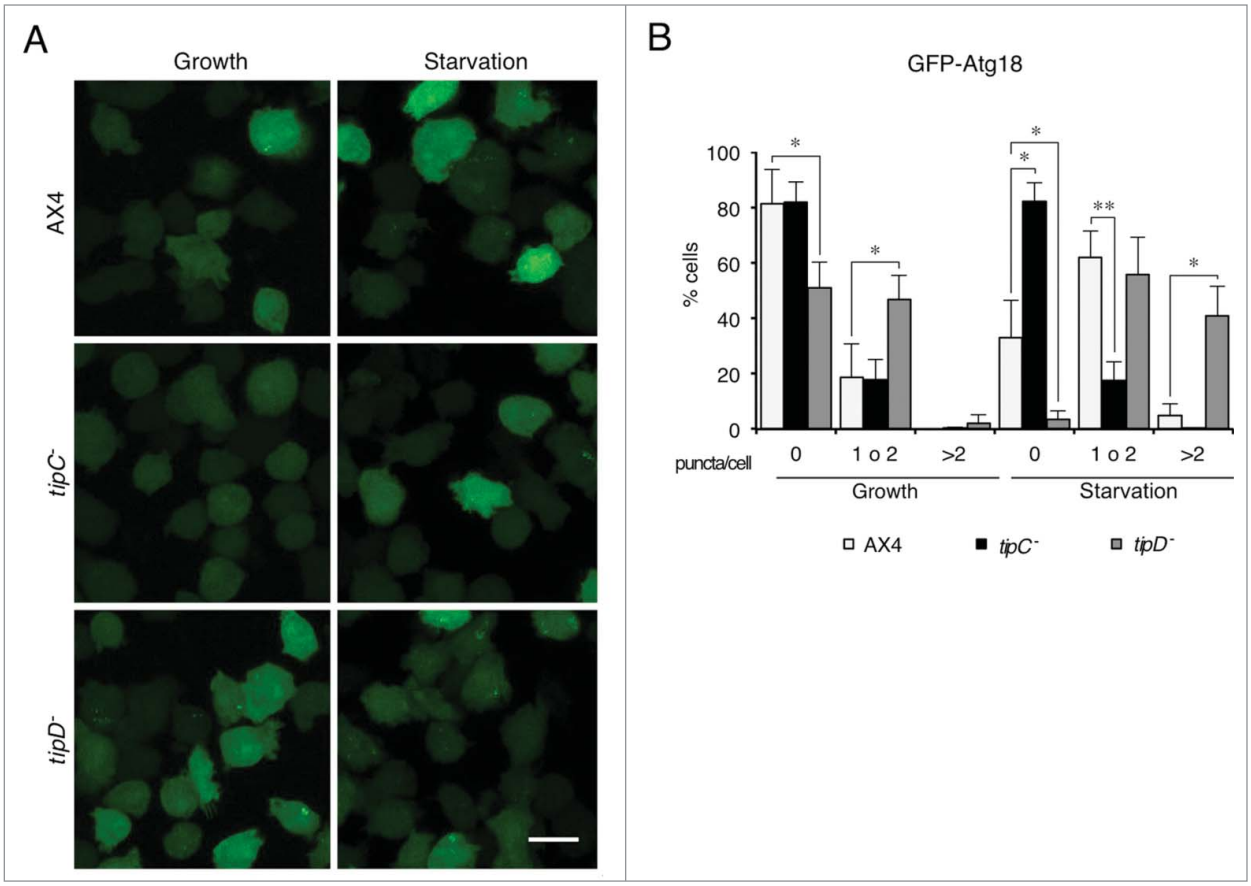

Figure 4. GFP-Atg18 puncta signaling is decreased in *tipC*$^{-}$ cells and accumulates in *tipD*$^{-}$ cells. (**A**) Cells expressing GFP-Atg18 were analyzed in vivo by confocal microscopy. Puncta formation is induced under starvation conditions in AX4 cells. However, most of *tipC*$^{-}$ cells do not display any puncta. Conversely, many puncta are observed *tipD*$^{-}$ cells regardless of the nutritional conditions. Scale bar: 10 μm. (**B**) Quantification of GFP-Atg18 puncta of at least 100 cells in blinded images from 3 independent experiments. Results are shown as mean values with standard deviations of the percentage of cells showing the indicated number of puncta. Asterisks indicate the level of significance of the Student *t* test (* < 0.05; ** < 0.01).

in the presence of chloroquine in starved *VPS13A*-depleted cells (**Fig. 6A, C**). These experiments indicate a lower autophagic flux during starvation.

The levels and turnover of endogenous LC3-I/-II were also quantified. Of note, the amount of LC3-I (the cytosolic form) in *VPS13A*-depleted cells was higher than in control cells, suggesting that conversion of LC3-I to LC3-II was affected (**Fig. 6A, D**). LC3 turnover was also consistent with a partial block of autophagic flux as the difference in the LC3-II levels between cells treated with or without chloroquine was reduced in *VPS13A*-silenced cells in both conditions (**Fig. 6A, E**). All together, these results indicate that VPS13A is required for efficient autophagy at basal and starvation conditions in human HeLa cells.

Discussion

We have characterized the role of TipC and TipD in *Dictyostelium* autophagy. TipD encodes a homolog of the *S. cerevisiae* Atg16 but shows a higher similarity to the human ATG16L1 because it contains a large C-terminal region that is not present in the yeast model. This is another example of the close similarity of the autophagy machinery between *Dictyostelium* and animal cells.[2]

Dictyostelium TipC and human VPS13A belong to the VPS13 family. To our knowledge, this is the first description of the role of this protein family in autophagy. *Dictyostelium* genome encodes other 5 Vps13 proteins, which have not been characterized yet. Similarly, the human genome also codes for several members of this family (VPS13A/B/C/D). Two of them, VPS13A and VPS13B, are responsible for the diseases chorea-acanthocytosis and Cohen syndrome, respectively. These diseases differ in many phenotypic and pathological aspects so it is likely that these proteins have diverged in their function. In addition, the analysis of amino acid identity shows that VPS13A and VPS13C are more similar, while VPS13B is more distantly related. The *Dictyostelium* TipC shows higher similarity to human VPS13A and VPS13C than to VPS13B. Interestingly, the expression of the C-terminal region of TipC allows the strain to progress in development, pass the finger stage, and form differentiated spores and stalks, a process dependent on autophagy. These results suggest that the C-terminal region is important for autophagy regulation.

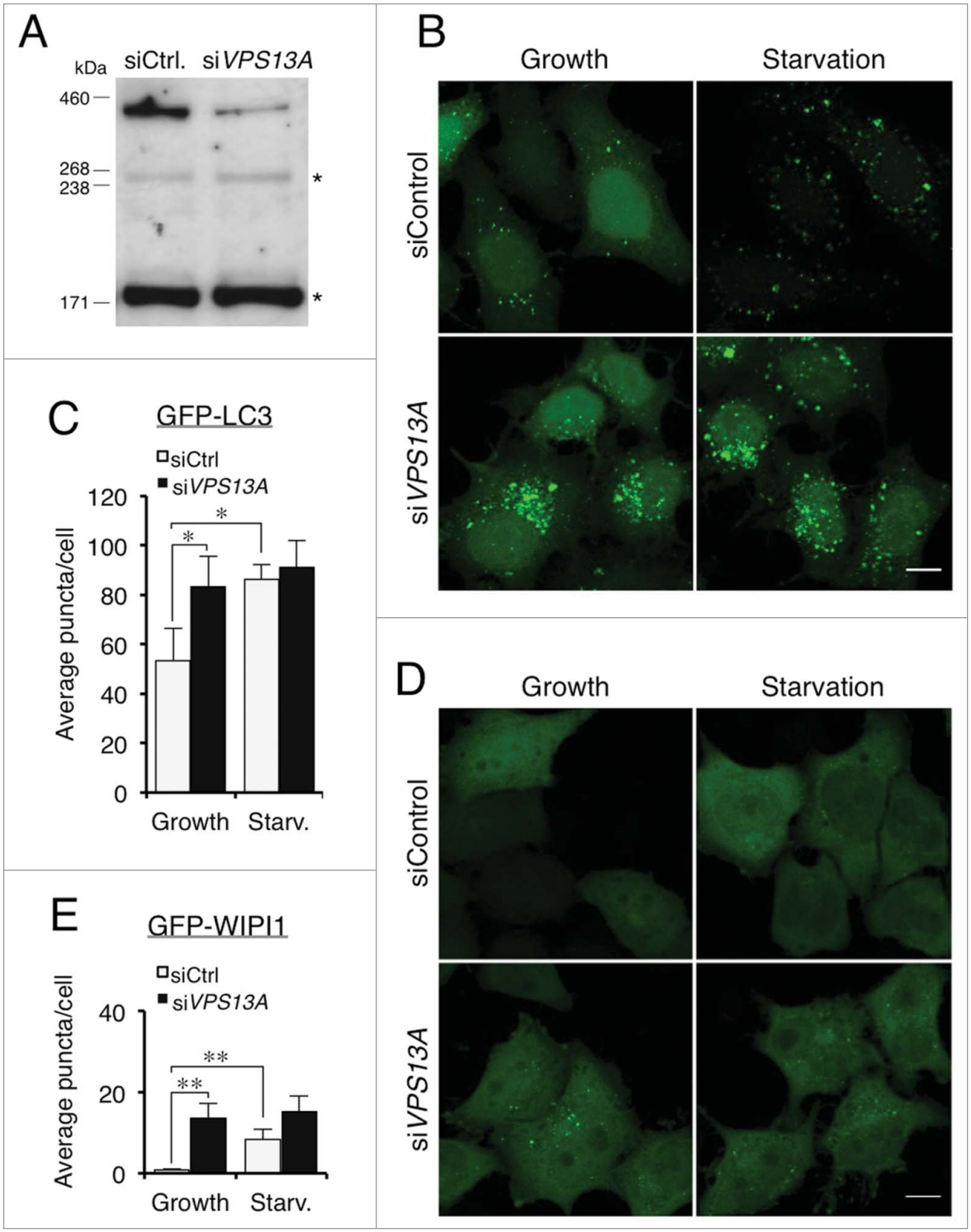

Figure 5. VPS13A downregulation causes GFP-LC3 and GFP-WIPI1 accumulation. (**A**) Western blot of control and *VPS13A* siRNA-transfected cells. A band of the VPS13A-predicted molecular weight decreases in the *VPS13A*-silenced cells. The asterisks indicate nonspecific immunoreactive bands. (**B and C**) HeLa cells stably expressing GFP-LC3 were transfected with control or *VPS13A* siRNAs and the pattern observed by confocal microscopy. *VPS13A*-depleted cells show accumulated puncta and less translocation from the nucleus to the cytoplasm during starvation. (**D** and **E**) HeLa cells were transfected with GFP-WIPI1 and the pattern observed by confocal microscopy. The number of puncta is higher in *VPS13A* siRNA-treated cells and does not significantly increase following starvation. The graphs show the mean and the standard deviation of puncta quantification of more than 40 cells from 3 independent experiments. Asterisks indicate the level of significance of the Student *t* test (* < 0.05; ** < 0.01). Scale bar: 10 μm.

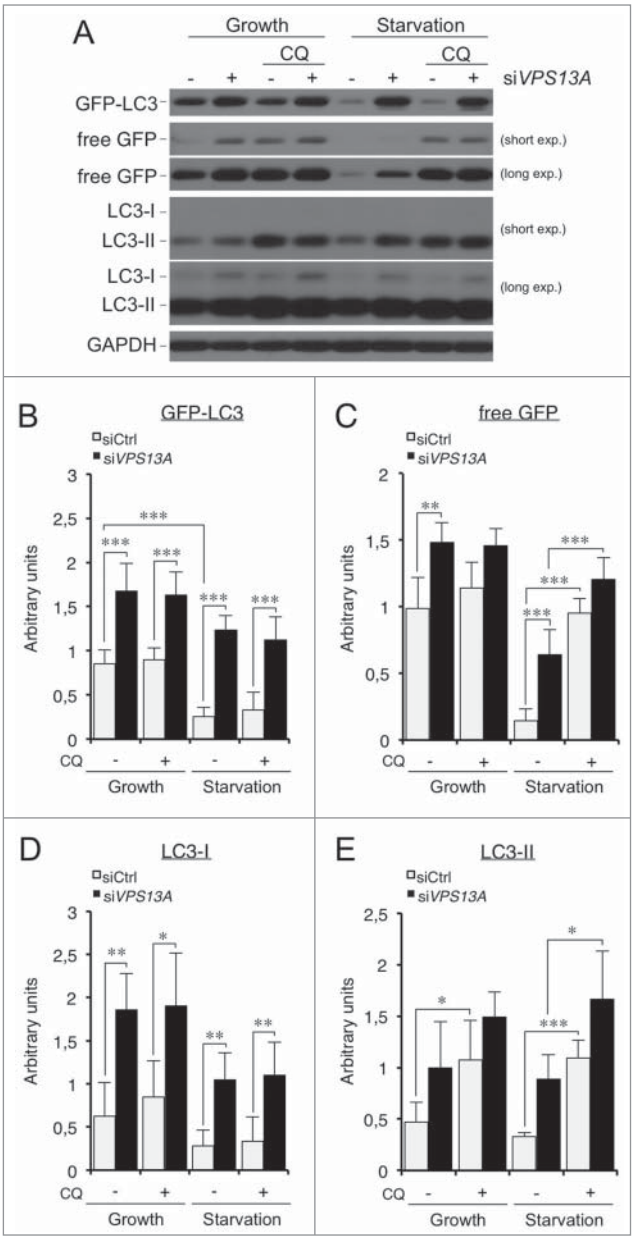

Figure 6. A reduced autophagic flux is observed in *VPS13A* siRNA-treated cells. (**A**) GFP-LC3, free GFP, and endogenous LC3-I/-II were analyzed by western blot from control or *VPS13A* siRNA-treated cells under growth or starvation conditions with or without 5 μM chloroquine (CQ). (**B**–**E**) Densitometric quantification showing the mean and the standard deviations of at least 3 independent experiments. The data was normalized against GAPDH. Asterisks indicate the level of significance of the Student *t* test (* < 0.05; ** < 0.01; *** < 0.001).

This region contains 2 conserved domains also present in the human VPS13 proteins (DUF1162, and ATG_C). The first one is a domain of unknown function, and the second one is a short region of similarity with Atg2, a protein that is recruited together with WIPI1/Atg18 to the sites of autophagosome formation.

The function of VPS13 proteins has been addressed in other model systems like the yeast *Saccharomyces cerevisiae* and the protozoa *Tetrahymena thermophila*. Interestingly, the *Tetrahymena* VPS13A localizes to the phagosome membrane and it is required for efficient phagocytosis.[27] A relationship between autophagy and phagocytosis pathways has been described in mammalian phagocytes and this connection seems to be required for efficient killing and digestion of extracellular pathogens.[34] The phagocytosis defect observed in *Dictyostelium tipC*$^{-}$ is not profound and could be due to a side effect of the autophagy blockade.

Yeast has only one Vps13 protein, which has been involved in membrane morphogenesis during sporulation but no defects in autophagy have been reported in the mutant strain so far. More specifically, the yeast *vps13*Δ cells show a depletion of PtdIns4P levels in prospore membranes.[26,39] Distinct PtdIns-phosphates play essential roles in autophagy at different levels. For example, PtdIns(3,4,5)P_3 is essential for the signaling pathway that regulates TORC1 (TOR complex 1), and PtdIns(4,5)P_2 is required for the formation of autophagosomes originated from the plasma membrane.[40] Another important PtdIns molecule is PtdIns3P, which is formed at the ER-derived omegasome by the action of the class III PtdIns3K/Vps34. This signaling lipid is required for the recruitment of Atg18 and Atg2 to the phagophore site. Our results in *Dictyostelium* show a lower recruitment of the marker GFP-Atg18 in cells lacking TipC, which might indicate a defect at the level of PdIns3P signaling. However, *VPS13A*-depleted HeLa cells, although impaired in autophagy flux, show the accumulation of autophagic markers, including WIPI1, the counterpart of Atg18. These results suggest that *Dictyostelium* TipC and human VPS13A regulate autophagy at different stages. Due to the large number of members of the VPS13 family in *Dictyostelium* and humans, we cannot be certain if the *Dictyostelium* TipC is the precise functional counterpart of human VPS13A. It is likely that the different members could regulate autophagy at different levels or even distinct but related processes, an issue that will require the complete characterization of the different proteins of the family in both species.

Previous studies in human cells report that silencing *VPS13A* in K562-erythrocytic cells and vascular endothelial cells leads to changes in cell shape and cytoskeletal architecture.[24,25] It has been suggested that *VPS13A*-depleted cells have lower activity of class I PI3K at the plasma membrane and this affects the control of actin cytoskeleton.[25] Class I PI3K inhibits autophagy through activation of TORC1, thus it is possible that *VPS13A*-depleted cells have a higher activation of the inductive stages of autophagy. However, even if this occurs, the concomitant accumulation of autophagic markers and the reduction in autophagic flux indicate that autophagosome maturation is impaired in *VPS13A*-silenced cells.

Malfunction of autophagy is associated with a variety of human diseases, including the most prominent neurodegenerative diseases,[41] and therefore, an increasing number of autophagy-modulating compounds are being tested in clinical trials.[29] The role of TipC and VPS13A in autophagy opens a new perspective in the functional studies of this protein family and warrants further explorations on the involvement of autophagy in VPS13-related diseases, and more specifically, in chorea-acanthocytosis.

Materials and Methods

Dictyostelium cell culture and genetic manipulations

Dictyostelium Tip mutants were obtained from Dicty-stock center (kindly deposited by William F. Loomis). The parent strain, AX4, was used as wild type. Cells were grown axenically in complete medium (HL-5 or SIH medium; Formedium, HLB0102; SIH0102), or in association with *Klebsiella planticola* on SM-agar plates. Transformations were carried out by electroporation as described previously.[42] For synchronous development, axenically grown cells were washed from culture media by centrifugation, resuspended in PDF buffer (20 mM KCl, 9 mM K_2HPO_4, 13 mM KH_2PO_4, 1 mM $CaCl_2$, 1 mM $MgSO_4$, pH 6.4) and deposited on nitrocellulose filters (Millipore, HABP04700). The C-terminal region of TipC was amplified by PCR from genomic DNA and cloned into the pCGFPCTAP vector (fused to GFP at the C terminus).

Calcofluor staining, sporulation, and phagocytosis assays

Calcofluor (Sigma, F3543) staining and sporulation assays were performed as described previously.[43] Sporulation efficiency was calculated by taking into account the spore production and the viability of the formed spores and given as a percentage related to the result of wild-type AX4 strain. For the phagocytosis assay, vegetative-grown cells were incubated with fluorescent latex beads (Fluotesbrite 1.0 Micron Microspheres; Polysciences, 18860) and treated as indicated previously.[44] The amount of internalized fluorescence was measured in a fluorimeter and corrected by protein concentration in each sample.

HeLa cell culture and small interfering (siRNA) experiments

HeLa cells stably expressing GFP-LC3 were kindly provided by Aviva M. Tolkovsky (John Van Geest Center for Brain Repair, Cambridge, UK) and described previously.[45] Cells were maintained in complete medium (DMEM, Dulbecco's modified Eagle's medium). Knockdown was performed by transfection of *VPS13A* siRNA (Ambion, s23340) or control siRNA (Ambion, control#2) with Lipofectamine RNAiMAX (Invitrogen, 13778-150), according to the manufacturer's instructions. Cells were transfected again with the same siRNAs after 2 d from the first transfection and the assays were carried out 3 d later. The level of depletion of *VPS13A* mRNA was measured by TaqMan PCR (Applied Biosystems, Hs00362891_m1) and found to be 89.5 ± 2.9% for all the experiments shown. GFP-WIPI-1 transfections were performed using Lipofectamine 2000 (Invitrogen, 11668-019) according to the manufacturer's instructions and the plasmid pMX-IP GFP-WIPI-1 (Addgene, 38272).

Autophagy detection in *Dictyostelium*

In vivo confocal analysis of autophagic markers GFP-Atg8 and GFP-Atg18, immunofluorescence of ubiquitin aggregates, and proteolytic cleavage assay were performed as described previously.[10,32,46] For starvation assays, complete medium was replaced with PDF buffer or SIH medium without arginine and lysine (Formedium, SIH1001) 1 h prior to visualization.

Autophagy detection in HeLa cells

For confocal visualization, cells were incubated in complete medium (DMEM, Dulbecco's modified Eagle's medium) or starvation medium (EBSS, Earle's balanced salt solution) for 2 h, fixed with 4% paraformaldehyde and mount with ProLongGold (Invitrogen, P36934) for visualization. For western blot analysis, total cell lysates were isolated using RIPA buffer from cells incubated in complete or starvation medium for 4 h in the presence or absence of 5 μM chloroquine.

Western blot and confocal microscopy

Immunoblots were performed using anti-GFP (Sigma-Aldrich, G1544), anti-LC3B (Cell Signaling Technology, 2775), anti-GAPDH (Enzo LifeSciences, ADI-CSA-335) and anti-VPS13A (Santa Cruz Biotechnology, sc-109138) antibodies and the appropriate HRP-conjugated secondary antibody (Santa Cruz Biotechnology, sc-2004; sc2005). VPS13A detection was performed as previously described.[21] The western blot bands were quantified by densitometry (ImageJ software). Confocal images were acquired using an inverted Zeiss LSM 710 laser-scanning microscope (Carl-Zeiss-Strasse 22, 73447 Oberkochen, Germany). Puncta were counted using ImageJ software.

Statistical analysis

Data were shown as mean with SD (standard deviation) and analyzed using the Student *t* test. A P value < 0.05, $P < 0.01$ or $P < 0.001$ was denoted by *, **, or ***, respectively.

Acknowledgments

Sequence data for *Dictyostelium* were obtained from the Genome Sequencing Centers of the University of Cologne, Germany; the Institute of Molecular Biotechnology, Department of Genome Analysis, Jena; the Baylor College of Medicine in Houston, Texas, USA; and the Sanger Center in Hinxton, Cambridge, UK. Tip-deficient strains were obtained from Dicty Stock Center and deposited by William F. Loomis. We thank Patricia Boya and Aviva Tolkovsky for providing the HeLa cells stably expressing GFP-LC3 and M. J. Obregón for providing the quantitative PCR instrument.

Funding

This work was supported by grants BFU2009–09050 and BFU2012–32536 from the Spanish Ministerio de Ciencia e Innovación. We also thank the help of Obra Social Caja de Burgos para Jóvenes Excelentes. SMB is recipient of a predoctoral fellowship from Universidad Autónoma de Madrid.

Supplemental data

Supplemental data for this article can be accessed on the publisher's website.

References

1. Yang Z, Klionsky DJ. Mammalian autophagy: core molecular machinery and signaling regulation. Curr Opin Cell Biol 2010; 22: 124-31; PMID:20034776; http://dx.doi.org/10.1016/j.ceb.2009.11.014
2. Calvo-Garrido J, Carilla-Latorre S, Kubohara Y, Santos-Rodrigo N, Mesquita A, Soldati T, Golstein P, Escalante R. Autophagy in Dictyostelium: genes and pathways, cell death and infection. Autophagy 2010; 6: 686-701; PMID:20603609; http://dx.doi.org/10.4161/auto.6.6.12513
3. Mizushima N, Yoshimori T, Ohsumi Y. The role of Atg proteins in autophagosome formation. Annu Rev Cell Dev Biol 2011; 27:107-32; PMID:21801009; http://dx.doi.org/10.1146/annurev-cellbio-092910-154005
4. Axe EL, Walker SA, Manifava M, Chandra P, Roderick HL, Habermann A, Griffiths G, Ktistakis NT. Autophagosome formation from membrane compartments enriched in phosphatidylinositol 3-phosphate and dynamically connected to the endoplasmic reticulum. J Cell Biol 2008; 182:685-701; PMID:18725538; http://dx.doi.org/10.1083/jcb.200803137
5. Itakura E, Mizushima N. Characterization of autophagosome formation site by a hierarchical analysis of mammalian Atg proteins. Autophagy 2010; 6:764-76; PMID:20639694; http://dx.doi.org/10.4161/auto.6.6.12709
6. King JS. Autophagy across the eukaryotes: Is S. cerevisiae the odd one out? Autophagy 2012; 8:1159-62; PMID:22722653; http://dx.doi.org/10.4161/auto.20527
7. King JS, Veltman DM, Insall RH. The induction of autophagy by mechanical stress. Autophagy 2011; 7:1490-9; PMID:22024750; http://dx.doi.org/10.4161/auto.7.12.17924
8. Otto GP, Wu MY, Kazgan N, Anderson OR, Kessin RH. Macroautophagy is required for multicellular development of the social amoeba Dictyostelium discoideum. J Biol Chem 2003; 278:17636-45; PMID:12626495; http://dx.doi.org/10.1074/jbc.M212467200
9. Otto GP, Wu MY, Kazgan N, Anderson OR, Kessin RH. Dictyostelium macroautophagy mutants vary in the severity of their developmental defects. J Biol Chem 2004; 279:15621-9; PMID:14736886; http://dx.doi.org/10.1074/jbc.M311139200
10. Calvo-Garrido J, Escalante R. Autophagy dysfunction and ubiquitin-positive protein aggregates in Dictyostelium cells lacking Vmp1. Autophagy 2010; 6:100-9; PMID:20009561; http://dx.doi.org/10.4161/auto.6.1.10697
11. Tung SM, Unal C, Ley A, Pena C, Tunggal B, Noegel AA, Krut O, Steinert M, Eichinger L. Loss of Dictyostelium ATG9 results in a pleiotropic phenotype affecting growth, development, phagocytosis and clearance and replication of Legionella pneumophila. Cell Microbiol 2010; 12:765-80; PMID:20070309; http://dx.doi.org/10.1111/j.1462-5822.2010.01432.x
12. Stege JT, Shaulsky G, Loomis WF. Sorting of the initial cell types in Dictyostelium is dependent on the tipA gene. Dev Biol 1997; 185:34-41; PMID:9169048; http://dx.doi.org/10.1006/dbio.1997.8538
13. Stege JT, Laub MT, Loomis WF. tip genes act in parallel pathways of early Dictyostelium development. Dev Genet 1999; 25:64-77; PMID:10402673; http://dx.doi.org/10.1002/(SICI)1520-6408(1999)25:1%3c64::AID-DVG7%3e3.0.CO;2-1
14. Dobson-Stone C, Rampoldi L, Bader B, Velayos Baeza A, Walker RH, Danek A, Monaco AP. Chorea-acanthocytosis. In: Pagon RA, Bird TD, Dolan CR, Stephens K, Adam MP, eds. GeneReviews. University of Washington: Seattle, WA, 1993.
15. Walterfang M, Looi JC, Styner M, Walker RH, Danek A, Niethammer M, Evans A, Kotschet K, Rodrigues GR, Hughes A, et al. Shape alterations in the striatum in chorea-acanthocytosis. Psychiatry Res 2011; 192:29-36; PMID:21377843; http://dx.doi.org/10.1016/j.pscychresns.2010.10.006
16. Neutel D, Miltenberger-Miltenyi G, Silva I, de Carvalho M. Chorea-acanthocytosis presenting as motor neuron disease. Muscle Nerve 2012; 45:293-5; PMID:22246890; http://dx.doi.org/10.1002/mus.22269
17. Ueno S, Maruki Y, Nakamura M, Tomemori Y, Kamae K, Tanabe H, Yamashita Y, Matsuda S, Kaneko S, Sano A. The gene encoding a newly discovered protein, chorein, is mutated in chorea-acanthocytosis. Nat Genet 2001; 28:121-2; PMID:11381254; http://dx.doi.org/10.1038/88825
18. Dobson-Stone C, Danek A, Rampoldi L, Hardie RJ, Chalmers RM, Wood NW, Bohlega S, Dotti MT, Federico A, Shizuka M, et al. Mutational spectrum of the CHAC gene in patients with chorea-acanthocytosis. Eur J Hum Genet: EJHG 2002; 10:773-81; PMID:12404112; http://dx.doi.org/10.1038/sj.ejhg.5200866
19. Velayos-Baeza A, Vettori A, Copley RR, Dobson-Stone C, Monaco AP. Analysis of the human VPS13 gene family. Genomics 2004; 84:536-49; PMID:15498460; http://dx.doi.org/10.1016/j.ygeno.2004.04.012
20. Tomiyasu A, Nakamura M, Ichiba M, Ueno S, Saiki S, Morimoto M, Kobal J, Kageyama Y, Inui T, Wakabayashi K, et al. Novel pathogenic mutations and copy number variations in the VPS13A gene in patients with chorea-acanthocytosis. Am J Med Genet B Neuropsychiatr Genet 2011; 156B:620-31; PMID:21598378; http://dx.doi.org/10.1002/ajmg.b.31206
21. Dobson-Stone C, Velayos-Baeza A, Filippone LA, Westbury S, Storch A, Erdmann T, Wroe SJ, Leenders KL, Lang AE, Dotti MT, et al. Chorein detection for the diagnosis of chorea-acanthocytosis. Ann Neurol 2004; 56:299-302; PMID:15293285; http://dx.doi.org/10.1002/ana.20200
22. Tomemori Y, Ichiba M, Kusumoto A, Mizuno E, Sato D, Muroya S, Nakamura M, Kawaguchi H, Yoshida H, Ueno S, et al. A gene-targeted mouse model for chorea-acanthocytosis. J Neurochem 2005; 92:759-66; PMID:15686477; http://dx.doi.org/10.1111/j.1471-4159.2004.02924.x
23. Kurano Y, Nakamura M, Ichiba M, Matsuda M, Mizuno E, Kato M, Agemura A, Izumo S, Sano A. In vivo distribution and localization of chorein. Biochem Biophys Res Commun 2007; 353:431-5; PMID:17188237; http://dx.doi.org/10.1016/j.bbrc.2006.12.059
24. Alesutan I, Seifert J, Pakladok T, Rheinlaender J, Lebedeva A, Towhid ST, Stournaras C, Voelkl J, Schäffer TE, Lang F. Chorein sensitivity of actin polymerization, cell shape and mechanical stiffness of vascular endothelial cells. Cell Physiol Biochem 2013; 32:728-42; PMID:24080826; http://dx.doi.org/10.1159/000354475
25. Foller M, Hermann A, Gu S, Alesutan I, Qadri SM, Borst O, Schmidt EM, Schiele F, vom Hagen JM, Saft C, et al. Chorein-sensitive polymerization of cortical actin and suicidal cell death in chorea-acanthocytosis. FASEB J: Off Pub Federat Am Soc Exp Biol 2012; 26:1526-34; PMID:22227296; http://dx.doi.org/10.1096/fj.11-198317
26. Park JS, Neiman AM. VPS13 regulates membrane morphogenesis during sporulation in Saccharomyces cerevisiae. J Cell Sci 2012; 125:3004-11; PMID:22442115; http://dx.doi.org/10.1242/jcs.105114
27. Samaranayake HS, Cowan AE, Klobutcher LA. Vacuolar protein sorting protein 13A, TtVPS13A, localizes to the tetrahymena thermophila phagosome membrane and is required for efficient phagocytosis. Eukar Cell 2011; 10:1207-18; PMID:21764909; http://dx.doi.org/10.1128/EC.05089-11
28. Brickner JH, Fuller RS. SOI1 encodes a novel, conserved protein that promotes TGN-endosomal cycling of Kex2p and other membrane proteins by modulating the function of two TGN localization signals. J Cell Biol 1997; 139:23-36; PMID:9314526; http://dx.doi.org/10.1083/jcb.139.1.23
29. Jiang P, Mizushima N. Autophagy and human diseases. Cell Res 2014; 24:69-79; PMID:24323045; http://dx.doi.org/10.1038/cr.2013.161
30. Yang ZJ, Chee CE, Huang S, Sinicrope F. Autophagy modulation for cancer therapy. Cancer Biol Ther 2011; 11:169-76; PMID:21263212; http://dx.doi.org/10.4161/cbt.11.2.14663
31. Xie M, Morales CR, Lavandero S, Hill JA. Tuning flux: autophagy as a target of heart disease therapy. Curr Opin Cardiol 2011; 26:216-22; PMID:21415729; http://dx.doi.org/10.1097/HCO.0b013e328345980a
32. Calvo-Garrido J, Carilla-Latorre S, Mesquita A, Escalante R. A proteolytic cleavage assay to monitor autophagy in Dictyostelium discoideum. Autophagy 2011; 7:1063-8; PMID:21876387; http://dx.doi.org/10.4161/auto.7.9.16629
33. Shui W, Sheu L, Liu J, Smart B, Petzold CJ, Hsieh TY, Pitcher A, Keasling JD, Bertozzi CR. Membrane proteomics of phagosomes suggests a connection to autophagy. Proc Natl Acad Sci U S A 2008; 105:16952-7; PMID:18971338; http://dx.doi.org/10.1073/pnas.0809218105
34. Mehta P, Henault J, Kolbeck R, Sanjuan MA. Noncanonical autophagy: one small step for LC3, one giant leap for immunity. Curr Opin Immunol 2014; 26:69-75; PMID:24556403; http://dx.doi.org/10.1016/j.coi.2013.10.012
35. Polson HE, de Lartigue J, Rigden DJ, Reedijk M, Urbe S, Clague MJ, Tooze SA. Mammalian Atg18 (WIPI2) localizes to omegasome-anchored phagophores and positively regulates LC3 lipidation. Autophagy 2010; 6:506-22; PMID:20505359; http://dx.doi.org/10.4161/auto.6.4.11863
36. Dorsey FC, Steeves MA, Prater SM, Schroter T, Cleveland JL. Monitoring the autophagy pathway in cancer. Methods Enzymol 2009; 453:251-71; PMID:19216910; http://dx.doi.org/10.1016/S0076-6879(08)04012-3
37. Klionsky DJ, Abdalla FC, Abeliovich H, Abraham RT, Acevedo-Arozena A, Adeli K, Agholme L, Agnello M, Agostinis P, Aguirre-Ghiso JA, et al. Guidelines for the use and interpretation of assays for monitoring autophagy. Autophagy 2012; 8:445-544; PMID:22966490; http://dx.doi.org/10.4161/auto.19496
38. Ni HM, Bockus A, Wozniak AL, Jones K, Weinman S, Yin XM, Ding WX. Dissecting the dynamic turnover of GFP-LC3 in the autolysosome. Autophagy 2011; 7:188-204; PMID:21107021; http://dx.doi.org/10.4161/auto.7.2.14181
39. Park JS, Okumura Y, Tachikawa H, Neiman AM. SPO71 encodes a developmental stage-specific partner for VPS13 in Saccharomcyes cerevisiae. Eukar Cell 2013; 12:1530-7; PMID:24036347; http://dx.doi.org/10.1128/EC.00239-13
40. Dall'armi C, Devereaux KA, Di Paolo G. The role of lipids in the control of autophagy. Curr Biol: CB 2013; 23:R33-45; PMID:23305670; http://dx.doi.org/10.1016/j.cub.2012.10.041
41. Schneider JL, Cuervo AM. Autophagy and human disease: emerging themes. Curr Opin Genet Dev 2014; 26C:16-23; ; http://dx.doi.org/10.1016/j.gde.2014.04.003
42. Pang KM, Lynes MA, Knecht DA. Variables controlling the expression level of exogenous genes in Dictyostelium. Plasmid 1999; 41:187-97; PMID:10366524; http://dx.doi.org/10.1006/plas.1999.1391
43. Escalante R, Sastre L. A serum response factor homolog is required for spore differentiation in Dictyostelium. Development 1998; 125:3801-8; PMID:9729488
44. Rivero F, Maniak M. Quantitative and microscopic methods for studying the endocytic pathway. Methods Mol Biol (Clifton, NJ) 2006; 346:423-38; PMID:16957305
45. Bampton ET, Goemans CG, Niranjan D, Mizushima N, Tolkovsky AM. The dynamics of autophagy visualized in live cells: from autophagosome formation to fusion with endolysosomes. Autophagy 2005; 1:23-36; PMID:16874023; http://dx.doi.org/10.4161/auto.1.1.1495
46. Mesquita A, Calvo-Garrido J, Carilla-Latorre S, Escalante R. Monitoring autophagy in Dictyostelium. Methods Mol Biol 2013; 983:461 70; PMID:23494324; http://dx.doi.org/10.1007/978-1-62703-302-2_26

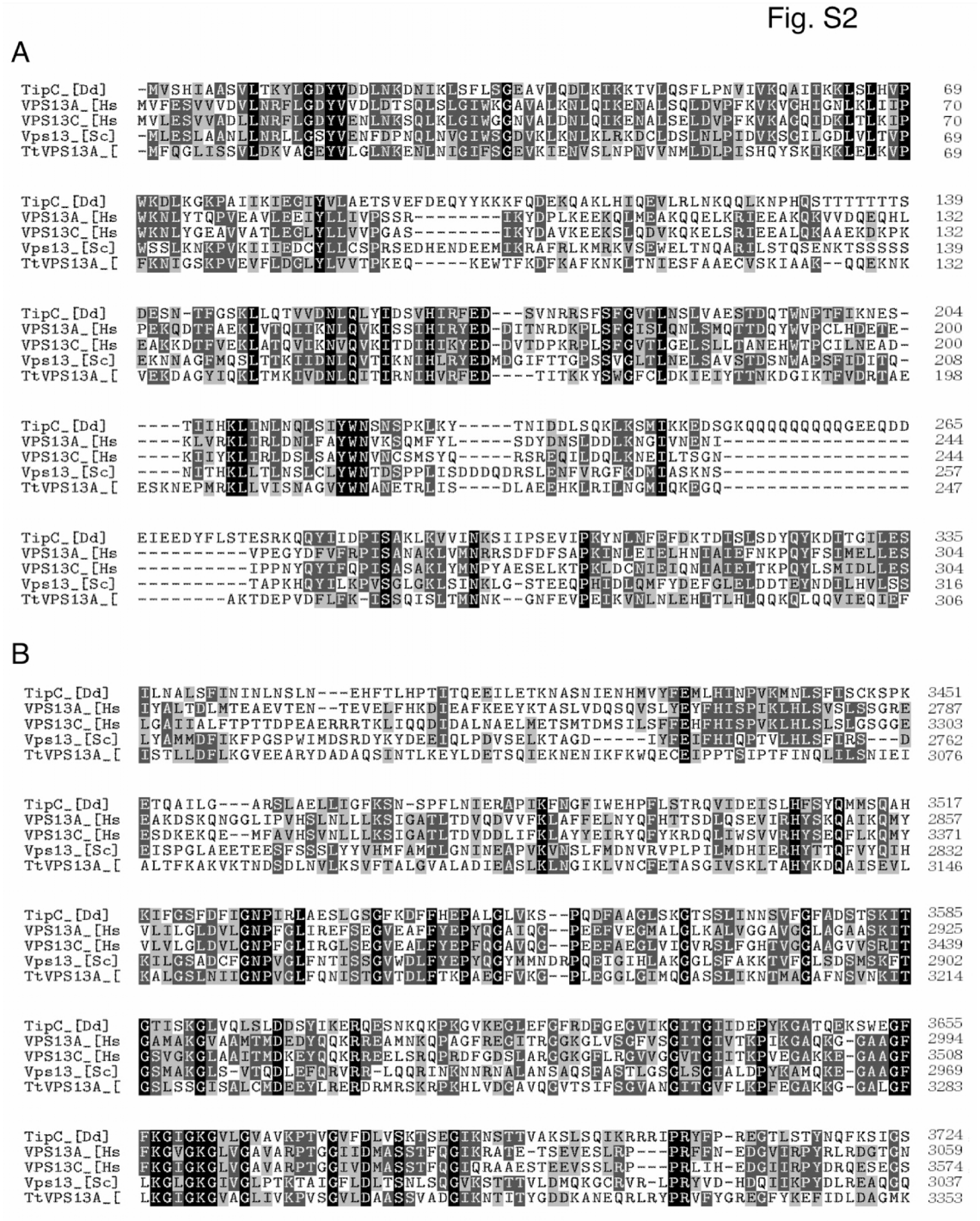

Figure S2. Amino acid alignment of the N (**A**) and C terminus (**B**) of TipC with VPS13 proteins of other organisms. *Dictyostelium discoideum* TipC (EAL73163.1) was aligned with *H. sapiens* VPS13A (NP_150648.2) and VPS13C (NP_060154.3), *S. cerevisiae* Vps13 (CAA97491.1) and *Tetrahymena termophila* VPS13A (ADM47433.1) using the ClustalW algorithm and shaded using the Textshade tool at the SDSC Biology WorkBench server (http://workbench.sdsc.edu/).

Chapter 20

Analysis of Relevant Parameters for Autophagic Flux Using HeLa Cells Expressing EGFP-LC3

Sandra Muñoz-Braceras and Ricardo Escalante

Abstract

Macroautophagy (called just autophagy hereafter) is an intracellular degradation machinery essential for cell survival under stress conditions and for the maintenance of cellular homeostasis. The hallmark of autophagy is the formation of double membrane vesicles that engulf cytoplasmic material. These vesicles, called autophagosomes, mature by fusion with endosomes and lysosomes that allows the degradation of the cargo. Autophagy is a dynamic process regulated at multiple steps. Assessment of autophagy is not trivial because the number autophagosomes might not necessarily reflect the real level of autophagic degradation, the so-called autophagic flux. Here, we describe an optimized protocol for the analysis of relevant parameters of autophagic flux using HeLa cells stably expressing EGFP-LC3. These cells are a convenient tool to determine the influence of the downregulation or overexpression of specific proteins in the autophagic flux as well as the analysis of autophagy-modulating compounds. Western blot analysis of relevant parameters, such as the levels of EGFP-LC3, free EGFP generated by autophagic degradation and endogenous LC3·I–II are analyzed in the presence and absence of the autophagic inhibitor chloroquine.

Key words Autophagy, Autophagosome, LC3, HeLa

1 Introduction

Autophagy is a degradative pathway in which cytoplasmic constituents are degraded in the lysosomes. The process comprises the formation of structures, called phagophores, which sequester the cytoplasmic cargo and elongate to form closed double membrane vesicles, the autophagosomes. Subsequently, they fuse with compartments of the endolysosomal pathway to form autolysosomes, where the inner membrane of the vesicle and its content are degraded [1]. It occurs constitutively at basal levels but it is further induced in response to starvation and to other circumstances that could threaten cellular homeostasis, such as the presence of defective organelles or accumulated protein aggregates [2, 3].

Although numerous proteins participate in the constant formation and degradation of autophagic structures [4–6], only

Rune Matthiesen (ed.), *Proteostasis: Methods and Protocols*, Methods in Molecular Biology, vol. 1449,
DOI 10.1007/978-1-4939-3756-1_20,

Atg8—and its homologs in other eukaryotes—remains associated to all those structures (phagophores, autophagosomes, and autolysosomes). Precisely because of its association to autophagic membranes until the end of the process, Atg8 is the quintessential protein for monitoring autophagy. In mammals, one of its homologs, microtubule-associated protein 1 light chain 3 (LC3), is the most widely used as an autophagic marker [7].

Membrane association of LC3 requires the posttranslational modification of the protein. Newly synthesized LC3 (proLC3) is cleaved by Atg4 at Gly120 at the C-terminus to form LC3-I, which is diffusely localized in the cytoplasm [8]. During autophagosome formation, LC3-I is conjugated to phosphatidylethanolamine in an ubiquitin-like reaction and the lipidated LC3 form (LC3-II) binds to the outer and the inner membranes of autophagosomes [9–11]. After autophagosome–lysosome fusion, outer membrane-bound LC3-II is again cleaved by Atg4 and dissociated from the membrane [12]. On the contrary, inner membrane-bound LC3-II is degraded within the autolysosome [8], *see* Fig. 1 for a schematic representation.

Most current assays to monitor autophagy are based on LC3 conversion and degradation. LC3 conversion can be traced by microscopy and immunoblotting techniques as LC3-II presents a punctate localization instead of a diffuse pattern and migrates faster

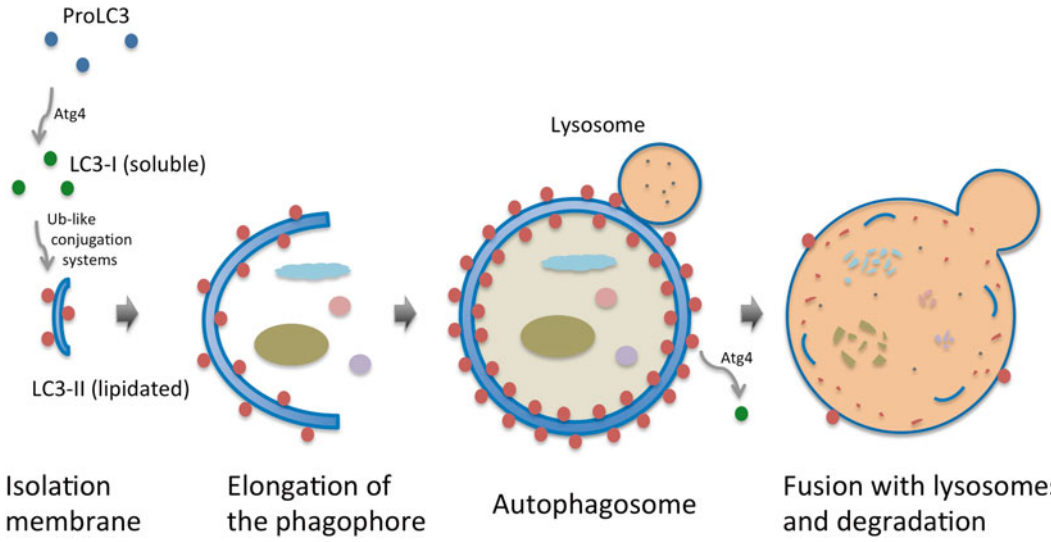

Fig. 1 Simplified representation of LC3 lipidation and turnover during autophagy. Cellular proLC3 is first cleaved by the protease Atg4 at the C-terminus to form LC3-I, also known as the soluble form. Upon autophagy induction, LC3-I is conjugated to the membrane of the nascent autophagosome and remains attached to both sides of the double membrane as the vesicle elongates, engulfs the cargo, and closes up. At that point, the outer LC3 is cleaved and recycled, the autophagosome fuses with lysosomes, and the internal LC3 is the degraded together with the inner membrane and the cargo. For cells expressing GFP-LC3, the fused protein suffers the same process as the endogenous LC3. The degradation of LC3 and GFP-LC3 in the autophagosome is the base for the methods described here, as their levels and localization change in the course of autophagic flux

than LC3-I on SDS-PAGE due to its hydrophobicity. LC3-II puncta and LC3-II levels correlate with the number of autophagic structures present in the cell but they do not inform about the actual autophagic activity. The reason is that autophagy is a dynamic process, in which the number of autophagosomes at a certain moment depends on their formation and degradation. This is referred to as autophagic flux and can be conveniently inferred from the assessment of LC3-II degradation in the lysosomes [13]. For that, LC3-II accumulation is monitored by immunoblotting after the addition of compounds that inhibit lysosomal degradation such as chloroquine.

The GFP-tagged version of LC3 at the N-terminus (GFP-LC3) is widely used to visualize autophagosomes. Following autophagy induction, GFP-LC3 is lipidated and associates to forming autophagosomes, resulting in a punctate pattern of the marker. Non-autophagic LC3 puncta can also occur due to the aggregation of the overexpressed GFP-LC3 [14] but this artifact is prevented in cell lines stably expressing GFP-LC3 at moderate levels. We would like to emphasize that not only the fluorescence of the lipidated membrane-bound form (GFP-LC3-II) can be used to monitor autophagy, but that the fluorescence of the soluble form (GFP-LC3-I) can also be informative of the autophagic process. In particular, when GFP-LC3 is overexpressed, GFP-LC3-I is diffusely located in the nucleus but translocates to the cytoplasm upon autophagy induction [15]. Thus, translocation of the diffuse fluorescence reflects autophagic activity. Differences in intensity of the diffuse fluorescence pattern can give a clue about the rate of LC3 conversion and degradation. However, it should be noted that differences of intensity can be due to different expression levels of the marker, so this is only applicable when using samples expressing a relatively homogeneous level of GFP-LC3, which is achieved in cell lines stably expressing the marker.

In addition, the potential of GFP-LC3 to monitor autophagy goes beyond its use as a fluorescent label. The fusion protein undergoes the same conversion and degradation of endogenous protein, but GFP is more resistant to lysosomal proteases than LC3. Thus, the appearance of free GFP also serves as an indicator of autophagic degradation [16]. We have found that most of the published studies limit the use of GFP-LC3 in immunoblotting to the detection of the free GFP band and that lysosomal inhibitors are not always added to properly characterize autophagic flux. However, as GFP-LC3 overexpression does not affect autophagic activity [17], we consider that the detection of both forms of the overexpressed and endogenous protein (GFP-LC3-I/II and LC3-I/II) together with the detection of the free GFP fragment, in the presence and absence of lysosomal inhibitors, provides a more complete view of the autophagic flux in a given experimental condition.

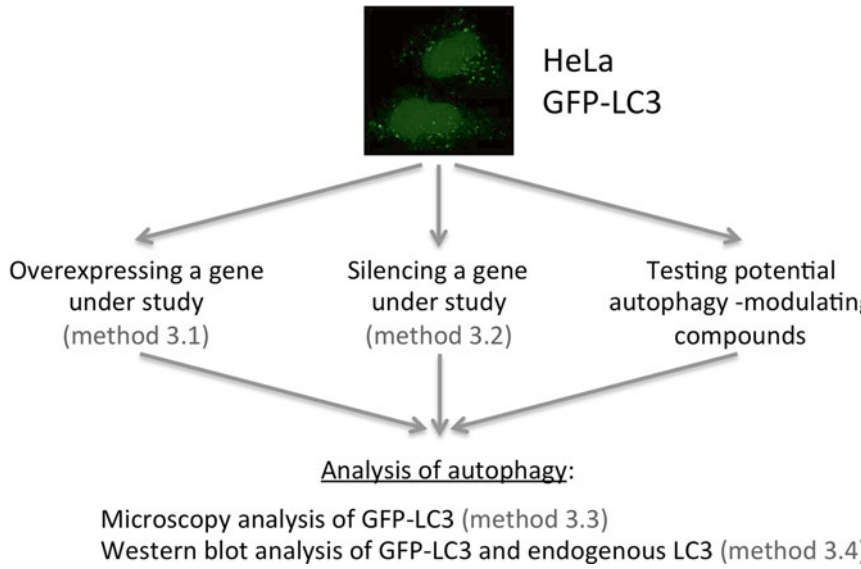

Fig. 2 Schematic representation of the methods described in this chapter. HeLa cells stably expressing the autophagosome marker GFP-LC3 can be used to determine autophagy changes upon overexpression (Subheading 3.1) or downregulation (Subheading 3.2) of genes under study as well as for testing the effect of compounds on autophagy (for example, in preclinical and high-throughput screenings). The effect of these alterations in autophagy can then be monitored by microscopy analysis (Subheading 3.3) or western blot to determine autophagic flux using the change in the levels of LC3-I and II (or GFP-LC3-I, II) and free GFP fragments upon autophagy inhibition with chloroquine (Subheading 3.4)

We describe in this chapter a series of protocols to efficiently assess autophagy using HeLa cells stably expressing EGFP-LC3 and a combination of fluorescence microscopy and immunoblotting procedures. These methods complement each other, which helps to interpret changes in the autophagic activity upon downregulation or overexpression of your favorite protein. This protocol can easily be adapted to the analysis of autophagy-modulating compounds. Figure 2 shows a diagram of the different methods described in this chapter.

2 Materials

2.1 Reagents

1. HeLa cells stably expressing EGFP-LC3 were kindly provided by Aviva M Tolkovsky (John Van Geest Center for Brain Repair, Cambridge, UK) and described previously [18].
2. Complete cell culture medium: DMEM (Dulbecco's Modified Eagle's Medium) (Sigma-Aldrich) supplemented with 10% FBS (Fetal Bovine Serum) (Gibco) and 1× penicillin-streptomycin (Gibco).

3. Starvation cell culture medium: EBSS, Earle's Balanced Salt Solution (Sigma-Aldrich).
4. PBS (phosphate-buffered saline) 1×: 133 mM NaCl, 8 mM Na_2HPO_4, 2 mM KH_2PO_4; pH 7.4.
5. TrypLE Express Enzyme (Gibco) for detachment of adherent cells.
6. Lipofectamine 2000 (Invitrogen).
7. Lipofectamine RNAiMAX (Invitrogen).
8. Opti-MEM (Invitrogen).
9. Silencer Select siRNA, target and negative control (Ambion).
10. 4% Paraformaldehyde (Merk) in PBS. Prepare the solution in a hood, heating it to approximately 60 °C and stirring it gently. 1 M NaOH is added drop by drop to clear the solution, but taking care that the pH is maintained around 7.4.
11. 100 mM Glycine (Carlo Erba) in PBS.
12. DAPI (4′,6-Diamidino-2-Phenylindole, Dihydrochloride) (Molecular Probes).
13. ProLongGold antifade mountant (Molecular Probes).
14. Chloroquine diphosphate salt (Sigma-Aldrich) stock solution at 1 mM, prepared with deionized distilled water (ddH_2O).
15. RIPA lysis buffer: 50 mM Tris–HCl pH 8, 1% NP-40, 0.1% SDS, 0.5% sodium deoxycholate, 150 mM NaCl, 2 mM EDTA. Protease inhibitor cocktail (Sigma-Aldrich) is added to the lysis buffer at a 1:100 dilution just before use.
16. Pierce BCA protein assay kit (Thermo Scientific).
17. Sample loading buffer 5×: 250 mM Tris–HCl pH 6.8, 10% SDS, 25% glycerol, 0.04% bromophenol blue, 100 mM dithiothreitol (DTT).
18. SDS-polyacrylamide resolving gel (14%). Recipe for 10 ml (enough to prepare a 1.5 mm thick mini-protean gel): 3.85 ml ddH_2O, 3.5 ml 40% acrylamide/bis-acrylamide solution 37.5:1 (Bio-Rad), 2.5 ml Tris buffer 1.5 M pH 8.8, 100 µl SDS 10%, 50 µl ammonium persulfate (APS) 10% in ddH_2O (Bio-Rad, 161-0700), 5 µl *N,N,N′,N′*-Tetramethylethylenediamine (TEMED) (Sigma-Aldrich).
19. SDS-polyacrylamide stacking gel (4%). Recipe for 4 ml (enough to prepare a 1.5 mm thick mini-protean gel): 3.04 ml ddH_2O, 0.4 ml 40% acrylamide/bis-acrylamide solution 37.5:1, 0.5 ml Tris buffer 1 M pH 6.8, 40 µl SDS 10%, 20 µl APS 10%, 4 µl TEMED.
20. SDS running buffer: 25 mM Tris Base, 192 mM glycine, 0.1% SDS in ddH_2O.
21. Transfer buffer: 25 mM Tris Base, 192 mM glycine, 20% methanol in ddH_2O.

22. Tris buffered saline containing tween (TBS-T): 0.136 mM NaCl, 20 mM Tris Base, 0.05% Tween-20 (Sigma-Aldrich). The pH should be adjusted to 7.4 with HCl.
23. Skim milk (Sigma-Aldrich).
24. Primary antibodies: anti-LC3 (Cell Signaling, 2775), anti-GFP (Sigma-Aldrich, G1544), anti-GAPDH antibody (Enzo LifeSciences, ADI-CSA-335).
25. Secondary antibodies are horseradish peroxidase (HRP)-conjugated antibodies: goat anti-rabbit IgG-HRP (Santa Cruz Biotechnology, sc-2004), goat anti-mouse IgG-HRP (Santa Cruz Biotechnology, sc-2005).
26. Amersham ECL Western Blotting detection reagent (GE Healthcare).

2.2 Other Materials and Equipment

1. Falcon 100 mm TC-treated polystyrene cell culture dishes (Corning), 6-well and 24-well clear TC-treated polystyrene multiwell cell culture plates (Corning).
2. CO_2 incubator.
3. 12 mm coverslips (Heinz Herenz) and microscope slides (VWR).
4. Inverted Zeiss LSM 710 laser confocal microscope (Zeiss) equipped with a Plan-Apochromat 63×/1.40 NA oil-immersion objective. ZEN2009 acquisition software and ImageJ processing software.
5. Mini-PROTEAN Electrophoresis System and Mini Trans-Blot Electrophoretic Transfer Cell (Bio-Rad).
6. BioTrace Polyvinylidene fluoride (PVDF) transfer membrane (Pall Life Sciences).
7. CURIX RP2 Plus film (Agfa) and an X-ray film processing machine. A digital imaging system (GE Healthcare ImageQuant LAS4000) can be used instead.

3 Methods

3.1 DNA Transfection

1. The day before, detach the adherent cells on culture with the aid of a dissociating solution, such as TrypLE Express Enzyme, centrifuge the cells, and seed approximately 2×10^6 cells in a 100 mm dish to become 80% confluent at the time of transfection. Incubate the cells in complete cell culture medium at 37 °C in a CO_2 incubator.
2. Prior to transfection, replace the growing medium with 8 ml of prewarmed complete medium without antibiotics because the presence of antibiotics during transfection may increase cell death.

3. For each sample, dilute 40 μl Lipofectamine 2000 in 1 ml of serum-free medium Opti-MEM, mix gently by pipetting and incubate at room temperature for 5 min.
4. Dilute 20 μg of plasmid DNA in 1 ml Opti-MEM. Make the equivalent dilution with the same amount of a control empty vector.
5. Add the Lipofectamine 2000 dilution to the DNA dilution (2 ml of final volume for each sample), mix by pipetting, and incubate at room temperature for 20 min.
6. Add the 2 ml of the solution with the DNA-Lipofectamine 2000 complexes to the cells slowly and move the dish to evenly distribute the solution.
7. Incubate the cells with the DNA-Lipofectamine 2000 complexes at 37 °C in a CO_2 incubator for 4 h to minimize toxicity, aspirate the medium, and add fresh complete medium.
8. Incubate for about 24–30 h to allow the cells to recover from transfection. The cells are now ready for the subsequent autophagy experiments (*see* Subheadings 3.3 and 3.4) (*see* **Note 1**).

3.2 siRNA Reverse Transfection

1. The day of the transfection, detach the adherent cells on culture, count, centrifuge the cells, and dilute approximately 1×10^6 cells in 8 ml of prewarmed complete medium without antibiotics. Keep the cells in the falcon until **step 6** or alternatively **step 1** can be performed during the 20 min incubation described in **step 4**.
2. To prepare the complexes, for each sample, dilute 35 μl Lipofectamine RNAiMAX in 1 ml Opti-MEM, mix gently by pipetting, and incubate at room temperature for 5 min.
3. Dilute 100 pmol (10 μl of a 10 μM solution) of siRNA in 1 ml Opti-MEM. Make the equivalent dilution with the same amount of a negative control siRNA.
4. Add the Lipofectamine RNAiMAX dilution to the siRNA dilution (2 ml of final volume for each sample), mix by pipetting, and incubate at room temperature for 20 min.
5. Add the siRNA-Lipofectamine RNAiMAX complexes to the 100 mm dish and move back and forth to cover the surface of the dish with the mixture.
6. Add the 8 ml dilution of the cells to the dish containing the 2 ml of siRNA-Lipofectamine RNAiMAX complexes (the final siRNA concentration is 10 nM). Rock the dish gently.
7. Incubate at 37 °C in a CO_2 incubator for 48 h. Changing the medium is not necessary.
8. Repeat the siRNA reverse transfection from **steps 1–6** (*see* **Note 2**) using again 1×10^6 cells and the same volumes of every reagent for each transfection.

9. Three days after the second transfection the cells can be used for the subsequent autophagy experiments (*see* Subheadings 3.3 and 3.4).

3.3 Microscopy Analysis of GFP-LC3 Fluorescence

1. The day before the experiment, seed approximately 40,000 transfected cells on sterilized coverslips in 24-well plates. The culture should be 60–70 % confluent at the time of the experiment (*see* **Note 3**).
2. For starvation treatment to induce autophagy, wash the cells twice with 1 ml of prewarmed PBS and once again with 1 ml of prewarmed starvation medium EBSS. Aspirate off the medium and add 1 ml of EBSS. Similarly, aspirate off the medium, wash the cells, and add 1 ml of prewarmed fresh complete medium (DMEM with 10 % FBS) to the samples in which basal autophagy will be analyzed.
3. Incubate the cells at 37 °C and 5 % CO_2 for 2 h (*see* **Note 4**).
4. Discard the medium and rinse the cells with PBS.
5. Fix the cells with 4 % paraformaldehyde in PBS, pH 7.4, for 15 min at room temperature (*see* **Note 5**).
6. Wash the cells three times with PBS.
7. To quench the possible fluorescence signal from free aldehyde groups in paraformaldehyde, it can be convenient to incubate with 100 mM glycine in PBS for 30 min at room temperature.
8. At this point, permeabilization and incubation with primary and fluorescent-secondary antibodies can also be performed if the detection of additional proteins is desired. A nuclear dye such as DAPI can also be employed to stain nuclei (*see* **Note 6**).
9. Mount the samples using an antifade reagent such as ProLongGold. Put 4 μl of ProLongGold onto a microscope slide and with the aid of a forceps, place the coverslip onto the drop with the cells facing down and avoiding air bubble trapping. Leave the mounted samples in the dark at room temperature until the ProLongGold reagent is dry and then store them in the dark at 4 °C until visualization.
10. Observe the cells under the microscope. We routinely use a 63× objective. Higher magnification (100×) can be used to visualize the ring-shape of the autophagosomes.
11. Acquire the necessary captures along the *z*-axis to image the whole cell. Then, perform the montage to obtain the maximum intensity *z*-projection of the stack (*see* **Note 7**). Figure 3a shows images of the control sample of a representative experiment.
12. Count the puncta (*see* **Notes 8** and **9**). Figure 3b illustrates an example of quantification of the puncta observed in the control samples of independent experiments.

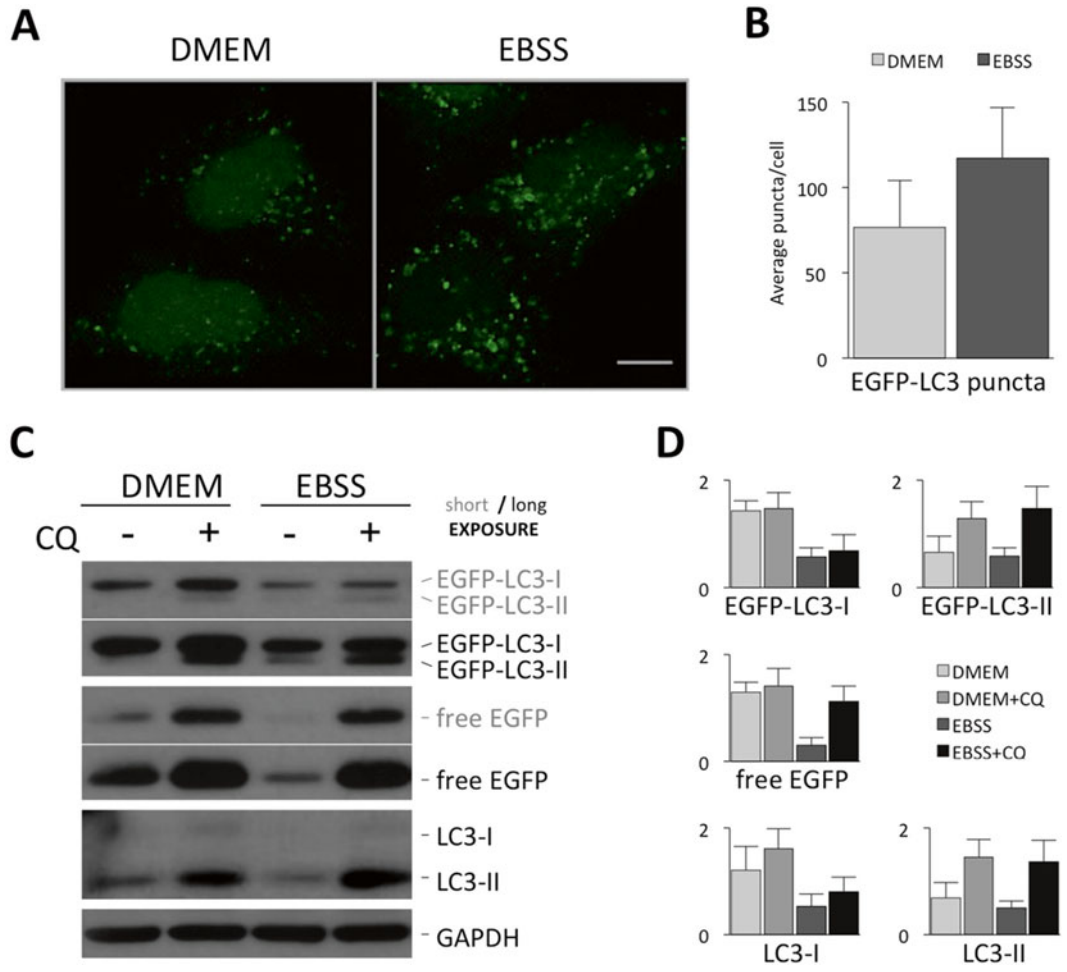

Fig. 3 HeLa cells stably expressing EGFP-LC3 and transfected with control siRNAs were incubated in complete (DMEM) or starvation (EBSS) medium for 2 h (**a**, **b**) or for 4 h in the absence or presence of 5 μM chloroquine (CQ) (**c**, **d**). Starvation causes the translocation of diffuse EGFP-LC3 fluorescence from the nucleus to the cytoplasm (**a**), an increase in the number of puncta per cell (**b**), a decrease in the amount of EGFP-LC3-I (45 kDa) and endogenous LC3-I (18 kDa) and the faster degradation of the free EGFP (27 kDa) generated by the cleavage of EGFP-LC3 (**c**, **d**). The block of the degradation caused by the presence of chloroquine shows the accumulation of the free EGFP fragment and the EGFP-LC3-II (43 kDa) and LC3-II (16 kDa) (**c**, **d**). The graphs show the mean values and standard deviations of the quantification of the puncta per cell in more than 300 cells for each condition from seven independent experiments (**b**) and of the densitometry of the protein bands observed in western blots of nine independent experiments, showing the comparison of the amounts of protein in arbitrary units (**d**). Scale bar: 10 μm

3.4 Western Blot Analysis

1. The day before the experiment, seed approximately 200,000 transfected cells in six-well plates. Cell confluence should be 60–70 % at the time of the experiment (*see* **Note 3**).
2. The day of the experiment, aspirate off the medium, wash the cells twice with 2 ml of prewarmed PBS and once again with 1 ml of the prewarmed incubation medium for each experimental condition (DMEM or EBSS, without or with

chloroquine) to avoid any undesirable variation in the final composition and chloroquine concentration of the experimental incubation medium. Aspirate off the medium and add 2 ml of DMEM or EBSS medium, for incubation in rich nutrient or starvation conditions, respectively. To the samples in which autophagic degradation will be blocked, chloroquine has to be added to the medium at a final concentration of 5 μM from a prediluted stock solution (*see* **Notes 10** and **11**).

3. Incubate the cells at 37 °C and 5 % CO_2 for 4 h (*see* **Note 12**).
4. Put the plate on ice, discard the medium, and wash the cells with ice-cold PBS.
5. Add approximately 50 μl of RIPA lysis buffer with the protease inhibitor cocktail added prior to use.
6. Harvest the cells using a cell scraper and transfer them into a cooled microcentrifuge tube.
7. Leave the cells on ice during 30 min, mixing the solution each 10 min by pipetting or vortexing.
8. Centrifuge at 13,500 × *g* for 15 min at 4 °C and transfer the supernatant to a new microcentrifuge tube.
9. Take an aliquot of the sample and make a 1:4 dilution for measuring protein concentrations by the BCA protein assay. Follow the manufacturer's instructions to determine protein concentration.
10. Prepare the samples to load 7 μg of protein per well in sample loading buffer (*see* **Note 13**).
11. Boil the samples at 98 °C for 5 min. If the samples are not going to be loaded immediately, store them at −80 °C.
12. Place the previously prepared gels in the electrophoresis chamber and fill it with SDS running buffer. For preparing the gels, pour the freshly prepared resolving gel solution (APS and TEMED are added just prior pouring) in the cassette of cleaned glasses. Pour on top some milliliters of water or isopropanol to facilitate polymerization. Retire the water, pour the stacking solution, place the comb on top, and allow the gel to polymerize.
13. Load the samples and the protein marker in the polyacrylamide gel. Proceed with the electrophoresis at a constant voltage of 150 V at room temperature until the sample buffer is at the bottom of the gel.
14. Disassemble the gel cassette, discard the stacking gel, wash the gel in transfer buffer and assemble the transference sandwich (gel and methanol-activated PVDF membrane between filter papers and sponges) (*see* **Note 14**).
15. For protein transference, we routinely use a wet-type transfer system. Place the sandwich in the electrophoretic transfer cell

and fill it with transfer buffer. Transfer the proteins at 100 V constant current at 4 °C for 1 h (*see* **Note 15**).

16. Optionally, after transference the membrane can be stained with 0.1 % Ponceau S in 5 % acetic acid for 5 min to verify transference efficiency.
17. Block the membrane by incubating with 5 % skim milk in TBS-T on a shaker at room temperature for at least 1 h.
18. Incubate the membrane first with anti-LC3 antibody diluted 1:1000 in 5 % skim milk TBS-T on a shaker at 4 °C overnight (*see* **Note 16**).
19. Wash the membrane with TBS-T at room temperature five times for 10 min each.
20. Incubate the membrane with secondary antibody (goat anti-rabbit IgG-HRP) diluted 1:5000 in 2 % skim milk TBS-T on a shaker at room temperature for 1 h.
21. Wash the membrane with TBS-T at room temperature five times for 10 min each.
22. Mix the developing ECL solution, add it to the membrane and incubate for 1 min.
23. Use an X-ray film to capture the chemiluminescent signal on the membrane (*see* **Note 17**).
24. Repeat **steps 18–23** using anti-GFP antibody diluted 1:4000 and the goat anti-rabbit IgG-HRP antibody (*see* **Note 18**).
25. Repeat **steps 18–23** for detection of GAPDH as a loading control using anti-GAPDH antibody at 1:2000. In this case, use the secondary goat anti-mouse IgG-HRP antibody at 1:4000. Actin or tubulin can be also used as loading control proteins. Figure 3c shows the protein bands of the control sample of a representative experiment.
26. Scan the film and quantify bands signal intensity by densitometry using ImageJ software (*see* **Notes 19–21**). Figure 3d contains the graphs obtained from the protein bands densitometry of the control sample in independent experiments.

4 Notes

1. It is preferably to perform the procedure in a single population of cells that will be split at least 16–18 h before the planned experiment and no longer than 24 h. This is important to avoid heterogeneity in protein overexpression or depletion levels and even in confluence rates, which can alter basal autophagy and even LC3 expression. Concerning confluence, in general, cells should be maintained subconfluent but at a density that does not compromise transfection efficiency.

2. In certain cases, a large level of downregulation might be necessary to observe an effect. This can be particularly important for long-lived proteins. Longer periods of silencing can be achieved by clonal selection using expression of small hairpin RNA (shRNA); however, knockdown for prolonged time periods is not recommended for autophagy-related proteins [19]. We prefer to perform two consecutive siRNA transfections to assure the maximal depletion of the protein. However, it should be kept in mind that repetitive transfection is an additional stress to the cells. The decision to perform single or double transfections will depend on the protein of interest.
3. As stated above, confluence has an effect on basal autophagy levels. Thus, density of the cultures evaluated within and between experiments should be similar and confluence should be avoided.
4. This time period has been established for HeLa cells stably expressing EGFP-LC3. It might have to be modified if other cell lines are used as it depends on the autophagic activity of the cell [7]. In any case, it is not recommended to extend too much this incubation time when neither chloroquine nor other similar compound are added to block lysosomal degradation because it has been reported that LC3-puncta fluorescence decreases when cells are starved for longer periods [20].
5. Although the expression of the fluorescent marker allows live cell imaging, we describe here a protocol for fixing cells. Live cell imaging has the advantage that the response to the autophagy induction stimulus can be monitored along the time and that mobility of autophagosomes can also be traced. The major drawback is that the proper equipment is required to control temperature and CO_2 concentration in the environment, necessary to maintain the culture in suitable healthy conditions during the period of imaging. Another consideration is that GFP signal diminishes at an acidic pH. As a consequence, GFP fluorescence is quenched inside the autolysosomes [20]. This attenuation of fluorescence can be circumvented by fixation of the samples. Paraformaldehyde fixation maintains the sample at a neutral pH and thus, GFP fluorescence is retained. Fixed samples have the additional advantage that they can be stored and also used for immunodetection of other proteins and colocalization studies.
6. For immunofluorescence, it is important to keep in mind that certain detergents can lead to the appearance of artifactual GFP-LC3 puncta [21]. Similar cautions apply with regard to methanol, which can also be used for cell fixation and permeabilization, but might reduce GFP intensity [22].
7. To avoid misinterpretation of results that could arise from an uneven distribution of autophagosomes within the cell and the selection of random sections along the *z*-axis, we routinely

image and count the puncta present of the whole cell. For this, we capture the necessary slices to imaging the entire cell. For showing purposes, we also consider that the maximum intensity *z*-stack projection provides a more objective view of the cell.

8. Puncta can be automatically quantified by using specialized imaging software (ImageJ, Imaris, or CellProfiler). In that case, manual evaluation of the analysis is highly recommended to verify the quantification or, if necessary, adjust the parameters that define what is considered "puncta". Manual quantification might be more accurate, but similarly, uniform criteria must be applied regarding the definition of puncta. An advantage of automated analysis is that other parameters, such as area, can be monitored. In particular, the average percentage of the total area of GFP-LC3 puncta on a per cell basis can be a more appropriate index in the cases when individual puncta quantification is not possible due to autophagosome clustering.
9. GFP-LC3 overexpression results in most of the cells displaying some puncta regardless of the experimental condition. Therefore, the percentage of cells with puncta is not a good indicator of autophagic activity. To circumvent this problem, a threshold can be established to classify the population in cells with basal or induced autophagy. However, the definition of this cut-off value is rather subjective, and can be dependent on the expression levels of GFP-LC3. GFP-LC3 expression is more uniform in cell lines stably expressing the marker, but variability of autophagic activity is still significant. We think that a more appropriate index is the average number of puncta per cell. As a consequence of the variability of the autophagic activity within the same population, this parameter also considerably fluctuates across cells. Thus, for a good quantification of puncta, a large number of cells (around 100) from multiple sections should be documented for each condition in at least three independent experiments.
10. We have observed that this nonsaturated concentration of chloroquine is enough to allow the simultaneous accumulation of free GFP and LC3-II in HeLa cells stably expressing GFP-LC3. If this concentration has to be increased for other cell types, it is important to ensure that it is low enough to allow the visualization of the cleavage of the GFP-LC3, which requires a nonsaturating concentration of chloroquine as described previously [16]. It is believed that GFP is relatively resistant to lysosomal degradation and can be accumulated using low concentrations of lysosomal inhibitors. Higher concentrations (saturating concentrations) would totally inhibit lysosomal proteases hampering the GFP-LC3 cleavage, so free GFP fragments will not be generated and the GFP cleavage assay would not be applicable. Besides, high concentrations of

chloroquine could induce autophagy or could also affect other pathways independent of autophagy. This kind of side-effect has to be also taken into account if other compounds are used to raise the lysosomal pH.

11. When deciding the experimental incubation conditions, it should be kept in mind that acidity of lysosomes regulates GFP-LC3 cleavage and free GFP accumulation. This also accounts for the use of EBSS as a starvation medium to induce autophagy. EBSS lowers lysosomal pH and this provokes that, while free GFP fragments can still be detected when the cells are incubated in complete medium in the absence of lysosomal inhibitors, free GFP is further degraded and might be undetectable when EBSS is used without lysosomal inhibitors.
12. Note that we have extended the incubation period with respect to the protocol for fluorescence microscopy because accumulation of the lipidated GFP-LC3-II and LC3-II as well as free GFP will increase in a time-dependent manner due to the altered lysosomal pH and thus, the differences, in comparison to the samples in the absence of chloroquine, will be more evident. Longer incubations are not advisable because the expression of some proteins can change. One example is the autophagy substrate p62/SQSTM1 [23] but changes in other autophagy-related proteins, even in LC3, might also occur [24–26]. Moreover, a secondary autophagic response could be induced due to the accumulation of nondegraded autophagosomes if the incubation period is too long.
13. Using small amounts of protein is advisable so the chemiluminiscent signal is less saturated, and minor differences between the bands of accumulated proteins are easier visualized. In contrast, it is probably necessary to load higher amounts of protein to visualize the LC3-I band, which is difficult to detect even after long exposure periods in this cell type.
14. PVDF membranes are preferred rather than nitrocellulose membranes due to their better retention of the lipidated LC3-II.
15. Time of transfer should be short because of the low molecular weight of endogenous LC3.
16. We recommend incubating first with anti-LC3 antibody because LC3 signal is more easily lost during subsequent hybridizations than the GFP signal, due to the lesser sensitivity of the anti-LC3 antibody. This might also help in the detection of little differences in the fusion protein GFP-LC3-I and GFP-LC3-II amounts, which might be more difficult to perceive using the more sensitive anti-GFP antibody.
17. Capture the signal at different exposure times to cover all the range of signal saturation levels. Discard for densitometry those with too low or too strong signals as they might not be

in the linear range and would not represent the real differences between the samples. Short exposure times can lead to too faint bands in conditions of induced and nonblocked autophagy, while long exposure times can mask differences between bands in conditions where autophagy degradation has been blocked. Thus, for illustrating purposes, it is usually helpful to show both a short and a long exposure. Nevertheless, for a quantitative evaluation, the lanes from all the conditions have to be measured from a unique exposure time.

18. Stripping of the membrane is not necessary as the molecular weights of the proteins are different and this procedure could be aggressive and affect latter signals.
19. ImageJ software tool is useful for this purpose. As with puncta quantification, there are some practical aspects to be considered. The most important one is that the bands that are going to be subjected to densitometry must not be overexposed. This accounts, in particular, for the samples corresponding to chloroquine incubation, where the accumulation of GFP and the lipidated forms of overexpressed and endogenous LC3-II results in a strong signal. As stated above, for comparison between all the samples, the densitometry has to be done from a unique exposure; and although it might be difficult in practice, this exposure should be in the linear range for all the bands, avoiding saturation as much as possible. The data must be normalized to the loading control protein and then, the mean and the standard deviations of the independent experiments can be used to compare between samples and determine the autophagic flux in each experimental setting.
20. We would like to add some important considerations regarding data interpretation in the following notes. LC3-I levels decrease in response to autophagy induction due to the conversion to the LC3-II form and therefore, changes in the LC3-I amount in a given experimental setting compared to controls suggest that LC3-I conversion is affected in that condition. The comparison of LC3-II levels between samples in the presence and absence of lysosomal inhibitors better represents autophagic activity than the comparison of the ratio of LC3-II to LC3-I. Although the later has been employed as a measure of autophagic induction, we believe that it is not a trustworthy indicator because LC3-II is degraded within the autophagolysosomes and its levels can increase or decrease depending on the rate of conjugation and degradation if the later is not blocked. Besides, we have experienced that this ratio might change depending on the antibody used for immunodetection. Certain antibodies barely detect LC3-I although they give a strong signal for LC3-II and, inversely, LC3-I is sensitive to detection by other antibodies that might result in a

less intense LC3-II band [7]. Moreover, it should be kept in mind than LC3-I seems to be more fragile and poorly conserved in stored samples, especially when they have been repetitively frozen and thawed [15].

21. The amounts of the soluble and the lipidated forms of LC3 can also be analyzed when the protein is fused to GFP. Conversion of GFP-LC3 parallels that of endogenous LC3 [18]. Therefore, the evaluation of the fused protein, in addition to that of the endogenous one, might be helpful to interpret the autophagic activity within the cell. As in the case of endogenous protein, GFP-LC3-I amount decreases in response to autophagy induction and thus its comparison between growth and starvation conditions can be used as a reliable parameter. While the detection of the endogenous LC3-I have some drawbacks, GFP-LC3-I detection is clear due to the overexpression and the higher sensitivity of anti-GFP detection. Similarly to endogenous LC3-II, GFP-LC3-II band intensity can increase or decrease in response to starvation or other autophagy induction stimulus if the autophagic degradation is not blocked. But in reference to its accumulation in the presence of lysosomal inhibitors, it may be less evident for GFP-LC3-II, which tends to accumulate less than endogenous LC3-II in certain conditions [20]. This effect might arise from GFP-LC3-II cleavage within the lysosome when a nonsaturating concentration of lysosomal inhibitor is being used. Regarding the evaluation of free GFP, we believe that the comparison between its levels in the presence and absence of lysosomal inhibitors informs about the autophagic flux mainly in starvation conditions.

Acknowledgments

This work was supported by grants BFU2012-32536 and BFU2015-64440-P from the Spanish Ministerio de Ciencia e Innovación. SMB is recipient of a predoctoral fellowship from Universidad Autónoma de Madrid. The authors would like to acknowledge networking support by the Proteostasis COST Action (BM1307).

References

1. Shibutani ST, Yoshimori T (2014) A current perspective of autophagosome biogenesis. Cell Res 24(1):58–68
2. Schneider JL, Cuervo AM (2014) Autophagy and human disease: emerging themes. Curr Opin Genet Dev 26C:16–23
3. Choi AM, Ryter SW, Levine B (2013) Autophagy in human health and disease. N Engl J Med 368(19):1845–1846
4. Mizushima N, Yoshimori T, Ohsumi Y (2011) The role of Atg proteins in autophagosome formation. Annu Rev Cell Dev Biol 27:107–132

5. Itakura E, Mizushima N (2010) Characterization of autophagosome formation site by a hierarchical analysis of mammalian Atg proteins. Autophagy 6(6):764–776
6. Feng Y, He D, Yao Z, Klionsky DJ (2014) The machinery of macroautophagy. Cell Res 24(1):24–41
7. Kimura S, Fujita N, Noda T, Yoshimori T (2009) Monitoring autophagy in mammalian cultured cells through the dynamics of LC3. Methods Enzymol 452:1–12
8. Kabeya Y, Mizushima N, Ueno T, Yamamoto A, Kirisako T, Noda T, Kominami E, Ohsumi Y, Yoshimori T (2000) LC3, a mammalian homologue of yeast Apg8p, is localized in autophagosome membranes after processing. EMBO J 19(21):5720–5728
9. Tanida I, Tanida-Miyake E, Ueno T, Kominami E (2001) The human homolog of Saccharomyces cerevisiae Apg7p is a protein-activating enzyme for multiple substrates including human Apg12p, GATE-16, GABARAP, and MAP-LC3. J Biol Chem 276(3):1701–1706
10. Tanida I, Tanida-Miyake E, Komatsu M, Ueno T, Kominami E (2002) Human Apg3p/Aut1p homologue is an authentic E2 enzyme for multiple substrates, GATE-16, GABARAP, and MAP-LC3, and facilitates the conjugation of hApg12p to hApg5p. J Biol Chem 277(16):13739–13744
11. Mizushima N, Sugita H, Yoshimori T, Ohsumi Y (1998) A new protein conjugation system in human. The counterpart of the yeast Apg12p conjugation system essential for autophagy. J Biol Chem 273(51):33889–33892
12. Kirisako T, Ichimura Y, Okada H, Kabeya Y, Mizushima N, Yoshimori T, Ohsumi M, Takao T, Noda T, Ohsumi Y (2000) The reversible modification regulates the membrane-binding state of Apg8/Aut7 essential for autophagy and the cytoplasm to vacuole targeting pathway. J Cell Biol 151(2):263–276
13. Mizushima N, Yoshimori T, Levine B (2010) Methods in mammalian autophagy research. Cell 140(3):313–326
14. Kuma A, Matsui M, Mizushima N (2007) LC3, an autophagosome marker, can be incorporated into protein aggregates independent of autophagy: caution in the interpretation of LC3 localization. Autophagy 3(4):323–328
15. Klionsky DJ, Abdalla FC, Abeliovich H, Abraham RT, Acevedo-Arozena A, Adeli K, Agholme L, Agnello M, Agostinis P, Aguirre-Ghiso JA, Ahn HJ, Ait-Mohamed O, Ait-Si-Ali S, Akematsu T, Akira S, Al-Younes HM, Al-Zeer MA, Albert ML, Albin RL, Alegre-Abarrategui J, Aleo MF, Alirezaei M, Almasan A, Almonte-Becerril M, Amano A et al (2012) Guidelines for the use and interpretation of assays for monitoring autophagy. Autophagy 8(4):445–544
16. Ni HM, Bockus A, Wozniak AL, Jones K, Weinman S, Yin XM, Ding WX (2011) Dissecting the dynamic turnover of GFP-LC3 in the autolysosome. Autophagy 7(2):188–204
17. Mizushima N, Yamamoto A, Matsui M, Yoshimori T, Ohsumi Y (2004) In vivo analysis of autophagy in response to nutrient starvation using transgenic mice expressing a fluorescent autophagosome marker. Mol Biol Cell 15(3):1101–1111
18. Bampton ET, Goemans CG, Niranjan D, Mizushima N, Tolkovsky AM (2005) The dynamics of autophagy visualized in live cells: from autophagosome formation to fusion with endo/lysosomes. Autophagy 1(1):23–36
19. Staskiewicz L, Thorburn J, Morgan MJ, Thorburn A (2013) Inhibiting autophagy by shRNA knockdown: cautions and recommendations. Autophagy 9(10):1449–1450
20. Tanida I, Minematsu-Ikeguchi N, Ueno T, Kominami E (2005) Lysosomal turnover, but not a cellular level, of endogenous LC3 is a marker for autophagy. Autophagy 1(2):84–91
21. Ciechomska IA, Tolkovsky AM (2007) Non-autophagic GFP-LC3 puncta induced by saponin and other detergents. Autophagy 3(6):586–590
22. Patergnani S, Pinton P (2015) Mitophagy and mitochondrial balance. Methods Mol Biol 1241:181–194
23. Sahani MH, Itakura E, Mizushima N (2014) Expression of the autophagy substrate SQSTM1/p62 is restored during prolonged starvation depending on transcriptional upregulation and autophagy-derived amino acids. Autophagy 10(3):431–441
24. Settembre C, Di Malta C, Polito VA, Garcia Arencibia M, Vetrini F, Erdin S, Erdin SU, Huynh T, Medina D, Colella P, Sardiello M, Rubinsztein DC, Ballabio A (2011) TFEB links autophagy to lysosomal biogenesis. Science 332(6036):1429–1433
25. Bartholomew CR, Suzuki T, Du Z, Backues SK, Jin M, Lynch-Day MA, Umekawa M, Kamath A, Zhao M, Xie Z, Inoki K, Klionsky DJ (2012) Ume6 transcription factor is part of a signaling cascade that regulates autophagy. Proc Natl Acad Sci U S A 109(28):11206–11210
26. Jin M, Klionsky DJ (2014) Regulation of autophagy: modulation of the size and number of autophagosomes. FEBS Lett 588(15):2457–2463

Autophagy

Taylor & Francis
Taylor & Francis Group

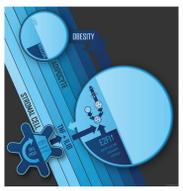

Autophagy

ISSN: 1554-8627 (Print) 1554-8635 (Online) Journal homepage: http://www.tandfonline.com/loi/kaup20

Autophagy in Dictyostelium: Mechanisms, regulation and disease in a simple biomedical model

Ana Mesquita, Elena Cardenal-Muñoz, Eunice Dominguez, Sandra Muñoz-Braceras, Beatriz Nuñez-Corcuera, Ben A. Phillips, Luis C. Tábara, Qiuhong Xiong, Roberto Coria, Ludwig Eichinger, Pierre Golstein, Jason S. King, Thierry Soldati, Olivier Vincent & Ricardo Escalante

To cite this article: Ana Mesquita, Elena Cardenal-Muñoz, Eunice Dominguez, Sandra Muñoz-Braceras, Beatriz Nuñez-Corcuera, Ben A. Phillips, Luis C. Tábara, Qiuhong Xiong, Roberto Coria, Ludwig Eichinger, Pierre Golstein, Jason S. King, Thierry Soldati, Olivier Vincent & Ricardo Escalante (2016): Autophagy in Dictyostelium: Mechanisms, regulation and disease in a simple biomedical model, Autophagy, DOI: 10.1080/15548627.2016.1226737

To link to this article: http://dx.doi.org/10.1080/15548627.2016.1226737

AUTOPHAGY
2016, VOL. 13, NO. 1, 1–17
http://dx.doi.org/10.1080/15548627.2016.1226737

Taylor & Francis
Taylor & Francis Group

REVIEW

Autophagy in *Dictyostelium*: Mechanisms, regulation and disease in a simple biomedical model

Ana Mesquita[a,b], Elena Cardenal-Muñoz[c], Eunice Dominguez[a,d], Sandra Muñoz-Braceras[a], Beatriz Nuñez-Corcuera[a], Ben A. Phillips[e], Luis C. Tábara[a], Qiuhong Xiong[f], Roberto Coria[d], Ludwig Eichinger[f], Pierre Golstein[g], Jason S. King[e], Thierry Soldati[c], Olivier Vincent[a], and Ricardo Escalante[a]

[a]Instituto de Investigaciones Biomédicas "Alberto Sols" (CSIC-UAM), Madrid, Spain; [b]University of Cincinnati College of Medicine, Cincinnati, OH, USA; [c]Départment de Biochimie, Faculté des Sciences, Université de Genève, Switzerland; [d]Departamento de Genética Molecular, Instituto de Fisiología Celular, Universidad Nacional Autónoma de México, Mexico City, México; [e]Department of Biomedical Sciences, University of Sheffield, UK; [f]Center for Biochemistry, Medical Faculty, University of Cologne, Cologne, Germany; [g]Centre d'Immunologie de Marseille-Luminy, Aix Marseille Université UM2, Inserm, U1104, CNRS UMR7280, Marseille, France

ABSTRACT

Autophagy is a fast-moving field with an enormous impact on human health and disease. Understanding the complexity of the mechanism and regulation of this process often benefits from the use of simple experimental models such as the social amoeba *Dictyostelium discoideum*. Since the publication of the first review describing the potential of *D. discoideum* in autophagy, significant advances have been made that demonstrate both the experimental advantages and interest in using this model. Since our previous review, research in *D. discoideum* has shed light on the mechanisms that regulate autophagosome formation and contributed significantly to the study of autophagy-related pathologies. Here, we review these advances, as well as the current techniques to monitor autophagy in *D. discoideum*. The comprehensive bioinformatics search of autophagic proteins that was a substantial part of the previous review has not been revisited here except for those aspects that challenged previous predictions such as the composition of the Atg1 complex. In recent years our understanding of, and ability to investigate, autophagy in *D. discoideum* has evolved significantly and will surely enable and accelerate future research using this model.

ARTICLE HISTORY
Received 6 June 2016
Revised 28 July 2016
Accepted 16 August 2016

KEYWORDS
Atg proteins; autophagic cell death; autophagy; *Dictyostelium*; infection; social amoeba

Introducing D. discoideum*, a simple model for autophagy with striking similarities to animal cells*

Dictyostelium discoideum is a protist that belongs to the Amoebozoa, a sister group of animals and fungi. They are known as social amoebae since the motile cells are able to aggregate and form a simple multicellular organism. Under starvation, groups of approximately 100,000 cells form a mound that goes through different stages of development to give rise to a fruiting body, in which vacuolated dead cells form a stalk that supports the spores (Fig. 1). Vegetative *D. discoideum* cells are more similar to animal cells than fungi or plant cells in many respects. For example, they lack rigid cell walls that might restrict movement, allowing the cells to perform typical animal-like processes such as phagocytosis, macropinocytosis, pseudopod-based cell motility and chemotaxis. The parallels with animal cells extends to the evolutionary conservation of many genes that have been lost during fungal evolution.[1]

The similarity to animal cells makes *D. discoideum* a suitable model to address the study of genes or processes relevant to human disease. These include the study of pathogen infections,[2] cell motility-related pathologies,[3] mitochondrial diseases,[4] the study of the mechanism of action of certain drugs,[5] cancer,[6] neurodegenerative disorders[7] and lysosomal-related disorders[8] among others. *D. discoideum* also provides useful ways to study the mechanisms and the physiological roles of autophagy.[9] As in in other organisms, autophagy is required for *D. discoideum* to survive starvation, for the turnover of proteins, to remove protein aggregates and is also fundamental during infection by intracellular pathogens. The first description of autophagic vacuoles in *D. discoideum* (defined at that time simply as "bodies containing partially degraded cytoplasmic material") comes from transmission electron microscopy (TEM) studies of germinating spores in 1969,[10] shortly after Christian de Duve coined the term autophagy.[11] We have come a long way from these initial morphological observations and now begin to understand the significance and the mechanisms of this crucial cellular process in the context of a whole organism.

During starvation, autophagy is responsible for the liberation of nutrients to maintain viability. Therefore, defects in autophagy drastically reduce the ability of cells to survive prolonged periods of nutrient deprivation. Typically, wild-type

CONTACT Ricardo Escalante rescalante@iib.uam.es Arturo Duperier 4. 28029-Madrid, Spain
Color versions of one or more of the figures in the article can be found online at www.tandfonline.com/kaup.
Supplemental data for this article can be accessed on the publisher's website.

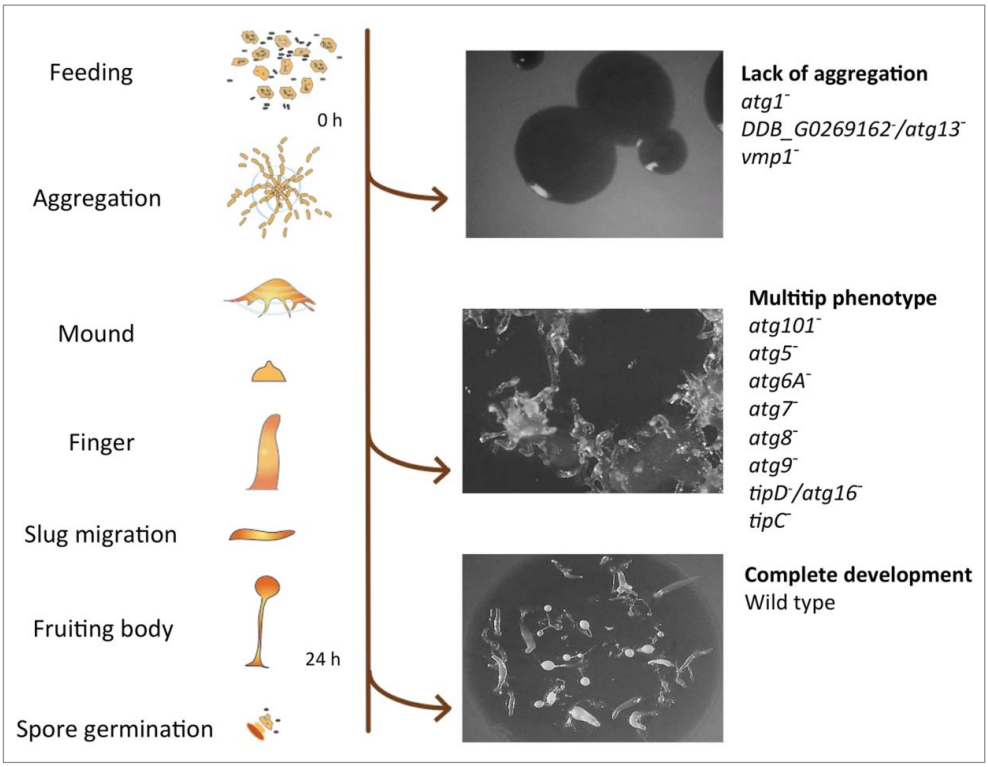

Figure 1. *D. discoideum's* life cycle and representative phenotypes associated with the lack of autophagy. Mutant strains have been described for the genes depicted at the right side (see details in the main text). The pictures correspond from top to bottom to the strains *DDB_G0269162*$^{-}$*/atg13*$^{-}$, *tipC*$^{-}$ and wild-type AX4.

D. discoideum cells survive for more than 10 d under amino acid starvation, whereas autophagy-deficient mutants start losing viability after just 24 h.[12,13] During starvation, autophagy is also responsible for a reduction in both cell volume and total protein.[12,13] The *D. discoideum* developmental program takes place in the absence of nutrients; therefore, the intracellular degradation and recycling of the cell's own material by autophagy becomes essential as a source of energy and simple metabolites required for the biosynthetic pathways taking place during development. Thus, it is not surprising that autophagic dysfunction leads to abnormal development, which facilitates the identification of autophagy mutants in the laboratory. The severity of the phenotype ranges from complete lack of aggregation to the formation of multi-tipped mounds, which are unable to form normal stalks and viable spores (Fig. 1).[13] It is unclear how much of the defects in development are simply the result of imbalanced nutrient homeostasis or whether more specific signaling events are involved. However, the signaling peptide SDF-2 (spore differentiation factor 2) is essential for spore formation, and its precursor protein, AcbA, is secreted by an unconventional mechanism that requires autophagy.[14] Moreover, terminal stalk differentiation also seems to require autophagy for the formation of the vacuoles that accompany stalk cell differentiation.[15] Nonrecyling roles for autophagy are therefore important for the terminal differentiation of both spores and stalk cells.

Three forms of autophagy have been described that differ in the mechanism by which the cargo is delivered to the lysosome. Chaperone-mediated autophagy,[16] microautophagy,[17] and macroautophagy. Macroautophagy (denoted here as autophagy for simplicity) is the best known, the most conserved autophagic pathway and the only one described in *D. discoideum* so far. Although autophagy was initially thought to simply be a mechanism to recycle nutrients by nonselective self-degradation (so called bulk autophagy), the enormous importance of selective autophagy is now becoming clear. The selective process is devoted to the specific degradation of abnormal protein aggregates (aggrephagy), organelles (mitophagy, pexophagy, ribophagy, reticulophagy, nucleophagy) or pathogens (xenophagy). Impaired selective autophagy is therefore thought to underlie the etiology of numerous diseases.[18]

The hallmark of autophagy is the formation of intracellular double-membrane vesicles (autophagosomes), which eventually fuse with lysosomes, leading to degradation of the cargo and the inner membrane. The basic molecular machinery that controls autophagy was initially discovered in *Saccharomyces cerevisiae*, in which the proteins involved were named Atg, for autophagy-related. These proteins form different complexes that are required for the induction, elongation and completion of the autophagic process. This has been extensively reviewed in the past few years.[19-21] Most of these proteins and complexes can be recognized in *D. discoideum* by sequence homology as summarized in Fig. 2. A more detailed description of the putative *D. discoideum* Atg protein homologs was included in a previous review.[9] The generation and analysis of a number of mutants from each complex have subsequently confirmed the functional conservation of the autophagic machinery in *D. discoideum* (the available mutants and their phenotypes are depicted in Fig. 1). Lack of aggregation is the phenotype observed for *atg1*$^{-}$,[22] *DDB_G0269162*$^{-}$*/atg13*$^{-}$,[23] and *vmp1*$^{-}$.[24] Formation of multiple tips in mounds is the phenotype observed in *atg101*$^{-}$,[23] *atg5*$^{-}$,[13] *atg6A*$^{-}$,[22] *atg7*$^{-}$,[13] *atg8*$^{-}$,[22] *atg9*$^{-}$,[25] *tipD*$^{-}$*/atg16*$^{-}$[26-28] and *tipC*$^{-}$.[27] Importantly, additional non-Atg proteins have been found to be involved in

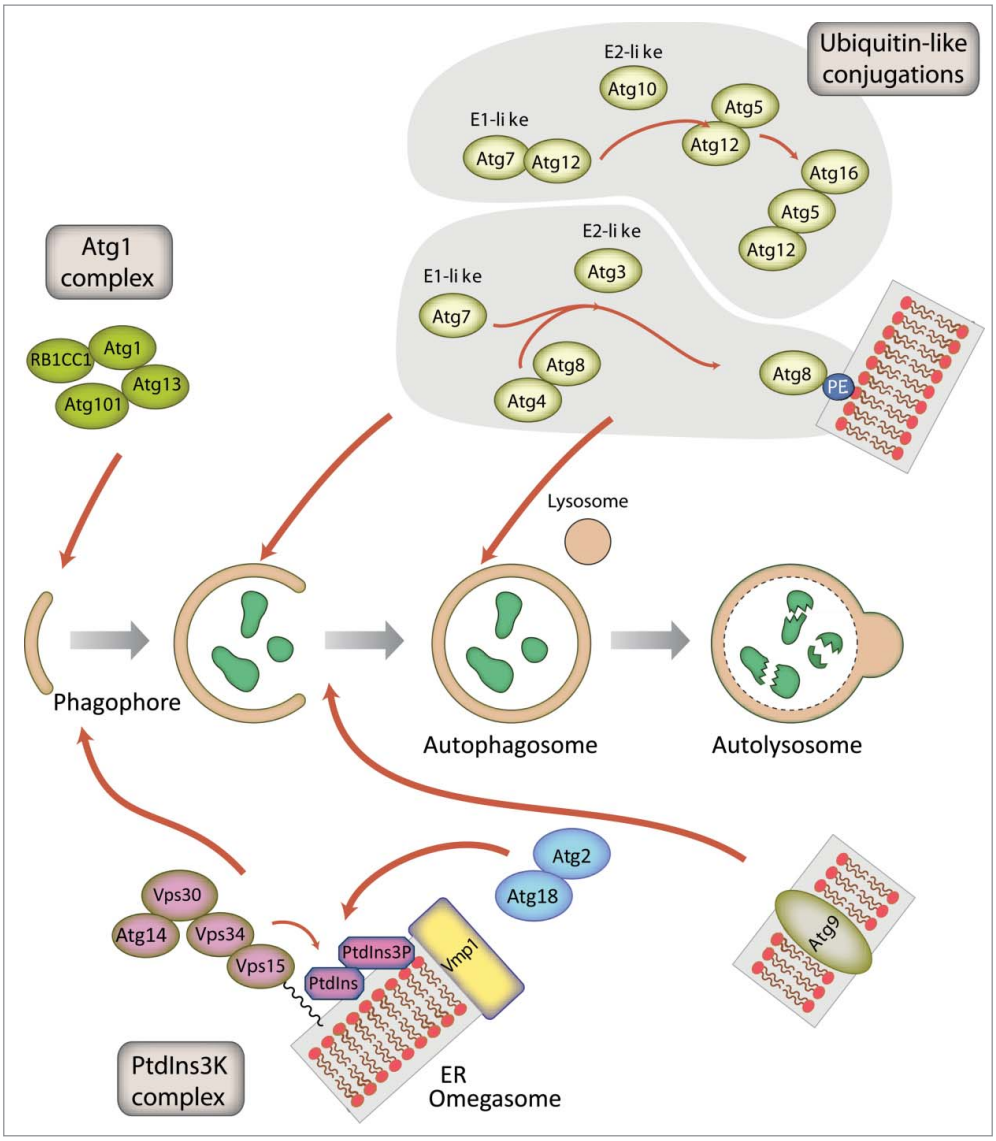

Figure 2. Schematic representation of autophagosome formation and the proteins involved in *D. discoideum*. The autophagic proteins were identified by sequence homology with those described in yeast and mammalian cells. The predicted complexes have been organized using the information available from the yeast *S. cerevisiae*, mammalian cells and *D. discoideum*. The inductive stage depends on the serine/threonine Atg1 kinase complex and the class III PtdIns3K complex. The latter complex generates the signaling lipid PtdIns3P, which is essential for the recruitment of Atg18 and Atg2. The elongation of the phagophore membrane requires 2 ubiquitin-like (Ubl) conjugation systems (upper right). In the first conjugation reaction Atg12 is covalently bound to Atg5. Atg12–Atg5 interacts with Atg16 and localizes to the phagophore membrane, from which it regulates the second conjugation reaction that attaches the protein Atg8 (known as LC3 in mammals) to phosphatidylethanolamine (PE) of the expanding phagophore membrane. Atg8 initially localizes to both sides of the phagophore and remains inside the completed autophagosome until fusion with the lysosome occurs; Atg8 on the cytosolic side of the autophagosome is cleaved from PE by Atg4 and recycled, whereas Atg8–PE of the lumenal leaflet of the bilayer is degraded. Atg9-containing vesicles supply membrane for phagophore expansion. Recent advances have clarified the composition of the Atg1 complex and the role of Vmp1 as a key protein in the origin of the autophagosomes from the ER.

Dictyostelium autophagy such as the ER transmembrane protein Vmp1 (vacuole membrane protein 1), which demonstrates the usefulness of *Dictyostelium* as an alternative simple genetic system to study autophagy.

Methods and tools to study autophagy in D. discoideum

Over recent years the number of tools available to study autophagy in *D. discoideum* has expanded greatly. TEM remains the gold standard for identifying the double-membrane autophagic structures, but it is difficult and time-consuming to obtain quantitative data. In particular, as each *D. discoideum* cell only contains approximately 5 autophagosomes under conditions of amino acid starvation,[29] very few are present in each of the thin sections required for TEM.[13] However, with recent advances in 3D electron microscopy it should now be possible to reconstruct complete amoeba, although quantification of autophagosomes has yet to be demonstrated. In contrast, light microscopy has been extensively used, allowing rapid quantification of large numbers of cells, and dynamic information to be captured.

It is often experimentally desirable to induce autophagy in a defined manner. Typically in mammalian cell cultures autophagy is induced using either starvation e.g. Hank's balanced salt solution or drug treatment, e.g., rapamycin, which inhibits MTORC1 (mechanistic target of rapamycin [serine/threonine

kinase] complex 1) function. In *D. discoideum*, complete starvation can be induced using non-nutrient buffers but this initiates development, complicating interpretation. To avoid this, it is preferable to use a defined medium such as SIH medium lacking arginine and lysine (available from ForMedium for use in SILAC). Within 5 min this gives a comparable induction of autophagy to complete starvation, without cells entering development.[29] Although *D. discoideum* has a functional rapamycin-sensitive TORC1 complex,[30] short-term rapamycin treatment is unable to activate autophagy.

Several markers have been used to study autophagy in *D. discoideum*. In mammalian systems the most commonly used markers are MAP1LC3/LC3 (microtubule associated protein 1 light chain 3) family proteins, the ubiquitin-like (Ubl) orthologs of yeast Atg8 that associate with autophagic entities from initiation until recycling.[31] *D. discoideum* possess 2 Atg8 paralogs (Atg8a and b), which are both good markers of autophagosomes although they play partially nonredundant roles (discussed below).[32] Another useful marker is Atg18, the ortholog of mammalian WIPI2. Atg18 localizes to omegasome-anchored phagophores (the precursors to autophagosomes) at initiation events but, in contrast to Atg8, dissociates immediately after autophagosome formation is completed.[29,33,34] Atg18 is therefore specific for the formation of new autophagosomes.

Immunolabeling of endogenous autophagy proteins allows a variety of markers to be observed, and several good antibodies against *D. discoideum* Atg8 have been generated.[32,35] While these antibodies are useful for many experiments, fixed samples lack dynamic information. It is therefore often useful to perform live-cell imaging and track markers in real-time to dissect the different phases of autophagosome formation. GFP-Atg8 fusions permit visualization from initiation through expansion, closure and fusion with the lysosome, whereupon the GFP fluorescence becomes quenched. Movement in the Z-axis, however, makes following individual autophagosomes over time challenging. To reduce this problem, sheets of agarose can be placed upon the cells to compress them, reducing cell height and improving image quality. This approach allows individual autophagosomes to be followed from an initial punctum, to a cup and then a complete circular autophagosome (Fig. 3 and Movie S1). The timing of each phase can be quantified from such movies, as well as the time it takes for the GFP fluorescence to be quenched, giving an indirect combined measure of acidification and proteolysis. This is a powerful method to directly quantify autophagosome dynamics, but does not represent basal autophagy levels, as the compression itself potently induces autophagosome initiation.[29]

An additional way to differentiate autolysosomes (the product of autophagosomes fusing with lysosomes) is by fusing Atg8 to both GFP and RFP in tandem.[36] As RFP is less sensitive to quenching by low pH, only the red signal can be observed in mammalian autolysosomes, whereas phagophores and autophagosomes emit both green and red fluorescence. Unfortunately, *D. discoideum* lysosomes have a much lower pH than their mammalian counterparts (3.5 compared to 4.5-5.0), which is sufficient to quench both GFP and RFP. Treatment with lysosomotropic agents such as ammonium chloride (NH_4Cl), however, can be used to partially elevate lysosomal pH, and reveal autolysosomes, with the caveat that this

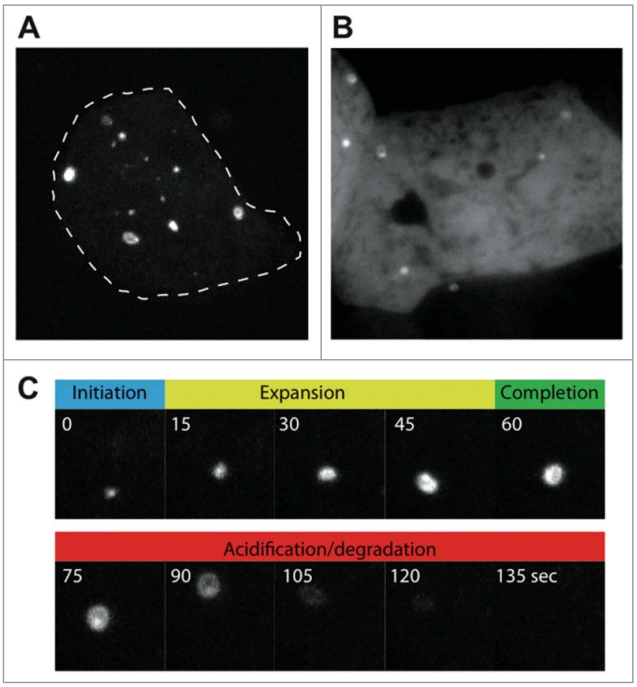

Figure 3. Live-cell imaging of autophagosome formation in *D. discoideum*, using (A) GFP-Atg8a, and (B) GFP-Atg18. Images were obtained under compression to improve clarity, and to allow individual autophagosomes to be followed over time. (C) Shows the different stages of autophagosome formation from the cell in (A) marked by GFP-Atg8a. The autophagosome shown in (C) has been marked by an arrow in Movie S1.

treatment itself will induce autophagy and lead to osmotically distended compartments with dilute content.[37,38]

Autophagic flux refers to the net amount of material that is captured and degraded by this pathway over time. This is an important but complex and dynamic measurement and is not a simple reflection of the number of autophagosomes. Currently, the best method to measure flux is based on observing the autophagic cleavage of GFP from its fusion with cytosolic proteins.[38] Although GFP fluorescence is rapidly quenched within acidic lysosomes, the GFP protein itself is relatively resistant to lysosomal proteolysis. When GFP is fused to cytosolic proteins, captured and delivered to lysosomes by autophagy, GFP fragments accumulate while the rest of the fusion protein is degraded.[39] GFP cleavage fragments can therefore be quantified by western blot analysis of whole cell lysates probed with anti-GFP antibodies. As *D. discoideum* are professional phagocytes, they possess an extremely efficient proteolytic machinery and free GFP is barely detectable due to rapid degradation. Therefore NH_4Cl treatment is again required to inhibit proteolysis sufficiently for cleaved GFP fragments to accumulate.[37,38] Band intensities for GFP-marker and free-GFP can then be quantified to give a measure of autophagic flux. It is again important to note that the concentrations of NH_4Cl required are very high (0.2-0.3 M), and likely to induce autophagy themselves. Nonetheless, this system provides a good measure of maximum autophagic capacity, and is useful to demonstrate gross effects of mutations on the pathway.[37,38]

The array of techniques available, coupled with orthologs of most mammalian autophagy genes, makes *D. discoideum* a robust model for the study of autophagy. While a system for studying autophagic flux in noninduced conditions is yet to be

established, significant progress has been made and *D. discoideum* provides many useful means in which to study this pathway.

Phagophore nucleation: The Atg1 complex in D. discoideum *is closely related to themammalian ULK1 complex*

The Atg1/ULK1 protein kinase complex works at the initiation step in both selective and nonselective autophagy.[40] In mammals, ULK1 phosphorylates BECN1 to activate the PIK3C3/VPS34 lipid kinase,[41] and phosphorylation of the transmembrane protein Atg9 by its budding yeast homolog Atg1 plays a key role in the recruitment of Atg18 and Atg8 to the phagophore assembly site (PAS).[42] Initial studies of nonselective autophagy in yeast identified the different components of the Atg1 complex: the Atg1 protein kinase itself, the regulatory subunit Atg13 and the Atg17-Atg31-Atg29 scaffolding subcomplex.[43] Selective autophagy processes, such as the cytoplasm-to-vacuole targeting (Cvt) pathway, involve a different scaffold protein, Atg11 (Fig. 4). Although not absolutely required in nonselective autophagy, Atg11 interacts with Atg29[44] and, thus, it is still unclear whether Atg11 and the Atg17-Atg31-Atg29 subcomplex form mutually exclusive complexes with Atg1. Dephosphorylation of the TOR kinase substrate Atg13 upon nutrient starvation promotes Atg1 complex assembly in nonselective autophagy.[45] In contrast, under nutrient-rich conditions, selective autophagy receptor-bound targets activate Atg1 via the scaffold protein Atg11.[46] Autophagy receptors have been identified in mitophagy (Atg32), pexophagy (Atg36), nucleophagy (Atg39), reticulophagy (Atg40) and the Cvt pathway (Atg19 and Atg34).[47]

The ULK1 protein complex in mammals differs from the budding yeast Atg1 complex in several aspects. This complex consists of the ULK1 protein kinase and 3 proteins, ATG13, ATG101 and the scaffold protein RB1CC1/FIP200 (Fig. 4). ATG101, which is absent in budding yeast, binds to and stabilizes Atg13.[48,49] The crystal structure of the Atg13-Atg101 complex revealed that the HORMA domains present in these 2 proteins heterodimerize.[50,51] In budding yeast, Atg13 contains a 3-strand β-sheet insertion in the HORMA domain that stabilizes this protein in the absence of ATG101. The scaffold protein RB1CC1 is the functional counterpart of both Atg17 and Atg11 in yeast, and results from phylogenetic analysis suggest that Atg17 arose via gene duplication of Atg11 and loss of the C-terminal region.[52] This gene duplication event and functional specialization appears to be essentially restricted to fungi. In mammals, the HTT (huntingtin) protein also shares structural similarity to yeast Atg11 and, like RB1CC1, functions as a scaffold protein in the ULK1 complex.[53]

The Atg1 complex in *D. discoideum* is evolutionarily closer to the mammalian ULK1 complex than its budding yeast counterpart. In addition to the Atg1 protein kinase,[54] Atg13 and Atg101 homologs have been identified[23] and interaction studies have shown that Atg13, like its mammalian homolog, binds to both Atg1 and Atg101 (Fig. 4). The likely RB1CC1/Atg11 homolog in *D. discoideum* is DDB_G0285767.[52] A putative Atg17 homolog has also been reported but functional studies argue against a role in autophagy,[23] thus supporting the idea that Atg17 proteins are restricted to fungi. Similarities between mammals and *D. discoideum* are not limited to the core components of the complex, as shown by the conservation of the mammalian selective autophagy receptor and Atg8-binding protein Sqstm1/p62 in *D. discoideum*.[23,55] Interestingly, *D. discoideum* Atg1 kinase also interacts with the pentose phosphate pathway (PPP) enzyme transketolase (Tkt).[23] Although no direct phosphorylation has been reported, the activity of TKT is altered in strains lacking or overexpressing Atg1, suggesting a possible crosstalk between autophagy and the PPP. Interestingly, a recent report shows that another component of the PPP, the ribose-5-phosphate isomerase (RpiA), regulate autophagy in HeLa cells.[56]

The origin of the autophagosomal membrane, function of Vmp1 and regulation of PtdIns3P

The origin and elongation of the phagophore membrane are still the subject of intense research. In mammalian cells the ER, establishing close contacts with other organelles such as mitochondria and lipid droplets, forms a specialized cradle-like

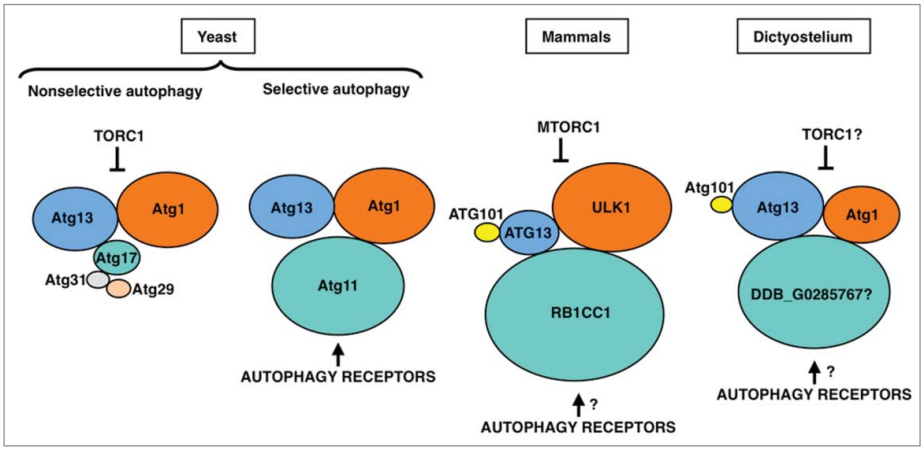

Figure 4. The Atg1/ULK1 complex in yeast, mammalian cells and *D. discoideum*. Proteins are colored according to their conservation, and protein size is proportional to the molecular weight. The inhibition of the Atg1/ULK1 kinase activity by TORC1, and its activation through binding of the autophagy receptors to the Atg11 subunit, are indicated.

structure known as the omegasome.[57] This structure is enriched in the signaling lipid PtdIns3P, generated by the class III phosphatidylinositol 3-kinase (PtdIns3K) PIK3C3/VPS34. It is thought that the phagophore expands by fusing with vesicles that originate from different cellular compartments. Some of these vesicles contain the transmembrane protein ATG9 and emanate from the Golgi and recycling endosomes,[58,59] whereas others can originate from the ER-Golgi intermediate compartment (ERGIC).[60-62]

D. discoideum autophagosomes form simultaneously in different locations of the ER[29] and are thus, in this respect, more similar to those in mammalian cells than yeast, in which autophagosomes originate from the PAS, a single spot near the vacuole. It has been proposed that *S. cerevisiae* has become highly specialized during evolution. As a result, some processes such as autophagy have diverged from a more universally conserved mechanism, which has remained unaltered in other organisms such as *D. discoideum*.[63] A valuable example of these differences is the presence in *D. discoideum* of the conserved protein Vmp1 that is required for correct formation of the omegasome, but absent in *S. cerevisiae* and other fungi.

The phenotype of Vmp1-deficient cells differs from that of cells lacking classical Atg proteins because it affects a wide array of processes apparently not connected to autophagy as described in *D. discoideum* and *Chlamydomonas reinhardtii*.[24,64] Autophagic flux is blocked in Vmp1-deficient *D. discoideum* but PtdIns3P production and subsequent recruitment of the autophagy machinery to the ER still occurs. Indeed, PtdIns3P is abnormally high in the mutants and correlates with the accumulation of enlarged omegasomes and LC3-containing structures in *D. discoideum*,[65] *C. elegans*[66] and mammalian cells.[67] Taken together, these studies suggest that Vmp1 might be required for the correct structure of the omegasome and/or the capacity of the phagophore to elongate and become a functional autophagosome. Since Vmp1 is an ER-resident protein it is tempting to speculate that Vmp1 generates an ER microenvironment that orchestrates the autophagic machinery to allow the correct expansion of the phagophore rather than the recruitment of Atg proteins (Fig. 5).

Another interesting phenotype of the Vmp1 mutant is the defect in macropinocytosis, a mechanism of nutrient uptake that allows *D. discoideum* to grow in liquid media. The abnormal accumulation of PtdIns3P in the mutant impairs macropinocytosis indirectly and prevents growth in liquid media. This conclusion is based on experiments that preclude the accumulation of PtdIns3P. Atg1 is upstream of the PtdIns3K and therefore a double mutant in Vmp1 and Atg1 lacks this abnormal signaling.[65] Remarkably, macropinocytosis and cell growth in liquid media is recovered in the double mutant, suggesting that additional nonautophagy-related defects may occur as a result of an abnormal regulation of PtdIns3P signaling at the omegasome.[65] It will be interesting to determine if such a phenomenon also occurs in mammalian cells.

The 2 ubiquitin-like (Ubl) conjugation systems are highly conserved in D. discoideum

The proteins involved in the 2 Ubl conjugation systems are highly conserved from yeast to mammalian cells and very likely function in an analogous manner in all eukaryotes including *D. discoideum*.[9] However, while yeast harbors only one isoform for each of the 8 different proteins of the 2 Ubl conjugation systems there are 2 paralogs for ATG16 (ATG16L1, L2), 4 for ATG4 (ATG4A, B, C, D) and 7 for ATG8/LC3 in mammals.[9,68,69] In particular, the large number of ATG8/LC3 paralogs in humans and mice complicates

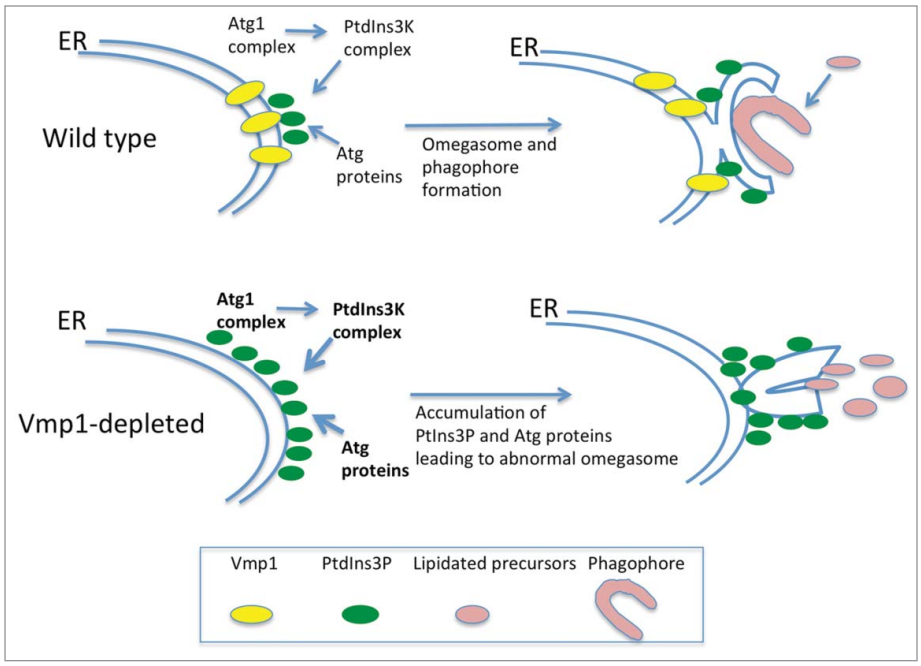

Figure 5. Vmp1 is essential for correct PtdIns3P signaling and omegasome formation in *D. discoideum* and mammalian cells. Vmp1 accumulates in subdomains of the ER where the autophagic machinery is recruited. PtdIns3P is formed at these domains to regulate omegasome formation and phagophore elongation. In the absence of Vmp1, PtdIns3P is aberrantly generated leading to persistent recruitment of autophagy proteins and unproductive autophagosome formation.

functional studies in these organisms. These proteins are grouped into the MAP1LC3 (microtubule associated protein 1 light chain 3) subfamily with 4 members (LC3A, B, B2 and C), and the GABARAP (GABA type A receptor-associated protein) subfamily with 3 members (GABARAP, GABARAPL1 and GABARAPL2/GATE16) protein.[68] The GABARAPL2 protein is approximately equally distant from the LC3 and the GABARAP subfamilies (Fig. 6) and the precise functions of the individual proteins are largely unresolved.[70] In contrast, fungi possess only a single *ATG8* gene, while plants, insects, nematodes and amoebozoa, like *D. discoideum*, usually have 2 genes for Atg8.

Phylogenetic analysis showed that *D. discoideum* Atg8a and *Acanthamoeba castellanii* Atg8 are situated in the same evolutionary branch as the orthologs from fungi and plants. In contrast, the 2 Atg8b proteins from *D. discoideum* and *A. castellanii* appear evolutionarily more closely related to the LC3 subfamily from animals (Fig. 6). Live cell imaging of *D. discoideum* cells expressing RFP-Atg8a and GFP-Atg8b showed that Atg8b associates with autophagosomes before ATG8a.[32] In mammals, LC3 subfamily members are involved in the elongation of the phagophore, whereas the GABARAP subfamily seem to be essential for a later stage in maturation.[71,72] Thus, Atg8b is likely the functional ortholog of the mammalian LC3 subfamily, which is also supported by the grouping in the evolutionary tree (Fig. 6), and Atg8a the ortholog of the GABARAP subfamily.[32] It appears therefore, that duplication of Atg8 early in eukaryotic evolution allowed specialization of the paralogs during autophagosome maturation. Expansion of the respective subfamilies in mammals likely led to the acquisition of further specialized functions in more complex animals.[70] Similarly, the Atg4 paralogs and the Atg16 paralog in the 2 Ubl conjugation systems may enable the fine-tuning of the activation of the different Atg8/LC3 family members.

Atg9 studies in D. discoideum *reveal new functions*

The multimembrane spanning Atg9 protein is the only known integral membrane protein of the core autophagic machinery and thought to be involved in the delivery of membrane lipids to the growing autophagosome.[73] Atg9 orthologs exist in all eukaryotic species so far examined and the protein is essential for autophagy. For example, in *Drosophila melanogaster*, Atg9 depletion reduces both the number and size of autophagosomes, and blocks the fusion of autophagosomes with lysosomes.[74] Modulation of Atg9 levels in yeast strains directly correlates with the frequency of autophagosome formation and autophagic activity.[75]

The PAS in yeast originates from Atg9-positive clusters, called Atg9 peripheral sites.[76] The origin of these clusters,

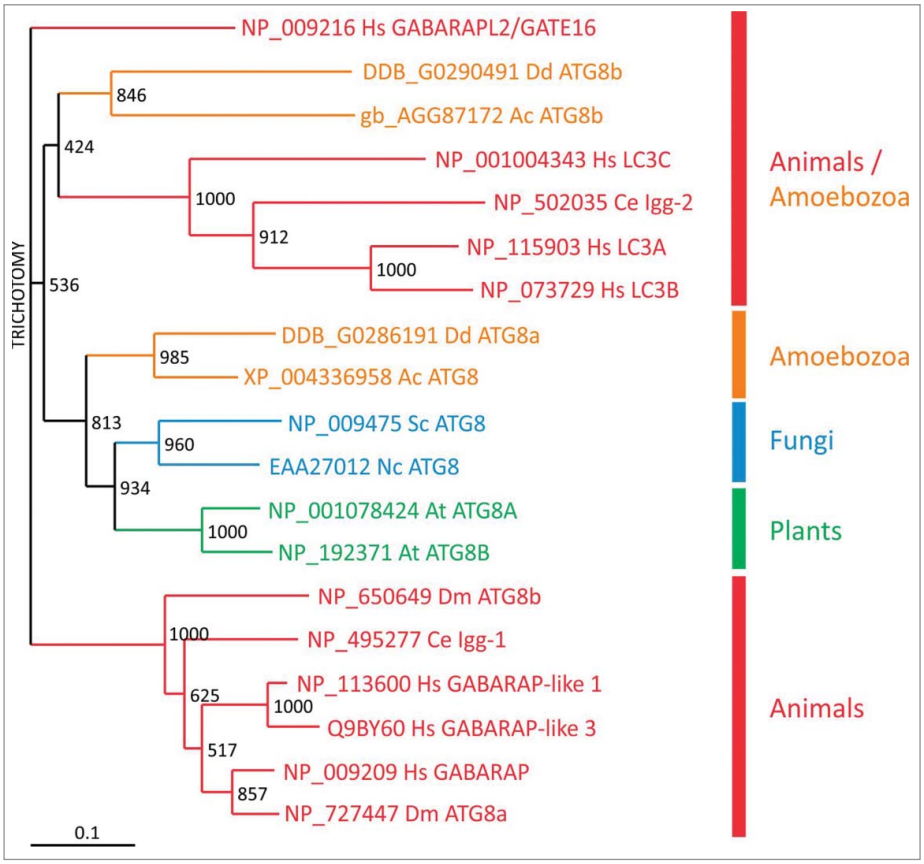

Figure 6. Evolutionary relationship of Atg8/LC3 family members. Phylogenetic analysis of Atg8/LC3 family proteins from animals (red), amoebozoa (orange), fungi (blue) and plants (green). A CLUSTALX alignment was used to create a phylogenetic tree with the TreeView program. The scale bar indicates amino acid substitutions per site. Bootstrap values are provided at the node of each branch. GenBank, SwissProt or dictyBase (http://dictybase.org/) accession numbers are provided on the right of the tree. Hs, *Homo sapiens*; Dm, *Drosophila melanogaster*; Ce, *Caenorhabditis elegans*; At, *Arabidopsis thaliana*; Nc, *Neurospora crassa*; Sc, *Saccharomyces cerevisiae*; Ac, *Acanthamoeba castellanii*; Dd, *D. discoideum*. LC3, microtubule-associated protein 1 light chain 3; GABARAP, GABA type A receptor-associated protein; GABARAPL2/GATE16, GABA type A receptor associated protein like 2; lgg: LC3, GABARAP and GATE-16 family.

however, has remained poorly understood. They localize in proximity to the mitochondrial membrane[77] and may represent vesicles derived from mitochondrial-ER contact sites. Alternatively, based on partial colocalization between Atg9 and the late Golgi protein marker Sec7, the Atg9 peripheral sites could emerge as a new organelle through the delivery of newly synthesized Atg9 to these sites via the secretory pathway.[76] Upon delivery of the lipids, Atg9 is no longer required and may be retrieved to the peripheral sites by an as yet unknown mechanism.

In mammals, there are 2 ATG9 paralogs, namely ATG9A/ATG9L1 and ATG9B/ATG9L2. ATG9A (ATG9 hereafter) is ubiquitously expressed in human adult tissues, whereas ATG9B is only expressed in placenta and pituitary gland.[78] Mammalian ATG9 is localized at the ER, the trans-Golgi network and early, late and recycling endosomes.[79,80] Recently, it was shown that in *D. melanogaster* and in human cells the Atg1/ULK1 protein kinase phosphorylates a MYLK/myosin light chain kinase, which in turn activates MYL/myosin II regulatory light chain. This is followed by myosin II activation, which apparently drives transport of ATG9-containing membranes to the phagophore.[81] *D. discoideum* Atg9 does not colocalize with mitochondria, the ER or lysosomes; however, there is a partial colocalization with the Golgi apparatus and many Atg9-GFP-containing vesicles localize along microtubules and accumulate around the microtubule organizing center.[25] Disruption of *Atg9* results in a pleiotropic phenotypes with severe impairments in development, slug migration, vegetative growth, phagocytosis, clearance of *Legionella pneumophila* and proteasomal activity.[25] A similar pleiotropic phenotype is observed in *tipD*$^{-}$*/atg16*$^{-}$ cells.[26]

Unexpectedly, some of the defects of the *atg9* knockout mutant can be partially or fully restored by expression of wild-type or point-mutated CdcD/p97, an evolutionarily highly conserved member of the AAA-ATPase family.[82] VCP/p97, the mammalian homologue, is a key player in ER-associated protein degradation, in the ubiquitin-proteasome system for protein degradation system, in aggresome formation and also in autophagosome maturation.[83-85] Heterozygous mutations in the human *VCP/p97* gene cause autosomal-dominant inclusion body myopathy with early onset Paget disease of bone and frontotemporal dementia and further neurological disorders;[86,87] however, the molecular basis of the pathogenesis remains unknown. VCP is essential for autophagosome maturation in mouse embryonic fibroblasts and, moreover, disease-causing VCP point mutations impair autophagy.[88]

Interestingly, *atg9*$^{-}$, *tipD*$^{-}$*/atg16*$^{-}$ and *atg9*$^{-}$ *tipD*$^{-}$*/atg16*$^{-}$ double mutant *D. discoideum* cells have a severe and counterintuitive defect in proteasomal activity. Since the amounts of proteasomal subunits are not altered in knockouts of *atg9* or *tipD/atg16*, this result suggests that intact autophagy is required for optimal proteasomal activity.[26,82] Furthermore, this phenotype is fully or partially suppressed by overexpression of wild-type or point-mutated *cdcD/p97* in *atg9*$^{-}$ cells. This result provides evidence that in *D. discoideum* CdcD/p97 and Atg9 are functionally directly or indirectly linked and supports the existence of a delicate balance between the 2 major protein degradation pathways, proteasomal degradation and autophagy. Disruption of this balance causes severe impairment of essential cellular functions in lower eukaryotes such as *D. discoideum* but ultimately may cause late-onset complex diseases in humans. How exactly the ubiquitin-proteasome system and autophagy are interconnected needs to be unraveled in the future.

Autophagy and disease: New leads from the social amoeba in human genetic disorders

Autophagic dysfunction may lead to defects in protein and organelle homeostasis associated with numerous human diseases.[89] A very relevant example is the connection of autophagy with major neurodegenerative diseases (including Alzheimer, Parkinson and Huntington diseases), often associated with the accumulation of abnormal protein aggregates or nonfunctional organelles. Autophagy dysfunction in *D. discoideum* often leads to the accumulation of large ubiquitinated protein aggregates.[55] Ubiquitin is a small regulatory protein that can be covalently linked to proteins to target them for proteasomal or autophagic degradation. These protein aggregates can be observed by both immunofluorescence microscopy using anti-ubiquitin antibodies and by western blot. As these aggregates are insoluble in 1% Triton X-100, they can rapidly be separated from whole cell lysates by centrifugation, separated by SDS-PAGE and detected using commercially available anti-ubiquitin antibodies. Ubiquitinated proteins are dramatically increased in the Triton-insoluble fraction of autophagy-deficient mutants.[55] The size and number of these aggregates correlates well with the severity of the phenotypes of the different autophagy mutants.[55] Interestingly, the protein aggregates formed in the Vmp1 mutant also accumulate the receptor protein Sqstm1,[55] which is involved in the clearance of several ubiquitinated cargos in mammalian cells and has been implicated in aggregation disorders and infectious diseases.[90]

Packing proteins into aggregates, if properly degraded by autophagy, could function as a regulated cellular mechanism to handle abnormal proteins that otherwise would be toxic. However, several studies in *D. discoideum* suggest that the protein aggregation phenotype might be deleterious for cell function. Overexpression of the actin-binding protein VasP fused to an endosomal targeting signal leads to the formation of huge actin aggregates reminiscent of Hirano bodies,[91] structures that are often present in neurodegenerative diseases. These actin aggregates sequester a number of actin binding and endosomal proteins promoting their disappearance from their normal location in the cytoplasm[91] leading to cytoskeletal defects. These findings open the possibility that protein sequestration might also contribute to neuronal malfunction in these pathologies. Hirano body-like aggregates can also be induced in *D. discoideum* by the overexpression of a truncated form of a 34-kDa actin-binding protein.[92] Another report showed that both autophagy and the proteasome pathway contribute to the degradation of Hirano bodies in *D. discoideum*.[91] The autophagosome marker protein GFP-Atg8 colocalizes with Hirano bodies in wild-type *D. discoideum* cells, but not in cells deficient in the autophagic proteins Atg5 or Atg1.[93] Interestingly, Hirano bodies can be released by exocytosis following autophagy, which could explain the presence of these aggregates in both intracellular and extracellular spaces in the brain.[93]

Another example using *D. discoideum* to study autophagy-related pathologies was the discovery of a possible connection of the rare disease Chorea-acanthocytosis (ChAc) with autophagy. ChAc is a neurodegenerative disease associated with abnormally shaped erythrocytes known as acanthocytes, leading to disability and premature death. ChAc is caused by loss-of-function mutations in *VPS13A*, most of which lead to a decrease or absence of the VPS13A protein (also known as Chorein).[94,95] The molecular function of this protein is not known and the literature provides fragmented and nonconclusive results. Proposed functions for VPS13A include membrane trafficking, membrane morphogenesis, phagocytosis and actin cytoskeleton regulation.[96-99] There are 3 additional VPS13 proteins in humans (VPS13B,C and D)[100] and mutations in 2 of them, VPS13B and C, lead to Cohen syndrome and Parkinson disease, respectively.[101,102] *D. discoideum* has 6 VPS13-related proteins, which are more similar to human VPS13A and C than to VPS13B or D. One of these proteins was initially named TipC since the phenotype of an insertional mutant was the formation of multiple tips in large mounds, a typical phenotype of autophagy mutants as pointed out above.[28] Several years later this mutant was revisited and the presence of a strong autophagy blockade was confirmed.[27] Subsequently, additional studies of the autophagic pathway in VPS13A-depleted human HeLa cells confirmed that autophagy could play a role in the etiology of this devastating disease.[27]

Defects in either the retromer or WASH (WAS protein family homolog) complexes also lead to endosomal trafficking and autophagy defects associated with human diseases. The WASH complex regulates the formation of actin filaments on endosomes, driving multiple endocytic protein sorting and recycling events,[103] and mutations in the gene encoding KIAA0196/strumpellin, a component of the WASH complex, cause a form of autosomal dominant hereditary spastic paraplegia.[104] Furthermore, an aspartate to asparagine substitution (D620N) in VPS35, a component of the retromer sorting complex that recruits WASH to endosomes, results in autosomal dominant familial Parkinson disease.[105] *D. discoideum* have all components of the WASH complex, and mutants in WASH also have a defect in autophagy. However, while defects either in the retromer or WASH lead to an early inhibition of autophagosome formation due to defective trafficking of ATG9-containing vesicles and deficient BECN1 activation in mammals,[105,106] *D. discoideum* WASH null cells do not have defects in the induction of autophagosome formation.[12] The observed blockade in autophagy is due to impaired recycling of vacuolar-type H^+-translocating ATPase (V-ATPase) subunits and lysosomal hydrolases that leads to a late defect in lysosome recycling that blocks degradation of the cargo.[12]

Mitochondrial diseases are complex degenerative disorders caused by mutations in mitochondrial proteins encoded in the nuclear or mitochondrial genome. *D. discoideum* has been used to study the cytopathology involved in mitochondrial disease, specially those involving alterations in pathways that affect AMP-activated protein kinase (AMPK), the kinase required to sense cellular energy levels and regulate autophagy through MTOR, ULK1 and BECN1.[4,107,108] Unexpected connections with autophagy are observed in *D. discoideum* cells deficient in components of the NADH:ubiquinone oxidoreductase or complex I, the first complex of the respiratory chain. Mutants affecting complex I assembly factors Ndufaf5 and MidA/Ndufaf7 have a strong activation of bulk autophagy,[109,110] but not mitophagy, which, in the case of MidA could be mediated by a chronic activation of AMPK. Given the importance of autophagy in cellular homeostasis, this connection might have relevance in human pathology and subsequently a similar phenomenon has been observed in skin fibroblast cultures derived from patients with mitochondrial disease.[111,112]

Autophagy and bacterial infectious diseases in D. discoideum

Autophagy also represents an efficient mechanism for eukaryotic cells to capture and kill invading pathogens. The killing of intracellular pathogens by autophagy, termed "xenophagy," is therefore emerging as a major regulator of both cytosolic and vacuolar pathogens. Many bacterial pathogens are able to manipulate, either by inhibition or induction, the host xenophagic response to take advantage of autophagy for their own benefits.[113] Since *D. discoideum* lives in the soil and feeds on bacteria and yeasts, it likely developed mechanisms to discriminate between food and pathogenic organisms early during evolution. Due to its easy experimental manipulation, *D. discoideum* has become a useful model to study host-pathogen interactions and xenophagy[9] and in the past 5 y has been used to study interactions of the host autophagic machinery with pathogenic microbes such as *Salmonella enterica* serovar Typhimurium (*S. enterica*), *L. pneumophila*, Francisella *noatunensis, Staphylococcus aureus* and *Mycobacterium marinum*.[26,35,114-118] Furthermore, *D. discoideum* has also been used to identify and dissect the mechanisms of action of drugs with potential utility in medical therapy against pathogens.[119-122]

M. marinum infects mainly fish and frogs, but it can also produce skin lesions in humans. Due to safety reasons and to the faster growth rate than its close relative *M. tuberculosis*,[123] *M. marinum* represents an easier tool to research mycobacterial pathogenesis. In mammalian cells and zebrafish, *M. marinum* induces an autophagic response that includes upregulation of some autophagy-related genes and LC3 recruitment to the mycobacteria-containing vacuole (MCV).[124-128] This recognition by the autophagy machinery requires the activity of the mycobacterial pore-forming toxin ESAT-6, and engagement of the host autophagy-related proteins SQSTM1, MYD88 (myeloid differentiation primary response 88), DRAM1 (DNA damage regulated autophagy modulator protein 1) and TMEM173/STING (transmembrane protein 173).[124,125,129,130] ESAT-6 is secreted by the type VII secretion system ESX-1, and induces permeabilization of the MCV membrane, exposing *M. marinum* to the cytosol.[131] As a consequence, the ESX-1-dependent membrane damage allows the host autophagy machinery to recognize bacterial products including DNA, and to induce an autophagic response dependent on the cytosolic DNA-sensing TMEM173/STING pathway.[125,129] However, apart from its indirect role in MCV permeabilization, ESX-1 seems to be dispensable for ubiquitination of *M. marinum* in macrophages.[130]

It has been recently shown that, in *D. discoideum*, the autophagy machinery is not only recruited to cytosolic *M. marinum*, but it also targets the bacteria escaping out of

hosts cell by the nonlytic mechanism called "ejection."[35,132] During this process, ubiquitin, Atg8, Sqstm1 and Atg18 localize at the distal pole of the ejecting bacteria, with a proposed function in sealing the plasma membrane wound.[35] This recruitment of autophagy to the ejecting bacteria seems to be independent on ESX-1, as well as on other *M. marinum* virulence factors. However, host Atg1, Atg5, Atg6A and Atg7 are all required for Atg8 association with the ejecting bacterium suggesting that this process may be entirely driven by the host. Furthermore, even though Atg1 is not necessary for ejectosome formation, it is essential for the tight membrane sealing during ejection, avoiding cytosolic leakage and, thereby, death upon bacterial egress.[35]

Interestingly, disruption of *Sqstm1*, encoding the only selective autophagy receptor protein described so far in *D. discoideum*, seems to have no effect on Atg8 recruitment to *M. marinum*. Gerstenmaier and collaborators thus suggest that other receptor proteins must exist in this amoeba.[35] Ubiquitin-binding CUE-domain containing proteins have been recently described to act as autophagy recepptors for protein aggregates in yeast and humans. Consistent with the evolutionary conservation of these proteins, 2 *D. discoideum* CUE domain-containing proteins, CnrD and DDB_G0274365/CueA also localize to MCVs (Drs. J. King and T. Soldati, unpublished results). In addition to the domain for ubiquitin binding, these proteins present LIR motifs in their sequences (Fig. 7), making them ideal selective autophagy receptor candidates.

The WASH complex is also necessary for *M. marinum* ejection and is possibly involved in *D. discoideum* xenophagy.[118] During infection, WASH-induced actin polymerization prevents MCV acidification by promoting recycling of the V-ATPase, rendering the compartment more permissive to infection.[118] This correlates with previous results in mammalian cells, in which *M. marinum* modifies the composition of its MCV by depleting the V-ATPase and the lysosomal protease CTSD (cathepsin D), as also observed during infection of *D. discoideum*.[124,133]

D. discoideum has also been recently established as a model host for another fish pathogen, *F. noatunensis*.[116] This Gram-negative bacterium exploits autophagy in human and murine macrophages.[134,135] In *D. discoideum*, the mRNA levels of *atg8* and *sqstm1* slightly increase during *F. noatunensis* infection, and Atg8, Sqstm1 and ubiquitin are recruited to the compartment containing this bacterium, suggesting an induction of

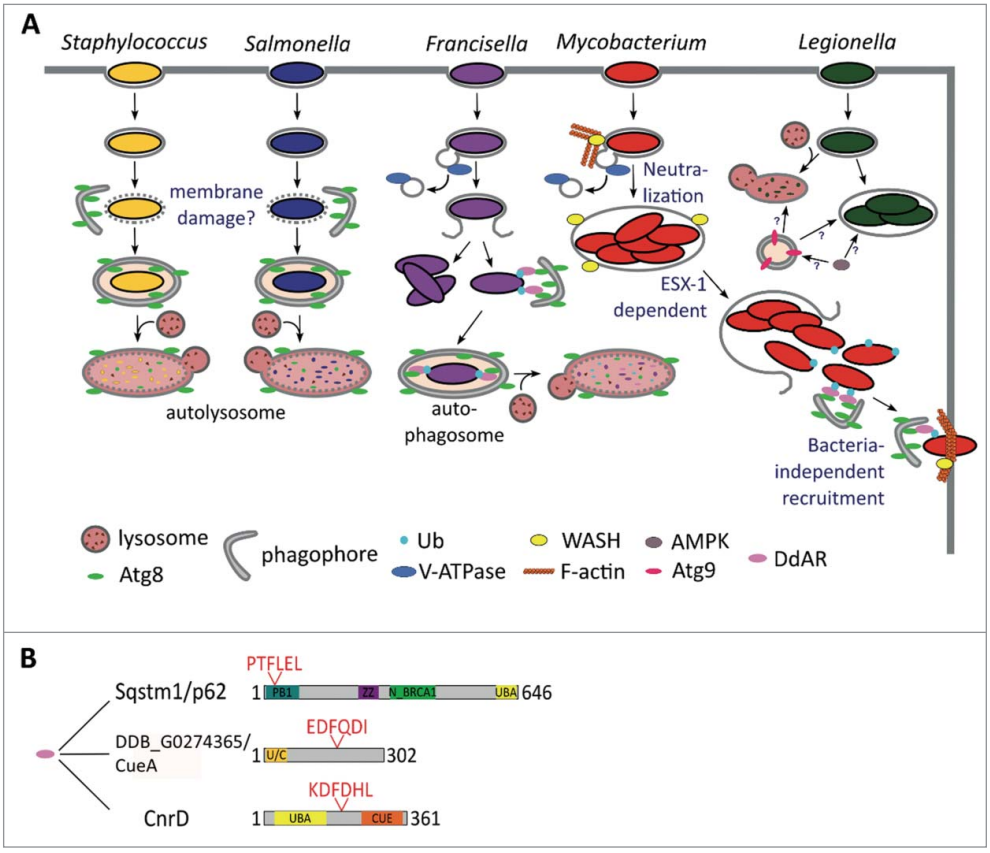

Figure 7. Xenophagy in *D. discoideum*. (A) The autophagosomal marker Atg8 is recruited to the compartment harboring both *S. aureus* and *S. enterica*, which might be a response to the putative membrane damage produced by these bacteria. As a consequence, the bacteria are engulfed in phagophores and killed in autolysosomes, where the lumenal leaflet Atg8 is digested. After uptake by *D. discoideum, F. noatunensis* escapes phagosomal maturation and resides in a compartment lacking the V-ATPase. The majority of *F. noatunensis* replicates in the cytosol, while a small proportion of bacteria succumb to autophagy; *M. marinum* also prevents phagosomal acidification by the V-ATPase via WASH-induced actin polymerization. After proliferation inside the MCV, *M. marinum* is released to the cytosol, where it recruits the autophagy machinery, but does not seem to be fully engulfed in autophagosomes (unpublished observations). Finally, *M. marinum* is ejected through the *D. discoideum* plasma membrane in an autophagy-dependent manner; Atg9 controls *L. pneumophila* infection, whereas the autophagy activator kinase AMPK enhances its proliferation. Therefore, the function of autophagy during *L. pneumophila* in *D. discoideum* remains unclear. (B) Domain and motif organization of the already characterized *D. discoideum* autophagy receptor (DdAR) Sqstm1 and the 2 additional putative adaptors CnrD and DDB_G0274365/CueA. PB1, Phox and Bem1 domain; ZZ, zinc finger, ZZ-type; N_BRCA1, Next to BRCA1, central domain; UBA, ubiquitin-associated domain; CUE, ubiquitin system component Cue; U/C, UBA and CUE domains. Protein domains and LIR motifs were predicted with the web prediciton resources InterPro (http://www.ebi.ac.uk/interpro) and iLIR, respectively.

autophagy. Furthermore, autophagy controls intracellular proliferation of *F. noatunensis*, since deletion of *atg1* in *D. discoideum* increases the bacterial burden after 24 h of infection.[116]

In contrast to growth of *F. noatunensis, L. pneumophila* shows similar proliferation kinetics when infecting wild-type and *atg1*$^{-}$, *atg5*$^{-}$, *atg6A*$^{-}$, *atg7*$^{-}$ and *atg8*$^{-}$ *D. discoideum* cells. Likewise, this intracellular pathogen of amoebae and macrophages, rarely recruits Atg8, suggesting that xenophagy is not involved in amoebal immunity against *L. pneumophila*.[136] Whether *L. pneumophila* actively escapes autophagic capture in *D. discoideum* by uncoupling Atg8 from the phagophore membrane, via action of the RavZ toxin, as it does in human cells,[137] remains to be studied. Interestingly, Atg9 might be involved in controlling *L. pneumophila*, because its expression rises after 24 h of infection, and bacterial clearance decreases in *atg9*$^{-}$ cells. Uptake of this bacterium is also decreased in *atg9*$^{-}$, *tipD*$^{-}$/*atg16*$^{-}$ and *atg9*$^{-}$ *tipD*$^{-}$/*atg16*$^{-}$ double-mutant *D. discoideum* cells.[25,26] However, the mechanism is unclear, because, contrary to *atg9*, the expression of TipD/Atg16 and Atg8a is downregulated after infection with *L. pneumophila*.[25] Interestingly, the intracellular proliferation of *L. pneumophila* in *D. discoideum* increases in cells overexpressing the catalytic subunit of AMPK. Since AMPK regulates ATG9 localization via the activation of ULK1 in mammalian cells,[138] the different *L. pneumophila* proliferation rates observed during infection of *atg1*$^{-}$, *atg9*$^{-}$ and AMPK-overexpressing cells may indicate autophagy-independent functions for Atg9 and TipD/Atg16 as suggested by Xiong and collaborators.[26]

Finally, it is controversial whether *S. enterica*, one of the Gram-negative bacteria more commonly used in laboratories to study the host innate immune responses at the molecular level,[139] is pathogenic or not for *D. discoideum*. *S. enterica* survives and proliferates inside very diverse human cell types,[140] but both its survival and death inside amoebae have been reported.[114,141,142] Sillo and collaborators proposed that the discrepancies observed might be due to the use of the antibiotic gentamicin, normally employed in *S. enterica* infection protocols for mammalian cells. Gentamicin is likely to be taken up in large quantities by macropinocytosis during *D. discoideum* infection, thus affecting intracellular bacteria.[114] Regardless, early during infection of *D. discoideum*, Atg8 is recruited to the compartment harboring *S. enterica*,[142] and concomitant cleavage of GFP-Atg8 suggests an enhanced autophagic response.[115] Together with the fact that *atg1*$^{-}$, *atg6A*$^{-}$ and *atg7*$^{-}$ cells are more permissive for *S. enterica* growth,[142] this observation implies a rapid autophagy-dependent killing of these bacteria by *D. discoideum* cells.

Autophagy has also been implicated during infection of lipopolysaccharide-treated *D. discoideum* cells with *S. aureus*.[115] The fate of this Gram-positive bacterium inside amoebae is affected by autophagy, since its uptake is reduced in *atg9*$^{-}$ cells.[25,115] Treatment with lipopolysaccharide, which also induces bacteria clearance in an Atg1- and Atg9-dependent manner, further increases the localization of Atg8 to the vacuoles containing *S. aureus*.[115] Because *S. aureus* localizes to LC3-labeled compartments and subverts the autophagy pathway in mammalian cells,[143-145] manipulating autophagy with protease inhibitors or compounds blocking autolysosome formation is needed to confirm the induction or blockade of autophagy by these bacteria.[146]

In conclusion, different bacterial species differentially subvert autophagy in *D. discoideum*, as occurs in mammalian cells. The *D. discoideum* autophagy machinery is recruited to *S. aureus, S. enterica, F. noatunensis* and *M. marinum* at different stages during infection (Fig. 7). This recruitment is normally induced by the damage or rupture of the bacteria-containing compartments and, as a consequence, the bacteria are killed in autolysosomes. However, both *F. noatunensis* and *M. marinum* are able to prevent phagosomal acidification by the V-ATPase, therefore, bypassing xenophagy.

Autophagy and cell death pathways in D. discoideum

In addition to caspase-mediated apoptosis in animal cells, an increasing number of nonapoptotic cell death types are being reported within and outside the animal kingdom. In these multiple different cell death types there might be common, conserved cell death core elements that can be analyzed through studying cell death in alternative model organisms[147] such *D. discoideum*.

The *D. discoideum* fruiting body includes a stalk made of vacuolized, cellulose-walled dead cells.[148] This developmental cell death can be mimicked in vitro in monolayer conditions[149-151] that include a stereotyped sequence of events[9,150] such as vacuolization and cellulose encasing (Fig. 8). The induction of this process requires 2 exogenous signals. The first signal, starvation and cAMP, sensitizes the cells. Only cells which have received this first signal can be induced to die by a second signal, classically the polyketide DIF-1.[152] In starved cells subjected to DIF-1, autophagy determines the type of cell

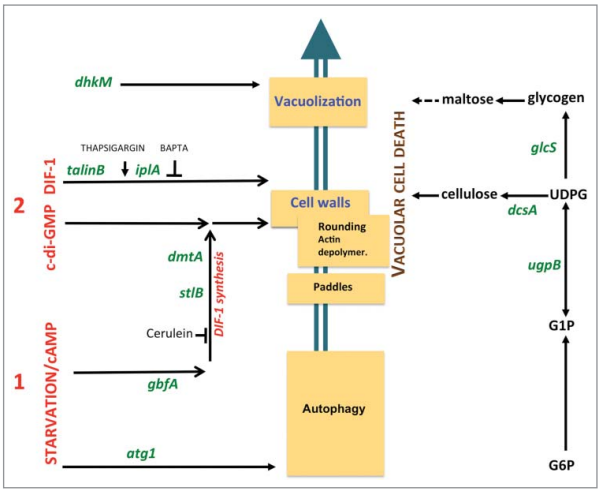

Figure 8. Genes and pathways governing *D. discoideum* vacuolar cell death. The cascade of subcellular cell death events is schematically depicted (*middle*). These include the formation of "paddle" cells, following by their rounding, biogenesis of a cellulose shell and extensive vacuolization. Random insertional mutagenesis and targeted mutagenesis identified a number of genes, here shown in green letters, encoding molecules required for this cell death. Details are given in the main text. These genes in turn helped define pathways to cell death, such as a polysaccharide pathway (*right*), a first signal pathway induced by starvation and cAMP (*lower left*) and second signal pathways (*upper left*). The latter include a DIF-1-induced autonomous pathway and a c-di-GMP pathway requiring endogenously synthesized or exogenous DIF-1. Ca^{2+}-related drugs such as thapsigargin and BAPTA affect DIF-1 signaling leading to cell death.

death. In the presence of autophagy, DIF-1 induces a normal vacuolar cell death. However, in the absence of autophagy, DIF-1 induces necrotic cell death.[153,154] This necrotic death includes mitochondrial uncoupling[155-157] and depends not only on the absence of autophagy upon starvation, but also on given targets of the DIF-1 molecule, distinct from those that induce vacuolar cell death.[158] These results are in line with the known mitochondrial uncoupling effects of DIF-1 treatment[159] and with the recently demonstrated multiplicity of DIF-1-induced effects.[160] Importantly, although both pathways result in programmed death, while vacuolar cell death is part of normal development, necrotic cell death is incompatible with it.[153]

Whether autophagy is also involved at the execution stage of vacuolar cell death has not been unambiguously proven. However, a large amount of debris is observed in the death-accompanying vacuoles indicating active degradation. Autophagy has also been proposed to have a structural role in terminal stalk differentiation.[15] Stalk-cell vacuoles seem to originate from acidic vesicles and autophagosomes, which fuse to form autolysosomes. Their repeated fusion expands the vacuole, accompanied by cellulose wall formation enabling the stalk cells to make the stalk rigid and hold the spores aloft.[15]

DIF-1-induced vacuolar cell death in monolayers has been studied by random insertional mutagenesis. This led to the identification of a number of molecules required for this pathway, including the ITPR/IP3R homolog Ca^{2+} flux-controlling IplA,[161] the UDP-glucose pyrophosphorylase UgpB, the glycogen synthase GlcS,[162] the histidine kinase DhkM,[163] the transcription factor GbfA and the integrin-cytoskeleton intermediate TalB/talinB.[157] These and other studies have contributed to defining molecular pathways required for DIF-1-induced vacuolar cell death (Fig. 8).

An important recent discovery was the demonstration that not only DIF-1, but also the cyclic dinucleotide c-di-GMP are able to induce *D. discoideum* cell death.[164,165] c-di-GMP is a universal bacterial second messenger[166] and can trigger innate immunity in bacterially-infected animal cells.[167] Unexpectedly, experiments using both inducers show marked synergy,[168] although c-di-GMP alone is insufficient to induce cell death in *D. discoideum* cell monolayers, requiring either DIF-1 or a DIF-1-related polyketide. The required DIF-1 can be endogenous, as shown by the inability of c-di-GMP to induce cell death when DIF-1 synthesis was blocked pharmacologically (by cerulenin), and by its rescue upon complementation by exogenous DIF-1.[168] This was confirmed genetically using mutants in the polyketide synthase *stlB* and the methylase *dmtA* genes that are required for DIF-1 biosynthesis.[169,170] The corresponding $stlB^-$ or $dmtA^-$ mutant cells cannot be induced to die by exogenous c-di-GMP, and this can be complemented by exogenous DIF-1.[168] Thus, c-di-GMP can only trigger cell death in the presence of DIF1 or DIF-1-related polyketides, providing an additional level of control to this, and perhaps other c-di-GMP-dependent pathways.

How c-di-GMP synergizes with endogenous DIF-1, to drive cell death is not clear. However, at least part of the c-di-GMP pathway seems to be distinct from the autonomous DIF-1 pathway, since mutants of the latter, $talB^-$ and $iplA^-$, do not impair the former.[168] Among several cytosolic molecules able to sense c-di-GMP in animal cells, DDX41[171] is especially well conserved and has a clear *D. discoideum* ortholog. Attempts to inactivate *D. discoideum* DDX41 by targeted mutagenesis have not led to alterations of cell death so far (Y. Song, unpublished) although several other c-di-GMP binding proteins have been reported.[172] Studying not only DIF-1- but also c-di-GMP-induced cell death in *D. discoideum* may provide important detail on the molecular mechanisms, including the role of autophagy, as well as suggestions as to how c-di-GMP acts in animal cells.

Concluding remarks

The strong conservation of the autophagic pathway between *D. discoideum* and mammalian cells justifies the use of this social amoeba as a model system for the study of the molecular mechanisms of autophagy and autophagy-related diseases. For basic studies *D. discoideum* can beautifully complement the enormous wealth of information obtained in *S. cerevisiae*, in particular those genes not conserved in yeast. In recent years, this potential has also become a reality in a wide range of biomedical conditions as exemplified in the use of *D. discoideum* as a surrogate host for studying the role of autophagy in infectious diseases.

Disclosure of potential conflicts of interest

No potential conflicts of interest were disclosed.

Funding

This work was supported by grant BFU2015-64440-P (MINECO/FEDER) to R.E. and O.V. from the Spanish Ministerio de Ciencia e Innovación. LE acknowledges support of this work by the German Research Foundation (Deutsche Forschungsgemeinschaft: CRC670, TP01) and by Köln Fortune.

References

[1] Muñoz-Braceras S, Mesquita A, Escalante R. *Dictyostelium discoideum* as a model in biomedical research. In: Romeralo M, Baldauf S, Escalante R, eds. Dictyostelids Evolution, Genomics and Cell Biology. Berlin: Springer, 2013:1-34.

[2] Steinert M. Pathogen-host interactions in Dictyostelium, Legionella, Mycobacterium and other pathogens. Semin Cell Dev Biol 2011; 22:70-6; PMID:21109012; http://dx.doi.org/10.1016/j.semcdb.2010.11.003

[3] Carnell MJ, Insall RH. Actin on disease - Studying the pathobiology of cell motility using *Dictyostelium discoideum*. Semin Cell Dev Biol 2010; 22:82-8; PMID:21145982; http://dx.doi.org/10.1016/j.semcdb.2010.12.003

[4] Francione LM, Annesley SJ, Carilla-Latorre S, Escalante R, Fisher PR. The Dictyostelium model for mitochondrial disease. Semin Cell Dev Biol 2011; 22:120-30; PMID:21129494; http://dx.doi.org/10.1016/j.semcdb.2010.11.004

[5] Ludtmann MH, Boeckeler K, Williams RS. Molecular pharmacology in a simple model system: implicating MAP kinase and phosphoinositide signalling in bipolar disorder. Semin Cell Dev Biol 2011; 22:105-13; PMID:21093602; http://dx.doi.org/10.1016/j.semcdb.2010.11.002

[6] Alexander S, Alexander H. Lead genetic studies in *Dictyostelium discoideum* and translational studies in human cells demonstrate that sphingolipids are key regulators of sensitivity to cisplatin and other anticancer drugs. Semin Cell Dev Biol 2011; 22:97-104; PMID:20951822; http://dx.doi.org/10.1016/j.semcdb.2010.10.005

[7] Myre MA. Clues to gamma-secretase, huntingtin and Hirano body normal function using the model organism *Dictyostelium discoideum*. J Biomed Sci 2012; 19:41; PMID:22489754; http://dx.doi.org/10.1186/1423-0127-19-41

[8] Maniak M. Dictyostelium as a model for human lysosomal and trafficking diseases. Semin Cell Dev Biol 2011; 22:114-9; PMID:21056680; http://dx.doi.org/10.1016/j.semcdb.2010.11.001

[9] Calvo-Garrido J, Carilla-Latorre S, Kubohara Y, Santos-Rodrigo N, Mesquita A, Soldati T, Golstein P, Escalante R. Autophagy in Dictyostelium: genes and pathways, cell death and infection. Autophagy 2010; 6:686-701; PMID:20603609; http://dx.doi.org/10.4161/auto.6.6.12513

[10] Cotter DA, Miura-Santo LY, Hohl HR. Ultrastructural changes during germination of *Dictyostelium discoideum* spores. J Bacteriol 1969; 100:1020-6; PMID:5391047

[11] De Duve C, Wattiaux R. Functions of lysosomes. Annu Rev Physiol 1966; 28:435-92; PMID:5322983; http://dx.doi.org/10.1146/annurev.ph.28.030166.002251

[12] King JS, Gueho A, Hagedorn M, Gopaldass N, Leuba F, Soldati T, Insall RH. WASH is required for lysosomal recycling and efficient autophagic and phagocytic digestion. Mol Biol Cell 2013; 24:2714-26; PMID:23885127; http://dx.doi.org/10.1091/mbc.E13-02-0092

[13] Otto GP, Wu MY, Kazgan N, Anderson OR, Kessin RH. Macroautophagy is required for multicellular development of the social amoeba *Dictyostelium discoideum*. J Biol Chem 2003; 278:17636-45; PMID:12626495; http://dx.doi.org/10.1074/jbc.M212467200

[14] Cabral M, Anjard C, Malhotra V, Loomis WF, Kuspa A. Unconventional secretion of AcbA in Dictyostelium discoideum through a vesicular intermediate. Eukaryot Cell 2010; 9:1009-17; PMID:20472692; http://dx.doi.org/10.1128/ec.00337-09

[15] Uchikawa T, Yamamoto A, Inouye K. Origin and function of the stalk-cell vacuole in Dictyostelium. Dev Biol 2011; 352:48-57; PMID:21256841; http://dx.doi.org/10.1016/j.ydbio.2011.01.014

[16] Cuervo AM, Wong E. Chaperone-mediated autophagy: roles in disease and aging. Cell Res 2014; 24:92-104; PMID:24281265; http://dx.doi.org/10.1038/cr.2013.153

[17] Li WW, Li J, Bao JK. Microautophagy: lesser-known self-eating. Cell Mol Life Sci 2012; 69:1125-36; PMID:22080117; http://dx.doi.org/10.1007/s00018-011-0865-5

[18] Zaffagnini G, Martens S. Mechanisms of selective autophagy. J Mol Biol 2016; 482:1714-24; http://dx.doi.org/10.1016/j.jmb.2016.02.004

[19] Feng Y, He D, Yao Z, Klionsky DJ. The machinery of macroautophagy. Cell Res 2014; 24:24-41; PMID:24366339; http://dx.doi.org/10.1038/cr.2013.168

[20] Parzych KR, Klionsky DJ. An Overview of autophagy: Morphology, mechanism, and regulation. Antioxid Redox Signal 2014; 20:460-73; PMID:23725295; http://dx.doi.org/10.1089/ars.2013.5371

[21] Ktistakis NT, Tooze SA. Digesting the expanding mechanisms of autophagy. Trends Cell Biol 2016; Apr. 2:S0962-8924(16)00045-3

[22] Otto GP, Wu MY, Kazgan N, Anderson OR, Kessin RH. Dictyostelium macroautophagy mutants vary in the severity of their developmental defects. J Biol Chem 2004; 279:15621-9; PMID:14736886; http://dx.doi.org/10.1074/jbc.M311139200

[23] Mesquita A, Tabara LC, Martinez-Costa O, Santos-Rodrigo N, Vincent O, Escalante R. Dissecting the function of Atg1 complex in Dictyostelium autophagy reveals a connection with the pentose phosphate pathway enzyme transketolase. Open Bio 2015; 5:pii: 150088.

[24] Calvo-Garrido J, Carilla-Latorre S, Lazaro-Dieguez F, Egea G, Escalante R. Vacuole membrane protein 1 is an endoplasmic reticulum protein required for organelle biogenesis, protein secretion, and development. Mol Biol Cell 2008; 19:3442-53; PMID:18550798; http://dx.doi.org/10.1091/mbc.E08-01-0075

[25] Tung SM, Unal C, Ley A, Pena C, Tunggal B, Noegel AA, Krut O, Steinert M, Eichinger L. Loss of Dictyostelium ATG9 results in a pleiotropic phenotype affecting growth, development, phagocytosis and clearance and replication of Legionella pneumophila. Cell Microbiol 2010; 12:765-80; PMID:20070309; http://dx.doi.org/10.1111/j.1462-5822.2010.01432.x

[26] Xiong Q, Unal C, Matthias J, Steinert M, Eichinger L. The phenotypes of ATG9, ATG16 and ATG9/16 knock-out mutants imply autophagy-dependent and -independent functions. Open Bio 2015; 5:150008; http://dx.doi.org/10.1098/rsob.150008

[27] Munoz-Braceras S, Calvo R, Escalante R. TipC and the chorea-acanthocytosis protein VPS13A regulate autophagy in Dictyostelium and human HeLa cells. Autophagy 2015; 11:918-27; PMID:25996471; http://dx.doi.org/10.1080/15548627.2015.1034413

[28] Stege JT, Laub MT, Loomis WF. tip genes act in parallel pathways of early Dictyostelium development. Dev Genet 1999; 25:64-77; PMID:10402673; http://dx.doi.org/10.1002/(SICI)1520-6408(1999)25:1%3c64::AID-DVG7%3e3.0.CO;2-1

[29] King JS, Veltman DM, Insall RH. The induction of autophagy by mechanical stress. Autophagy 2011; 7:1490-9; PMID:22024750; http://dx.doi.org/10.4161/auto.7.12.17924

[30] Rosel D, Khurana T, Majithia A, Huang X, Bhandari R, Kimmel AR. TOR complex 2 (TORC2) in Dictyostelium suppresses phagocytic nutrient capture independently of TORC1-mediated nutrient sensing. J Cell Sci 2012; 125:37-48; PMID:22266904; http://dx.doi.org/10.1242/jcs.077040

[31] Kabeya Y, Mizushima N, Ueno T, Yamamoto A, Kirisako T, Noda T, Kominami E, Ohsumi Y, Yoshimori T. LC3, a mammalian homologue of yeast Apg8p, is localized in autophagosome membranes after processing. EMBO J 2000; 19:5720-8; PMID:11060023; http://dx.doi.org/10.1093/emboj/19.21.5720

[32] Matthias J, Messling S, Eichinger L. The two Dictyostelium autophagy eight proteins, ATG8a and ATG8b, associate with the autophagosome in succession. Eur J Cell Biol 2016; 95:15-25; PMID:26697781; http://dx.doi.org/10.1016/j.ejcb.2015.10.007

[33] Krick R, Henke S, Tolstrup J, Thumm M. Dissecting the localization and function of Atg18, Atg21 and Ygr223c. Autophagy 2008; 4:896-910; PMID:18769150; http://dx.doi.org/10.4161/auto.6801

[34] Polson HE, de Lartigue J, Rigden DJ, Reedijk M, Urbe S, Clague MJ, Tooze SA. Mammalian Atg18 (WIPI2) localizes to omegasome-anchored phagophores and positively regulates LC3 lipidation. Autophagy 2010; 6:506-22; PMID:20505359; http://dx.doi.org/10.4161/auto.6.4.11863

[35] Gerstenmaier L, Pilla R, Herrmann L, Herrmann H, Prado M, Villafano GJ, Kolonko M, Reimer R, Soldati T, King JS, et al. The autophagic machinery ensures nonlytic transmission of mycobacteria. Proc Natl Acad Sci U S A 2015; 112:E687-92; PMID:25646440; http://dx.doi.org/10.1073/pnas.1423318112

[36] Kimura S, Noda T, Yoshimori T. Dissection of the autophagosome maturation process by a novel reporter protein, tandem fluorescent-tagged LC3. Autophagy 2007; 3:452-60; PMID:17534139; http://dx.doi.org/10.4161/auto.4451

[37] Mesquita A, Calvo-Garrido J, Carilla-Latorre S, Escalante R. Monitoring autophagy in Dictyostelium. Methods Mol Biol 2013; 983:461-70; PMID:23494324; http://dx.doi.org/10.1007/978-1-62703-302-2_26

[38] Calvo-Garrido J, Carilla-Latorre S, Mesquita A, Escalante R. A proteolytic cleavage assay to monitor autophagy in Dictyostelium discoideum. Autophagy 2011; 7:1063-8; PMID:21876387; http://dx.doi.org/10.4161/auto.7.9.16629

[39] Welter E, Thumm M, Krick R. Quantification of nonselective bulk autophagy in *S. cerevisiae* using Pgk1-GFP. Autophagy 2010; 6:794-7; PMID:20523132; http://dx.doi.org/10.4161/auto.6.6.12348

[40] Lin MG, Hurley JH. Structure and function of the ULK1 complex in autophagy. Curr Opin Cell Biol 2016; 39:61-8; PMID:26921696; http://dx.doi.org/10.1016/j.ceb.2016.02.010

[41] Russell RC, Tian Y, Yuan H, Park HW, Chang YY, Kim J, Kim H, Neufeld TP, Dillin A, Guan KL. ULK1 induces autophagy by phosphorylating Beclin-1 and activating VPS34 lipid kinase. Nat Cell Biol 2013; 15(7):741-50; PMID:23685627

[42] Papinski D, Schuschnig M, Reiter W, Wilhelm L, Barnes CA, Maiolica A, Hansmann I, Pfaffenwimmer T, Kijanska M, Stoffel I, et al. Early steps in autophagy depend on direct phosphorylation of Atg9 by the Atg1 kinase. Mol Cell 2014; 53:471-83; PMID:24440502; http://dx.doi.org/10.1016/j.molcel.2013.12.011

[43] Noda NN, Fujioka Y. Atg1 family kinases in autophagy initiation. Cell Mol Life Sci 2015; 72(16):3083-96; PMID:25948417

[44] Mao K, Chew LH, Inoue-Aono Y, Cheong H, Nair U, Popelka H, Yip CK, Klionsky DJ. Atg29 phosphorylation regulates

coordination of the Atg17-Atg31-Atg29 complex with the Atg11 scaffold during autophagy initiation. Proc Natl Acad Sci U S A 2013; 110:E2875-84; PMID:23858448; http://dx.doi.org/10.1073/pnas.1300064110

[45] Kamada Y, Yoshino K, Kondo C, Kawamata T, Oshiro N, Yonezawa K, Ohsumi Y. Tor directly controls the Atg1 kinase complex to regulate autophagy. Mol Cell Biol 2010; 30:1049-58; PMID:19995911; http://dx.doi.org/10.1128/mcb.01344-09

[46] Kamber RA, Shoemaker CJ, Denic V. Receptor-bound targets of selective autophagy use a scaffold protein to activate the Atg1 kinase. Mol Cell 2015; 59:372-81; PMID:26166702; http://dx.doi.org/10.1016/j.molcel.2015.06.009

[47] Khaminets A, Behl C, Dikic I. Ubiquitin-dependent and independent signals in selective autophagy. Trends Cell Biol 2016; 26:6-16; PMID:26437584; http://dx.doi.org/10.1016/j.tcb.2015.08.010

[48] Hosokawa N, Sasaki T, Iemura S, Natsume T, Hara T, Mizushima N. Atg101, a novel mammalian autophagy protein interacting with Atg13. Autophagy 2009; 5:973-9; PMID:19597335; http://dx.doi.org/10.4161/auto.5.7.9296

[49] Mercer CA, Kaliappan A, Dennis PB. A novel, human Atg13 binding protein, Atg101, interacts with ULK1 and is essential for macroautophagy. Autophagy 2009; 5:649-62; PMID:19287211; http://dx.doi.org/10.4161/auto.5.5.8249

[50] Suzuki H, Kaizuka T, Mizushima N, Noda NN. Structure of the Atg101-Atg13 complex reveals essential roles of Atg101 in autophagy initiation. Nat Struct Mol Biol 2015; 22:572-80; PMID:26030876; http://dx.doi.org/10.1038/nsmb.3036

[51] Qi S, Kim do J, Stjepanovic G, Hurley JH. Structure of the human Atg13-Atg101 HORMA heterodimer: an interaction hub within the ULK1 complex. Structure 2015; 23:1848-57; PMID:26299944; http://dx.doi.org/10.1016/j.str.2015.07.011

[52] Li F, Chung T, Vierstra RD. Autophagy-related 11 plays a critical role in general autophagy- and senescence-induced mitophagy in Arabidopsis. Plant Cell 2014; 26:788-807; PMID:24563201; http://dx.doi.org/10.1105/tpc.113.120014

[53] Rui YN, Xu Z, Patel B, Chen Z, Chen D, Tito A, David G, Sun Y, Stimming EF, Bellen HJ, et al. Huntingtin functions as a scaffold for selective macroautophagy. Nat Cell Biol 2015; 17:262-75; PMID:25686248; http://dx.doi.org/10.1038/ncb3101

[54] Tekinay T, Wu MY, Otto GP, Anderson OR, Kessin RH. Function of the Dictyostelium discoideum Atg1 kinase during autophagy and development. Eukaryot Cell 2006; 5:1797-806; PMID:17031001; http://dx.doi.org/10.1128/ec.00342-05

[55] Calvo-Garrido J, Escalante R. Autophagy dysfunction and ubiquitin-positive protein aggregates in Dictyostelium cells lacking Vmp1. Autophagy 2010; 6:100-9; PMID:20009561; http://dx.doi.org/10.4161/auto.6.1.10697

[56] Heintze J, Costa JR, Weber M, Ketteler R. Ribose 5-phosphate isomerase inhibits LC3 processing and basal autophagy. Cell Signal 2016; 28:1380-8; PMID:27328773; http://dx.doi.org/10.1016/j.cellsig.2016.06.015

[57] Axe EL, Walker SA, Manifava M, Chandra P, Roderick HL, Habermann A, Griffiths G, Ktistakis NT. Autophagosome formation from membrane compartments enriched in phosphatidylinositol 3-phosphate and dynamically connected to the endoplasmic reticulum. J Cell Biol 2008; 182:685-701; PMID:18725538; http://dx.doi.org/10.1083/jcb.200803137

[58] Puri C, Renna M, Bento CF, Moreau K, Rubinsztein DC. Diverse autophagosome membrane sources coalesce in recycling endosomes. Cell 2013; 154:1285-99; PMID:24034251; http://dx.doi.org/10.1016/j.cell.2013.08.044

[59] He S, Ni D, Ma B, Lee JH, Zhang T, Ghozalli I, Pirooz SD, Zhao Z, Bharatham N, Li B, et al. PtdIns(3)P-bound UVRAG coordinates Golgi-ER retrograde and Atg9 transport by differential interactions with the ER tether and the beclin 1 complex. Nat Cell Biol 2013; 15:1206-19; PMID:24056303; http://dx.doi.org/10.1038/ncb2848

[60] Ge L, Zhang M, Schekman R. Phosphatidylinositol 3-kinase and COPII generate LC3 lipidation vesicles from the ER-Golgi intermediate compartment. eLife 2014; 3:e04135; PMID:25432021; http://dx.doi.org/10.7554/eLife.04135

[61] Carlsson SR, Simonsen A. Membrane dynamics in autophagosome biogenesis. J Cell Sci 2015; 128:193-205; PMID:25568151; http://dx.doi.org/10.1242/jcs.141036

[62] Lemus L, Ribas JL, Sikorska N, Goder V. An ER-localized SNARE protein is exported in specific COPII vesicles for autophagosome biogenesis. Cell Rep 2016; 14:1710-22; PMID:26876173; http://dx.doi.org/10.1016/j.celrep.2016.01.047

[63] King JS. Autophagy across the eukaryotes: Is *S. cerevisiae* the odd one out? Autophagy 2012; 8:1159-62; PMID:22722653; http://dx.doi.org/10.4161/auto.20527

[64] Tenenboim H, Smirnova J, Willmitzer L, Steup M, Brotman Y. VMP1-deficient Chlamydomonas exhibits severely aberrant cell morphology and disrupted cytokinesis. BMC Plant Biol 2014; 14:121; PMID:24885763; http://dx.doi.org/10.1186/1471-2229-14-121

[65] Calvo-Garrido J, King JS, Munoz-Braceras S, Escalante R. Vmp1 regulates PtdIns3P signaling during autophagosome formation in *Dictyostelium discoideum*. Traffic 2014; 15:1235-46; PMID:25131297; http://dx.doi.org/10.1111/tra.12210

[66] Tian Y, Li Z, Hu W, Ren H, Tian E, Zhao Y, Lu Q, Huang X, Yang P, Li X, et al. C. elegans screen identifies autophagy genes specific to multicellular organisms. Cell 2010; 141:1042-55; PMID:20550938; http://dx.doi.org/10.1016/j.cell.2010.04.034

[67] Itakura E, Mizushima N. Characterization of autophagosome formation site by a hierarchical analysis of mammalian Atg proteins. Autophagy 2010; 6:764-76; PMID:20639694; http://dx.doi.org/10.4161/auto.6.6.12709

[68] Mizushima N, Yoshimori T, Ohsumi Y. The role of Atg proteins in autophagosome formation. Annu Rev Cell Dev Biol 2011; 27:107-32; PMID:21801009; http://dx.doi.org/10.1146/annurev-cellbio-092910-154005

[69] Zhang L, Li J, Ouyang L, Liu B, Cheng Y. Unraveling the roles of Atg4 proteases from autophagy modulation to targeted cancer therapy. Cancer Lett 2016; 373:19-26; PMID:26805760; http://dx.doi.org/10.1016/j.canlet.2016.01.022

[70] Shpilka T, Weidberg H, Pietrokovski S, Elazar Z. Atg8: an autophagy-related ubiquitin-like protein family. Genome Biol 2011; 12:226; PMID:21867568; http://dx.doi.org/10.1186/gb-2011-12-7-226

[71] Weidberg H, Shvets E, Elazar Z. Biogenesis and cargo selectivity of autophagosomes. Annu Rev Biochem 2011; 80:125-56; PMID:21548784; http://dx.doi.org/10.1146/annurev-biochem-052709-094552

[72] Weidberg H, Shpilka T, Shvets E, Abada A, Shimron F, Elazar Z. LC3 and GATE-16 N termini mediate membrane fusion processes required for autophagosome biogenesis. Dev Cell 2011; 20:444-54; PMID:21497758; http://dx.doi.org/10.1016/j.devcel.2011.02.006

[73] Xie Z, Klionsky DJ. Autophagosome formation: core machinery and adaptations. Nat Cell Biol 2007; 9:1102-9; PMID:17909521; http://dx.doi.org/10.1038/ncb1007-1102

[74] Bader CA, Shandala T, Ng YS, Johnson IR, Brooks DA. Atg9 is required for intraluminal vesicles in amphisomes and autolysosomes. Bio Open 2015; 4:1345-55; http://dx.doi.org/10.1242/bio.013979

[75] Jin M, He D, Backues SK, Freeberg MA, Liu X, Kim JK, Klionsky DJ. Transcriptional regulation by Pho23 modulates the frequency of autophagosome formation. Curr Biol 2014; 24:1314-22; PMID:24881874; http://dx.doi.org/10.1016/j.cub.2014.04.048

[76] Mari M, Griffith J, Rieter E, Krishnappa L, Klionsky DJ, Reggiori F. An Atg9-containing compartment that functions in the early steps of autophagosome biogenesis. J Cell Biol 2010; 190:1005-22; PMID:20855505; http://dx.doi.org/10.1083/jcb.200912089

[77] Reggiori F, Shintani T, Nair U, Klionsky DJ. Atg9 cycles between mitochondria and the pre-autophagosomal structure in yeasts. Autophagy 2005; 1:101-9; PMID:16874040; http://dx.doi.org/10.4161/auto.1.2.1840

[78] Yamada T, Carson AR, Caniggia I, Umebayashi K, Yoshimori T, Nakabayashi K, Scherer SW. Endothelial nitric-oxide synthase antisense (NOS3AS) gene encodes an autophagy-related protein (APG9-like2) highly expressed in trophoblast. J Biol

Chem 2005; 280:18283-90; PMID:15755735; http://dx.doi.org/10.1074/jbc.M413957200

[79] Young AR, Chan EY, Hu XW, Kochl R, Crawshaw SG, High S, Hailey DW, Lippincott-Schwartz J, Tooze SA. Starvation and ULK1-dependent cycling of mammalian Atg9 between the TGN and endosomes. J Cell Sci 2006; 119:3888-900; PMID:16940348; http://dx.doi.org/10.1242/jcs.03172

[80] Puri C, Renna M, Bento CF, Moreau K, Rubinsztein DC. ATG16L1 meets ATG9 in recycling endosomes: additional roles for the plasma membrane and endocytosis in autophagosome biogenesis. Autophagy 2014; 10:182-4; PMID:24257061; http://dx.doi.org/10.4161/auto.27174

[81] Tang HW, Wang YB, Wang SL, Wu MH, Lin SY, Chen GC. Atg1-mediated myosin II activation regulates autophagosome formation during starvation-induced autophagy. EMBO J 2011; 30:636-51; PMID:21169990; http://dx.doi.org/10.1038/emboj.2010.338

[82] Arhzaouy K, Strucksberg KH, Tung SM, Tangavelou K, Stumpf M, Faix J, Schroder R, Clemen CS, Eichinger L. Heteromeric p97/p97 (R155C) complexes induce dominant negative changes in wild-type and autophagy 9-deficient Dictyostelium strains. PLoS ONE 2012; 7:e46879; PMID:23056506; http://dx.doi.org/10.1371/journal.pone.0046879

[83] Dai RM, Li CC. Valosin-containing protein is a multi-ubiquitin chain-targeting factor required in ubiquitin-proteasome degradation. Nat Cell Biol 2001; 3:740-4; PMID:11483959; http://dx.doi.org/10.1038/35087056

[84] Lilley BN, Ploegh HL. Multiprotein complexes that link dislocation, ubiquitination, and extraction of misfolded proteins from the endoplasmic reticulum membrane. Proc Natl Acad Sci U S A 2005; 102:14296-301; PMID:16186509; http://dx.doi.org/10.1073/pnas.0505014102

[85] Ye Y, Shibata Y, Yun C, Ron D, Rapoport TA. A membrane protein complex mediates retro-translocation from the ER lumen into the cytosol. Nature 2004; 429:841-7; PMID:15215856; http://dx.doi.org/10.1038/nature02656

[86] Kazamel M, Sorenson EJ, McEvoy KM, Jones LK, Jr., Leep-Hunderfund AN, Mauermann ML, Milone M. Clinical spectrum of valosin containing protein (VCP)-opathy. Muscle Nerve 2016; 54:94-9; PMID:26574898; http://dx.doi.org/10.1002/mus.24980

[87] Kimonis VE, Mehta SG, Fulchiero EC, Thomasova D, Pasquali M, Boycott K, Neilan EG, Kartashov A, Forman MS, Tucker S, et al. Clinical studies in familial VCP myopathy associated with Paget disease of bone and frontotemporal dementia. Am J Med Genet A 2008; 146A:745-57; PMID:18260132; http://dx.doi.org/10.1002/ajmg.a.31862

[88] Tresse E, Salomons FA, Vesa J, Bott LC, Kimonis V, Yao TP, Dantuma NP, Taylor JP. VCP/p97 is essential for maturation of ubiquitin-containing autophagosomes and this function is impaired by mutations that cause IBMPFD. Autophagy 2010; 6:217-27; PMID:20104022; http://dx.doi.org/10.4161/auto.6.2.11014

[89] Schneider JL, Cuervo AM. Autophagy and human disease: emerging themes. Curr Opin Genet Dev 2014; 26C:16-23; http://dx.doi.org/10.1016/j.gde.2014.04.003

[90] Katsuragi Y, Ichimura Y, Komatsu M. p62/SQSTM1 functions as a signaling hub and an autophagy adaptor. FEBS J 2015; 282:4672-8; PMID:26432171; http://dx.doi.org/10.1111/febs.13540

[91] Schmauch C, Claussner S, Zoltzer H, Maniak M. Targeting the actin-binding protein VASP to late endosomes induces the formation of giant actin aggregates. Eur J Cell Biol 2009; 88:385-96; PMID:19324455; http://dx.doi.org/10.1016/j.ejcb.2009.02.185

[92] Maselli AG, Davis R, Furukawa R, Fechheimer M. Formation of Hirano bodies in Dictyostelium and mammalian cells induced by expression of a modified form of an actin-crosslinking protein. J Cell Sci 2002; 115:1939-49; PMID:11956325

[93] Kim DH, Davis RC, Furukawa R, Fechheimer M. Autophagy contributes to degradation of Hirano bodies. Autophagy 2009; 5:44-51; PMID:18989098; http://dx.doi.org/10.4161/auto.5.1.7228

[94] Rampoldi L, Dobson-Stone C, Rubio JP, Danek A, Chalmers RM, Wood NW, Verellen C, Ferrer X, Malandrini A, Fabrizi GM, et al. A conserved sorting-associated protein is mutant in chorea-acanthocytosis. Nat Genet 2001; 28:119-20; PMID:11381253; http://dx.doi.org/10.1038/88821

[95] Ueno S, Maruki Y, Nakamura M, Tomemori Y, Kamae K, Tanabe H, Yamashita Y, Matsuda S, Kaneko S, Sano A. The gene encoding a newly discovered protein, chorein, is mutated in chorea-acanthocytosis. Nat Genet 2001; 28:121-2; PMID:11381254; http://dx.doi.org/10.1038/88825

[96] Foller M, Hermann A, Gu S, Alesutan I, Qadri SM, Borst O, Schmidt EM, Schiele F, vom Hagen JM, Saft C, et al. Chorein-sensitive polymerization of cortical actin and suicidal cell death in chorea-acanthocytosis. FASEB J 2012; 26:1526-34; PMID:22227296; http://dx.doi.org/10.1096/fj.11-198317

[97] Alesutan I, Seifert J, Pakladok T, Rheinlaender J, Lebedeva A, Towhid ST, Stournaras C, Voelkl J, Schaffer TE, Lang F. Chorein sensitivity of actin polymerization, cell shape and mechanical stiffness of vascular endothelial cells. Cell Physiol Biochem 2013; 32:728-42; PMID:24080826; http://dx.doi.org/10.1159/000354475

[98] Park JS, Neiman AM. VPS13 regulates membrane morphogenesis during sporulation in *Saccharomyces cerevisiae*. J Cell Sci 2012; 125:3004-11; PMID:22442115; http://dx.doi.org/10.1242/jcs.105114

[99] Samaranayake HS, Cowan AE, Klobutcher LA. Vacuolar protein sorting protein 13A, TtVPS13A, localizes to the tetrahymena thermophila phagosome membrane and is required for efficient phagocytosis. Eukaryot Cell 2011; 10:1207-18; PMID:21764909; http://dx.doi.org/10.1128/ec.05089-11

[100] Velayos-Baeza A, Vettori A, Copley RR, Dobson-Stone C, Monaco AP. Analysis of the human VPS13 gene family. Genomics 2004; 84:536-49; PMID:15498460; http://dx.doi.org/10.1016/j.ygeno.2004.04.012

[101] Balikova I, Lehesjoki AE, de Ravel TJ, Thienpont B, Chandler KE, Clayton-Smith J, Traskelin AL, Fryns JP, Vermeesch JR. Deletions in the VPS13B (COH1) gene as a cause of Cohen syndrome. Hum Mutat 2009; 30:E845-54; PMID:19533689; http://dx.doi.org/10.1002/humu.21065

[102] Wang L, Cheng L, Li NN, Yu WJ, Sun XY, Peng R. Association of four new candidate genetic variants with Parkinson's disease in a Han Chinese population. Am J Med Genet B 2016; 171:342-7; http://dx.doi.org/10.1002/ajmg.b.32410

[103] Duleh SN, Welch MD. WASH and the Arp2/3 complex regulate endosome shape and trafficking. Cytoskeleton 2010; 67:193-206; PMID:20175130

[104] Freeman C, Seaman MN, Reid E. The hereditary spastic paraplegia protein strumpellin: characterisation in neurons and of the effect of disease mutations on WASH complex assembly and function. Biochim Biophys Acta 2013; 1832:160-73; PMID:23085491; http://dx.doi.org/10.1016/j.bbadis.2012.10.011

[105] Zavodszky E, Seaman MN, Moreau K, Jimenez-Sanchez M, Breusegem SY, Harbour ME, Rubinsztein DC. Mutation in VPS35 associated with Parkinson's disease impairs WASH complex association and inhibits autophagy. Nat Commun 2014; 5:3828; PMID:24819384; http://dx.doi.org/10.1038/ncomms4828

[106] Xia P, Wang S, Du Y, Zhao Z, Shi L, Sun L, Huang G, Ye B, Li C, Dai Z, et al. WASH inhibits autophagy through suppression of Beclin 1 ubiquitination. EMBO J 2013; 32:2685-96; PMID:23974797; http://dx.doi.org/10.1038/emboj.2013.189

[107] Sarkar S. Regulation of autophagy by mTOR-dependent and mTOR-independent pathways: autophagy dysfunction in neurodegenerative diseases and therapeutic application of autophagy enhancers. Biochem Soc Trans 2013; 41:1103-30; PMID:24059496; http://dx.doi.org/10.1042/BST20130134

[108] Francione L, Smith PK, Accari SL, Taylor PE, Bokko PB, Bozzaro S, Beech PL, Fisher PR. Legionella pneumophila multiplication is enhanced by chronic AMPK signalling in mitochondrially diseased Dictyostelium cells. Dis Model Mech 2009; 2:479-89; PMID:19638422; http://dx.doi.org/10.1242/dmm.003319

[109] Carilla-Latorre S, Gallardo ME, Annesley SJ, Calvo-Garrido J, Grana O, Accari SL, Smith PK, Valencia A, Garesse R, Fisher PR, et al. MidA is a putative methyltransferase that is required for mitochondrial complex I function. J Cell Sci 2010; 123:1674-83; PMID:20406883; http://dx.doi.org/10.1242/jcs.066076

[110] Carilla-Latorre S, Annesley SJ, Munoz-Braceras S, Fisher PR, Escalante R. Ndufaf5 deficiency in the Dictyostelium model: new roles in autophagy and development. Mol Biol Cell 2013; 24:1519-28; PMID:23536703; http://dx.doi.org/10.1091/mbc.E12-11-0796

[111] Peng M, Ostrovsky J, Kwon YJ, Polyak E, Licata J, Tsukikawa M, Marty E, Thomas J, Felix CA, Xiao R, et al. Inhibiting cytosolic translation and autophagy improves health in mitochondrial disease. Hum Mol Genet 2015; 24:4829-47; PMID:26041819; http://dx.doi.org/10.1093/hmg/ddv207

[112] Moran M, Delmiro A, Blazquez A, Ugalde C, Arenas J, Martin MA. Bulk autophagy, but not mitophagy, is increased in cellular model of mitochondrial disease. Biochim Biophys Acta 2014; 1842:1059-70; PMID:24704045; http://dx.doi.org/10.1016/j.bbadis.2014.03.013

[113] Escoll P, Rolando M, Buchrieser C. Modulation of host autophagy during bacterial infection: Sabotaging host munitions for pathogen nutrition. Frontiers Immunol 2016; 7:81; http://dx.doi.org/10.3389/fimmu.2016.00081

[114] Sillo A, Matthias J, Konertz R, Bozzaro S, Eichinger L. Salmonella typhimurium is pathogenic for Dictyostelium cells and subverts the starvation response. Cell Microbiol 2011; 13:1793-811; PMID:21824247; http://dx.doi.org/10.1111/j.1462-5822.2011.01662.x

[115] Pflaum K, Gerdes K, Yovo K, Callahan J, Snyder ML. Lipopolysaccharide induction of autophagy is associated with enhanced bactericidal activity in Dictyostelium discoideum. Biochem Biophys Res Commun 2012; 422:417-22; PMID:22575510; http://dx.doi.org/10.1016/j.bbrc.2012.05.006

[116] Lampe EO, Brenz Y, Herrmann L, Repnik U, Griffiths G, Zingmark C, Sjostedt A, Winther-Larsen HC, Hagedorn M. Dissection of Francisella - host cell interactions in Dictyostelium discoideum. Appl Environ Microbiol 2015; 82:1586-98; PMID:26712555; http://dx.doi.org/10.1128/aem.02950-15

[117] Barisch C, Paschke P, Hagedorn M, Maniak M, Soldati T. Lipid droplet dynamics at early stages of Mycobacterium marinum infection in Dictyostelium. Cell Microbiol 2015; 17:1332-49; PMID:25772333; http://dx.doi.org/10.1111/cmi.12437

[118] Kolonko M, Geffken AC, Blumer T, Hagens K, Schaible UE, Hagedorn M. WASH-driven actin polymerization is required for efficient mycobacterial phagosome maturation arrest. Cell Microbiol 2014; 16:232-46; PMID:24119059; http://dx.doi.org/10.1111/cmi.12217

[119] Schiebler M, Brown K, Hegyi K, Newton SM, Renna M, Hepburn L, Klapholz C, Coulter S, Obregon-Henao A, Henao Tamayo M, et al. Functional drug screening reveals anticonvulsants as enhancers of mTOR-independent autophagic killing of Mycobacterium tuberculosis through inositol depletion. EMBO Mol Med 2014; 7:127-39; PMID:25535254; http://dx.doi.org/10.15252/emmm.201404137

[120] Jaiswal P, Soldati T, Thewes S, Baskar R. Regulation of aggregate size and pattern by adenosine and caffeine in cellular slime molds. BMC Dev Biol 2012; 12:5; PMID:22269093; http://dx.doi.org/10.1186/1471-213X-12-5

[121] Kicka S, Trofimov V, Harrison C, Ouertatani-Sakouhi H, McKinney J, Scapozza L, Hilbi H, Cosson P, Soldati T. Establishment and validation of whole-cell based fluorescence assays to identify anti-mycobacterial compounds using the Acanthamoeba castellanii-Mycobacterium marinum host-pathogen system. PLoS ONE 2014; 9:e87834; PMID:24498207; http://dx.doi.org/10.1371/journal.pone.0087834

[122] Swer PB, Lohia R, Saran S. Analysis of rapamycin induced autophagy in Dictyostelium discoideum. Indian J Exp Biol 2014; 52:295-304; PMID:24772931

[123] Tobin DM, Ramakrishnan L. Comparative pathogenesis of Mycobacterium marinum and Mycobacterium tuberculosis. Cell Microbiol 2008; 10:1027-39; PMID:18298637; http://dx.doi.org/10.1111/j.1462-5822.2008.01133.x

[124] Lerena MC, Colombo MI. Mycobacterium marinum induces a marked LC3 recruitment to its containing phagosome that depends on a functional ESX-1 secretion system. Cell Microbiol 2011; 13:814-35; PMID:21447143; http://dx.doi.org/10.1111/j.1462-5822.2011.01581.x

[125] van der Vaart M, Korbee CJ, Lamers GE, Tengeler AC, Hosseini R, Haks MC, Ottenhoff TH, Spaink HP, Meijer AH. The DNA damage-regulated autophagy modulator DRAM1 links mycobacterial recognition via TLP-MYD88 to authophagic defense. Cell Host Microbe 2014; 15:753-67; PMID:24922577; http://dx.doi.org/10.1016/j.chom.2014.05.005

[126] Sato E, Imafuku S, Ishii K, Itoh R, Chou B, Soejima T, Nakayama J, Hiromatsu K. Vitamin D-dependent cathelicidin inhibits Mycobacterium marinum infection in human monocytic cells. Journal Dermatol Sci 2013; 70:166-72; http://dx.doi.org/10.1016/j.jdermsci.2013.01.011

[127] Hosseini R, Lamers GE, Hodzic Z, Meijer AH, Schaaf MJ, Spaink HP. Correlative light and electron microscopy imaging of autophagy in a zebrafish infection model. Autophagy 2014; 10:1844-57; PMID:25126731; http://dx.doi.org/10.4161/auto.29992

[128] Mohanty S, Jagannathan L, Ganguli G, Padhi A, Roy D, Alaridah N, Saha P, Nongthomba U, Godaly G, Gopal RK, et al. A mycobacterial phosphoribosyltransferase promotes bacillary survival by inhibiting oxidative stress and autophagy pathways in macrophages and zebrafish. J Biol Chem 2015; 290:13321-43; PMID:25825498; http://dx.doi.org/10.1074/jbc.M114.598482

[129] Watson RO, Manzanillo PS, Cox JS. Extracellular M. tuberculosis DNA targets bacteria for autophagy by activating the host DNA-sensing pathway. Cell 2012; 150:803-15; PMID:22901810; http://dx.doi.org/10.1016/j.cell.2012.06.040

[130] Collins CA, De Maziere A, van Dijk S, Carlsson F, Klumperman J, Brown EJ. Atg5-independent sequestration of ubiquitinated mycobacteria. PLoS Pathog 2009; 5:e1000430; PMID:19436699; http://dx.doi.org/10.1371/journal.ppat.1000430

[131] Smith J, Manoranjan J, Pan M, Bohsali A, Xu J, Liu J, McDonald KL, Szyk A, LaRonde-LeBlanc N, Gao LY. Evidence for pore formation in host cell membranes by ESX-1-secreted ESAT-6 and its role in Mycobacterium marinum escape from the vacuole. Infect Immun 2008; 76:5478-87; PMID:18852239; http://dx.doi.org/10.1128/iai.00614-08

[132] Hagedorn M, Rohde KH, Russell DG, Soldati T. Infection by tubercular mycobacteria is spread by nonlytic ejection from their amoeba hosts. Science 2009; 323:1729-33; PMID:19325115; http://dx.doi.org/10.1126/science.1169381

[133] Hagedorn M, Soldati T. Flotillin and RacH modulate the intracellular immunity of Dictyostelium to Mycobacterium marinum infection. Cell Microbiol 2007; 9:2984; http://dx.doi.org/10.1111/j.1462-5822.2007.01064.x

[134] Checroun C, Wehrly TD, Fischer ER, Hayes SF, Celli J. Autophagy-mediated reentry of Francisella tularensis into the endocytic compartment after cytoplasmic replication. Proc Natl Acad Sci U S A 2006; 103:14578-83; PMID:16983090; http://dx.doi.org/10.1073/pnas.0601838103

[135] Steele S, Brunton J, Ziehr B, Taft-Benz S, Moorman N, Kawula T. Francisella tularensis Harvests Nutrients Derived via ATG5-Independent Autophagy to Support Intracellular Growth. PLoS Pathog 2013; 9:e1003562; PMID:23966861; http://dx.doi.org/10.1371/journal.ppat.1003562

[136] Otto GP, Wu MY, Clarke M, Lu H, Anderson OR, Hilbi H, Shuman HA, Kessin RH. Macroautophagy is dispensable for intracellular replication of Legionella pneumophila in Dictyostelium discoideum. Mol Microbiol 2004; 51:63-72; PMID:14651611; http://dx.doi.org/10.1046/j.1365-2958.2003.03826.x

[137] Choy A, Dancourt J, Mugo B, O'Connor TJ, Isberg RR, Melia TJ, Roy CR. The Legionella effector RavZ inhibits host autophagy through irreversible Atg8 deconjugation. Science 2012; 338:1072-6; PMID:23112293; http://dx.doi.org/10.1126/science.1227026

[138] Mack HI, Zheng B, Asara JM, Thomas SM. AMPK-dependent phosphorylation of ULK1 regulates ATG9 localization. Autophagy 2012; 8:1197-214; PMID:22932492; http://dx.doi.org/10.4161/auto.20586

[139] LaRock DL, Chaudhary A, Miller SI. Salmonellae interactions with host processes. Nat Rev Microbiol 2015; 13:191-205; PMID:25749450; http://dx.doi.org/10.1038/nrmicro3420

[140] Garai P, Gnanadhas DP, Chakravortty D. Salmonella enterica serovars Typhimurium and Typhi as model organisms: revealing

paradigm of host-pathogen interactions. Virulence 2012; 3:377-88; PMID:22722237; http://dx.doi.org/10.4161/viru.21087

[141] Skriwan C, Fajardo M, Hagele S, Horn M, Wagner M, Michel R, Krohne G, Schleicher M, Hacker J, Steinert M. Various bacterial pathogens and symbionts infect the amoeba Dictyostelium discoideum. Int J Med Microbiol 2002; 291:615-24; PMID:12008915; http://dx.doi.org/10.1078/1438-4221-00177

[142] Jia K, Thomas C, Akbar M, Sun Q, Adams-Huet B, Gilpin C, Levine B. Autophagy genes protect against Salmonella typhimurium infection and mediate insulin signaling-regulated pathogen resistance. Proc Natl Acad Sci U S A 2009; 106:14564-9; PMID:19667176; http://dx.doi.org/10.1073/pnas.0813319106

[143] Mestre MB, Fader CM, Sola C, Colombo MI. Alpha-hemolysin is required for the activation of the autophagic pathway in Staphylococcus aureus-infected cells. Autophagy 2010; 6:110-25; PMID:20110774; http://dx.doi.org/10.4161/auto.6.1.10698

[144] Schnaith A, Kashkar H, Leggio SA, Addicks K, Kronke M, Krut O. Staphylococcus aureus subvert autophagy for induction of caspase-independent host cell death. J Biol Chem 2007; 282:2695-706; PMID:17135247; http://dx.doi.org/10.1074/jbc.M609784200

[145] O'Keeffe KM, Wilk MM, Leech JM, Murphy AG, Laabei M, Monk IR, Massey RC, Lindsay JA, Foster TJ, Geoghegan JA, et al. Manipulation of Autophagy in Phagocytes Facilitates Staphylococcus aureus Bloodstream Infection. Infect Immun 2015; 83:3445-57; PMID:26099586; http://dx.doi.org/10.1128/iai.00358-15

[146] Klionsky DJ, Abdelmohsen K, Abe A, Abedin MJ, Abeliovich H, Acevedo Arozena A, Adachi H, Adams CM, Adams PD, Adeli K, et al. Guidelines for the use and interpretation of assays for monitoring autophagy (3rd edition). Autophagy 2016; 12:1-222; PMID:26799652; http://dx.doi.org/10.1080/15548627.2015.1100356

[147] Golstein P, Aubry L, Levraud JP. Cell-death alternative model organisms: why and which? Nature Rev Mol Cell Biol 2003; 4:798-807; http://dx.doi.org/10.1038/nrm1224

[148] Whittingham WF, Raper KB. Non-viability of stalk cells in Dictyostelium. Proc Natl Acad Sci USA 1960; 46:642-9; PMID:16590653; http://dx.doi.org/10.1073/pnas.46.5.642

[149] Kay RR. Cell differentiation in monolayers and the investigation of slime mold morphogens. Methods Cell Biol 1987; 28:433-48; PMID:3600415; http://dx.doi.org/10.1016/S0091-679X(08)61661-1

[150] Cornillon S, Foa C, Davoust J, Buonavista N, Gross JD, Golstein P. Programmed cell death in Dictyostelium. J Cell Sci 1994; 107:2691-704; PMID:7876338

[151] Giusti C, Tresse E, Luciani MF, Golstein P. Autophagic cell death: analysis in Dictyostelium. Biochim Biophys Acta 2009; 1793:1422-31; PMID:19133302; http://dx.doi.org/10.1016/j.bbamcr.2008.12.005

[152] Morris HR, Taylor GW, Masento MS, Jermyn KA, Kay RR. Chemical structure of the morphogen differentiation inducing factor from Dictyostelium discoideum. Nature 1987; 328:811-4; PMID:3627228; http://dx.doi.org/10.1038/328811a0

[153] Luciani MF, Giusti C, Harms B, Oshima Y, Kikuchi H, Kubohara Y, Golstein P. Atg1 allows second-signaled autophagic cell death in Dictyostelium. Autophagy 2011; 7:501-8; PMID:21301205; http://dx.doi.org/10.4161/auto.7.5.14957

[154] Kosta A, Roisin-Bouffay C, Luciani MF, Otto GP, Kessin RH, Golstein P. Autophagy gene disruption reveals a non-vacuolar cell death pathway in Dictyostelium. J Biol Chem 2004; 279:48404-9; PMID:15358773; http://dx.doi.org/10.1074/jbc.M408924200

[155] Kosta A, Laporte C, Lam D, Tresse E, Luciani MF, Golstein P. How to assess and study cell death in Dictyostelium discoideum. Methods Mol Biol 2006; 346:535-50; PMID:16957313

[156] Laporte C, Kosta A, Klein G, Aubry L, Lam D, Tresse E, Luciani MF, Golstein P. A necrotic cell death model in a protist. Cell Death Differ 2007; 14:266-74; PMID:16810325; http://dx.doi.org/10.1038/sj.cdd.4401994

[157] Giusti C, Luciani MF, Klein G, Aubry L, Tresse E, Kosta A, Golstein P. Necrotic cell death: From reversible mitochondrial uncoupling to irreversible lysosomal permeabilization. Exp Cell Res 2009; 315:26-38; PMID:18951891; http://dx.doi.org/10.1016/j.yexcr.2008.09.028

[158] Luciani MF, Kubohara Y, Kikuchi H, Oshima Y, Golstein P. Autophagic or necrotic cell death triggered by distinct motifs of the differentiation factor DIF-1. Cell Death Differ 2009; 16:564-70; PMID:19079140; http://dx.doi.org/10.1038/cdd.2008.177

[159] Shaulsky G, Loomis WF. Mitochondrial DNA replication but no nuclear DNA replication during development of Dictyostelium. Proc Natl Acad Sci USA 1995; 92:5660-3; PMID:7777565; http://dx.doi.org/10.1073/pnas.92.12.5660

[160] Sugden C, Urbaniak MD, Araki T, Williams JG. The Dictyostelium prestalk inducer differentiation-inducing factor-1 (DIF-1) triggers unexpectedly complex global phosphorylation changes. Mol Biol Cell 2015; 26:805-20; PMID:25518940; http://dx.doi.org/10.1091/mbc.E14-08-1319

[161] Lam D, Golstein P. A specific pathway inducing autophagic cell death is marked by an IP3R mutation. Autophagy 2008; 4:349-50; PMID:18196962; http://dx.doi.org/10.4161/auto.5521

[162] Tresse E, Kosta A, Giusti C, Luciani MF, Golstein P. A UDP-glucose derivative is required for vacuolar autophagic cell death. Autophagy 2008; 4:680-91; PMID:18424909; http://dx.doi.org/10.4161/auto.6084

[163] Giusti C, Luciani MF, Ravens S, Gillet A, Golstein P. Autophagic cell death in Dictyostelium requires the receptor histidine kinase DhkM. Mol Biol Cell 2010; 21:1825-35; PMID:20375146; http://dx.doi.org/10.1091/mbc.E09-11-0976

[164] Chen ZH, Schaap P. The prokaryote messenger c-di-GMP triggers stalk cell differentiation in Dictyostelium. Nature 2012; 488:680-3; PMID:22864416; http://dx.doi.org/10.1038/nature11313

[165] Chen ZH, Schaap P. Secreted cyclic-di-GMP induces stalk cell differentiation in the eukaryote Dictyostelium discoideum. J Bacteriol 2016; 198:27-31; PMID:26013485; http://dx.doi.org/10.1128/jb.00321-15

[166] Romling U, Galperin MY, Gomelsky M. Cyclic di-GMP: the first 25 years of a universal bacterial second messenger. Microbiol Mol Biol Rev 2013; 77:1-52; PMID:23471616; http://dx.doi.org/10.1128/mmbr.00043-12

[167] Danilchanka O, Mekalanos JJ. Cyclic dinucleotides and the innate immune response. Cell 2013; 154:962-70; PMID:23993090; http://dx.doi.org/10.1016/j.cell.2013.08.014

[168] Song Y, Luciani MF, Giusti C, Golstein P. c-di-GMP induction of Dictyostelium cell death requires the polyketide DIF-1. Mol Biol Cell 2015; 26:651-8; PMID:25518941; http://dx.doi.org/10.1091/mbc.E14-08-1337

[169] Thompson CRL, Kay RR. The role of DIF-1 signaling in Dictyostelium development. Mol Cell 2000; 6:1509-14; PMID:11163223; http://dx.doi.org/10.1016/S1097-2765(00)00147-7

[170] Saito T, Kato A, Kay RR. DIF-1 induces the basal disc of the Dictyostelium fruiting body. Dev Biol 2008; 317:444-53; PMID:18402932; http://dx.doi.org/10.1016/j.ydbio.2008.02.036

[171] Parvatiyar K, Zhang Z, Teles RM, Ouyang S, Jiang Y, Iyer SS, Zaver SA, Schenk M, Zeng S, Zhong W, et al. The helicase DDX41 recognizes the bacterial secondary messengers cyclic di-GMP and cyclic di-AMP to activate a type I interferon immune response. Nat Immunol 2012; 13:1155-61; PMID:23142775; http://dx.doi.org/10.1038/ni.2460

[172] Chou SH, Galperin MY. Diversity of c-di-GMP-binding proteins and mechanisms. J Bacteriol 2015; 198:32-46; http://dx.doi.org/10.1128/jb.00333-15